

JOURNAL OF

CHROMATOGRAPHY A

INCLUDING ELECTROPHORESIS AND OTHER SEPARATION METHODS

EDITORS

U.A.Th. Brinkman (Amsterdam)
R.W. Giese (Boston, MA)
J.K. Haken (Kensington, N.S.W.)
L.R. Snyder (Orinda, CA)
S. Terabe (Hyogo)

EDITORS, SYMPOSIUM VOLUMES,
E. Heftmann (Orinda, CA), Z. Deyl (Prague)

EDITORIAL BOARD

D.W. Armstrong (Rolla, MO)
W.A. Aue (Halifax)
P. Boček (Brno)
A.A. Boulton (Saskatoon)
P.W. Carr (Minneapolis, MN)
N.H.C. Cooke (San Ramon, CA)
V.A. Davankov (Moscow)
G.J. de Jong (Weesp)
Z. Deyl (Prague)
S. Dilli (Kensington, N.S.W.)
Z. El Rassi (Stillwater, OK)
H. Engelhardt (Saarbrücken)
F. Erni (Basle)
M.B. Evans (Hatfield)
J.L. Glajch (N. Billerica, MA)
G.A. Guiochon (Knoxville, TN)
P.R. Haddad (Hobart, Tasmania)
I.M. Hais (Hradec Králové)
W.S. Hancock (Palo Alto, CA)
S. Hjertén (Uppsala)
S. Honda (Higashi-Osaka)
Cs. Horváth (New Haven, CT)
J.F.K. Huber (Vienna)
K.-P. Hupe (Waldbronn)
J. Janák (Brno)
P. Jandera (Pardubice)
B.L. Karger (Boston, MA)
J.J. Kirkland (Newport, DE)
E. sz. Kováts (Lausanne)
K. Macek (Prague)
A.J.P. Martin (Cambridge)
L.W. McLaughlin (Chestnut Hill, MA)
E.D. Morgan (Keele)
J.D. Pearson (Kalamazoo, MI)
H. Poppe (Amsterdam)
F.E. Regnier (West Lafayette, IN)
P.G. Righetti (Milan)
P. Schoenmakers (Amsterdam)
R. Schwarzenbach (Dübendorf)
R.E. Shoup (West Lafayette, IN)
R.P. Singhal (Wichita, KS)
A.M. Siouffi (Marseille)
D.J. Strydom (Boston, MA)
N. Tanaka (Kyoto)
K.K. Ungor (Mainz)
R. Verpoorte (Leiden)
Gy. Vigh (College Station, TX)
J.T. Watson (East Lansing, MI)
B.D. Westerlund (Uppsala)

EDITORS, BIBLIOGRAPHY SECTION

Z. Deyl (Prague), J. Janák (Brno), V. Schwarz (Prague)

ELSEVIER

JOURNAL OF CHROMATOGRAPHY A

INCLUDING ELECTROPHORESIS AND OTHER SEPARATION METHODS

Scope. The *Journal of Chromatography A* publishes papers on all aspects of **chromatography, electrophoresis** and related methods. Contributions consist mainly of research papers dealing with chromatographic theory, instrumental developments and their applications. In the *Symposium volumes*, which are under separate editorship, proceedings of symposia on chromatography, electrophoresis and related methods are published. *Journal of Chromatography B: Biomedical Applications*—This journal, which is under separate editorship, deals with the following aspects: developments in and applications of chromatographic and electrophoretic techniques related to clinical diagnosis or alterations during medical treatment; screening and profiling of body fluids or tissues related to the analysis of active substances and to metabolic disorders; drug level monitoring and pharmacokinetic studies; clinical toxicology; forensic medicine; veterinary medicine; occupational medicine; results from basic medical research with direct consequences in clinical practice.

Submission of Papers. The preferred medium of submission is on disk with accompanying manuscript (see *Electronic manuscripts* in the Instructions to Authors, which can be obtained from the publisher, Elsevier Science B.V., P.O. Box 330, 1000 AH Amsterdam, Netherlands). Manuscripts (in English; *four* copies are required) should be submitted to: Editorial Office of *Journal of Chromatography A*, P.O. Box 681, 1000 AR Amsterdam, Netherlands, Telefax (+31-20) 5862 304, or to: The Editor of *Journal of Chromatography B: Biomedical Applications*, P.O. Box 681, 1000 AR Amsterdam, Netherlands. Review articles are invited or proposed in writing to the Editors who welcome suggestions for subjects. An outline of the proposed review should first be forwarded to the Editors for preliminary discussion prior to preparation. Submission of an article is understood to imply that the article is original and unpublished and is not being considered for publication elsewhere. For copyright regulations, see below.

Publication information. *Journal of Chromatography A* (ISSN 0021-9673): for 1995 Vols. 683–714 are scheduled for publication. *Journal of Chromatography B: Biomedical Applications* (ISSN 0378-4347): for 1995 Vols. 663–674 are scheduled for publication. Subscription prices for *Journal of Chromatography A*, *Journal of Chromatography B: Biomedical Applications* or a combined subscription are available upon request from the publisher. Subscriptions are accepted on a prepaid basis only and are entered on a calendar year basis. Issues are sent by surface mail except to the following countries where air delivery via SAL is ensured: Argentina, Australia, Brazil, Canada, China, Hong Kong, India, Israel, Japan, Malaysia, Mexico, New Zealand, Pakistan, Singapore, South Africa, South Korea, Taiwan, Thailand, USA. For all other countries airmail rates are available upon request. Claims for missing issues must be made within six months of our publication (mailing) date. Please address all your requests regarding orders and subscription queries to: Elsevier Science B.V., Journal Department, P.O. Box 211, 1000 AE Amsterdam, Netherlands. Tel.: (+31-20) 5803 642; Fax: (+31-20) 5803 598. Customers in the USA and Canada wishing information on this and other Elsevier journals, please contact Journal Information Center, Elsevier Science Inc., 655 Avenue of the Americas, New York, NY 10010, USA, Tel. (+1-212) 633 3750, Telefax (+1-212) 633 3764.

Abstracts/Contents Lists published in Analytical Abstracts, Biochemical Abstracts, Biological Abstracts, Chemical Abstracts, Chemical Titles, Chromatography Abstracts, Current Awareness in Biological Sciences (CABS), Current Contents/Life Sciences, Current Contents/Physical, Chemical & Earth Sciences, Deep-Sea Research/Part B: Oceanographic Literature Review, Excerpta Medica, Index Medicus, Mass Spectrometry Bulletin, PASCAL-CNRS, Referativnyi Zhurnal, Research Alert and Science Citation Index.

US Mailing Notice. *Journal of Chromatography A* (ISSN 0021-9673) is published weekly (total 52 issues) by Elsevier Science B.V., (Sara Burgerhartstraat 25, P.O. Box 211, 1000 AE Amsterdam, Netherlands). Annual subscription price in the USA US\$ 5389.00 (US\$ price valid in North, Central and South America only) including air speed delivery. Second class postage paid at Jamaica, NY 11431. **USA POSTMASTERS:** Send address changes to *Journal of Chromatography A*, Publications Expediting, Inc., 200 Meacham Avenue, Elmont, NY 11003. Airfreight and mailing in the USA by Publications Expediting.

See inside back cover for Publication Schedule, Information for Authors and information on Advertisements.

© 1994 ELSEVIER SCIENCE B.V. All rights reserved.

0021-9673/94/\$07.00

No part of this publication may be reproduced, stored in a retrieval system or transmitted in any form or by any means, electronic, mechanical, photocopying, recording or otherwise, without the prior written permission of the publisher, Elsevier Science B.V., Copyright and Permissions Department, P.O. Box 521, 1000 AM Amsterdam, Netherlands.

Upon acceptance of an article by the journal, the author(s) will be asked to transfer copyright of the article to the publisher. The transfer will ensure the widest possible dissemination of information.

Special regulations for readers in the USA—This journal has been registered with the Copyright Clearance Center, Inc. Consent is given for copying of articles for personal or internal use, or for the personal use of specific clients. This consent is given on the condition that the copier pays through the Center the per-copy fee stated in the code on the first page of each article for copying beyond that permitted by Sections 107 or 108 of the US Copyright Law. The appropriate fee should be forwarded with a copy of the first page of the article to the Copyright Clearance Center, Inc., 222 Rosewood Drive, Danvers, MA 01923, USA. If no code appears in an article, the author has not given broad consent to copy and permission to copy must be obtained directly from the author. The fee indicated on the first page of an article in this issue will apply retroactively to all articles published in the journal, regardless of the year of publication. This consent does not extend to other kinds of copying, such as for general distribution, resale, advertising and promotion purposes, or for creating new collective works. Special written permission must be obtained from the publisher for such copying.

No responsibility is assumed by the Publisher for any injury and/or damage to persons or property as a matter of products liability, negligence or otherwise, or from any use or operation of any methods, products, instructions or ideas contained in the materials herein. Because of rapid advances in the medical sciences, the Publisher recommends that independent verification of diagnoses and drug dosages should be made.

Although all advertising material is expected to conform to ethical (medical) standards, inclusion in this publication does not constitute a guarantee or endorsement of the quality or value of such product or of the claims made of it by its manufacturer.

② The paper used in this publication meets the requirements of ANSI/NISO Z39.48-1992 (Permanence of Paper).

Printed in the Netherlands

CONTENTS

(Abstracts/Contents Lists published in *Analytical Abstracts*, *Biochemical Abstracts*, *Biological Abstracts*, *Chemical Abstracts*, *Chemical Titles*, *Chromatography Abstracts*, *Current Awareness in Biological Sciences (CABS)*, *Current Contents/Life Sciences*, *Current Contents/Physical, Chemical & Earth Sciences*, *Deep-Sea Research/Part B: Oceanographic Literature Review*, *Excerpta Medica*, *Index Medicus*, *Mass Spectrometry Bulletin*, *PASCAL-CNRS*, *Referativnyi Zhurnal*, *Research Alert* and *Science Citation Index*)

REGULAR PAPERS

Column Liquid Chromatography

- Evaluation of a chiral stationary phase based on mixed immobilized proteins
by A.-F. Aubry and N. Markoglou (Montreal, Canada), V. Descorps (Talence, France), I.W. Wainer (Montreal, Canada) and G. Félix (Talence, France) (Received 18 July 1994) 1
- Interpretation of enantioselective activity of albumin used as the chiral selector in liquid chromatography and electrophoresis
by Z. Šimek and R. Vespaľec (Brno, Czech Republic) (Received 29 June 1994) 7
- Structural factors affecting the enantiomeric separation of barbiturates and thiobarbiturates with a chiral side-chain by various β -cyclodextrin supports. Effects of the presence of hydroxypropyl substituents on the chiral selector
by N. Thuaud and B. Sebillé (Thiais, France) (Received 18 July 1994) 15
- Analytical conditions for the determination of 23 phenylthiocarbamyl amino acids and ethanolamine in musts and wines by high-performance liquid chromatography
by M. Puig-Deu and S. Buxaderas (Barcelona, Spain) (Received 18 July 1994) 21
- Resolution of proteins on a phenyl-Superose HR5/5 column and its application to examining the conformation homogeneity of refolded recombinant staphylococcal nuclease
by G. Jing, B. Zhou, L. Liu, J. Zhou and Z. Liu (Beijing, China) (Received 19 July 1994) 31
- High-performance liquid chromatographic analysis of low-molecular-mass products synthesized by polynucleotide phosphorylase in polymerization reaction
by A.L. Simanov (Moscow, Russian Federation) (Received 24 June 1994) 39
- Purification of beet molasses by ion-exclusion chromatography: fixed-bed modelling
by M.-L. Lameloise and R. Lewandowski (Massy, France) (Received 21 July 1994) 45
- Ion chromatographic determination of fluoride in welding fumes with elimination of high contents of iron by solid-phase extraction
by M.T.S.D. Vasconcelos, C.A.R. Gomes and A.A.S.C. Machado (Porto, Portugal) (Received 15 July 1994) 53

Gas Chromatography

- Preparation of deactivated metal capillary for gas chromatography
by Y. Takayama and T. Takeichi (Toyohashi, Japan) (Received 21 June 1994) 61

Supercritical Fluid Extraction

- Analysis of volatile organics by supercritical fluid extraction coupled to gas chromatography. I. Optimization of chromatographic parameters
by M.D. Burford, S.B. Hawthorne and D.J. Miller (Grand Forks, ND, USA) (Received 5 July 1994) 79
- Analysis of volatile organics by supercritical fluid extraction coupled to gas chromatography. II. Quantitation of petroleum hydrocarbons from environmental sample
by M.D. Burford, S.B. Hawthorne and D.J. Miller (Grand Forks, ND, USA) (Received 5 July 1994) 95
- Solute collection after off-line supercritical fluid extraction into a moving liquid layer
by J. Vejrosta, J. Planeta, M. Mikešová, A. Ansorgová and P. Karásek (Brno, Czech Republic) and J. Fanta and V. Janda (Prague, Czech Republic) (Received 22 July 1994) 113
- Preparation of highly condensed polyacrylamide gel-filled capillaries with low detection background
by Y. Chen, J.-V. Höltje and U. Schwarz (Tübingen, Germany) (Received 25 July 1994) 121

(Continued overleaf)

ห้องสมุดวิทยาศาสตร์บริการ

12 ต.ค. ๒๕๓๘

Contents (continued)

Micellar electrokinetic capillary chromatography with in situ charged micelles. IV. Influence of the nature of the alkylglycoside surfactant by J.T. Smith and Z. El Rassi (Stillwater, OK, USA) (Received 12 July 1994)	131
Capillary zone electrophoresis with indirect UV detection of organic anions using 2,6-naphthalenedicarboxylic acid by E. Dabek-Zlotorzynska and J.F. Dlouhy (Ottawa, Canada) (Received 13 June 1994)	145
Practical aspects in chiral separation of pharmaceuticals by capillary electrophoresis. II. Quantitative separation of naproxen enantiomers by A. Guttman and N. Cooke (Fullerton, CA, USA) (Received 5 July 1994)	155
Optimisation of separation selectivity in capillary zone electrophoresis of inorganic anions using binary cationic surfactant mixtures by A.H. Harakuwe, P.R. Haddad and W. Buchberger (Hobart, Australia) (Received 18 July 1994)	161

SHORT COMMUNICATIONS

Column Liquid Chromatography

Immobilization of peralkylated β -cyclodextrin on silica gel for high-performance liquid chromatography by I. Ciucanu and W.A. König (Hamburg, Germany) (Received 25 May 1994)	166
Determination of Stokes radii and molecular masses of sodium hyaluronates by Sephacryl gel chromatography by E. Shimada and K.T. Nakamura (Tokyo, Japan) (Received 29 July 1994)	172
Silver ion high-performance liquid chromatographic separation of fatty acid methyl esters labelled with deuterium atoms on the double bonds by R.O. Adlof and E.A. Emken (Peoria, IL, USA) (Received 19 August 1994)	178
Single-run analysis of isomers of retinoyl- β -D-glucuronide and retinoic acid by reversed-phase high-performance liquid chromatography by J.O. Sass and H. Nau (Berlin, Germany) (Received 23 August 1994)	182

Gas Chromatography

Formation of Schiff bases with acetone as a solvent in the determination of anilines by M. Kolb and M. Bahadir (Braunschweig, Germany) (Received 28 July 1994)	189
---	-----

Planar Chromatography

High-performance thin-layer chromatographic method for monitoring degradation products of rifampicin in drug excipient interaction studies by K.C. Jindal, R.S. Chaudhary, S.S. Gangwal, A.K. Singla and S. Khanna (Aurangabad, India) (Received 3 August 1994)	195
--	-----

BOOK REVIEW

Modern Methods and Applications in Analysis of Explosives (by J. Yinon and S. Zitrin), reviewed by P.A. D'Agostino (Medicine Hat, Canada)	200
---	-----

JOURNAL OF CHROMATOGRAPHY A

VOL. 685 (1994)

JOURNAL OF CHROMATOGRAPHY A

INCLUDING ELECTROPHORESIS AND OTHER SEPARATION METHODS

EDITORS

U.A.Th. BRINKMAN (Amsterdam), R.W. GIESE (Boston, MA), J.K. HAKEN (Kensington, N.S.W.),
L.R. SNYDER (Orinda, CA)

EDITORS, SYMPOSIUM VOLUMES

E. HEFTMANN (Orinda, CA), Z. DEYL (Prague)

EDITORIAL BOARD

D.W. Armstrong (Rolla, MO), W.A. Aue (Halifax), P. Boček (Brno), A.A. Boulton (Saskatoon), P.W. Carr (Minneapolis, MN), N.H.C. Cooke (San Ramon, CA), V.A. Davankov (Moscow), G.J. de Jong (Weesp), Z. Deyl (Prague), S. Dilli (Kensington, N.S.W.), Z. El Rassi (Stillwater, OK), H. Engelhardt (Saarbrücken), F. Erni (Basle), M.B. Evans (Hatfield), J.L. Glajch (N. Billerica, MA), G.A. Guiochon (Knoxville, TN), P.R. Haddad (Hobart, Tasmania), I.M. Hais (Hradec Králové), W.S. Hancock (Palo Alto, CA), S. Hjertén (Uppsala), S. Honda (Higashi-Osaka), Cs. Horváth (New Haven, CT), J.F.K. Huber (Vienna), K.-P. Hupe (Waldbronn), J. Janák (Brno), P. Jandera (Pardubice), B.L. Karger (Boston, MA), J.J. Kirkland (Newport, DE), E. sz. Kováts (Lausanne), K. Macek (Prague), A.J.P. Martin (Cambridge), L.W. McLaughlin (Chestnut Hill, MA), E.D. Morgan (Keele), J.D. Pearson (Kalamazoo, MI), H. Poppe (Amsterdam), F.E. Regnier (West Lafayette, IN), P.G. Righetti (Milan), P. Schoenmakers (Amsterdam), R. Schwarzenbach (Dübendorf), R.E. Shoup (West Lafayette, IN), R.P. Singhal (Wichita, KS), A.M. Siouffi (Marseille), D.J. Strydom (Boston, MA), N. Tanaka (Kyoto), S. Terabe (Hyogo), K.K. Unger (Mainz), R. Verpoorte (Leiden), Gy. Vigh (College Station, TX), J.T. Watson (East Lansing, MI), B.D. Westerlund (Uppsala)

EDITORS, BIBLIOGRAPHY SECTION

Z. Deyl (Prague), J. Janák (Brno), V. Schwarz (Prague)



ELSEVIER

Amsterdam – Lausanne – New York – Oxford – Shannon – Tokyo

J. Chromatogr. A, Vol. 685 (1994)

© 1994 ELSEVIER SCIENCE B.V. All rights reserved.

0021-9673/94/\$07.00

No part of this publication may be reproduced, stored in a retrieval system or transmitted in any form or by any means, electronic, mechanical, photocopying, recording or otherwise, without the prior written permission of the publisher, Elsevier Science B.V., Copyright and Permissions Department, P.O. Box 521, 1000 AM Amsterdam, Netherlands.

Upon acceptance of an article by the journal, the author(s) will be asked to transfer copyright of the article to the publisher. The transfer will ensure the widest possible dissemination of information.

Special regulations for readers in the USA – This journal has been registered with the Copyright Clearance Center, Inc. Consent is given for copying of articles for personal or internal use, or for the personal use of specific clients. This consent is given on the condition that the copier pays through the Center the per-copy fee stated in the code on the first page of each article for copying beyond that permitted by Sections 107 or 108 of the US Copyright Law. The appropriate fee should be forwarded with a copy of the first page of the article to the Copyright Clearance Center, Inc., 222 Rosewood Drive, Danvers, MA 01923, USA. If no code appears in an article, the author has not given broad consent to copy and permission to copy must be obtained directly from the author. The fee indicated on the first page of an article in this issue will apply retroactively to all articles published in the journal, regardless of the year of publication. This consent does not extend to other kinds of copying, such as for general distribution, resale, advertising and promotion purposes, or for creating new collective works. Special written permission must be obtained from the publisher for such copying.

No responsibility is assumed by the Publisher for any injury and/or damage to persons or property as a matter of products liability, negligence or otherwise, or from any use or operation of any methods, products, instructions or ideas contained in the materials herein. Because of rapid advances in the medical sciences, the Publisher recommends that independent verification of diagnoses and drug dosages should be made.

Although all advertising material is expected to conform to ethical (medical) standards, inclusion in this publication does not constitute a guarantee or endorsement of the quality or value of such product or of the claims made of it by its manufacturer.

© The paper used in this publication meets the requirements of ANSI/NISO Z39.48-1992 (Permanence of Paper).

Printed in the Netherlands



ELSEVIER

Journal of Chromatography A, 685 (1994) 1–6

JOURNAL OF
CHROMATOGRAPHY A

Evaluation of a chiral stationary phase based on mixed immobilized proteins

Anne-Françoise Aubry^{a,*}, Nektaria Markoglou^a, Vincent Descorps^b,
Irving W. Wainer^a, Guy Félix^b

^aDepartment of Oncology, McGill University, 687 Pine Avenue W., Room M7.19, Montreal, P.Q. H3A 1A1, Canada

^bENSCB/CNRS URA 35, 351 Cours de la Libération, 33405 Talence, France

First received 21 June 1994; revised manuscript accepted 18 July 1994

Abstract

The preparation of a new chiral stationary phase (CSP) based on mixed immobilized human serum albumin (HSA) and α_1 -acid glycoprotein (AGP) is reported. Enantiomeric separations of basic, acidic and neutral compounds on this AGP–HSA CSP were compared to those obtained on a HSA CSP and on a AGP CSP. The results show that the new CSP has a wider range of applications than the initial CSPs. For two compounds, the enantioselectivity on the mixed CSP was higher than on the HSA CSP.

1. Introduction

In the past few years there has been a rapid development of high-performance liquid chromatographic (HPLC) chiral stationary phases (CSPs) for the analytical and preparative separation of enantiomeric compounds [1]. At present there are over a hundred commercially available CSPs based on a variety of mechanistic approaches. One of the most successful approaches has employed protein stationary phases (PSPs) created by the immobilization of various proteins on silica supports. PSPs based upon α_1 -acid glycoprotein (AGP) [2,3], ovomucoid [4], cellulase [5], bovine serum albumin [2] and human serum albumin (HSA) [6–9] have been reported. Proteins can interact with small mole-

cules in a variety of ways. These multiple recognition mechanisms allow protein phases to separate a large number of solutes with very different structural characteristics [1,9].

Here, we report the preparation of a mixed CSP based on immobilized proteins. The term “mixed” stationary phase refers to phases prepared by a combination of two existing phases and which retain characteristics of both phases. The most notable example in chiral HPLC is the production of π -donor/ π -acceptor Pirkle-type CSPs. Several of these mixed phases were synthesized by grafting a π -donor and a π -acceptor chiral moiety on the same silica [10], by mixing a π -donor and a π -acceptor bonded silica [10] or by bonding to the silica one moiety which contains both a π -donor and a π -acceptor group [11–13]. The objective was to prepare a new CSP with an extended range of application in

* Corresponding author.

comparison with CSPs containing only one group [10–13].

Considering the already wide scope of protein based CSPs, a mixed protein CSP is expected to have an extremely broad applicability. The choice of HSA and AGP as the immobilized proteins was justified by the fact that their applications were quite complementary: HSA is most useful for acidic compounds while AGP is more favourable for cationic compounds [2]. Both are plasmatic proteins and the major carrier proteins for drug compounds.

A column was packed with a 50:50 mixture of HSA CSP and AGP CSP. We report the preliminary chromatographic results on this column and compare them to those obtained on columns packed with pure HSA CSP or pure AGP CSP.

2. Experimental

2.1. Chemicals

The compounds and proteins used in this study were obtained from the following suppliers: HSA (fatty acid free fraction V) and human AGP, (*R,S*)-temazepam, (*R,S*)-oxazepam, (*R,S*)-oxprenolol, (*R,S*)-propranolol, (*R,S*)-sufrofen, (*R,S*)-ketoprofen, (*R,S*)-disopyramide, were from Sigma (St. Louis, MO, USA); (*R,S*)-promethazine, (*R,S*)-hexobarbital, (*R,S*)-pentobarbital, (*R,S*)-benzoin, *S*-benzoin and octanoic acid were obtained from Aldrich (Milwaukee, WI, USA); (*R,S*)-warfarin, *R*-warfarin and *S*-warfarin were gifts of DuPont–Merck (Wilmington, DE, USA); (*R,S*)-ketorolac, *R*-ketorolac and *S*-ketorolac were gifts from Syntex (Palo Alto, CA, USA); (*R,S*)-verapamil was a gift from GD Searle (Skokie, IL, USA). (*Rac*)-Mefloquine was a gift from Hoffman–La Roche (Basel, Switzerland); (*Rac*)-enproline was a gift from the Walter Reed Army Institute of Research (Washington, DC, USA).

The silica Kromasil 200 Å, 10 µm was a gift from Eka-Nobel (Sweden), (3-glycidoxypropyl)trimethoxysilane was obtained from Aldrich. Other chemicals were of analytical grade and were obtained from local suppliers.

2.2. Synthesis of the stationary phases

The silica gel was heated for 15 h at 180°C and 1 mmHg (1 mmHg = 133.322 Pa). To 5.17 g of silica in 100 ml of dry xylene 2 g of distilled (3-glycidoxypropyl)trimethoxysilane in 5 ml of dry xylene were added dropwise and the mixture was refluxed for 36 h. After filtration on a fritted disc of porosity 4, the product was washed twice with dry xylene and dry acetone. The bonded silica was dried for 18 h at 40°C under vacuum. The activated silica was then packed into 150 × 4.6 mm I.D. HPLC columns. The column was washed with 100 ml of acetone and dried at 70°C under helium. A solution of protein (10 mg/ml) in potassium phosphate buffer (0.05 *M*, pH 7.5) containing 2 *M* of ammonium sulphate was circulated through the column, in closed circuit for 24 h. The column was washed with 100 ml of potassium phosphate buffer (0.05 *M*, pH 7.5). The amount of protein immobilized was determined by UV absorbance at 280 nm of the protein solution before and after the immobilization procedure. Two HSA and two AGP CSP columns were prepared. One of each was used directly, the other was emptied. The HSA and AGP CSPs were mixed in equal proportion and repacked in an analytical column to produce the AGP–HSA CSP.

The amount of protein immobilized on each of the analytical columns was as follow: HSA CSP: 85 mg HSA per g silica; AGP CSP: 105 mg AGP per g of silica; AGP–HSA column: HSA CSP 80 mg HSA per g of silica and AGP CSP 100 mg per g of silica.

2.3. Chromatography

Three chromatographic systems were used in this study. They consisted of a SpectraSystem P1000 isocratic pump, a Spectra 100 variable-wavelength UV detector and a Data Jet integrator, all from Thermo Separation Products (San Jose, CA, USA). All columns were 150 × 4.6 mm I.D. The injection volume was 20 µl and the flow-rate was maintained at 0.8 ml/min. The separations were carried out at room temperature. Mobile phases composition: (1) phosphate buffer (pH 7, 0.02 *M*); (2) phosphate buffer (pH

7, 0.02 M)–acetonitrile (90:10, v/v); (3) phosphate buffer (pH 5, 0.02 M)–acetonitrile (85:15, v/v); (4) phosphate buffer (pH 7, 0.02 M)–*n*-propanol (94:6, v/v); (5) phosphate buffer (pH 5.5, 0.02 M)–*n*-propanol (94:6, v/v) containing 2 mM octanoic acid.

3. Results and discussion

The immobilization procedure was different to those used to prepare commercial HSA- or AGP-based stationary phases. In particular, the proteins did not undergo any further modifications after immobilization and it is expected that their binding characteristics should be closer to the native proteins.

In theory, if there is no special effect due to the proximity of the two proteins, the capacity factor on the AGP–HSA CSP can be expressed by:

$$k'_{\text{AGP-HSA}} = (0.95k'_{\text{AGP}} + 0.94k'_{\text{HSA}})/2 \quad (1)$$

The factors 0.95 and 0.94 were introduced in this expression to take into account the lower amount of protein immobilized on the AGP–HSA column (80 mg/g silica vs. 85 for HSA and 100 mg/g vs. 105 for AGP). The same factors should be used in the calculation of the enantioselectivity but in this case their effect is negligible. Therefore, the enantioselectivity can be expressed by:

$$\alpha = \frac{k'_{\text{B,AGP}} + k'_{\text{B,HSA}}}{k'_{\text{A,AGP}} + k'_{\text{A,HSA}}}$$

where A and B are the first and the second eluted enantiomers on the AGP–HSA CSP, respectively. These expressions indicate that α and k' on the mixed phase are expected to take intermediate values between those obtained on the HSA and AGP CSPs. The maximum α is obtained when a compound is only retained on one of the initial CSPs. In that case α is equal to the α obtained on the CSP on which the compound separated.

3.1. Chromatographic results

The separation of a series of chiral compounds including anionic, cationic and neutral compounds was studied on the HSA, the AGP and the AGP–HSA CSPs under various conditions. The separations were not systematically optimized but the retention and enantioselectivity of test compounds were compared on the three columns under the same conditions. The three columns were used on three separate chromatographic systems so that all the results were collected simultaneously. The mobile phases were used in the same order on each system. The capacity factor of the first eluted enantiomer and the enantioselectivity on all three CSPs for 16 compounds are summarized in Table 1. This table also includes the values calculated from the expressions above for $k'_{\text{AGP-HSA}}$ and $\alpha_{\text{AGP-HSA}}$.

As the eluting conditions on the AGP and HSA CSPs for a given compound can be quite different, a large number of solutes tested could not be separated on both AGP and HSA in the same conditions even though the enantiomeric separation was possible on both columns. The separations reported here were carried out in conditions where the solute was eluted from all three columns.

Compounds which could not be separated on the HSA CSP in the conditions necessary for their elution from the AGP CSP, included verapamil, promethazine, propranolol, oxprenolol, disopyramide, enpiroline and mefloquine. For all of them, the observed k' and α were within 20% of the calculated values which suggest that the AGP–HSA CSP is performing as the sum of the two initial phases. As expected, oxprenolol which had a very low retention on HSA ($k' = 1.6$), was separated on the AGP–HSA CSP with an α value of 1.17, equal to the α observed on the AGP CSP. Examples of chromatograms are given on Fig. 1 for disopyramide.

Acidic compounds such as non steroidal anti-inflammatory drugs and warfarin had extremely low retentions on the AGP CSP in the conditions used to elute them on the HSA CSP. The chromatographic parameters obtained for warfarin were in relatively good accordance with calculated values. However, for ketoprofen, sup-

Table 1

Capacity factor of the first eluted enantiomer (k'_1) and enantioselectivity (α) on the AGP, HSA and mixed AGP-HSA CSPs and calculated k'_1 and α for the mixed stationary phase

Compound	MP	AGP		HSA		AGP-HSA observed		AGP-HSA calculated	
		k'_1	α	k'_1	α	k'_1	α	k'_1	α
<i>Compounds separated on AGP-HSA CSP</i>									
Hexobarbital	1	5.5	1.44	3.8	1.34	2.8	1.00	4.4	1.10
Pentobarbital	1	7.7	1.33	5.2	1.08	3.8	1.1	6.1	1.16
Benzoin	1	14.8	1.06	13.9	1.21	12.5	1.12	13.5	1.13
Temazepam	2	6.7	1.77	2.8	6.05	5.6	1.23	6.9	1.62
Oxazepam	2	5.5	2.15	3.5	3.35	3.6	2.40	4.2	2.60
<i>Compounds separated on AGP CSP</i>									
Verapamil	2	12.8	1.33	6.04	1.00	7.3	1.23	8.9	1.22
Promethazine	2	6.8	1.35	5.33	1.00	5.8	1.14	5.7	1.20
Propranolol	2	40.3	1.30	4.9	1.00	19.8	1.2	21.4	1.26
<i>Oxprenolol</i>	2	24.3	1.17	1.6	1.00	11.1	1.17	12.3	1.16
<i>Disopyramide</i>	2	10.0	1.23	1.81	1.00	4.63	1.10	5.6	1.19
Enpiroline	3	15.6	2.09	2.5	1.00	12.2	1.65	9.1	1.94
Mefloquine	3	6.0	1.30	3.1	1.00	4.0	1.20	4.3	1.20
<i>Compounds separated on HSA CSP</i>									
<i>Ketorolac</i>	2	0.15	1.00	24.8	2.65	6.5	4.4	12.5	2.64
Warfarin	2	2.5	1.00	28.0	1.64	12.2	1.45	15.2	1.59
Suprofen	5	3.3	1.00	9.1	1.19	6.2	1.33	10.5	1.16
Ketoprofen	4	3.6	1.00	18.1	1.64	6.7	1.10	10.2	1.11

Italics indicate solutes which are retained by one CSP only (k' on the other CSP is less than 2). Mobile phase (MP) numbers are given in the Experimental section.

rofen and ketorolac, the observed capacity factors were 40% lower on average than their expected value. Moreover, for ketorolac and suprofen, α values greater than the expected values were obtained on the mixed stationary phase.

Some test solutes could be separated on both the AGP and the HSA CSPs under the same experimental conditions. They included hexobarbital, pentobarbital, benzoin, temazepam and oxazepam. For all these compounds, the final separation factor on the mixed phase depended on the elution order on the initial phases. For oxazepam, the elution order was the same on AGP and HSA CSPs and the α value was 2.40, intermediate between the α values on both initial phases. For all the four other compounds, the elution order was different on AGP and HSA and the resulting α was lower on the

mixed phase than on either original phases. As shown in Fig. 2, hexobarbital separated on both the AGP and the HSA CSPs with α values of 1.44 and 1.34, respectively. When chromatographed on the mixed phase there was a complete loss of enantioselectivity. The separations induced by both CSP compensate each other so that the enantioselectivity is lost. Among the five solutes in this category, two (hexobarbital and pentobarbital) had significantly lower retention on the mixed CSP than expected. These two compounds were acidic compounds but as opposed to ketoprofen, suprofen and ketorolac were not ionized in the conditions of the assay.

The reason for this unexpected chromatographic behavior of acidic compounds is not clear. It does not seem to be due to a partial loss or inactivation of the HSA since the few cationic compounds which had a quite high retention on

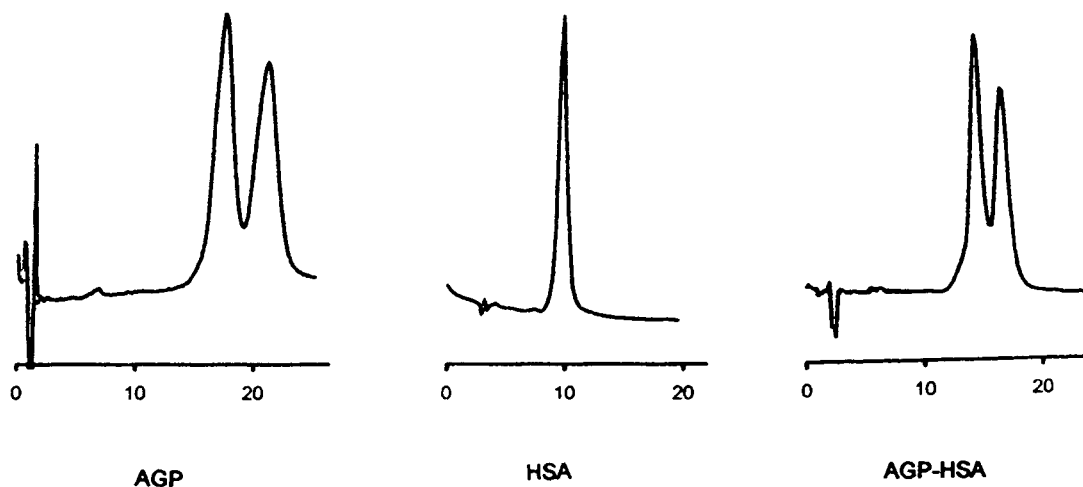


Fig. 1. Enantiomeric separation of disopyramide on (A) AGP, (B) HSA and (C) AGP-HSA CSPs. Column dimensions: 150×4.6 mm I.D., mobile phase: phosphate buffer (pH 7, 0.02 M)-acetonitrile (90:10, v/v), flow-rate: 0.8 ml/min, detection UV absorbance at 254 nm, injection volume: 20 μ l.

the HSA CSP were not affected to the same extent. Column-to-column variability is possible but would certainly affect all the compounds, not just the acidic solutes. Another possibility is that the presence of the AGP creates an obstacle to the interaction of acidic drugs with the HSA. It is unlikely that the proteins could physically interact with each other since they were immobilized on different particles of silica. When

the AGP and the HSA columns were coupled on-line with no possible interaction between the proteins, the results for ketorolac were within 2% of the expected values of k' and α .

3.2. Stability of the stationary phases

Pentobarbital and benzoin were chromatographed with mobile phase 1 at the beginning of

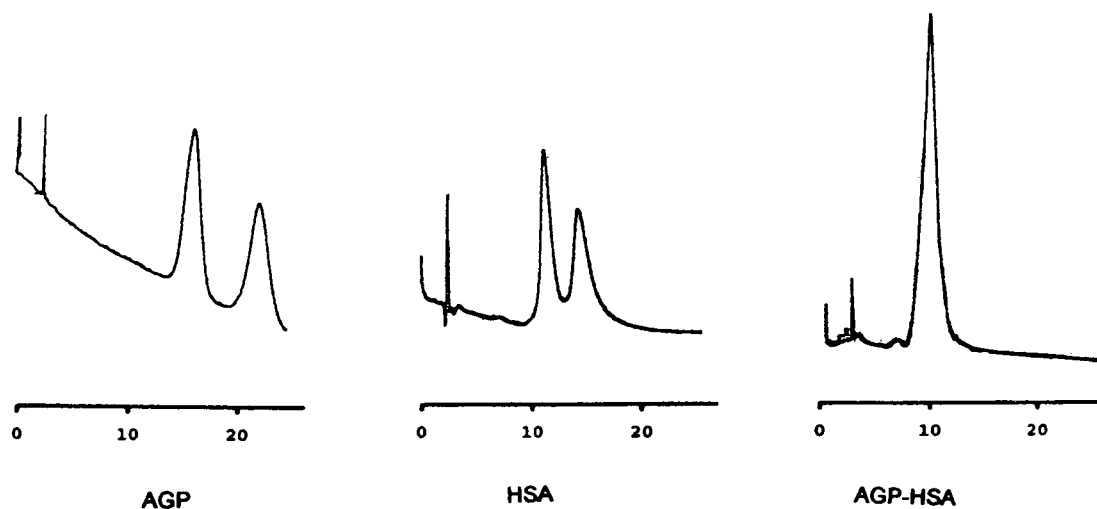


Fig. 2. Enantiomeric separation of hexobarbital on (A) AGP, (B) HSA and (C) AGP-HSA CSPs. Mobile phase: phosphate buffer (pH 7, 0.02 M), other conditions as in Fig. 1.

the column life and after seven different mobile phases were passed through the column including solutions containing ionized modifiers such as octanoic acid and dimethyloctylamine and about 200 injections were made. No apparent column degradation (peak broadening or peak splitting) was observed. A decrease in enantioselectivity was observed for benzoin on the HSA CSP (α decreased from 1.12 to 1.07) and on the AGP–HSA CSP (1.21 to 1.16) but an increase in α from 1.06 to 1.18 was observed on the AGP CSP. Capacity factors were almost unchanged. For pentobarbital, very little change in k' and α was observed on the AGP–HSA and HSA CSPs but a large decrease in k' from 7.7 to 3.9 for the first eluted enantiomer and from 10.3 to 5.5 for the second eluted one on the AGP CSP. The observed changes in retention and enantioselectivity could be due to insufficient conditioning of the stationary phases prior to the first use. Another explanation can be a modification of the protein structure due to insufficient washing of the mobile phase modifiers.

4. Conclusions

The new AGP–HSA CSP has an even wider range of applications than either initial CSP; only one out of 16 compounds tested could not be separated on the mixed protein column. The mixed protein phase combines the useful enantioselectivity of both individual proteins except for the small number of samples for which both proteins show enantioselectivity but with enantioselectivity in opposing senses. When both proteins were involved in the retention, not only

chiral but also non-chiral interactions were increased; the resulting enantioselectivity was generally intermediate between the values obtained on the two initial CSPs. The best α values were obtained in conditions where only one of the original CSPs participated in the retention and separation.

References

- [1] I.W. Wainer, in W.J. Lough (Editor), *Chiral Liquid Chromatography*, Chapman & Hall, New York, 1989, pp. 129–147.
- [2] S. Allenmark, in A.M. Krstulovic (Editor), *Chiral Separations by HPLC — Applications to Pharmaceutical Compounds*, Ellis Horwood, Chichester, 1989, pp. 287–315.
- [3] J. Hermansson, *Trends Anal. Chem.*, 8 (1989) 251–259.
- [4] T. Miwa, M. Ichikawa, M. Tsuno, T. Hattori, T. Miyakawa, M. Kayano, Y. Miyake, *Chem. Pharm. Bull.*, 35 (1987) 682–686.
- [5] P. Erlandsson, I. Marle, L. Hansson, R. Isaksson, C. Pettersson and G. Petersson, *J. Am. Chem. Soc.*, 112 (1990) 4573.
- [6] E. Domenici, C. Bertucci, P. Salvadori, G. Felix, I. Cahagne, S. Motellier and I.W. Wainer, *Chromatographia*, 29 (1990) 170–176.
- [7] E. Domenici, C. Bertucci, P. Salvadori and I.W. Wainer, *Chirality*, 2 (1990) 263–268.
- [8] E. Domenici, C. Bertucci, P. Salvadori and I.W. Wainer, *J. Pharm. Sci.*, 80 (1991) 164–166.
- [9] T.A.G. Noctor, G. Felix and I.W. Wainer, *Chromatographia*, 31 (1991) 55–59.
- [10] O. Oliveros, C. Minguillon, B. Desmaziere and P.-L. Desbene, *J. Chromatogr.*, 543 (1991) 277–286.
- [11] M.H. Hyun and W.H. Pirkle, *J. Chromatogr.*, 393 (1987) 357.
- [12] A. Tambute, L. Siret, M. Caude, A. Begos and R. Rosset, *Chirality*, 2 (1990) 106–119.
- [13] W.H. Pirkle and C.J. Welch, *J. Liq. Chromatogr.*, 15 (1992) 1947.

Interpretation of enantioselective activity of albumin used as the chiral selector in liquid chromatography and electrophoresis

Zdeněk Šimek^{a,*}, Radim Vespaľec^b

^a*Faculty of Chemistry, Technical University of Brno, Veslařská 230, 637 00 Brno, Czech Republic*

^b*Institute of Analytical Chemistry, Czech Academy of Sciences, Veveří Street 97, 611 42 Brno, Czech Republic*

First received 5 April 1994; revised manuscript received 29 June 1994

Abstract

The possibility of constructing a hypothesis on albumin enantioselectivity allowing consistent interpretation of retention and selectivity data for D,L-monocarboxylic acids, D,L-dicarboxylic acids and D,L-amino acids, measured by liquid chromatography and capillary zone electrophoresis, is demonstrated. An explanation of effects caused by high temperature, mildly alkaline aqueous solutions and methanol, consistent with the explanation of the retention and selectivity data, is also possible. The hypothesis considers the conformational variability of albumin.

1. Introduction

Recently, we published a study of albumin as a chiral selector for liquid chromatographic [1–3] and electrophoretic [4] chiral separations. Aqueous buffers served as the albumin wetting medium in both separation techniques. The chromatographic sorbent was prepared by chemical bonding on albumin on a hydroxyethylmethacrylate (HEMA) polymeric matrix possessing a high hydrolytic stability [5,6]. This allowed us to widen the range in which the influence of pH on the separation selectivity was investigated from the acidic and neutral regions, applicable with silica gel-based sorbents [7], to the whole pH range of the albumin titration

curve. Racemates of monocarboxylic acids, dicarboxylic acids and amino acids served as solutes in the study.

Fast and slow changes in albumin enantioselectivity, influenced by the pH value, were observed. The well known fast, virtually immediate and reversible changes, effective over the whole pH range of the albumin titration curve, are commonly utilized as the most effective tool in the control of both solute retentions and its separation selectivity [7,8]. The shape of the pH dependence of retention data was the same for compounds of a similar structure, e.g., for amino acids. However, characteristic differences in the shape of the dependence were found for monocarboxylic acids, dicarboxylic acids and amino acids. The same is valid for the influence of pH on the separation selectivity changes [3].

Slow changes in the albumin enantioselectivity and in its capability to bind solutes of various

* Corresponding author.

types occur in weakly alkaline mobile phases in the pH range 7–10. The changes, irreversible in aqueous medium and qualitatively identical for solutes of a particular type, e.g., amino acids, may be qualitatively different for solutes of different structural types, e.g., amino acids and dicarboxylic acids. Treatment with methanol and subsequent washing with an aqueous buffer of the appropriate pH restores the albumin enantioselectivity altered by the slow process [3]. Qualitatively, the same irreversible changes in both retention and separation selectivity are observed for tryptophan as a solute with the sorbent heated to 90°C in a buffer of pH 5 and then washed with methanol and mobile phase [2].

None of the published models, ideas or hypotheses on the enantioselectivity of albumin, based on liquid chromatographic experiments, allows a satisfactory interpretation of our results. The hypothesis described below, allowing such an interpretation, stems from our experiments with bovine serum albumin (BSA) chemically bonded to the porous matrix HEMA [1–3] and from the successful transfer of these results to capillary zone electrophoresis [4], from common constituents of hitherto published chromatography-based ideas and hypotheses on albumin enantioselectivity and from a knowledge of albumin research.

2. Hypothesis

Albumin enantioselectivity is conceived as the general capability of albumin to discriminate differences in the steric arrangements of the members of enantiomeric pairs. The chromatographic properties of a sorbent with chemically bonded albumin are conferred by both the matrix and albumin. The capability of an albumin macromolecule, chemically bonded to a solid matrix at a few points only, to interact with solutes and discriminate the members of enantiomeric pairs may be approximated by those of dissolved albumin.

The requirement for three interaction points, necessary for chiral discrimination [9], does not necessitate three qualitatively different interactions. Cooperating interactions may be either attractive or repulsive; a preponderance of attractive interactions results in the solute retention. A change or a difference in the sum of the mutual solute–albumin interactions is reflected in a corresponding retention change or in a retention difference, respectively. The influence of a solute–albumin interaction on the retention of the solute depends on the intensity of the interaction. As a result, coulombic interactions are the most important.

Coulombic interactions come into effect by means of electrostatic fields formed by electrical charges. An electrostatic field interacting with a charge may be created by one charge, and also by a set of charges of identical or opposite polarities. As a result, a space point in which the resulting field, created by contributions from two or more albumin charges, interacts most strongly with the field of a solute charge acts as the coulombic interaction point of albumin, dependent on albumin conformation. A coulombic interaction point independent of albumin conformation is created by one charged albumin group only. Albumin charges forming inner ionic pairs (interacting charges) [10] do not participate in albumin–solute interactions.

The ionization state of a solute follows from its distribution diagram. The ionization state of albumin is described by the albumin titration curve (Fig. 1) [11]. The change in the albumin ionization state is connected with changes in albumin conformation in general; the former may also be attended by a change in the number of functional groups capable of forming hydrogen bonds.

The types, number and accessibility of binding sites capable of interacting with a given solute depend on the albumin conformation. The mobile phase composition, pH, temperature and other experimental variables affect the solute retention and the separation selectivity via changes in albumin charge, in albumin conformation and in solute ionization state.

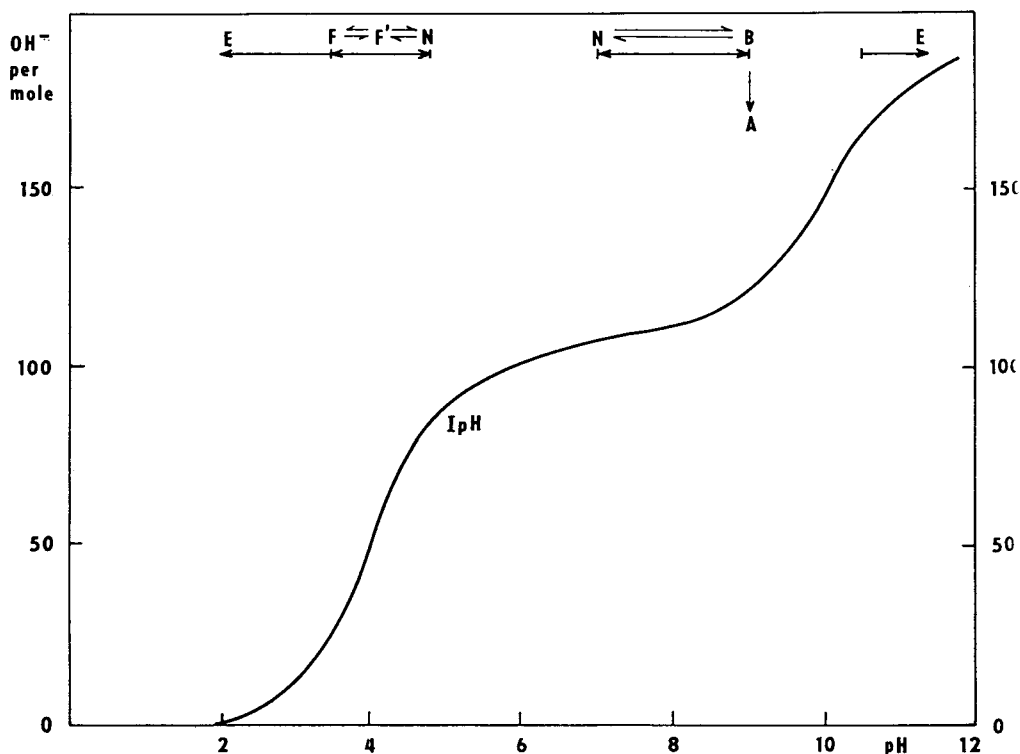


Fig. 1. Titration curve of human serum albumin according to Peters [11], with a diagram of albumin conformations according to Foster [10].

3. Interpretation of pH dependences

3.1. Monocarboxylic acids

Different retentions of D- and L-enantiomers at any $\text{pH} < 11$ and a monotonic decrease in their retention with increasing pH are characteristic of monocarboxylic acids (Fig. 2). The steep pH dependence of the retention of monocarboxylic acids may be understood as an indication that a strong and pronouncedly pH-dependent interaction is involved in their interaction with albumin. The marked influence of 1-propanol on the retention of both enantiomers [3] reveals the contribution of hydrophobic interaction to retention. Supposing that D,L-indolelactic acid is bound at the binding site of indolyl compounds [12], the hydrophobic interaction of

the indolyl group and the coulombic interaction of the ionized carboxylic group with albumin should also be the participating interactions in the retention of this acid. One can assume that the third interaction is due to the hydrogen bond formed by the hydroxyl group attached to the asymmetric carbon atom and that it is responsible for chiral discrimination.

The decrease in retention with increasing pH may be explained easily as the consequence of a decline in the total positive albumin charge. Weakening of the coulombic interaction and alkaline unfolding of albumin with pH increase enhance the relative contribution of non-coulombic interactions; this results in a small transient increase in separation selectivity. The decrease in enantioselectivity at $\text{pH} > 9$ results from the strengthening of the repulsion of the solute anion

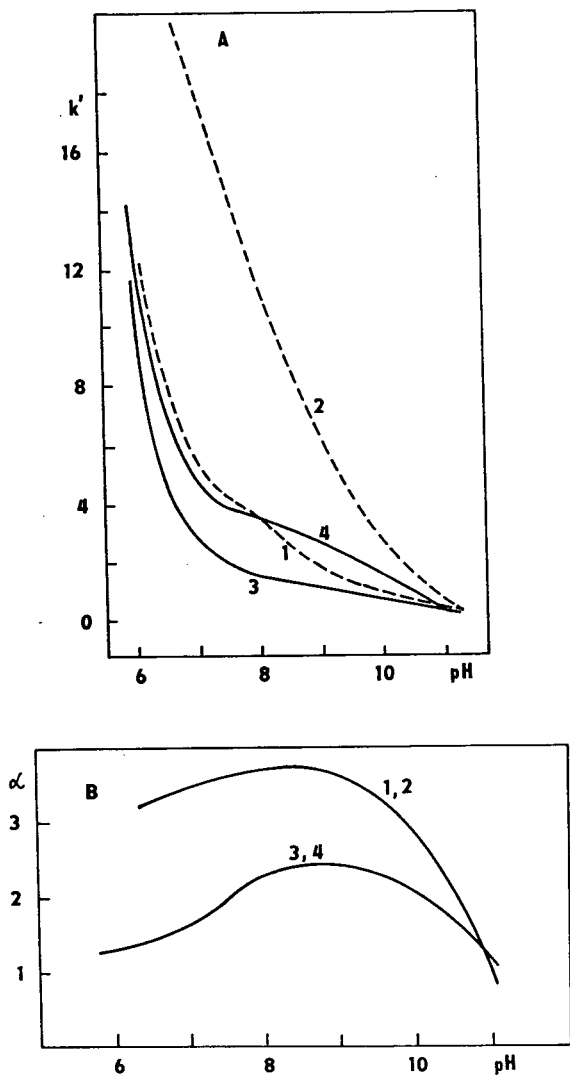


Fig. 2. pH dependences of (A) retention and (B) separation selectivity of D,L-indolelactic acid (1,2) and of N-benzoyl-D,L-phenylalanine (3,4) on the HEMA-BSA sorbent [3].

by the growing negative charge of albumin. At pH 11, the attractive interactions are totally eliminated by anionic repulsion.

The pH dependences of the retentions of N-benzoyl-D,L-phenylalanine may be explained analogously, assuming that the difference in the interaction of the substituted amine group in the D- or L-enantiomer with albumin is critical for chiral discrimination. The group may interact

with albumin hydrophobically (benzene ring) or by the hydrogen bond (carbonyl or secondary amine group).

3.2. Dicarboxylic acids

The retention and selectivity dependences of all three dicarboxylic acids studied on pH [3] have the form illustrated in the Fig. 3. The

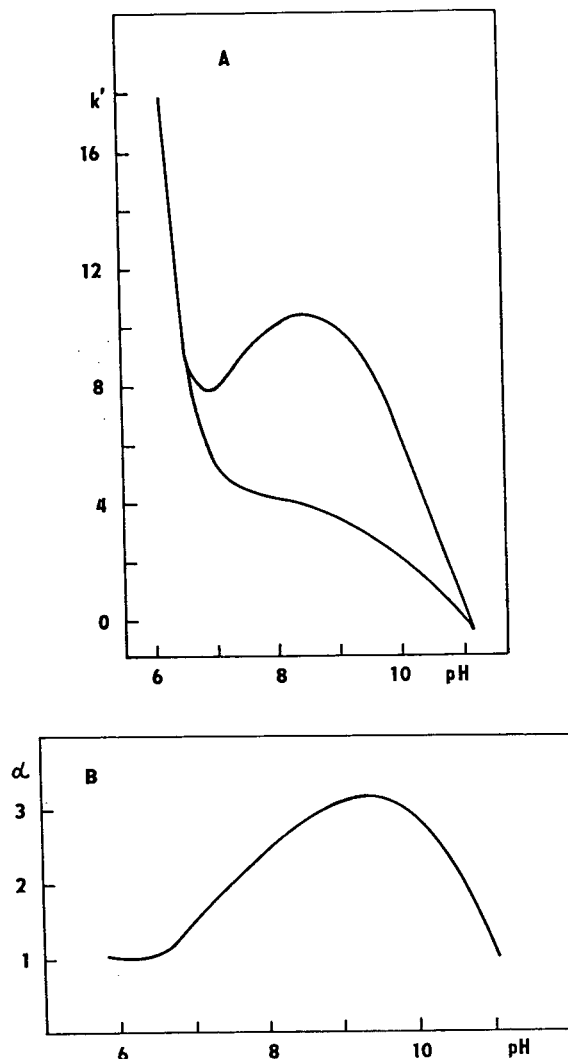


Fig. 3. pH dependences of (A) retention and (B) separation selectivity of N-2,4-dinitrophenyl-D,L-glutamic acid as the representative of dicarboxylic acids, separated on the HEMA-BSA sorbent [3].

necessity to utilize a mobile phase containing an alcohol, the strong decrease in retention with increasing pH and the unmeasurable difference in the retentions of the D- and L-enantiomers at $\text{pH} < 7$ indicate that chiral discrimination is probably caused by a relatively weak non-ionic interaction. The nature of the interaction is determined by one of the two non-ionized functional groups bonded to the asymmetric carbon atom.

Strong attractive interactions of negatively charged groups of the solute with positive albumin domains [10] prevail in the vicinity of the albumin isoelectric point. The anionic interaction points become weaker with increase in pH. As a result, the retentions of both enantiomers of a dicarboxylic solute decrease. Near pH 7, the contribution of the non-ionic interaction, causing the differentiation of the retentions of D- and L-enantiomers, becomes effective. Basic unfolding of the albumin macromolecule [10] enhances the differentiating non-coulombic interaction more strongly. As a result, the decrease in

retentions is interrupted and the separation selectivity increases transiently. The increases in both the retention and selectivity are stopped by continuing deprotonation of the basic albumin functional groups near pH 9. At higher pH, the positive albumin charge vanishes totally; anionic repulsion outweighs the non-ionic attractive interaction at first and then even precludes the diffusion of solutes to negatively charged pores of the sorbent. As a result, the electrostatically excluded solutes are eluted from the column in a retention volume lower than that of uncharged non-retained solutes near pH 11.

3.3. Amino acids

In contrast to mono- and dicarboxylic acids, the pH dependence of the retention data of amino acids is characterized by low retentions in the acidic region, independent of both pH and the steric configuration of the considered amino acid (Fig. 4); for D-amino acids, less retained at $\text{pH} > 6$, this independence reaches the alkaline

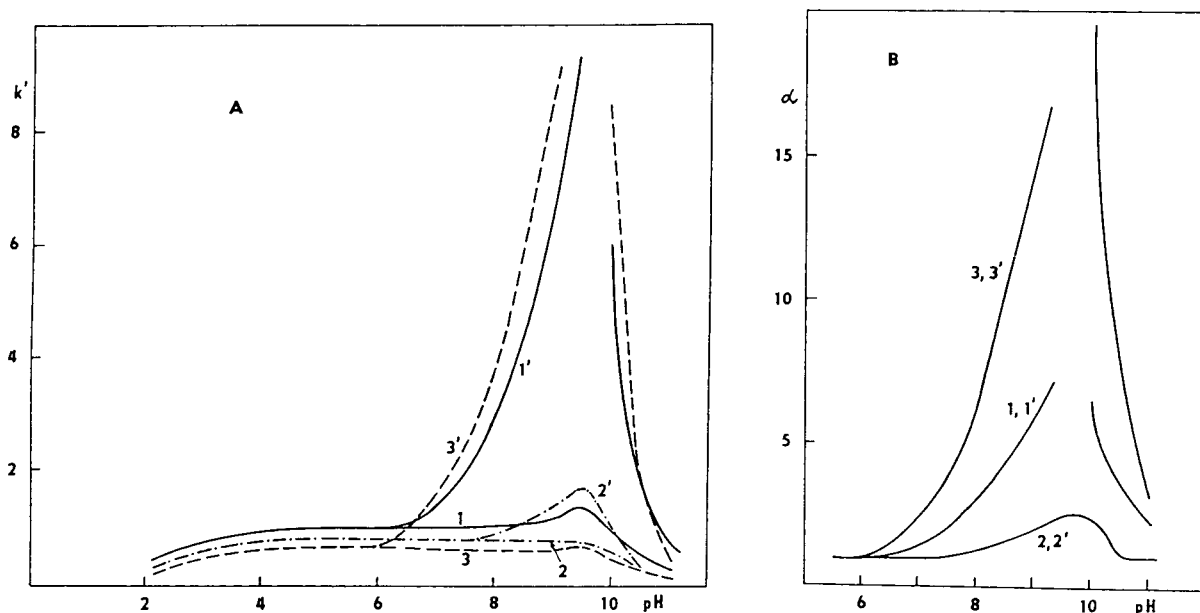


Fig. 4. pH dependences of (A) retentions and (B) separation selectivity of D,L-tryptophan, 5-hydroxy-D,L-tryptophan and D,L-kynurenine on the HEMA-BSA sorbent [3]. (A) 1 = D-tryptophan; 1' = L-tryptophan; 2 = 5-hydroxy-D-tryptophan; 2' = 5-hydroxy-L-tryptophan; 3 = D-kynurenine; 3' = L-kynurenine. (B) 1, 1' = D,L-tryptophan; 2, 2' = 5-hydroxy-D,L-tryptophan; 3, 3' = D,L-kynurenine.

region. The magnitude of retentions in this pH range is comparable to those on HEMA matrix without bonded albumin [3], free of charged groups. As a result, a strong coulombic interaction of the carboxylic group of amino acids with albumin is either absent or compensated for by a coulombic repulsion interaction in the pH region of constant retentions of amino acids.

Let us suppose that the change for the enantioselectively non-specific bonding of amino acids by albumin to enantioselectively specific bonding is not attended by migration of solutes. Then, an attractive non-coulombic interaction between amino acids and albumin must be active at least in one of the interaction points of the binding site.

A binding site allowing for contributions from coulombic interactions of both charged groups of an amino acid in the acid pH range does not make it possible to explain experimentally established data. The idea of the formation of coulombic interaction points, starting from approximately pH 6, allows a formal interpretation of dependences in Fig. 4 if the binding site given in Fig. 5A is considered. However, the formation of positively charged interaction points above the albumin isoelectric point is not probable, taking into consideration the structure of the tryptophan binding site [12].

A simple explanation of the dependences in Fig. 4 is possible by presuming the absence of coulombic interaction of the carboxylic group of amino acids with albumin and considering the formation of a hydrogen bond between the carboxylic group and albumin (Fig. 5B). Applying such an approach to D,L-tryptophan, it is advantageous to assume that the albumin interaction point, forming the hydrogen bond, is identical with the hydroxyl group of Tyr 30 having $pK_a = 10.07$ [10].

Starting from the structure of the binding site given in Fig. 5B, a pH-independent retention of amino acids may result from non-ionic interactions of the carboxylic anion and the aryl group with albumin. The increase in the retention of the D-enantiomer may be explained as the consequence of alkaline unfolding of albumin. The formation of a negatively charged interaction

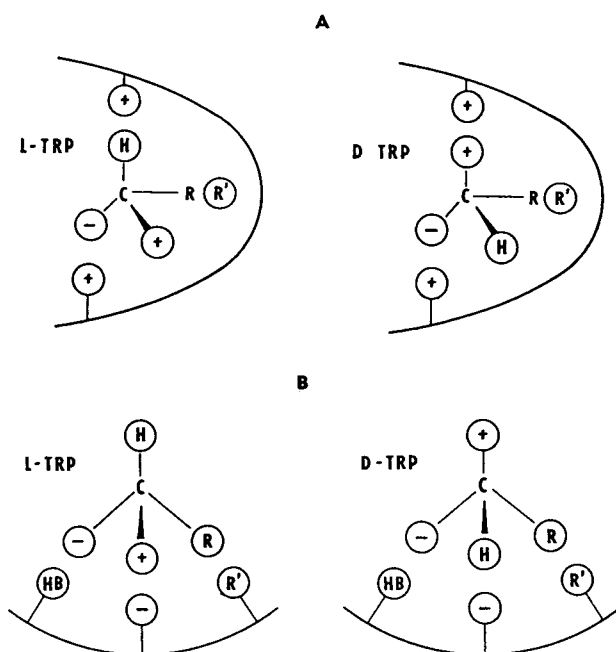


Fig. 5. Structure of hypothetical binding sites for interpretation of dependences from Fig. 4. (A) binding site with coulombic interaction of the ionized carboxylic group; (B) binding site with the hydrogen bond formed by the ionized carboxylic group.

point of albumin, causing a steeper increase in the L-enantiomer interaction, may result from splitting off of the inner ionic pairs with increasing pH due to either deprotonation of the histidine amino group ($pK_a = 6.5$) or from alkaline unfolding of albumin at $pH > 7$. The stopping of the retention increase in the proximity of pH 10 and the subsequent retention decrease may result from three processes: dissociation of the protonated amine group of the amino acid, disappearance of the hydrogen bond caused by dissociation of an albumin hydroxylic group and repulsion of the amino acid anion by the growing excess of the negative albumin charge.

4. Other results

The versatility of the hypothesis allowing a consistent interpretation of the pH dependences of retention and selectivity determined for three

types of compounds in the range of 10 pH units is mainly due to the incorporation of the conformational variability. The link between albumin conformation and its ability to bind enantioselectively solutes of various types enables one to understand alterations in albumin enantioselectivity as a result of changed pH, temperature and methanol treatment [2–4].

The slow decrease in D- and L-tryptophan retentions and in the separation selectivity of D,L-tryptophan, evoked by mobile phases of pH 7–10 [3], and the loss of enantioselectivity of dissolved albumin for amino acids in the same pH region, observed in capillary zone electrophoresis [4], suggest that the binding sites capable of discriminating D- and L-amino acids are linked with an albumin conformation that is unstable in that pH region. The same holds for binding sites capable of discriminating monocarboxylic acid enantiomers [4]. It follows from the albumin conformation equilibria in Fig. 1 that the B conformation is relevant. The increase in separation selectivity of dicarboxylic acids may then be ascribed to the link with the increase in the content of the A form, arising spontaneously in that pH range. The A form is identified as a covalently stabilized conformation with equivalent carboxylic groups, incapable of interacting with albumin positive charges [10]. Evidently, an analogous situation must hold for positive charges of albumin.

Organic solvents are stronger solvation agents for albumin than water [11]. The restitution of albumin enantioselectivity for amino acids and monocarboxylic acids (damaged by prolonged action of pH > 7) by methanol can be interpreted as follows. Methanol, being a sufficiently strong solvation agent, breaks the bonds causing stability of the A form in aqueous medium. During subsequent flushing of the column with aqueous buffer, methanol is replaced by water, present in great excess. The rehydrated chain of the albumin macromolecule is liable to conformational changes determined by the buffer pH.

The N–B–A transition of albumin in mildly alkaline medium is catalysed by sulfhydryl residues of the mercaptalbumin, created to a greater extent at elevated temperature [10]. There-

fore, the short (10 min) mild (up to 60°C) heating of the electrophoretic background electrolyte, containing dissolved albumin [4], speeds up the disappearance of the electrolyte enantioselectivity for amino acids and monocarboxylic acids and also the stabilization of the electrolyte enantioselectivity for dicarboxylic acids. The markedly higher rate of the process in the free solution may be ascribed to the absence of kinetic deceleration of the process, effective in the matrix pores.

The loss of ability of chemically bonded albumin to separate D,L-tryptophan, observed after heating the chromatographic column at 96°C in a stream of mobile phase of pH 5.6, and restoration of the column enantioselectivity by methanol treatment [2] may be a consequence of above-mentioned processes or processes analogous to them.

Although the hypothesis presented on the enantioselectivity of albumin makes it possible to treat all our experimental observations consistently [1–4], it can be hardly considered as anything more than a contribution to the likely explanation of the enantioselectivity of albumin acting as a chiral selector. It needs further thorough verification. However, knowledge gained from additional separation experiments only cannot lead to a pronounced improvement in the ideas presented.

References

- [1] Z. Šimek and R. Vespalec, *J. High Resolut. Chromatogr.*, 12 (1989) 610.
- [2] Z. Šimek, R. Vespalec and J. Šubert, *J. Chromatogr.*, 543 (1991) 475.
- [3] Z. Šimek and R. Vespalec, *J. Chromatogr.*, 629 (1993) 153.
- [4] R. Vespalec, V. Šustáček and P. Boček, *J. Chromatogr.*, 638 (1993) 255.
- [5] J. Turková, K. Bláha, J. Horáček, J. Vajčner, A. Frydrychová and J. Čoupek, *J. Chromatogr.*, 215 (1981) 165.
- [6] *Catalogue of Sorbents for LC*, Tessek, Prague, 1987.
- [7] S. Allenmark, B. Bomgrén and H. Borén, *J. Chromatogr.*, 237 (1982) 473.
- [8] K.K. Sterward and R.F. Doherty, *Proc. Natl. Acad. Sci. U.S.A.*, 70 (1973) 2850.

- [9] S. Allenmark, *Chromatographic Enantioseparation, Methods and Application*, Ellis Horwood, Chichester, 1988.
- [10] J.F. Foster, in V. Rosenoer, M. Oratz and M. Rothshild (Editors), *Albumin Structure, Function and Uses*, Pergamon Press, New York, 1977, pp. 53–84.
- [11] T. Peters, Jr., in F.W. Putnam (Editor), *The Plasma Proteins*, Vol. I., Academic Press, New York, 2nd ed., 1975, pp. 133–181.
- [12] R. McMenamy, in V. Rosenoer, M. Oratz and M. Rothshild (Editors), *Albumin Structure, Function and Uses*, Pergamon Press, New York, 1977, pp. 143–157.

Structural factors affecting the enantiomeric separation of barbiturates and thiobarbiturates with a chiral side-chain by various β -cyclodextrin supports. Effects of the presence of hydroxypropyl substituents on the chiral selector

N. Thuaud*, B. Sebillé

Laboratoire de Physicochimie des Biopolymères, UM 27 CNRS, Université Paris XII, 2 Rue H. Dunant, 94320 Thiais, France

First received 26 May 1994; revised manuscript received 18 July 1994

Abstract

The chromatographic separation of barbiturate and thiobarbiturate enantiomers on β -cyclodextrin (β -CD) HPLC columns was studied. The effect of the nature of the side-chain bearing the chiral centre was examined. The stationary phases used were of two types, commercial with native β -CD or hydroxypropyl- β -CD residues linked to silica and laboratory-made with β -CD polymers adsorbed on silica. The chiral recognition of the studied compounds is mainly dependent on the presence of hydroxypropyl substituents in the β -CD cavity.

1. Introduction

In recent years, various chiral cyclodextrin stationary phases (CDSP) have been developed. Two types of packing have been synthesized.

The first relies on the covalent bonding of cyclodextrins (CD) or derivatives to silica via different spacers. Columns packed with this type of support are commercially available: Cyclobond (Astec) columns containing an ether arm through which α -, β - and γ -native CD [1] or some derivatized CDs are linked to 5- μ m silica [2,3], and the Chiradex column (Merck) with native β -CD bonded to 5- μ m LiChrospher via a carbamate-type spacer. These supports exhibit

excellent properties allowing the enantiomeric resolution of numerous compounds.

The second type of packing was obtained by absorption of β -CD polymers on silica. Two polymers have been prepared, either by condensation of β -CD molecules with a bifunctional reagent (EP- β -CD- N^+ polymer) [4], or by grafting a monosubstituted β -CD derivative on to a linear polymer (polyvinylimidazole, PVI) [5]. The ability of these stationary phases to resolve racemic mixtures usually separated on commercial supports has been demonstrated. Moreover, we have shown that the chemical microenvironment of the β -CD influences the selectivity of the chromatographic phases. Thus, pendant β -CD residues linked to the PVI chain by a single spacer arm exhibit a chemical environment different to that observed with β -CD

* Corresponding author.

cavities bearing 6–7 hydroxypropyl groups in the EP- β -CD- N^+ polymer. The overcrowding resulting from this structure generates steric hindrance for the penetration of guest molecules into the cavities and/or additional interactions [5].

Preliminary results on the discrimination of chiral barbiturates by β -CD complexation have been obtained both on β -CD chiral columns and on reversed-phase achiral columns with β -CD in the mobile phase. The most commonly studied barbiturates, such as hexobarbital and mephobarbital, which have their chiral centre at the C-5 position on the pyrimidine ring, have been reported to be resolved on CDSP [4,6] or with β -CD complexation in the mobile phase [7–9]. In contrast, it has been reported that it is more difficult to resolve barbiturates bearing the chiral centre outside the heterocyclic ring. Little information is available on the resolution of this type of compound by β -CD complexation. Cyclobond columns failed to resolve butabarbital and pentobarbital [10]. This latter racemate could not be resolved either on PVI- β -CD polymer [5] or with β -CD in the eluent [7]. With this HPLC mode, secobarbital [7,9], thiopental [7] and butabarbital [9] enantiomers also were not separated. To our knowledge we have reported the only example of the resolution of a

barbiturate of this type, pentobarbital, using a CDSP, the EP- β -CD- N^+ support [5]. Chiral recognition of thiamylal enantiomers have also been reported using an achiral reversed-phase column and addition of β -CD to the mobile phase [8].

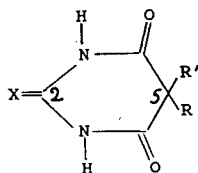
This paper describes the chiral separation of a series of barbiturates (BA) and thiobarbiturates (TBA), bearing the chiral centre on a substituent at the C-5 position, by employing several CDSPs, commercial with β -CD residues covalently linked to silica and laboratory-made with β -CD polymers adsorbed on silica. It has been pointed out that the structure of the guest, i.e., the nature of the heteroatom at C-2 and that of the substituents at C-5, greatly influences the chiral recognition of the racemates. Stationary phases with β -CD hydroxypropyl substituents allow some separations of BA that cannot be resolved with native β -CD.

2. Experimental

2.1. Chemicals

The structures of the optically active BA and TBA studied are shown in Table 1. These racemic compounds were kindly provided by

Table 1
Structural formulae of the investigated TBA and BA



Compound	Name	X	R	R'
1	Butabarbital	O	Ethyl	<i>sec.</i> -Butyl
2	Talbutal	O	Allyl	<i>sec.</i> -Butyl
3	Pentobarbital	O	Ethyl	1-Methylbutyl
4	Secobarbital	O	Allyl	1-Methylbutyl
5	Cyclopental	O	Allyl	2-Cyclopentenyl
6	Brevital	O	Allyl	1-Methyl-2-pentenyl
7	Thiopental	S	Ethyl	1-Methylbutyl
8	Thiamylal	S	Allyl	1-Methylbutyl

Professor Dr. J. Bojarski, Department of Organic Chemistry, N. Copernicus Academy of Medicine, Krakow, Poland. An examination of these structures revealed that, owing to the absence of a substituent at the N-3 position of the pyrimidine ring, all these compounds are not chiral at C-5, but do possess chiral side-chains 5-R'.

2.2. HPLC chiral columns

Polymeric HPLC supports, EP- β -CD-N⁺ and PVI- β -CD, were prepared by absorption on 5- μ m silica of the corresponding polymers, as described previously [5], and were packed by a slurry packing technique in 25 cm \times 4.6 mm I.D. stainless-steel columns. These supports were characterized from the amount of carbon determined by elemental analysis (Table 2). Compared with the procedures reported previously [5], in order to obtain similar loadings for both supports (in terms of the number of β -CD cavities per gram of silica), a more concentrated aqueous solution (20%, w/w) was used for the adsorption of the EP- β -CD-N⁺ polymer.

Three commercially available HPLC columns (25 cm \times 4.6 mm I.D.) were used: Cyclobond I and Cyclobond I RSP columns were obtained from Astec (Whippany, NY, USA) and a Chiradex LiChroCART cartridge was obtained from Merck (Darmstadt, Germany).

2.3. Chromatographic experiments

Sodium phosphate solutions (0.1 M) adjusted to pH 4 were used as eluents. The organic modifier was methanol. The flow-rate was 1.0 ml/min.

3. Results and discussion

3.1. Influence of the nature of the heteroatom at the C-2 position on the resolution of the racemates

The data in Tables 3 and 4 demonstrate the influence of the presence of a sulfur or an oxygen atom at the C-2 position of the ring, comparing the results for TBA compounds (7 and 8) with those of BA compounds (3 and 4). It can be seen that the pairs 7–3 and 8–4 have similar 5-R and 5-R' substituents.

Both TBA were resolved, at least partially, on each CDSP, whereas the enantiomers of 3 and 4 were not discriminated on Cyclobond I, Chiradex and PVI- β -CD columns. An enantioselectivity for 3 and 4 racemates was observed on EP- β -CD-N⁺ and Cyclobond I RSP columns for 3 and 4 BA racemates but the resolution was lower than for the 7 and 8 TBA enantiomers. Typical chromatograms obtained on these both supports are shown in Fig. 1.

Hence the presence of the sulfur atom at the C-2 position in the guest molecules promotes considerably their chiral recognition by CDSP. Moreover, the nature of the stationary phase modifies the selectivity resulting from the environment of the β -CD residues.

Some comments can also be made based on the examination of the retention data of these compounds. On all supports the order of elution is the same for TBA and BA compounds. Moreover, it is observed that the enantioselectivities increase as the retentions increase. The observed greater TBA affinity for the CDSP can be related to previous studies on β -CD complexes in solution. The stability constant of the

Table 2
 β -CD-polymer HPLC supports

Polymer	Support	
	Carbon content (%)	β -CD moieties (μ mol/g)
PVI- β -CD	7.5	87
EP- β -CD-N ⁺	7.4	94

Table 3
Comparison of capacity factors (k'), selectivity factors (α) and resolutions (R_s) of BA and TBA obtained on the CDSP

Compound	Mobile phase ^a	Cyclobond I			Chiradex			PVI- β -CD		
		k' ^b	α	R_s	k' ^b	α	R_s	k' ^b	α	R_s
1	15:85	14.6	1.0	0	12.3	1.0	0	5.2	1.0	0
2	15:85	14.1	1.0	0	16.3	1.0	0	6.8	1.0	0
3	30:70	4.9	1.0	0	5.4	1.0	0	2.0	1.0	0
4	15:85	18.3	1.0	0	17.3	1.0	0	7.1	1.0	0
	30:70	7.2	1.0	0	6.5	1.0	0	2.5	1.0	0
5	20:80	13.3	1.0	0	17.1	1.0	0	7.0	1.0	0
	30:70	7.7	1.07	0.9	6.9	1.03	NC ^c	3.0	1.0	0
6	15:85							11.1	1.05	0.5
	30:70	0.9	1.15	NC	5.1	1.57	2.9	1.0	1.52	1.8
7	15:85	3.0	1.15	0.9				10.7	1.39	2.4
	30:70	10.4	1.05	0.5	6.1	1.05	NC	2.8	1.04	NC
8	15:85							10.9	1.05	0.4
	30:70	14.1	1.07	1.0	9.3	1.08	0.9	3.3	1.07	0.5
	15:85							15.4	1.07	0.8

^a Methanol–0.1 M phosphate buffer (v/v).

^b Capacity factors for the first-eluted peaks.

^c NC = the resolution could not be calculated.

thiopental- β -CD complex has been reported to be twice that of the pentobarbital- β -CD complex, as measured by UV spectrophotometry [11]. Similar results were obtained by ion-exchange HPLC with addition of β -CD to the mobile phase [12].

Moreover, from the different patterns of the induced Cotton effect previously observed for TBA- and BA- β -CD complexes, circular dichroism experiments suggested that the configuration of TBA within the cavity of β -CD is different from that of BA [11]. The difference

Table 4
Comparison of capacity factors (k'), selectivity factors (α) and resolution (R_s) of BA and TBA obtained on the CDSP

Compound	Mobile phase ^a	EP- β -CD-N ⁺			Cyclobond I RSP		
		k' ^b	α	R_s	k' ^b	α	R_s
1	30:70	4.0	1.0	0	3.0	1.0	0
2	30:70	7.0	1.0	0	4.0	1.0	0
3	30:70	6.2	1.07	0.7	3.5	1.08	0.94
4	30:70	7.8	1.08	0.70	5.13	1.09	1.02
5	30:70	11.2	1.08	0.70	8.8	1.08	0.74
6	30:70	0.6	1.22	0.54	1.47	1.43	3.6
	15:85	1.2	1.28	1.22			
7	30:70	11.7	1.14	1.25	9.17	1.17	2.04
8	30:70	18.0	1.15	1.20	11.37	1.19	1.8

^{a,b} See Table 3.

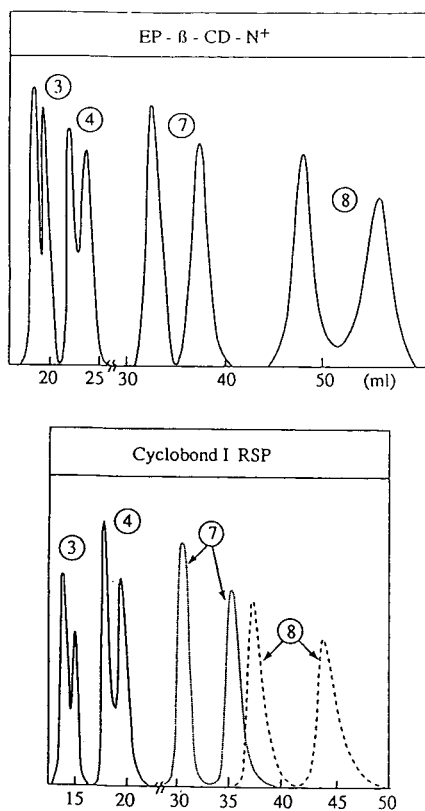


Fig. 1. Elution profiles of compounds **3**, **4**, **7** and **8** on EP- β -CD- N^+ and Cyclobond I RSP columns. Eluent: methanol-0.1 M phosphate solution (pH 4) (30:70).

resulting from fitting these two types of compounds into the β -CD cavity could explain the different chiral discrimination observed by the CDSP, with a TBA arrangement more favourable to chiral recognition.

On the other hand, it has been reported from thermodynamic studies that the inclusion of BA or TBA in β -CD involves forces other than hydrophobic forces such as hydrogen bonding and dipole-dipole interactions [11].

Similar observations have recently been made with an enhanced interaction with CDs in the presence of a thiocarbonyl function compared with that observed in presence of a carbonyl group. By HPLC, using a CD as a mobile phase additive, it was found that N-arylthiazoline-2-thiones have higher association constants than

N-arylthiazoline-2-ones with γ -CD, leading to better chiral recognition of their atropisomers [13]. Dipole-dipole interactions rather than hydrogen bonding has been suggested to be at the origin of the large association constants of thiocarbonyl derivatives with CDs as these compounds have a smaller proton-accepting ability than their oxygen analogues [13].

In summary, the sulfur atom at the C-2 position of the pyrimidine ring enhances the affinity of the solutes with the CDSP, and the occurrence of a polar interaction involving this atom leads to a better fitting of TBA with the β -CD cavities, favouring their chiral recognition.

3.2. Influence of the nature of the C-5 TBA substituents

Changing the substituent at the C-5 position from ethyl to allyl (comparing compounds **3** with **4** and **7** with **8**) leads to only a slight change in the chiral recognition by β -CD (α -values from Tables 3 and Table 4). Hence there is a small increase in enantioselectivity in the presence of the longer allyl substituent, when nevertheless a chiral discrimination is observed, i.e., for BA compounds (**3** and **4**) on EP- β -CD- N^+ and Cyclobond I RSP supports only, and for TBA compounds (**7** and **8**) on each column.

However, changing the other C-5 substituent from *sec.*-butyl to 1-methylbutyl, 2-cyclopentenyl or 1-methyl-2-pentenyl greatly influences the enantioselectivity observed. Thus, compounds **1** and **2**, with the shortest 5-R' substituent, are not resolved by the CDSP, the presence of a *sec.*-butyl group together with an allyl or an ethyl group precluding the resolution of the barbiturates on all the columns. However, the presence of a 1-methylbutyl group allows the recognition of **3** and **4** by EP- β -CD- N^+ and Cyclobond I RSP stationary phases only. This substituent is not effective for chiral recognition on the other columns. The presence of more bulky groups such as 1-methyl-2-pentenyl and 2-cyclopentenyl (**5** and **6**) is more favourable, with preference for 1-methyl-2-pentenyl, which provides the greatest enantioselectivity on all the columns.

The capacity factors in Tables 3 and 4 (com-

paring compounds **1** with **2**, **3** with **4** and **7** with **8**) show that higher retention times are obtained in the presence of an allyl than with an ethyl substituent. Increased retentions are observed also on passing from a *sec.*-butyl (BA **1** or **2**) to a 1-methylbutyl group (BA **3** and **4**), and then to a 2-cyclopentenyl group (BA **5**). A 1-methyl-2-pentenyl substituent reduces considerably the retention of the guest (**6**), except on Chiradex. The decrease in affinity for the other four stationary phases does not affect their chiral recognition as this BA has the best enantioselectivity values on all the columns.

Previous ^{13}C NMR experiments indicated that the cyclic moiety of BA is at least partly accommodated in the hydrophobic cavity of β -CD with the 5-substituents participating in inclusion formation and that their size affects the equilibrium constants of the β -CD complexes, with lower constants for smaller or too bulky substituents [11,14]. These results are in good agreement with our capacity factor results.

3.3. Influence of the β -CD stationary phase structure

Among the stationary phases used, only EP- β -CD- N^+ and Cyclobond I RSP can separate the enantiomers of pentobarbital and secobarbital. We conclude that the overcrowding due to the presence of substituents on the β -CD cavity edges of these supports allows a better adjustment of these guest molecules, resulting in a more favourable position of their chiral centre relative to the host for enantiomeric discrimination.

The presence of more bulky substituents than the 1-methylbutyl group on BA at the C-5 position of the pyrimidine ring is needed for chiral recognition when using the native β -CD supports PVI- β -CD, Cyclobond I and Chiradex.

Better enantioselectivities are also observed for TBA on columns with β -CD hydroxypropyl substituents. Nevertheless, the supports bearing native β -CD residues can discriminate both TBA enantiomers (with a 1-methylbutyl group at the C-5 position).

It has been reported that the presence of hydroxypropyl substituents on the Cyclobond I RSP support allows the resolution of several enantiomers that could not be separated on native β -CD phases [3,15], but to our knowledge, experiments dealing with a chiral centre located on the side-chain of BA have not been reported for this type of support.

In conclusion, the chiral recognition of the studied compounds is highest when they have a thiocarbonyl instead of a carbonyl group and when their substituents at the C-5 position have an adequate size.

The presence of β -CD hydroxypropyl substituents on CDSP favours the enantiomeric discrimination of the BA and TBA. It is emphasized that these supports resulting from different synthetic routes lead to very similar results.

References

- [1] D.W. Armstrong, *U.S. Pat.*, 4 539 399 (1985).
- [2] D.W. Armstrong, A.M. Stalcup, M.L. Hilton, J.D. Duncan, J.R. Faulkner and S.C. Chang, *Anal. Chem.*, 62 (1990) 1610.
- [3] A.M. Stalcup, S.C. Chang, D.W. Armstrong and J. Pitha, *J. Chromatogr.*, 513 (1990) 181.
- [4] N. Thuaud, B. Sébille, A. Deratani and G. Lelièvre, *J. Chromatogr.*, 555 (1991) 53.
- [5] N. Thuaud, B. Sébille, A. Deratani, B. Popping and C. Pellet, *Chromatographia*, 36 (1993) 373.
- [6] W.L. Hinze, T.E. Riehl, D.W. Armstrong, W. Demond, A. Alak and T. Ward, *Anal. Chem.*, 57 (1985) 237.
- [7] D. Sybilska, J. Zukowski and J. Bojarski, *J. Liq. Chromatogr.*, 9 (1986) 591.
- [8] S. Eto, H. Noda and A. Noda, *J. Chromatogr.*, 579 (1992) 253.
- [9] P. Mitchell and B.J. Clark, *Anal. Proc.*, 30 (1993) 101.
- [10] D.W. Armstrong and W. Demond, *J. Chromatogr. Sci.*, 22 (1984) 411.
- [11] M. Otagiri, T. Miyaji, K. Uekama and K. Ikeda, *Chem. Pharm. Bull.*, 24 (1976) 1146.
- [12] K. Uekama, F. Hirayama, S. Nasu, N. Matsuo and T. Irie, *Chem. Pharm. Bull.*, 26 (1978) 3477.
- [13] C. Roussel and A. Favrou, *Chirality*, 5 (1993) 471.
- [14] S.M. Han and N. Purdie, *Anal. Chem.*, 56 (1984) 2825.
- [15] S.C. Chang, L.R. Wang and D.W. Armstrong, *J. Liq. Chromatogr.*, 15 (1992) 1411.

Analytical conditions for the determination of 23 phenylthiocarbamyl amino acids and ethanolamine in musts and wines by high-performance liquid chromatography

M. Puig-Deu, S. Buxaderas*

Unidad de Nutrición y Bromatología, Departamento de Ciencias Fisiológicas Humanas y de la Nutrición, Facultad de Farmacia, Universidad de Barcelona, 08028 Barcelona, Spain

First received 11 April 1994; revised manuscript received 18 July 1994

Abstract

An improved HPLC method, using phenyl isothiocyanate (PITC) as derivatization agent, was developed for the separation and determination of 23 amino acids and triethanolamine in must and wine, without any pretreatment of the samples. The stability of dry and dissolved phenylthiocarbamyl derivatives was studied. The effects of pH, polarity, temperature and the addition of an ion-pairing reagent to facilitate the chromatographic separation were investigated. Four Penedès musts and their wines, from Macabeo and Parellada varieties, were analysed. The free amino acid contents found were compared with published results for the same varieties.

1. Introduction

Nitrogen compounds, especially amino acids, are particularly important in enology with regard to their influence on the organoleptic profile of wines and they can contribute to varietal characterization [1].

High-performance liquid chromatography in the reversed-phase mode (C_{18} column) and detection after derivatization is the technique of choice for the separation and identification of these compounds. Several compounds have been used as derivatization agents, e.g., dansyl chloride [2,3], orthophthaldehyde (OPA) [4,5] and phenyl isothiocyanate (PITC) [6–8]. All of them have advantages and disadvantages. We chose PITC, because it combines with primary and

secondary amine groups (proline and hydroxyproline), it has sufficient sensitivity, the reaction times are short and their derivatives are more stable than the others. Moreover, it is a pre-column derivative that does not need any special equipment, so the versatility of the instrumental is not lost.

Other investigators have also used the advantages of phenylthiocarbamyl (PTC) derivatives in application to wines; however, a prior amino acid extraction was applied to the sample [6]. We propose an elution system that allows the separation of 23 PTC-amino acids and ethanolamine (ETA) in musts and wines without any prepurification of the sample.

The mobile phase plays a very important role in the resolution of these compounds with regard to the amino acid structure. The amino acids have a dipolar character and some of them have

* Corresponding author.

an additional acidic or basic group. The basic amino acids show less resolution owing their interaction with the stationary phase. Hence the selection of the ionic strength, pH and polarity of the mobile phase is important. Buffer solutions with a pH between 5.0 and 6.5 and acetonitrile have been reported as eluents [6–8]. Sodium pentanesulphonate is added to the mobile phase because it forms an ion pair with the amino acids, improving the elution of basic compounds.

A diode-array detector was used because it not only gives results as a fixed-wavelength detector, it also indicates the peak purity and corroborates their identification, comparing the absorbance spectrum of the sample with those of standards. With these data correct amino acid identification and determination are possible; the mobile phase and chromatographic column are used frequently and, as no sample pretreatment was carried out, the peaks of some compounds present in must and wine could overlap with those of the PTC-amino acids.

2. Experimental

Stock standard solutions of amino acids (obtained from Sigma) were prepared by dissolving each acid in 0.1 M acetic acid to give a 20 nmol/ μ l concentration; tyrosine was dissolved in 1 M NaOH. From these solutions working standard solutions of 8, 12, 40, 80 and 120 mM for each amino acid were prepared; as proline is present at a higher concentration in must and wines, working standard solutions containing 0.4, 0.6, 0.8, 1.6 and 2.4 M were prepared. A 400 mM solution of norleucine (Nle) in 0.1 M acetic acid was used as an internal standard.

The derivatization reagent [PITC–water–ethanol–triethylamine (1:1:7:1)] was prepared daily. PITC was kept in a freezer (-20°C).

The samples were four white Penedès musts from the 1991 harvest, two Macabeos (M1 and M2) and two Parelladas (P1 and P2), and their four wines. The samples were kept at -20°C until analysis; also, 1 g/l of sodium fluoride was

added to the must samples to prevent fermentation. The samples were centrifuged at 4000 g for 15 min to eliminate large particles before derivatization.

2.1. Derivatization procedure

A 20- μ l volume of the standard solutions or 40 or 100 μ l of must or wine, with 20 μ l of the internal standard (Nle) and 20 μ l of a triethylamine (TEA) solution [TEA–water–ethanol (1:2:2)] were added to a 35 \times 4 mm I.D. tube. The solution was evaporated to dryness under vacuum and then the procedure described by Bidlingmeyer et al. [8] was followed. The dry residues containing the PTC derivatives were kept in a freezer. The dry residue was dissolved in 100 μ l of acetonitrile–water (95:5) and filtered through a 0.45- μ m cellulose acetate filter before injection.

2.2. Chromatographic conditions

A Hewlett-Packard Model 1040 gradient liquid chromatograph with an HP 1050 diode-array UV–visible detector was used. The separation was carried out using a Spherisorb C₁₈ ODS-2 column (25 \times 4.6 mm I.D.) of 5- μ m particle size; the precolumn contained the same stationary phase.

The following solvents were used: (A) an aqueous buffer containing 0.1 M sodium acetate, 0.680 ml/l of triethylamine and 0.2 mg/ml of

Table 1
Linear solvent gradient for elution

Time (min)	Solvent A (%)	Solvent B (%)	Solvent C (%)
0	35.0	62.8	2.2
3	35.0	62.0	3.0
15	35.0	62.0	3.0
16	35.0	58.0	7.0
30	35.0	50.0	15.0
45	35.0	42.0	23.0
50	0.0	0.0	100.0
60	0.0	0.0	100.0
65	35.0	62.8	2.2

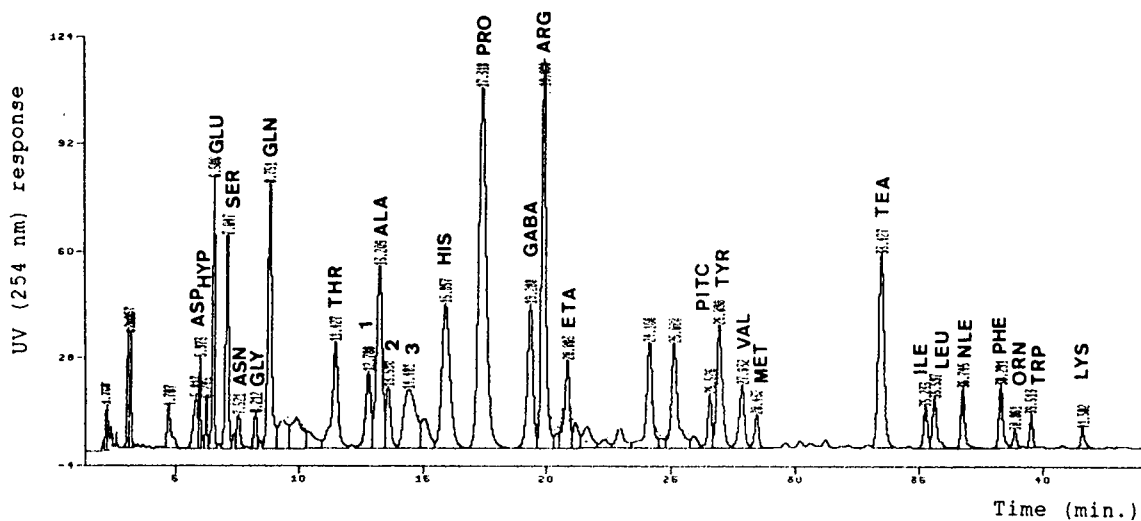


Fig. 1. Chromatogram of Parellada (P1) grape must.

sodium pentanesulphonate, adjusted to pH 5.27 with glacial acetic acid; (B) water; and (C) acetonitrile. The separation was carried out using a linear multi-step solvent gradient, as shown in Table 1. The flow-rate was 1 ml/min, the column temperature was 35°C and the detection wavelength was 254 nm.

3. Results and discussion

Twenty-three amino acids and ethanolamine (ETA) were satisfactorily separated from must and wine samples (Figs. 1 and 2). The effects of ionic strength, pH, mobile phase polarity, ion pair formation and column temperature are

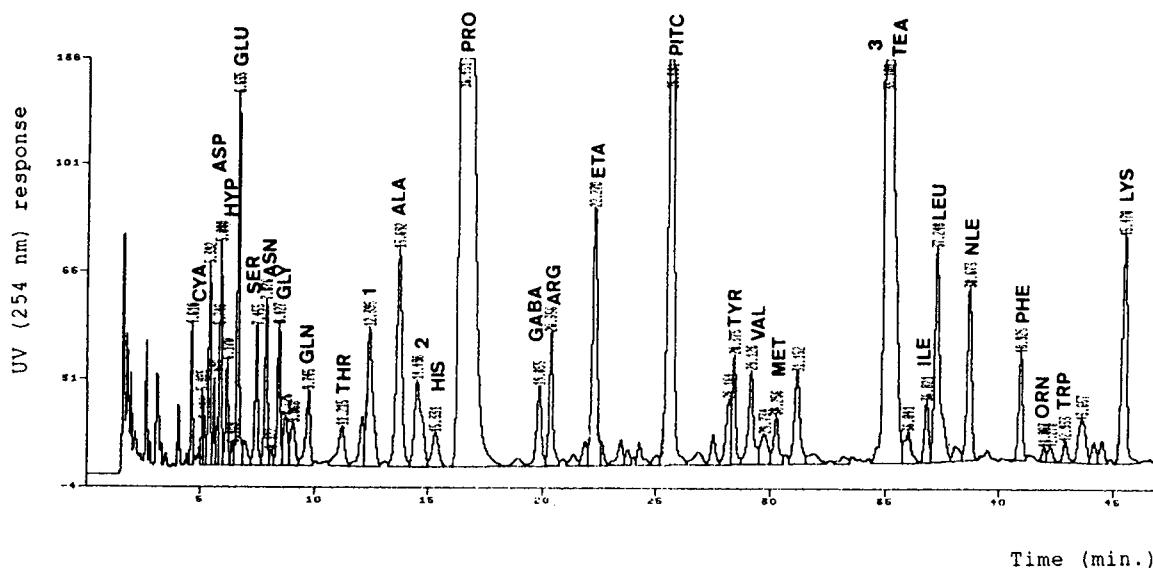


Fig. 2. Chromatogram of Parellada (P1) wine.

different for each amino acid, depending on their structure. An increase in the ionic strength of the mobile phase leads to an increase in the retention times of the amino acids, except for the basic compounds, which appear earlier. An increase in the buffer acidity produces a delay in the retention times. The addition of sodium pentanesulphonate or any other salt that

produces an ion pair with the amino acids improves the resolution of the basic amino acids and prolongs their elution times. The effect of the ion pair depends not only on the salt concentration in the mobile phase, but also on the ionic strength, the amino acid polarity and the percentage of acetonitrile in the mobile phase. Almost all the amino acids, with or without basic

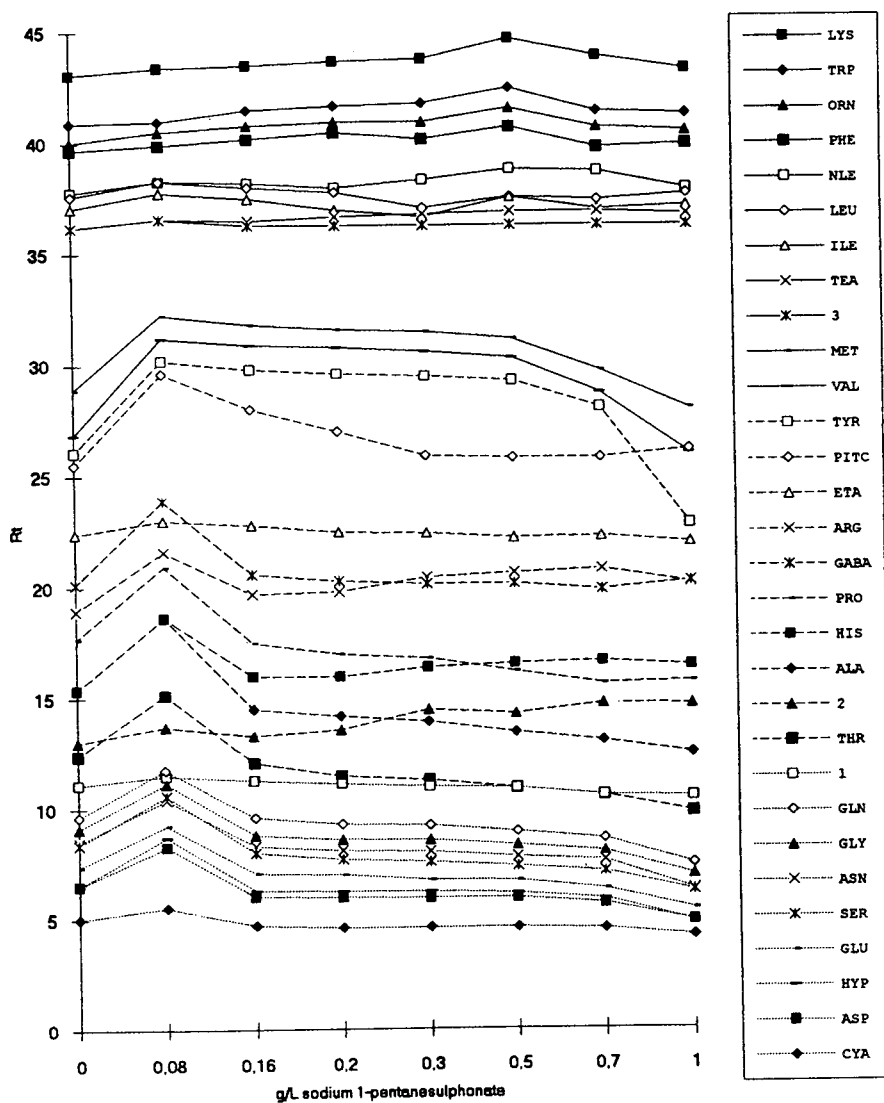


Fig. 3. Changes in retention time in HPLC of wine sample with variation in sodium 1-pentanesulphonate concentration in the mobile phase.

character, show increased retention times on addition of 0.08 g/l of sodium pentanesulphonate to the mobile phase (Fig. 3); however, adding more salt decreases their retention times. This effect was observed previously by Zoest et al. [9], who pointed out that the relationship between the salt concentration and the retention time of the basic compounds follows a parabolic curve. Exceptions are the basic amino acids (His, Arg and Lys) and ETA, which continue to show increasing retention times.

The addition of sodium pentanesulphonate allowed the separations of His-Ala, Asp-Hyp, Gly-Asn and Arg-Pro (Fig. 4). With the salt addition, Arg moves towards GABA, separating from Pro that is present at high concentration compared with the Arg present in must and wines, so Arg can be overlapped by Pro. A

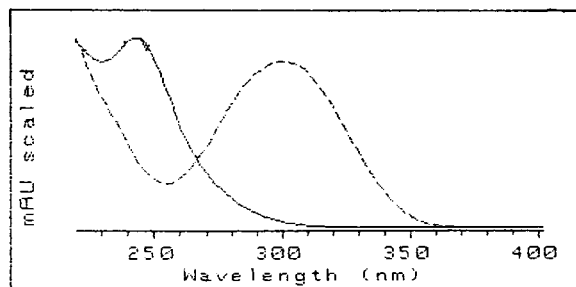


Fig. 5. Comparison of two spectra from a wine chromatogram. Solid line, Pro; dashed line, peak 1 (see Fig. 2).

better separation of all the amino acids was achieved when 0.2 g/l was added.

Changes in the ionic strength, pH and sodium pentanesulphonate affect the first part of the chromatogram (Figs. 1 and 2), but the amino

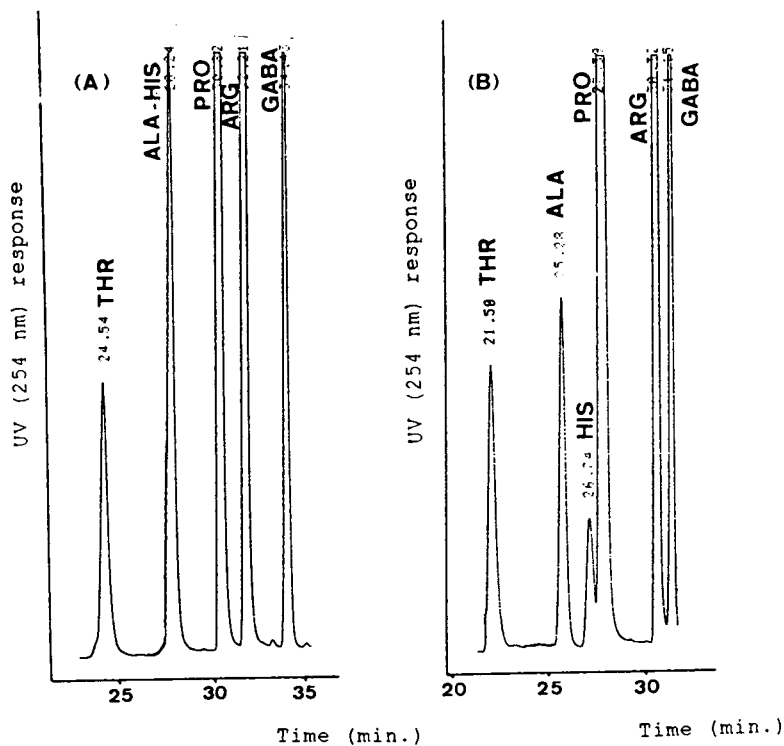


Fig. 4. HPLC of standards (Thr, Ala, His, Pro, Arg and GABA) eluted with mobile phases (A) without sodium 1-pentanesulphonate and (B) containing 0.1 mg/ml of sodium 1-pentanesulphonate.

acids that elute after 30 min are not affected by these parameters and their retention times depend primarily on the polarity of the mobile phase.

Temperature has the same effect on all the amino acids. At higher temperatures the chromatograms are shorter and show better resolution, but the lifetime of the chromatographic column decreases.

Figs. 1 and 2 show the must and wine chromatograms. Very good resolution (separation) was observed not only for the identified peaks, but also for other compounds that elute in the same chromatogram.

The amino acid spectra obtained with the diode-array detector indicate that the purity of each of these peaks is >99% and the corre-

spondence between the standard spectra and the measured peaks is also 99%. The spectra of the other peaks (1, 2 and 3) in Figs. 1 and 2 indicate that they are not PTC derivatives. In Fig. 5, the spectra of a PTC-amino acid (Pro) with an unidentified peak are compared (peak 1).

3.1. Method validation

Different parameters were considered to establish the reliability of the method (derivatization and chromatographic separation) (Table 2).

The variation in the retention time, studied with six aliquots of the same sample (Parellada wine), was <3%. The precision of amino acid determination was lower than 7%, except for

Table 2

Repeatability of retention time (t_R), precision, recovery, linearity, limit of detection (L.D.) and limit of quantification (L.Q.) for amino acids and ethanolamine

Compound	Repeatability, t_R (%)	Precision (%)	Recovery (%) ($n = 4$)	Linearity (r)	L.D. (nmol)	L.Q. (nmol)
Cya	3.00	9.85	100.1 ± 7.5	0.9999	0.020	0.052
Asp	1.83	6.87	100.8 ± 2.7	0.9989	0.025	0.063
Hyp	1.72	2.06	100.7 ± 1.8	0.9995	0.015	0.039
Glu	2.71	5.98	103.1 ± 4.4	0.9991	0.018	0.046
Ser	1.16	4.23	99.4 ± 1.8	0.9992	0.016	0.046
Asn	1.89	4.63	94.0 ± 2.8	0.9992	0.016	0.041
Gly	1.78	5.69	102.7 ± 10.4	0.9997	0.016	0.040
Gln	1.52	3.66	100.6 ± 4.8	0.9997	0.016	0.041
Thr	1.07	5.75	97.9 ± 7.9	0.9989	0.017	0.042
Ala	1.05	3.18	102.9 ± 8.9	0.9999	0.015	0.039
His	0.96	6.15	95.4 ± 2.8	0.9999	0.018	0.045
Pro ^a	1.24	2.16	99.9 ± 0.8	0.9990	0.013	0.033
GABA	0.88	2.46	98.2 ± 4.8	0.9995	0.021	0.054
Arg	0.94	6.94	102.5 ± 3.5	0.9997	0.017	0.044
ETA ^b	0.84	3.22	107.1 ± 1.8	0.9998	0.017	0.044
Tyr	0.77	4.09	96.5 ± 3.3	0.9996	0.017	0.044
Val	0.45	2.79	100.6 ± 4.3	0.9994	0.021	0.053
Met	0.49	9.34	103.3 ± 5.1	0.9999	0.020	0.052
Ile	0.21	4.08	102.3 ± 2.9	0.9998	0.021	0.053
Leu	0.11	5.82	99.6 ± 3.4	0.9999	0.017	0.043
Phe	0.15	4.79	95.0 ± 4.7	0.9999	0.018	0.047
Orn	0.18	3.56	93.7 ± 3.2	0.9997	0.011	0.027
Trp	0.31	6.97	95.2 ± 5.2	0.9995	0.014	0.035
Lys	0.51	6.71	95.6 ± 5.1	0.9992	0.012	0.031

^a $n = 3$.

^b Ethanolamine.

Met and Cya, for which it was 9.34% and 9.85%, respectively, because they are present at lower concentrations than the other amino acids in the sample studied.

The determinations of amino acids and ETA were carried out with three calibration graphs for each. The correlation coefficient (r) was >0.9990 , except for Asp and Thr ($r = 0.9989$) (see Linearity column in Table 2).

The recovery was studied by adding different concentrations (10, 20, 40 and 80 mM) of each of the amino acids and ETA, except for Pro (400, 600 and 800 mM), to the same sample. The recoveries obtained (see Table 2) for each amino acid and ETA were $>90\%$ and independent of the concentration added.

The limit of detection (L.D.) was calculated according to the IUPAC equation [10]:

$$\text{L.D.} = X + tS_{n-1}$$

where X = mean noise, t = Student's t for a probability of 99.99% and S = standard deviation. X was determined by running nine blanks using the maximum sensitivity allowed by the integration system.

The limit of quantification (L.Q.) was calculated according to the equation of the American Chemical Society [11]:

$$\text{L.Q.} = X + 10S_{n-1}$$

where X is the same as for the limit of detection L.D.

The L.D. for the amino acids ranges between 0.011 nmol for Orn and 0.025 nmol for Asp and the L.Q. between 0.027 nmol for Orn and 0.063 nmol for Asp. Hence the method is sufficiently

Table 3
Stability of dry and solution PTC-amino acids (mg of amino acid/l of wine)

Compound	Solution					Dry				
	Time (min)					Time (weeks)				
	0	15	45	60	90	0	1	2	3	4
Cya	10.2	9.9	9.5	10.1	10.2	10.2	12.0	10.7	10.9	11.6
Asp	17.5	17.8	17.4	17.3	17.2	17.5	17.2	17.7	17.0	17.1
Hyp	14.3	14.2	14.7	14.0	13.9	14.3	14.0	13.8	14.7	14.6
Glu	20.1	19.7	20.4	19.8	20.0	20.1	20.5	18.0	20.5	20.5
Ser	12.3	11.9	12.5	12.4	12.0	12.3	12.9	12.3	13.1	12.9
Asn	10.1	9.9	10.0	9.8	10.2	10.1	10.3	10.8	10.2	10.9
Gly	12.5	12.4	12.7	12.3	12.8	12.5	13.1	12.9	13.9	13.0
Gln	11.1	11.0	11.4	11.2	10.5	11.1	11.4	10.2	10.8	7.5
Thr	8.4	8.2	8.0	7.9	8.3	8.4	7.9	8.2	8.7	8.4
Ala	12.1	12.5	11.9	12.3	12.5	12.1	12.1	13.3	13.5	12.6
His	9.1	8.9	9.0	9.1	8.9	9.1	9.0	9.1	9.6	9.0
Pro	287.3	280.1	279.1	290.4	285.4	287.3	302.2	310.6	313.4	298.3
Arg	10.2	10.3	10.6	9.9	10.3	10.2	11.2	10.0	11.7	10.8
GABA	11.8	11.5	11.4	11.9	11.7	11.8	11.6	11.7	11.0	11.6
ETA	21.6	21.5	21.8	21.4	21.5	21.6	20.5	22.3	22.4	22.0
Tyr	12.5	12.4	12.6	12.4	12.0	12.5	13.9	13.6	12.9	13.8
Val	7.5	7.2	7.3	7.9	7.3	7.5	7.9	8.0	8.9	7.6
Met	8.4	8.2	8.4	8.1	8.2	8.4	8.1	8.6	8.4	8.5
Ile	6.9	6.3	6.8	6.4	6.2	6.9	6.7	7.1	7.3	6.5
Leu	12.0	12.4	11.8	11.9	12.0	12.0	13.0	12.0	12.5	12.4
Phe	9.5	9.2	9.1	9.6	9.3	9.5	9.7	9.1	10.1	9.9
Orn	5.4	5.2	5.3	5.9	5.4	5.4	5.6	5.2	5.8	5.6
Trp	18.4	18.2	18.1	18.5	17.2	18.4	17.8	19.3	20.3	15.0
Lys	2.8	2.6	2.9	2.8	2.6	2.8	3.1	2.7	2.7	2.6

sensitive for the determination of the amino acids in the samples studied.

3.2. Stability of PTC derivatives

The stability was studied for dry samples (kept at -20°C) and for samples in solution (kept in a refrigerator at 4°C). (Table 3).

Dry derivatives

The PTC-amino acids were injected every week during 1 month. The variations are lower than those calculated for the method accuracy. However, after the third week Gln and Trp began to decline in concentration. Hence dry derivatives can be kept at 20°C for 3 weeks.

In solution

The same sample was injected at 15, 45, 60 and 90 min, after being dissolved. The amino acids were stable in solution for 1 h, then they became degraded. For this reason, the solution must be injected within 1 h after preparation.

3.3. Sample results

Table 4 gives the results obtained for the amino acids in the four musts and wines are shown. The amino acid concentrations in the wines are very similar to those observed by other workers for other Penedès wines of the same varieties, considering that they are from different harvests and the methods used to analyse them

Table 4
Results for must and wine samples

Compound	Must ^a (mg/l)				Wine ^a (mg/l)			
	M1	M2	P1	P2	M1	M2	P1	P2
Cya	N.D. ^b	N.D.	N.D.	N.D.	1.0	0.1	0.1	0.1
ASp	40.4	6.8	12.4	6.6	6.2	2.8	9.3	5.5
Hyp	1.6	0.7	12.4	6.6	2.1	2.3	3.2	2.9
Glu	51.1	13.2	11.2	11.2	10.2	5.6	13.3	10.1
Ser	28.8	11.8	21.0	16.3	2.1	1.3	2.5	1.6
Asn	8.8	4.7	3.9	2.4	2.5	1.5	8.3	1.0
Gly	3.3	2.9	2.7	2.0	1.4	2.4	2.2	2.5
Gln	73.4	29.9	39.9	37.0	3.8	1.3	6.1	12.3
Thr	27.6	11.9	28.1	18.3	2.8	0.8	1.3	1.2
Ala	39.6	29.4	27.3	27.3	8.3	5.3	9.5	15.8
His	12.0	8.5	8.8	12.3	1.6	1.3	1.8	2.0
Pro	125.1	92.7	103.7	57.5	167.5	162.6	354.0	251.6
Arg	249.6	81.3	241.3	172.4	6.1	4.4	7.3	6.5
GABA	25.3	27.9	16.4	21.2	3.9	2.8	5.0	6.6
ETA	13.4	7.0	14.2	10.5	35.8	33.2	82.0	70.4
Tyr	20.9	8.8	21.8	18.2	3.4	3.1	5.0	3.7
Val	8.6	5.3	8.9	7.1	4.2	2.3	3.1	2.1
Met	2.8	1.2	2.8	1.2	2.4	1.3	2.7	1.8
Ile	6.5	3.5	7.1	5.7	5.1	2.8	4.5	2.0
Leu	15.0	5.1	11.9	11.0	8.2	7.5	10.3	3.9
Phe	15.0	7.5	19.6	15.7	4.4	2.9	5.8	6.4
Orn	5.3	2.1	3.3	5.9	1.9	1.3	6.3	6.1
Trp	8.9	4.7	17.4	12.9	2.5	3.3	2.9	1.8
Lys	5.0	2.2	3.9	6.5	6.7	7.3	6.8	4.3

^a M1 and M2 = Macabeo variety; P1 and P2 = Parellada variety.

^b N.D. = not detected.

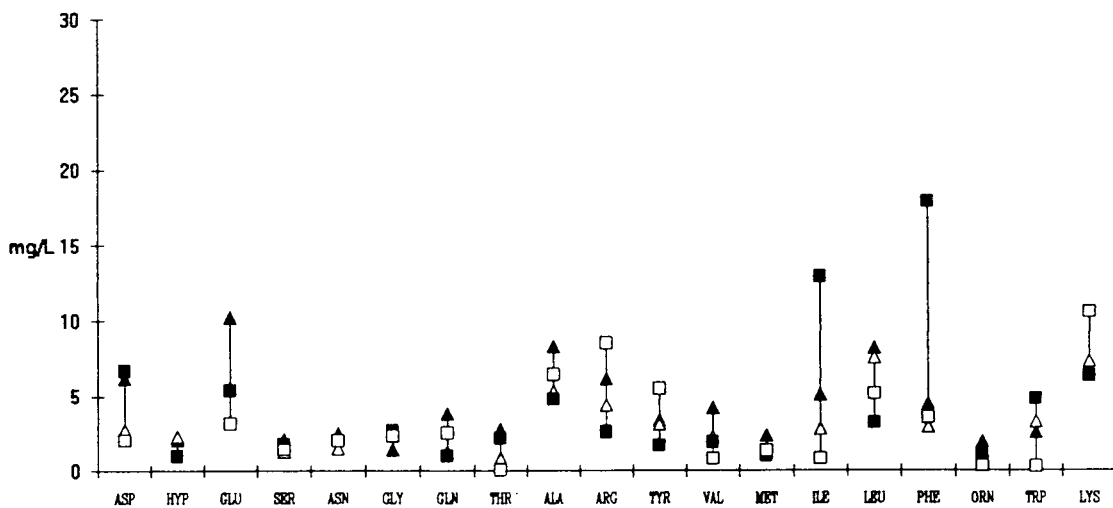


Fig. 6. Amino acid concentrations in Macabeo wine. ▲ = M1; △ = M2; ■ = MARCE (12); □ = CASTRO (4).

are different (Figs. 6 and 7). In one, the analysis was carried out following Sep-Pak pretreatment of the sample using PITC precolumn derivatization [12] and in the other the derivatization was carried out postcolumn with OPA [4].

Acknowledgements

The authors thank the Ministerio de Educación y Ciencia for funding Mariona Puig-Deu and the CICYT for grant No. ALI88-0495.

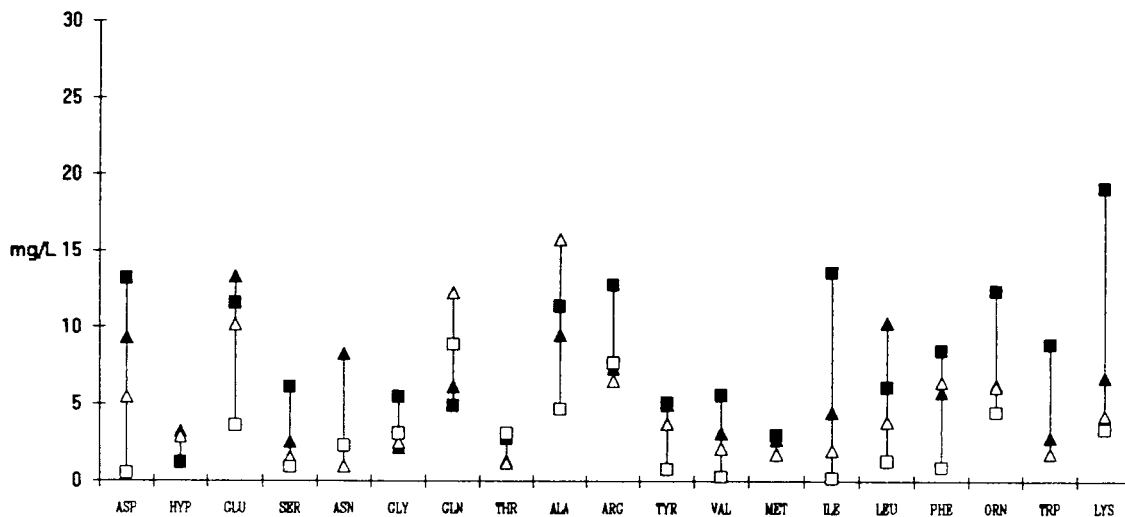


Fig. 7. Amino acid concentrations in Parellada wine. ▲ = P1; △ = P2; ■ = MARCE (12); □ = CASTRO (4).

References

- [1] Z. Huang and C.S. Ough, *Am. J. Enol. Vitic.*, 42 (1991) 261–267.
- [2] P. Martin, C. Polo, M.D. Cabezedo and M.V. Dabrio, *J. Liq. Chromatogr.*, 7 (1984) 539–558.
- [3] A. Casoli and O. Colagrange, *Am. J. Enol. Vitic.*, 33 (1982) 135–139.
- [4] J. Castro, paper presented at the *10th Congreso del Cava, October 15, 1992, Sant Sadurni d'Anoia, Spain*.
- [5] E.M. Sanders and C.S. Ough, *Am. J. Enol. Vitic.*, 36 (1985) 43–46.
- [6] R.M. Marce, M. Calull, J. Guasch and F. Borrull, *Am. J. Enol. Vitic.*, 40 (1989) 1–5.
- [7] J.L. Tedesco and R. Schafer, *J. Chromatogr.*, 403 (1987) 299–306.
- [8] B.A. Bidlingmeyer, S.A. Cohen and T.L. Tarvin, *J. Chromatogr.*, 336 (1984) 93–104.
- [9] A.R. Zoest, C.T. Hung, F.C. Lam, R.B. Taylor and S. Wanwimolruk, *J. Liq. Chromatogr.*, 15 (1992) 395–410.
- [10] G.L. Long and J.D. Winefordner, *Anal. Chem.*, 55 (1983) 712A–724A.
- [11] American Chemical Society, Committee on Environmental Improvement, Subcommittee on Environmental Chemistry, *Anal. Chem.*, 52 (1980) 2242–2249.
- [12] R.M. Marcé, *Tesina de Licenciatura en Ciències Químiques de Tarragona*, Universitat de Barcelona, Barcelona, 1988.

Resolution of proteins on a phenyl-Superose HR5/5 column and its application to examining the conformation homogeneity of refolded recombinant staphylococcal nuclease

Guozhong Jing*, Bo Zhou, Lijun Liu, Junxian Zhou, Zhige Liu
Institute of Biophysics, Academia Sinica, Beijing 100101, China

First received 17 May 1994; revised manuscript received 19 July 1994

Abstract

In order to examine the effect of amino acid substitutions on protein retention in hydrophobic interaction chromatography and the resolution of a phenyl-Superose HR5/5 column, two groups of staphylococcal nucleases, named Y113/W140 (wild-type), Y113W/W140 and Y113/W140F, Y113W/W140F, were produced by substituting tryptophan (W) for tyrosine (Y) at residue 113 and phenylalanine (F) for tryptophan (W) at residue 140. For each group, the proteins have the same amino acid at residue 140, but a different amino acid at residue 113. The solvent perturbation of nuclease fluorescence and 1,8-anilinoaphthalene-8-sulfonate binding studies showed that the substitutions do not change the side-chain positions of amino acids at residues 113 and 140. Chromatography of the proteins on the Phenyl-Superose HR5/5 column showed that the proteins with tryptophan at residue 113 have longer retention times than the proteins having tyrosine at residue 113; the proteins with the same amino acid at residue 113 have almost the same retention time regardless of substituting phenylalanine for tryptophan at residue 140. The studies clearly indicate that not all amino acid substitutions have an effect on protein retention; the contribution to retention of a given amino acid substitution depends on its position in a protein. Single amino acid substitutions at the exterior surface of a protein, which change the strength of hydrophobic interaction, can affect the protein retention in hydrophobic interaction chromatography. Staphylococcal nuclease and its mutants with only one amino acid difference on their surfaces can be discriminated by the phenyl-Superose column. The high resolving power of the Phenyl-Superose column makes it suitable not only for separating proteins, but also for providing a workable method for the analysis of the conformation homogeneity of refolded recombinant protein molecules by examining the hydrophobicity changes of protein molecules.

1. Introduction

Hydrophobic interaction chromatography (HIC) is a purification technique used to separate proteins on the basis of surface hydrophobicity [1,2]. Since HIC can preserve protein conformation and minimize denaturation, it is

used to separate proteins that span a wide range of surface hydrophobicity. The role of protein structure in chromatographic behaviour has been studied by Regnier and co-workers [3,4]. They used different lysozymes isolated from related bird species as model proteins to determine the contribution of certain amino acid substitutions in the proteins to retention. They predicted that amino acid substitutions did not affect the size of

* Corresponding author.

the hydrophobic contact surface area, but rather the strength of hydrophobic interactions, and only those residues at or near the exterior surface of a protein would have a major impact on chromatographic behaviour. However, systematic studies of the relationships between protein structure and chromatographic behaviour in HIC are still in the early stages, and more direct evidence is needed. Staphylococcal nuclease (EC 3.1.4.7) is a small globular protein of 149 residues containing no disulfide bonds or cysteines. X-ray crystal analysis of the protein indicates that a single tryptophan at residue 140 is buried in the interior of the protein, a tyrosine at residue 113 is not involved in the formation of any intramolecular hydrogen bonds and its side-chain is located on the protein surface [5]. Here we can take advantage of the structural characteristics of the protein to create two groups of staphylococcal nucleases, Y113/W140 (wild-type), Y113W/W140 and Y113/W140F, Y113W/W140F, by substituting tryptophan (W) for tyrosine (Y) at residue 113, and phenylalanine (F) for tryptophan (W) at residue 140. For each group, the proteins have different amino acids at residue 113 and the same amino acids at residue 140. The proteins provide good materials for examining the effect of amino acid substitutions at different regions of a protein on chromatographic behaviour. In this paper, we focus on examining the effect of single amino acid residue substitutions on chromatographic retention and the extent to which hydrophobic differences on surface of proteins can be discriminated by HIC using staphylococcal nuclease and its mutants as model proteins. The possibility of using HIC to examine the conformation homogeneity of refolded recombinant protein molecules is also discussed.

2. Experimental

2.1. Materials

All chemicals were of analytical-reagent grade. 1-Anilino-naphthalene-8-sulfonate (1,8-ANS) was purchased from Sigma.

The phenyl-Superose HR5/5 column (1 ml) was obtained from Pharmacia Laboratory Separation Division, which is used with a Pharmacia fast protein liquid chromatographic (FPLC) system.

2.2. Generating mutants and purification of staphylococcal nucleases

Plasmid pBVS-2 for expression of the staphylococcal nuclease (Y113/W140) was constructed by Jing et al. [6]; the nuclease was overproduced as inclusion bodies in *Escherichia coli* cells under the transcriptional control of P_{RPL} promoters regulated by cI857 temperature-sensitive repressors. Three mutants of the nuclease with different amino acid substitutions at residue 113 or/and 140, named Y113W/W140, Y113/W140F and Y113W/W140F, were obtained by the site-directed mutagenesis method described by Kunkel et al. [7], and overproduced in *E. coli* cells under the same transcriptional control as described above. The nuclease and its mutants were purified from *E. coli* cells harbouring the appropriate recombinant plasmid. *E. coli* cells grown to an absorbance of around 0.5–0.6 at 600 nm at 30°C in LB broth were induced at 42°C for 3–5 h. Partial purification was performed according to Shortle's cold-ethanol precipitation method [8]. For further purification, the partially purified protein was resuspended in a buffer of 1 M Tris-HCl (pH 9.2)–2.5 mM EDTA at 4°C overnight, and chromatographed on a Bio-Rex 70 column (15 cm × 2.6 cm I.D.) once or twice according to Shortle's procedure [9]. The peak containing the protein was collected and dialysed against distilled water. The purified proteins appeared to be homogeneous as judged by sodium dodecylsulfate polyacrylamide gel electrophoresis.

2.3. Fluorescence measurements

Fluorescence measurements were made with a Hitachi F4010 spectrofluorimeter at 25°C. Solvent perturbation of nuclease fluorescence was carried out according to the method described by Cuatrecasas et al. [10]. The enhancement of

tryptophanyl fluorescence by ethanol is used as a structural probe. Each solution contained 8 μM nuclease in 20 mM Tris-HCl (pH 7.4)–0.1 M NaCl and 0–30% (v/v) of ethanol. The tryptophanyl fluorescence intensities were measured at 360 nm with an excitation wavelength of 280 nm. For 1,8-ANS binding studies, each sample contained 180 μM of 1,8-ANS and 16 μM of nuclease protein in 20 mM Tris-HCl (pH 7.4), the fluorescence spectrum was measured after incubation of the sample for 20 min at 25°C, the wavelength of excitation was 345 nm and the slit width was 10 nm.

2.4. Circular dichroism

CD spectra were obtained on a Jasco J-500A spectropolarimeter. Samples were scanned from 250 to 195 nm using a quartz cuvette with a pathlength of 1 mm at 20°C; the concentration of each sample was 0.4 mg/ml in 20 mM Tris-HCl (pH 7.4).

2.5. Activity assays

The enzyme activity was measured with a Shimadzu UV-250 spectrophotometer by monitoring the increase in absorbance at 260 nm on addition of enzyme to 1 ml of a solution containing 50 $\mu\text{g}/\text{ml}$ of boiled salmon sperm DNA, 25 mM Tris-HCl (pH 7.4) and 10 mM CaCl_2 [11].

2.6. Hydrophobic interaction chromatography on phenyl-Superose HR5/5

Phenyl-Superose is a derivative of the rigid, cross-linked agarose-based gel Superose 12 and contains covalently bonded hydrophobic phenyl groups. The average particle size is 10 μm . Phenyl-Superose has a negligible amount of charged groups, ensuring true hydrophobic interaction chromatography. All the buffers and samples used in the chromatography were filtered through a 0.22- μm sterile filter. Each sample was dissolved in buffer A [50 mM potassium phosphate (pH 7.0)–1.7 M ammonium sulfate] to give a final concentration of 1 mg/ml.

A 50- μg amount of each sample was injected into the column equilibrated with buffer A. Chromatography was performed with a linear gradient from 0 to 100% buffer B with buffer A [buffer B = 50 mM potassium phosphate (pH 7.0)] at room temperature. A gradient volume of 15 ml at a flow-rate of 0.5 ml/min was used for testing the retention time of each sample individually on the phenyl-Superose column. The effluent was monitored at 280 nm. When the sample was a mixture of Y113/W140 and Y113W/W140 or Y113/W140F and Y113W/W140F, a gradient volume of 20 ml at a flow-rate of 0.25 ml/min was used.

3. Results and discussion

3.1. Positions of amino acids at residue 113 and 140 of the nucleases

The X-ray crystal analysis of staphylococcal nuclease (Y113/W140) showed that a single tryptophan at residue 140 is buried in the interior of the protein and a tyrosine at residue 113 is located on its surface [5]. Fig. 1 shows the results of solvent perturbation of nuclease fluorescence; increasing the ethanol concentration from 0 to 30% produces a linear increase in the tryptophanyl fluorescence of Y113W/W140 and Y113W/W140F. In contrast, no effect is observed on the tryptophanyl fluorescence of Y113W/W140 (wild-type). As low-molecular-mass tryptophanyl compounds showed a significant increase in ethanol [12], it is clear that the tryptophan residues at residue 113 of the mutants are also located on the surface of proteins. Y113W/W140 shows a less significant tryptophanyl fluorescence change than Y113W/W140F due to ethanol perturbation, as it contains two tryptophanyl residues, which make the mutant have a higher background fluorescence at 360 nm without ethanol perturbation.

It is known that 1,8-ANS can serve as a probe for hydrophobic sites on proteins [13], so the fluorescence of 1,8-ANS bound to the nucleases will provide another evidence to support the results mentioned above. Fig. 2 shows the fluo-

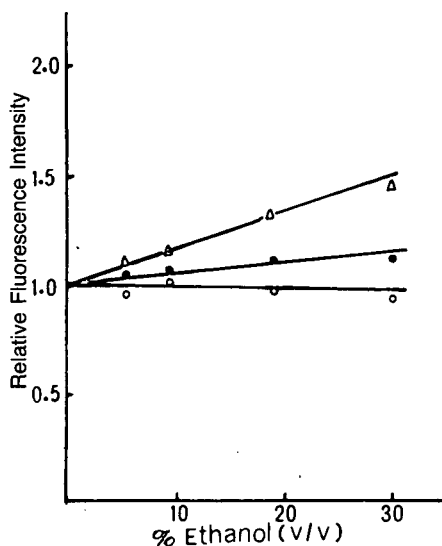


Fig. 1. Effect of ethanol on tryptophanyl fluorescence intensities of (○) staphylococcal nuclease and its mutants: (Δ) Y113W/W140F and (●) Y113W/W140. Solutions contained the nucleases ($8 \mu\text{M}$) in 20 mM Tris-HCl (pH 7.4)– 0.1 M NaCl and the indicated amount of ethanol. The tryptophanyl fluorescence was measured at 360 nm with an excitation wavelength of 280 nm . For each protein, the fluorescence intensity in absence of ethanol was taken as 100%.

rescence spectra of 1,8-ANS bound to the nuclease and its mutants. The fluorescence intensities of 1,8-ANS bound to the nucleases having same amino acid at residue 113 are almost the same regardless of the substitution of phenylalanine for tryptophan at residue 140. When 1,8-ANS is bound to the nucleases having tryptophan at residue 113, there is an apparent increase in fluorescence intensity and a blue shift of the fluorescence maximum compared with the fluorescence of 1,8-ANS bound to the nucleases with tyrosine at residue 113. The results again indicate that the tryptophan at residue 113 is located on the surface of proteins. The increase in fluorescence intensity and the blue shift of the fluorescence maximum occur because tryptophan has a higher hydrophobicity than tyrosine [14]. In addition, the results also show that the substitution of phenylalanine for tryptophan at residue 140 does not affect the hydrophobic properties of the proteins, which means that the phenylalanine

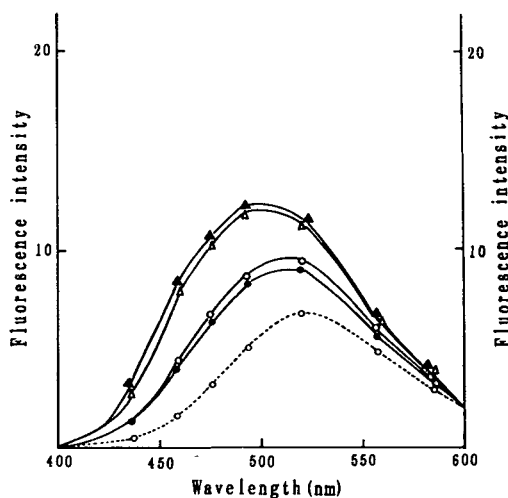


Fig. 2. Fluorescence emission spectra of 1,8-ANS in the presence of staphylococcal nuclease and its mutants. Spectra for 1,8-ANS with (●) Y113/W140, (○, solid line) Y113/Y140F, (Δ) Y113W/W140 and (▲) Y113W/W140F and (○, dashed line) a control with no protein. Each sample contained $180 \mu\text{M}$ of 1,8-ANS and $16 \mu\text{M}$ of the nuclease in 20 mM Tris-HCl (pH 7.4). The fluorescence spectra were measured after incubation of the samples for 20 min at 25°C ; the wavelength of excitation was 345 nm .

at residue 140 is buried in the interior of the proteins.

3.2. Effect of single amino acid substitution on protein retention in HIC and resolution of phenyl-Superose HR5/5 column

As described above, the effect of amino acid substitutions on the chromatographic retention of proteins was analysed by utilizing staphylococcal nuclease and its mutants. As shown in Fig. 3, the proteins with tryptophan at residue 113 were eluted at longer retention times than those having tyrosine at residue 113; the proteins with the same amino acid at residue 113 have almost the same retention time regardless of substituting phenylalanine for tryptophan at residue 140. It is unlikely that the differences in retention time between the nucleases are mainly caused by gross conformational changes as all the nucleases have almost the same CD spectra (Fig. 4) and

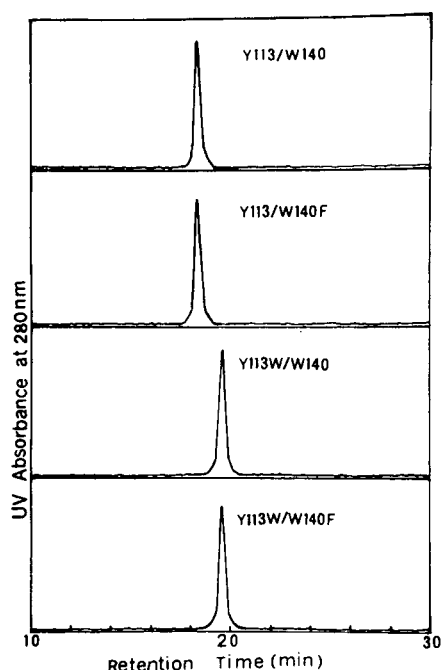


Fig. 3. Chromatographic retentions of staphylococcal nuclease (Y113/W140) and its mutants (Y113W/W140, Y113/W140F and Y113W/W140F) on the phenyl-Superose HR5/5 column. Chromatography was performed with a linear gradient (15 ml) from 0 to 100% buffer B with buffer A at room temperature. The effluent was monitored at 280 nm. Mobile phase: buffer A, 50 mM potassium phosphate (pH 7.0)–1.7 M ammonium sulfate; buffer B, 50 mM potassium phosphate (pH 7.0). Flow-rate, 0.5 ml/min.

the same activities (about 1000 units/mg), so the reason is that the substitution of tryptophan for tyrosine at residue 113 makes the nucleases with Y113W more hydrophobic than the nucleases with Y113 on their surfaces. Hence they would undergo stronger hydrophobic interactions with the Phenyl-Superose adsorbent. Of course, subtle changes in local conformation between the proteins caused by the substitution of tryptophan for tyrosine at residue 113 probably make some contribution to retention. However, there is no change in retention time when tryptophan at residue 140 is changed to phenylalanine, although phenylalanine is less hydrophobic than tryptophan [14]. A reasonable explanation is that the substitution does not make any changes in

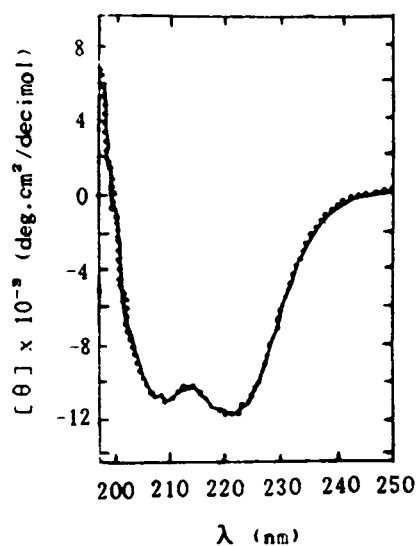


Fig. 4. Circular dichroism spectra of staphylococcal nuclease: Y113/W140 (solid line) and its mutants Y113W/W140, Y113W/W140F and Y113/W140F (dotted line). Refer to the Experimental section for the conditions of the spectra.

the hydrophobicity on their surfaces as the phenylalanine is buried in the interior of the mutants as described above. The studies clearly indicate that the contribution to retention of a given amino acid substitution depends on its position in the protein. Single amino acid substitution at the exterior surface of a protein can affect its retention in HIC if it changes the strength of the hydrophobic interactions.

In order to examine further what differences in hydrophobicity at the protein surface can be discriminated by HIC on the phenyl-Superose column, a mixture of Y113/W140 and Y113W/W140 or Y113/W140F and Y113W/W140F was applied to the phenyl-Superose column using the conditions described under Experimental. The proteins with only one amino acid difference on their surfaces can be well separated (Fig. 5). In agreement with earlier studies [4], the variant separation mechanism involves specific protein surface contact with the adsorbent in the region of primary structure protein differences. This indicates that the phenyl-Superose column has a high resolving power, and the properties of phenyl-Superose HIC can be used not only to

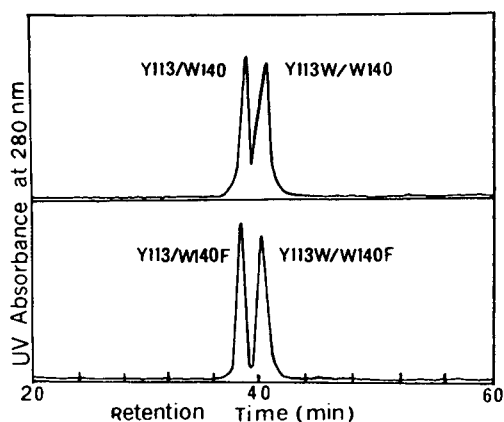


Fig. 5. Chromatography of the mixtures of Y113/W140 (wild-type) and Y113W/W140 or Y113/W140F and Y113W/W140F on the phenyl-Superose HR5/5 column. Chromatographic conditions in Fig. 3 except that the gradient volume was 20 ml at a flow-rate of 0.25 ml/min.

separate proteins but also to determine the relative hydrophobic characters of closely related proteins.

As numerous proteins have been shown to accumulate in an insoluble form when they are highly expressed in *E. coli* cells by the recombinant DNA technique, the protein of interest may be solubilized and require refolding to restore to it the same biological activity as for native protein after renaturation. However, there is no guarantee that the conformation among these soluble protein molecules is homogeneous. Therefore, finding a convenient way to discriminate the correctly folded molecules from the soluble but improperly folded molecules will be significant in both basic and applied research. The following experimental results may show the possibility of examining the conformation state of refolded recombinant proteins by using the phenyl-Superose column.

When the nuclease, which was purified from inclusion bodies as described above, was analysed on the HIC column, two peaks were sometimes eluted (Fig. 6B). Peak 1 has the same retention time and enzyme activity as the native enzyme, whereas peak 2 has a longer retention time and only 24% activity of the native enzyme. However, only one peak with the same retention

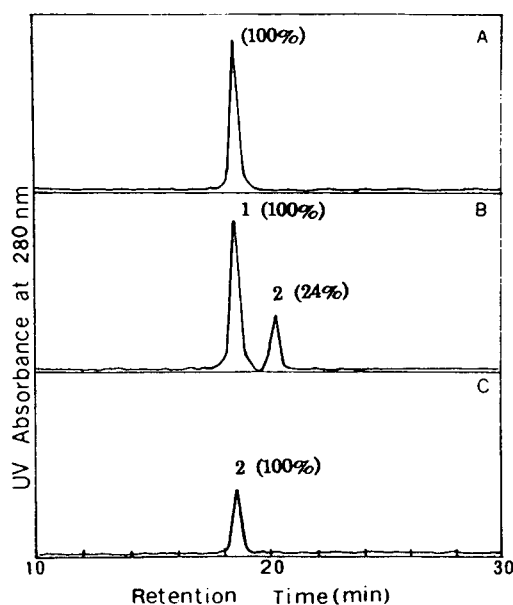


Fig. 6. Examination of the conformation homogeneity of the recombinant-derived staphylococcal nuclease by using HIC on the phenyl-Superose HR5/5 column. Chromatography was performed under the conditions described in Fig. 3. (A) Native nuclease; (B) nuclease purified from inclusion bodies; sometimes two peaks were eluted from the column; (C) re-chromatography of peak 2 on the column after denaturation and renaturation treatment. The values in parentheses represent the relative activities of the nucleases in different peaks.

time and activity as the native enzyme was obtained after peak 2 was further denatured in 4 M urea and renatured by dialysis against distilled water (Fig. 6C). It seems that peak 1 represents the correctly folded molecules of the enzyme and peak 2 represents the soluble but improperly folded molecules of the enzyme. As HIC is used to separate proteins on the basis of the surface hydrophobicity of proteins [1,2], the differences in retention time between molecules of the nuclease indicate that there are some differences in hydrophobicity between peaks 1 and 2, which ought to be caused by a conformational or structural change (e.g., improper folding) during the denaturation–renaturation process. Although refolding is easily achieved with some small polypeptides, there are no general rules for efficient refolding, and consequently appropriate conditions must be determined by trial and

error. Sometimes for recombinant proteins, especially for some proteins with high molecular masses and disulfide bonds, even when denaturation–renaturation treatment is carried out with great care there is still a small proportion of soluble molecules with improper folding. As long as there is a certain difference in surface hydrophobicity among them, in specific cases HIC may provide a workable method for the analysis of conformation homogeneity of recombinant proteins.

Acknowledgements

We thank Professor C.L. Tsou for his encouragement and critical reading and Professor J.M. Zhou for helpful discussions. This work was funded by a grant from National Natural Science Foundation of China.

References

- [1] H. Barth, W. Barber, C.R. Lochmuller, R. Majors and F.F. Regnier, *Anal. Chem.*, 60 (1988) 387R–429R.
- [2] G.G. Osthoff, A.I. Louw and L. Visser, *Anal. Biochem.*, 164 (1987) 315–319.
- [3] J.L. Fausnaugh and F.E. Regnier, *J. Chromatogr.*, 359 (1986) 131–146.
- [4] F.E. Regnier, *Science*, 238 (1987) 319–323.
- [5] T.R. Hynes and R.O. Fox, *Proteins*, 10 (1991) 92–105.
- [6] G.Z. Jing, L.J. Liu, Z.G. Liu, B. Zhou and Q. Zou, *Chin. J. Biotechnol.*, 10 (1994) 18–23.
- [7] T.A. Kunkel, J.D. Roberts and R.Z. Zakour, *Methods Enzymol.*, 154 (1987) 367–382.
- [8] D. Shortle and A.K. Meeker, *Biochemistry*, 28 (1989) 936–944.
- [9] D. Shortle, *J. Cell. Biochem.*, 30 (1986) 281–289.
- [10] P. Cuatrecasas, H. Edelhoich and C.B. Anfinsen, *Proc. Natl. Acad. Sci. U.S.A.*, 58 (1967) 2043–2050.
- [11] P. Cuatrecasas, S. Fuchs and C.B. Anfinsen, *J. Biol. Chem.*, 242 (1967) 1541–1547.
- [12] R.F. Steiner, R.E. Lippoldt, H. Edelhoich and V. Frattali, *Biopolymers, Symp.*, 1 (1964) 355.
- [13] D.C. Turner and L. Brand, *Biochemistry*, 7 (1968) 3381–3390.
- [14] C.H. Luan, T.M. Parker, D.C. Gowda and D.W. Urry, *Biopolymers*, 32 (1992) 1251–1261.



ELSEVIER

Journal of Chromatography A, 685 (1994) 39–44

JOURNAL OF
CHROMATOGRAPHY A

High-performance liquid chromatographic analysis of low-molecular-mass products synthesized by polynucleotide phosphorylase in polymerization reaction[☆]

Andrew L. Simanov

Moscow State University, BioChemMack Joint Venture, Leninskie Gory, 119899, Moscow GSP-3, Russian Federation

First received 7 September 1993; revised manuscript received 24 June 1994

Abstract

HPLC was used for the simultaneous analysis of low- and high-molecular-mass products of nucleotide polymerization. Oligonucleotides with chain lengths of less than 5 monomer units were found in the reaction mixture at the very beginning of the reaction. These oligomers were not the products of non-specific polymer degradation. An increase in NaCl concentration from 0 to 1 M resulted in the appearance of a short lag period and the oligonucleotide accumulation. A simultaneous increase in Mg^{2+} concentration eliminated the lag. It is concluded that high ionic strength affects both the formation of the metal–monomer–polymer complex and the affinity of the polynucleotide phosphorylase molecule for the reaction products.

1. Introduction

Polynucleotide phosphorylase (PNPase) is known to catalyze both the polymerization of ribonucleoside 5'-diphosphates (followed by inorganic phosphate release) and the reverse reaction of phosphorolysis [1]. These reactions proceed in the presence of divalent metal cations, such as Mg^{2+} or Mn^{2+} . PNPase was used for investigations of RNA structure and processing [2,3] and proved to be a suitable tool for the synthesis of a variety of oligo- and polynu-

cleotides that are widely used in many areas of molecular biology [1].

The mechanism of action of the enzyme is “non-synchronous” [1]. In the case of polymerization the polyribonucleotide chain is elongated by successive addition of monomers. If the synthesis is primed, the primer is incorporated into the chain of the product [4]. But data from the literature indicate that the molecular mass distribution (MMD) of the products formed in the absence of primer is a matter of controversy. The conclusion that the MMD is broad was based on the results obtained by electrophoresis in polyacrylamide gel [5]. Although the authors refrained from analyzing products of less than 17 units in length, their data do not allow to exclude the existence of such molecules. On the other hand, it was argued that no oligomers can be detected in the reaction mixture upon de novo

[☆] Presented at the symposium on *Applications of HPLC and CE in the Biosciences (12th International Symposium on Biomedical Applications of Chromatography/2nd International Symposium on the Applications of HPLC in Enzyme Chemistry)*, Verona and Soave, 7–10 September 1993. The proceedings of this symposium were published in *J. Chromatogr. B*, Vol. 656, No. 1 (1994).

polymerization; rather, the high-molecular-mass polymer is the only product formed [6]. However, analysis of products formed by oligonucleotide phosphorolysis (the reverse process) indicates that all intermediate oligomer types are present in the reaction mixture [7,8], i.e. the mechanism of oligonucleotide phosphorolysis is rather “synchronous”. Besides, the affinity of the enzyme molecule for polynucleotide chains is 10 000-fold higher in the case of a polymer compared to an oligomer [9]. Given that both polymerization and phosphorolysis involve the same steps, the array of short intermediates, whose formation is associated with the phosphorolysis, may be formed during the polymerization as well. Therefore, the presence of intermediates in the reaction mixture cannot be completely excluded.

The methods used until now for the analysis of the whole spectrum of nucleotide polymerization products are time-consuming. Gel permeation [6] and paper chromatography [4] give some idea of the overall distribution of the components of the reaction mixture. Gel electrophoresis [5] demonstrates molecular mass polymorphism of the products of polymerization, but fails to provide accurate data regarding the smallest oligomers. Unfortunately, oligonucleotides (with a chain length of less than 10 monomer units) could not be analyzed by electrophoresis together with polymers, although it is the short oligomer that was of interest to us. In this study we report for the first time on the utilization of an HPLC technique for the analysis of the products of a ribonucleoside 5'-diphosphate polymerization. The method involves simultaneous determination of high- and extremely low-molecular-mass components of the reaction mixture.

2. Experimental

2.1. Polymerization assay and sample preparation

Adenosine 5'-diphosphate (ADP) (87% purity) was purchased from Vector (Berdsk, Russian

Federation). The preparation contained adenosine 5'-monophosphate (AMP) and adenosine 5'-triphosphate (ATP) as contaminants. The increase in the content of ATP was determined independently by the bioluminescent method [10].

The preparation of PNPase from the thermophilic microorganism *Thermus thermophilus* (“Biolar”, Latvia) had a specific activity of $2.0 \cdot 10^{-2}$ U/ml (0.3 mg protein per ml, 3% of nucleic acids) in the reaction of ADP polymerization (one unit of activity is defined as the amount of the enzyme sufficient to release 1 μ mol inorganic phosphate, P_i , per minute at 70°C and pH 8.1).

The polymerization reaction was carried out in 50 mM Tris-HCl buffer, pH 8.55 (room temperature), in the presence of 1 mM EDTA, 10 mM ADP, the enzyme, and the desired concentrations of $MgCl_2 \cdot 6H_2O$ and NaCl (for details, see the captions to relevant figures). The mixture was incubated at 70°C and aliquots were taken to measure the amount of P_i released [11]. In addition to phosphate determination the reaction was monitored by HPLC as well. Samples were diluted 8-fold with the starting buffer (see below) supplemented with 30 mM EDTA.

For the raw estimation of the oligomer mass the reaction mixture was desalted by passing it through small Bio-Spin-like columns prepacked with Bio-Gel P-2, P-4, P-6 (Bio-Rad, USA); the supports had exclusion limits of M_r 1800, 4000 and 6000, respectively. High-molecular-mass components, including the enzyme, were eluted without any impediment, while small molecules were retained in the gel pores in accordance with exclusion limits of a particular support. ADP was used as an internal retention standard for low-molecular-mass components.

Phosphorolysis was carried out as follows. The process of polymerization was stopped by cooling the samples on ice. The reaction mixture was desalted as described above. The same volume of the two-fold more concentrated reaction buffer containing P_i instead of ADP was added. The final concentrations of $MgCl_2 \cdot 6H_2O$ and KH_2PO_4 were equal to 25 and 50 mM, respectively.

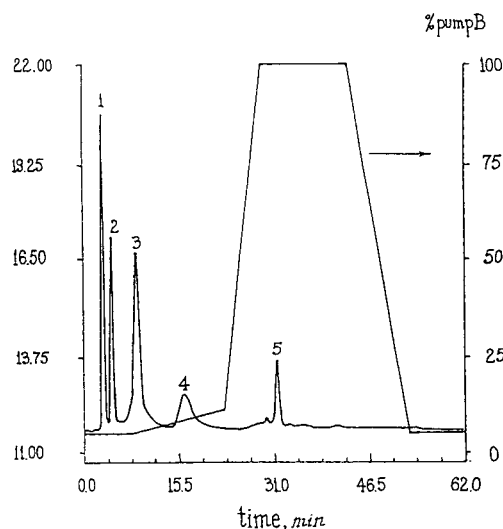


Fig. 1. Ion-exchange HPLC of ADP polymerization mixture and model compounds with our gradient scheme. Values on the left-hand y-axis are percentages of detector 1 V output. Peaks: 1 = adenosine (retention time 3.0 min); 2 = AMP (4.1 min); 3 = ADP (7.2 min); 4 = ATP (16.2 min); 5 = poly(A) (31.0 min).

2.2. High-performance liquid chromatography

The reaction mixture was analyzed at 55°C on a Bio-Rad 800 HPLC gradient system using a Bio-Gel DEAE-5-PW ion-exchange column (75 × 7.5 mm I.D.). The following solutions were used for separating the reaction mixture components: 75 mM Tris-HCl (pH 7.6) served as the starting buffer (A) and buffer A containing 1 M NH₄Cl, as the eluting buffer (B). The effluent was monitored at 260 nm; the scheme of the gradient is depicted in Fig. 1.

3. Results and discussion

The selected operating conditions made it possible to identify both small molecules (such as adenosine, AMP, ADP, ATP), and derivatives of higher molecular mass (Fig. 1). The distribution of the polynucleotide product with respect to chain lengths was previously shown by gel electrophoresis to range from thousands of monomer units to tens of residues [5]. Nevertheless, the polynucleotide was eluted as a single peak.

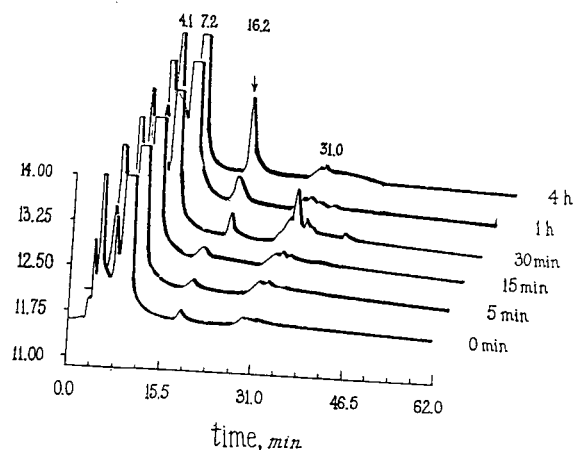


Fig. 2. HPLC separation of the components of the reaction mixture obtained by polymerization of 10 mM ADP for varying times. Conditions are specified in the Experimental section; the reaction mixture contained 0.01 U/ml enzyme and 5 mM MgCl₂ · 6H₂O.

However, a simple modification of the gradient scheme allowed to broaden the poly(A) distribution observed.

A substance with a retention time close to that of ATP was accumulated (Figs. 2–4, the peak is indicated with an arrow). During the first 15 min its concentration was increased 1.5–2-fold. However, according to the results of a bioluminescence analysis, there was no increase in ATP

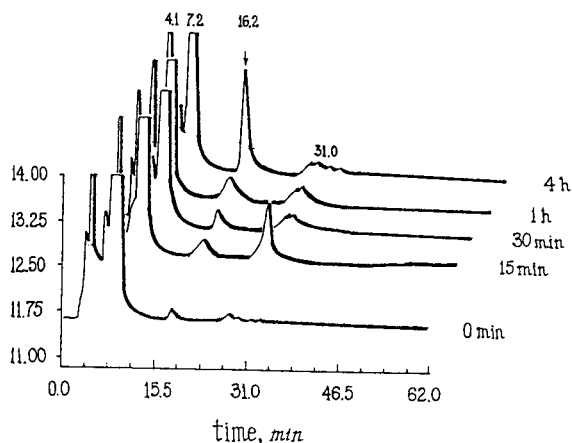


Fig. 3. HPLC separation of the components of the reaction mixture obtained by polymerization of 10 mM ADP for varying times. Reaction conditions as in Fig. 2, the medium was supplemented with 1 M NaCl. Retention times (min) are presented.

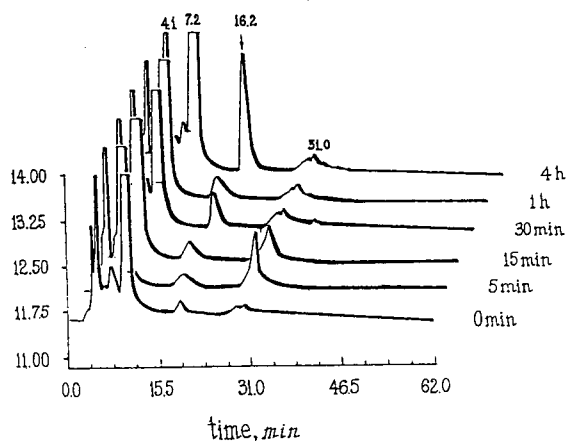


Fig. 4. HPLC separation of the components of the reaction mixture obtained by polymerization of 10 mM ADP for varying times. Reaction conditions are specified in the Experimental section, and the reaction mixture contained 0.01 U/ml enzyme, 20 mM $\text{MgCl}_2 \cdot 6\text{H}_2\text{O}$ and 1 M NaCl.

concentration ($4 \cdot 10^{-4}$ M), at least within 1 h of incubation. On the other hand, this substance, as well as ADP, was retained in the gel pores when Bio-Gel P-2 support (exclusion limit of M_r 1800) was used for the separation of the reaction mixture; this was not the case with components of higher molecular mass. Given the correlation between the charge of phosphates and the retention times (Fig. 1), it was reasonable to assume that this substance was an oligonucleotide with a net charge of phosphate groups similar to that of ATP (-4 under these conditions). It should be noted that a 5'-pyrophosphate-terminated product was not detected in the polymerization mixture [5]. Judging from the results of desalting experiments, the molecular mass of this substance did not exceed 1800 and corresponded to a chain of no more than 5 residues in length (provided that the molecular mass of the monomer is equal to that of AMP). Furthermore, the dinucleotide was shown to be resistant to PNPase-catalyzed phosphorolysis [9]. Since it was not the peak under consideration that was finally increased in the course of the reversed phosphorolysis reaction (Fig. 5), the oligonucleotide was not a dimer. Therefore, the

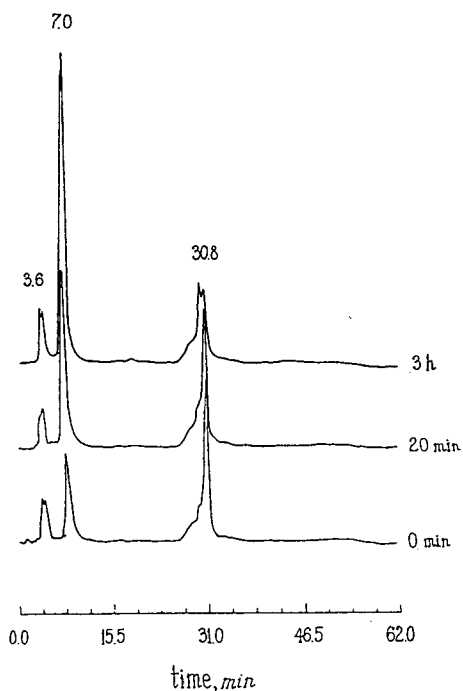


Fig. 5. Reaction of poly(A) phosphorolysis. HPLC separations of the reaction mixture components at indicated times. Conditions as in the Experimental section, except that the mixture contained 0.055 U/ml enzyme.

component appeared to be a short oligomer (3 to 5 monomer units), most likely, a trimer.

This oligomer was unlikely to arise from either phosphorolysis or non-specific degradation [12] of the produced polynucleotide and the endogenous primer. First, the primer content of the enzyme preparation was low (3%, or 5 $\mu\text{g}/\text{ml}$). Judging from the chromatographic data, the yield was at least 10 times higher than it would have been observed, had the product been formed by the primer decomposition in 5 min. Secondly, the amount of inorganic phosphate accumulated 5 min after the onset of the reaction would be insufficient to start the reverse process of phosphorolysis resulting in the formation of a detectable amount of the product (Figs. 2–4). Since endogenous primers were reported [13] to exceed in length the studied oligonucleotide, it can be concluded from this work that an extremely short oligonucleotide synthesized de

novo was found in the reaction mixture soon after the start of the polymerization.

At high NaCl concentration the appearance of detectable phosphate in the medium was preceded by a short lag period (Fig. 6, curve 2), as reported previously [1,14]. The same effect was observed in the presence of low Mg^{2+} concentrations [15]. The simultaneous accumulation of the oligomer was more pronounced at 1 M NaCl (Fig. 3) than in media with low ionic strength (Fig. 2), in spite of the decrease in the overall rate of the reaction (Fig. 6, curves 2 and 1, respectively). This could be expected, given the electrostatic nature of enzyme–nucleic acid interactions. In other words, an increase in NaCl concentration resulted in the dissociation of the complex formed by the enzyme molecule and short oligonucleotide chains. The accumulation of longer oligomers and short polymers takes

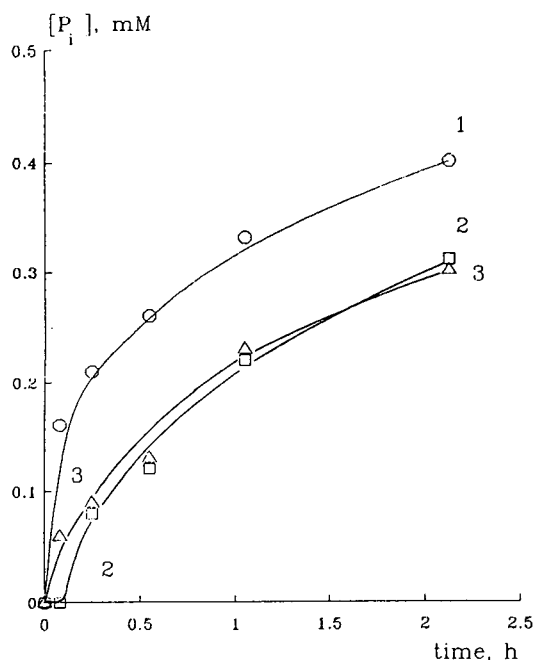


Fig. 6. Release of inorganic phosphate in the course of ADP polymerization. Reaction conditions are specified in the Experimental section. The reaction mixture contained 0.01 U/ml enzyme and 10 mM ADP. Additions: (1) 5 mM $MgCl_2 \cdot 6H_2O$; (2) 5 mM $MgCl_2 \cdot 6H_2O$ and 1 M NaCl; (3) 20 mM $MgCl_2 \cdot 6H_2O$ and 1 M NaCl.

place at low ionic strengths as well [5]. This was demonstrated by gel electrophoresis with other preparations of the enzyme [5], suggesting that high salt concentrations only promoted the process.

If the level of Mg^{2+} in the medium containing 1 M NaCl was increased, the lag was eliminated (Fig. 6, curve 3) and the elongation of the polynucleotide chain became more efficient (Fig. 4, the peak with a retention time of 31.0 min). Given the importance of magnesium ions for the initial step of the reaction [15,16], it can be suggested that the divalent cation takes part in the formation of the active complexes at either the initiation step (monomer–monomer interactions) or during the process of elongation (the interaction of the monomer and the growing chain), as is the case of other polymerases [17]. The appearance of the lag is likely due to the need for the accumulation of a certain amount of oligomers, which would be sufficient for further elongation of the chain [1]. Of course, the phosphorolysis also requires Mg^{2+} ions, so the latter may facilitate the adjustment of the long charged chain on the enzyme molecule by neutralizing the charge. Thus, high salt concentration affects the metal–monomer–chain complex and the affinity of the enzyme molecule for the reaction products.

Acknowledgements

I thank Dr. Gusakov for stimulating discussions and Dr. Simanova for her expert assistance in bioluminescence ATP assay.

References

- [1] T. Godefroy-Colburn and M. Grunberg-Manago, in P.D. Boyer (Editor), *The Enzymes*, Vol. 7, Academic Press, New York, 3rd ed., 1972, p. 533.
- [2] M.N. Thang, B. Beltchev and M. Grunberg-Manago, *Eur. J. Biochem.*, 19 (1971) 184.
- [3] G. Guarneros and C. Portier, *Biochimie*, 73 (1991) 543.
- [4] T. Godefroy, M. Cohn and M. Grunberg-Manago, *Eur. J. Biochem.*, 12 (1970) 236.

- [5] M. Sulewski, S.P. Marchese-Ragona, K.A. Johnson and S.J. Benkovic, *Biochemistry*, 28 (1989) 5855.
- [6] M.N. Thang, R.A. Harvey and M. Grunberg-Manago, *J. Mol. Biol.*, 53 (1970) 261.
- [7] J.Y. Chou and M.F. Singer, *J. Biol. Chem.*, 245 (1970) 995.
- [8] M.F. Singer, R.J. Hilmoie and M. Grunberg-Manago, *J. Biol. Chem.*, 235 (1960) 2705.
- [9] T. Godefroy, *Eur. J. Biochem.*, 14 (1970) 222.
- [10] N.N. Ugarova, G.D. Rozhkova and I.V. Berezin, *Biochim. Biophys. Acta*, 570 (1979) 31.
- [11] A.V. Gusakov, A.L. Simanov, E.G. Becker, A.P. Sinitsyn, *Vestn. Mosk. Univ., Ser. 2: Khim.*, 32 (1991) 523.
- [12] L.G. Marzilli and T.J. Kistenmacher, in T.G. Spiro (Editor), *Nucleic Acid–Metal Ion Interactions (Metal Ions in Biology, Vol. 1)*, Wiley, New York, 1980, p. 180.
- [13] S. Ochoa and S. Mii, *J. Biol. Chem.*, 236 (1961) 3303.
- [14] R.E. Thach and P. Doty, *Science*, 147 (1965) 1310.
- [15] F.R. Williams and M. Grunberg-Manago, *Biochim. Biophys. Acta*, 89 (1964) 66.
- [16] Y. Kikuchi, K. Hirai, F. Hishinuma and K. Sakaguchi, *Biochim. Biophys. Acta*, 476 (1977) 287.
- [17] A.S. Mildvan, *Magnesium*, 6 (1987) 28.

Purification of beet molasses by ion-exclusion chromatography: fixed-bed modelling

Marie-Laure Lameloise*, Richard Lewandowski

ENSIA (Ecole Nationale Supérieure des Industries Agricoles et Alimentaires), 1 avenue des Olympiades, 91305 Massy, France

First received 5 April 1994; revised manuscript received 21 July 1994

Abstract

Sucrose recovery from beet molasses was studied by ion-exclusion chromatography. On the basis of sucrose and NaCl adsorption isotherms, a simple equilibrium model was computed that gave good agreement with molasses band profiles on a single column. At high concentration, it was found necessary to introduce mass transfer resistance to account for band broadening.

1. Introduction

Molasses is a by-product of the sugar industry that still contains about 50% of sucrose. The current development of continuous chromatographic processes [simulated moving bed (SMB)] has given a new impetus to molasses desugarization by ion exclusion in countries where sucrose recovery is economically or technically justified. Many process suppliers have proposed continuous systems for molasses purification and have already built some plants [1–4]. However, very little information is available about the optimum design method, procedural strategy and performance. Optimization of a SMB system requires modelling. The first step consists in modelling the separation on a single column.

Industrial plants involving the SMB principle (about 100 according to Hotier [5]) process purified mixtures, often containing not more than two or three well identified compounds; an

example in the food industry is the extensively studied glucose–fructose separation. Actually, most current or potential applications of preparative chromatography in the food industry concern inputs having complex and often variable compositions, as illustrated in Table 1 for molasses. If the principle of molasses purification is based on Donnan exclusion of ionic species together with a weak adsorption of sucrose, other phenomena may take place to some extent. Modelling of such complex systems requires appropriate methodology.

Most studies addressing preparative-scale chromatographic modelling have dealt with separations in which compounds exhibit favourable, generally Langmuir-type, equilibrium isotherms. Now, ion-exclusion isotherms are well known to be unfavourable and those interested in applications of ion exclusion, whatever the field, have generally not tried to model them. Working on cane molasses desugarization, Saska et al. [7] were one of the very few groups to propose a model including a mathematical representation

* Corresponding author.

Table 1
Typical beet molasses composition (from Ref. [6])

Component	Content (g per 100 g)
Dry matter	75
Total sugar	48–52
Sucrose	48–52
Glucose/fructose	0.2–1.2
Raffinose	0.5–2
Organic matter	12–17
Nitrogeous	6–10
Non-nitrogeous	6–7
Mineral matter	10–12
Sodium	0.3–0.7
Potassium	2–7
Calcium	0.1–0.5
Chloride	0.5–1.5
Phosphorus	0.02–0.07

of unfavourable isotherms; however, owing to the non-linearity, a simplified version had to be derived to allow easy simulation of SMB purification.

The methodology we decided to adopt in this study has been detailed in a previous publication [8]: molasses is assimilated to a binary mixture containing sucrose and a salt; as resin used for molasses desugarization is generally in the Na⁺ form (at least at the beginning) NaCl is selected as the salt and its concentration is taken as equal to that of the ash, representative of ionic-excluded compounds in molasses. Sucrose and NaCl adsorption isotherms have been measured by frontal analysis on single compounds and on mixtures in a broad range of concentrations (up to nearly 600 g/l for sucrose and 110 g/l for NaCl) and found to be unfavourable and interdependent (Figs. 1 and 2). A second-order polynomial was found convenient to represent each set of isotherms, with appropriate coefficients:

Sucrose:

$$q_1 = 0.167c_1 + 0.307 \cdot 10^{-3}c_1^2 + 0.172 \cdot 10^{-2}c_1c_2$$

NaCl:

$$q_2 = 0.068c_2 + 0.176 \cdot 10^{-2}c_2^2 + 0.293 \cdot 10^{-3}c_2c_1$$

As equilibrium data play the major role in shaping the band profiles, a simple equilibrium

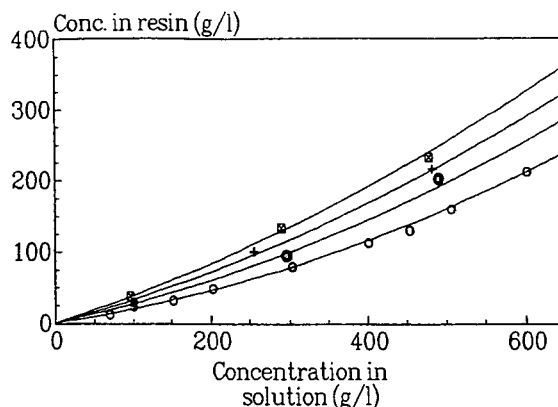


Fig. 1. Equilibrium isotherms of sucrose in mixtures with NaCl at various concentrations: ○ = 0; ● = 42; + = 75; ◻ = 110 g/l. Conditions: 70°C on Dowex C326 resin (from [8]).

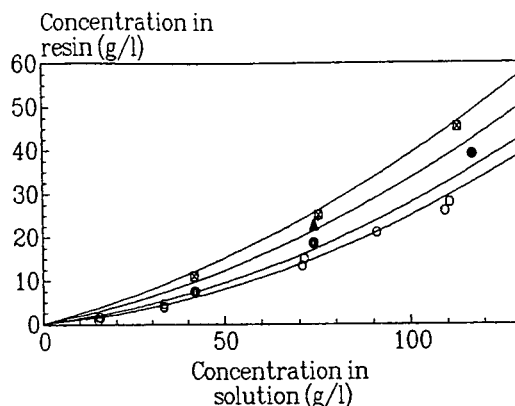


Fig. 2. Equilibrium isotherms of NaCl in mixtures with sucrose at various concentrations: ○ = 0; ● = 98; ▲ = 292; ◻ = 483 g/l. Conditions: 70°C on Dowex C326 resin (from [8]).

model based on previously measured isotherms is now computed to simulate the experimental elution of molasses.

2. Simple equilibrium model

This model is described by the following equations:

Mass balance in the liquid phase for the two solutes:

Sucrose:

$$u \cdot \frac{\partial c_1}{\partial z} + \frac{\partial c_1}{\partial t} + \frac{(1-\varepsilon)}{\varepsilon} \cdot \frac{\partial q_1}{\partial t} = 0 \quad (1)$$

NaCl:

$$u \cdot \frac{\partial c_2}{\partial z} + \frac{\partial c_2}{\partial t} + \frac{(1-\varepsilon)}{\varepsilon} \cdot \frac{\partial q_2}{\partial t} = 0 \quad (2)$$

Equilibrium isotherms:

Sucrose:

$$q_1 = ac_1 + bc_1^2 + dc_1c_2 \quad (3)$$

NaCl:

$$q_2 = a'c_2 + b'c_2^2 + d'c_1c_2 \quad (4)$$

Using normalized coordinates [$x = z/L$ and $\tau = t/t_0 = t(u/L)$], the following set of equations is obtained:

$$\frac{\partial c_1}{\partial x} + A \cdot \frac{\partial c_1}{\partial \tau} + B \cdot \frac{\partial c_2}{\partial \tau} = 0 \quad (5)$$

$$\frac{\partial c_2}{\partial x} + A' \cdot \frac{\partial c_2}{\partial \tau} + B' \cdot \frac{\partial c_1}{\partial \tau} = 0 \quad (6)$$

A , A' , B and B' depend on c_1 and c_2 .

Numerical solution of this set of partial differential equations cannot be achieved by Laplace or Fourier transform methods, because of the nonlinearity of the isotherms. Resolution with a finite difference method was undertaken.

Time derivatives are calculated at $(x, \tau + \Delta\tau/2)$ and a second-order Crank–Nicolson scheme is applied:

$$\frac{\partial c}{\partial \tau} \Big|_{x, \tau + \Delta\tau/2} = \frac{c(x, \tau + \Delta\tau) - c(x, \tau)}{\Delta\tau} \quad (7)$$

For space derivatives, a first-order backward difference is applied:

$$\begin{aligned} \frac{\partial c}{\partial x} \Big|_{x, \tau + \Delta\tau/2} &= \frac{1}{2} \cdot \frac{\partial c}{\partial x} \Big|_{x, \tau} + \frac{1}{2} \cdot \frac{\partial c}{\partial x} \Big|_{x, \tau + \Delta\tau} \\ &= \frac{1}{2} \cdot \frac{[c(x, \tau) - c(x - \Delta x, \tau) + c(x, \tau + \Delta\tau) - c(x - \Delta x, \tau + \Delta\tau)]}{\Delta x} \end{aligned} \quad (8)$$

with the following approximations:

$$c_1(x, \tau + \Delta\tau/2) = c_1(x, \tau) \quad (9)$$

$$c_2(x, \tau + \Delta\tau/2) = c_2(x, \tau) \quad (10)$$

The set of Eqs. 5 and 6 becomes a simple linear system of two equations with two unknowns:

$$c_1(x, \tau + \Delta\tau)P + c_2(x, \tau + \Delta\tau)Q + R = 0 \quad (11)$$

$$c_2(x, \tau + \Delta\tau)P' + c_1(x, \tau + \Delta\tau)Q' + R' = 0 \quad (12)$$

Given initial and boundary conditions, iterative calculation allows the column response $c_1(1, \tau)$ and $c_2(1, \tau)$ to be readily obtained.

For a rectangular injection of concentration c_1^0 in sucrose and c_2^0 in NaCl and of normalized duration τ_e , the initial conditions are expressed as follows:

$$0 < \tau \leq \tau_e \quad c_1(0, \tau) = c_1^0 \quad c_2(0, \tau) = c_2^0 \quad (13)$$

$$\tau > \tau_e \quad c_1(0, \tau) = 0 \quad c_2(0, \tau) = 0 \quad (14)$$

$$\tau = 0 \quad c_1(x, 0) = 0 \quad c_2(x, 0) = 0 \quad (15)$$

A proper choice of time and space increments $\Delta\tau$ and Δx has to be made to ensure stability and precision of the result; in practice, we have found that $\Delta\tau = 0.007$ and $\Delta x = 0.0025$ gave a satisfactory evaluation of the response.

This model is now used to simulate experimental band profiles resulting from more or less diluted molasses loads.

3. Experimental

The resin used in the experiments was Dowex C326 purchased from Dow Chemical; it is a sulphonated styrene–divinylbenzene cation-exchange resin of the gel type. The cross-linking is 6% and the mean diameter of the beads is 326 μm .

Softened beet molasses was furnished by Aplexion. Softening is a necessary preliminary step in the purification process because exclusion is much more efficient when the resin counter ion is monovalent and the resin has a stronger affinity for divalent than for monovalent cations.

In order to simulate as closely as possible industrial operating conditions and especially to ensure that the ionic form of the resin is in equilibrium with the molasses ionic composition, a large amount of molasses was allowed to

percolate through the resin bed; the bed was then washed and was ready to be used.

The experimental device on which elutions were carried out consisted of a jacketed glass column (1 m × 5 cm I.D.) furnished by Pignat. It was equipped with a piston allowing introduction of the feed solution exactly at the top of the resin through a PTFE frit. A purge line ensured that a perfect and non-delayed step signal could be achieved at the entrance of the bed. Feed solutions and water used for rinsing were pumped from a thermostated bath at 70°C by a Gilson Minipuls peristaltic pump. All experiments were performed at 70°C and at a constant flow-rate of about 36 ml/min.

Molasses elution curves were obtained from the rectangular injection of 210 ml of more or less diluted molasses (the injection size corresponds to about 10% of the bed volume); the highest concentration tested corresponded to a molasses diluted twice, comparable to concentrations involved in industrial applications. Samples were collected with a Gilson 201 fraction collector and analysed according to the official methods recommended in the sugar industry for molasses analysis [9]: the sucrose concentration was determined by polarimetry after precipitation by lead acetate and ash was measured by conductivity after dilution.

The results are related to the normalized time t/t_0 , where t_0 is the mean residence time of a non-adsorbing tracer; it was evaluated from Blue Dextran breakthrough curves, as Blue Dextran has proved in previous work [10] to be a good external tracer; its concentration was measured by spectrophotometry with a Carl Zeiss PMQ II spectrophotometer at a wavelength of 635 nm.

Table 2 gives the operating conditions for each elution.

4. Results and discussion

The results obtained are fairly satisfactory (Fig. 3). However, in both cases considered (runs 1 and 2), the simulation overestimates the maximum of the sucrose peak and the steepness of the rear part and makes ash leave the column later than in experiments. As the general features are correctly predicted, however, we tried to improve the quality of the simulation by modifying the isotherm parameters. Empirically, it can be seen that parameters a and a' influence mainly the peak positions and b and b' influence the peak asymmetry; although effective, the influence of d and d' is less easy to characterize. Isotherm parameters were then optimized using a simplex algorithm so that the model response matched the experimental band profiles obtained with the less concentrated molasses load (run 1). Optimized parameters are given in Table 3 and the resulting elution curves are shown in Fig. 4. It can be verified also from Fig. 5 that the parameters so obtained allow the model to simulate fairly well the experiment on a more concentrated molasses (run 2). It is worth noting that the new sucrose equilibrium isotherm is linear in the absence of any other compound ($b = 0$), and that mutual influences of sucrose and ash are lowered.

It is not surprising that we had to modify the isotherm coefficients to account for the sucrose and ash behaviour in such a complex medium as molasses. First, contrary to the simple system

Table 2
Operating conditions for molasses elutions

Run No.	DM (g/l)	Sucrose (g/l)	Ash (g/l)	L (cm)	Injection size (min)	Q (ml/min)	ε	t_0 (min)
1	157	98.3	17.7	110.7	5.86	35.5	0.39	23.88
2	320	196.8	36.1	112.2	5.86	35.5	0.38	23.58
3	476	288.6	51.0	109.8	5.86	35.8	0.39	23.49

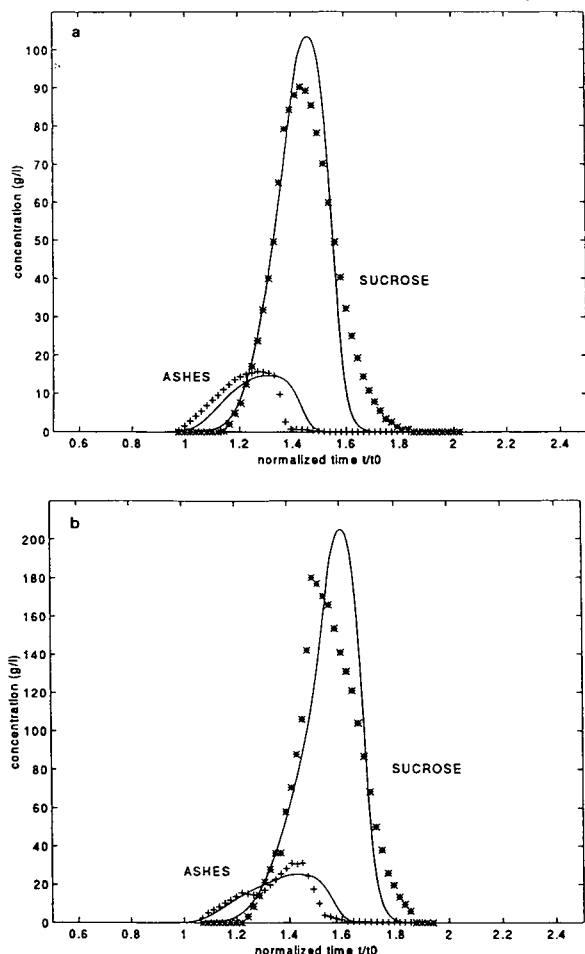


Fig. 3. Molasses elution curves: experiment (points) and simulation (solid line) by the simple equilibrium model with isotherm parameters measured on the sucrose–NaCl system. Operating conditions in Table 2. (a) Run 1; (b) run 2.

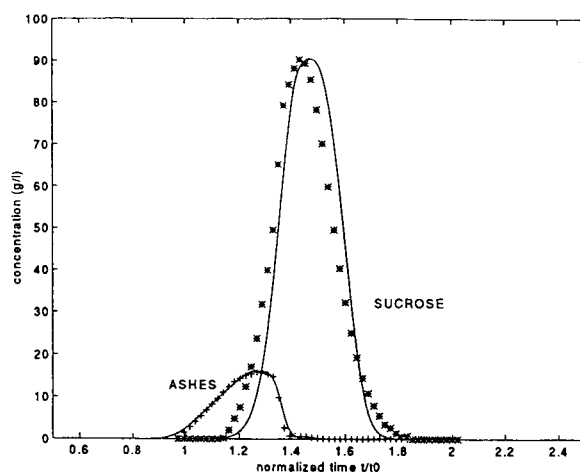


Fig. 4. Molasses elution curves (run 1): experiment (points) and best fit obtained with the simple equilibrium model (solid line).

sucrose–NaCl–Na⁺ resin, which served as a basis for modelling, ion exchange occurs: the actual ionic form of the resin results from an equilibrium with the molasses ionic composition during the elution; it is roughly estimated that about two thirds of the resin is converted into the K⁺ form. Fig. 6 shows the influence of the ionic form of the resin (Na⁺ and $\frac{1}{3}\text{Na}^+/\frac{2}{3}\text{K}^+$ resulting from equilibrium with molasses) on the adsorption of pure sucrose solutions at different concentrations: replacing even partially Na⁺ with K⁺ increases the sucrose retention significantly. Moreover, it should not be forgotten that

Table 3

Isotherm parameters obtained by frontal analysis of sucrose–NaCl mixtures and by fitting the simple equilibrium model with the molasses elution curve (run 1)

Method	Sucrose			Ash		
	<i>a</i>	<i>b</i>	<i>d</i>	<i>a'</i>	<i>b'</i>	<i>d'</i>
Measured by frontal analysis on sucrose–NaCl mixtures ^a	0.167	$0.307 \cdot 10^{-3}$	$0.172 \cdot 10^{-2}$	0.068	$0.176 \cdot 10^{-2}$	$0.293 \cdot 10^{-3}$
Fitted on molasses elution (run 1)	0.24	0.0	$0.172 \cdot 10^{-3}$	0.0134	$0.4 \cdot 10^{-2}$	$0.05 \cdot 10^{-3}$

^a From Lewandowski and Lameloise [8].

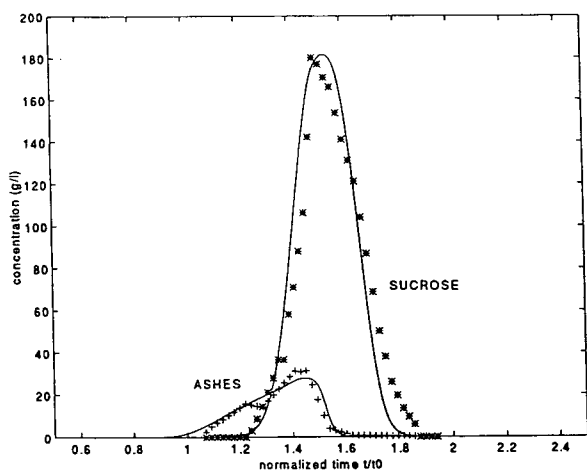


Fig. 5. Molasses elution curves (run 2): experiment (points) and simulation (solid line) by the simple equilibrium model with isotherm parameters optimized on run 1.

coloured matter, organic compounds such as betaine and other impurities contained in molasses may influence the sucrose and ash adsorption.

At higher concentrations of molasses (run 3: 288.6 g sucrose/l), modifications of the band profiles occur (Fig. 7): they broaden and flatten out, and a shoulder appears on the rear part of the band, almost visible on the sucrose peak. Simulation with previously optimized parameters

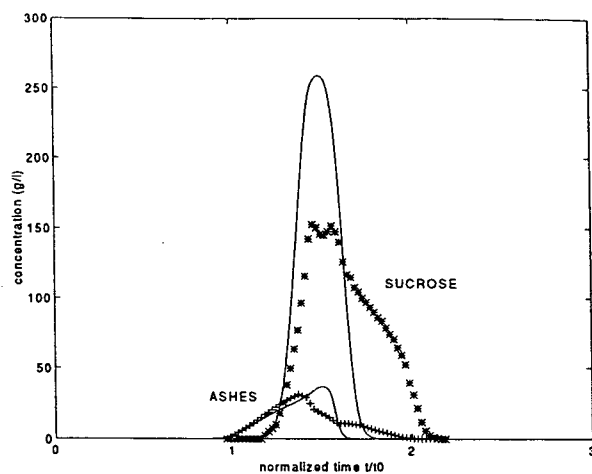


Fig. 7. Molasses elution curves (run 3): experiment (points) and simulation (solid line) by the simple equilibrium model with isotherm parameters optimized on run 1.

gives very poor results. Such deformations have also been observed when eluting highly concentrated sucrose–NaCl mixtures; therefore, they are not to be attributed to the influence of impurities in molasses such as betaine or coloured matter. At such concentration levels, mass transfer resistance is perhaps no longer negligible. A model accounting for sucrose transfer resistance was elaborated.

4.1. Mass transfer resistance model

As indicated by Ruthven [11], under most practically realizable conditions, the intraparticle resistance is more important than film resistance in determining the mass transfer rate. Therefore, film resistance was neglected.

As a gel-type resin was used here, a diffusion model characterized by an equivalent diffusivity D_e has a reasonable chance of describing sucrose migration inside resin beads. To avoid complexities rising from the second-order derivatives, the diffusion equation is often approximated by a linear driving force model with a mass transfer coefficient k_d . Glueckauf [12] has demonstrated the equivalence of the two models when isotherms are linear, provided $k_d = 5(D_e/R_p)$. Ruthven [11] showed that this equivalence is still

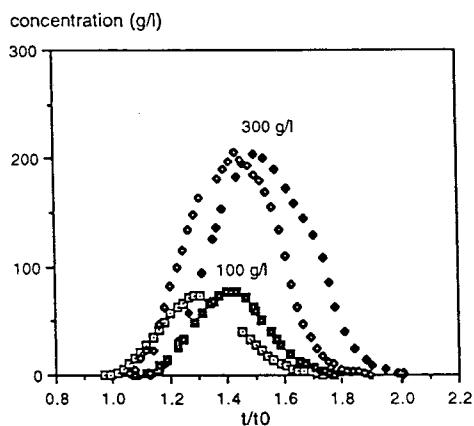


Fig. 6. Influence of ionic form of the resin on sucrose adsorption. Sucrose 100 g/l; resin in (\square) Na^+ form and (\blacksquare) Na^+/K^+ form. Sucrose 300 g/l; resin in (\diamond) Na^+ form and (\blacklozenge) Na^+/K^+ form. Other operating conditions as in Table 2.

acceptable in the case of unfavourable or moderately favourable isotherms.

The following system is then to be solved:

$$u \cdot \frac{\partial c_1}{\partial z} + \frac{\partial c_1}{\partial t} + \frac{(1-\varepsilon)}{\varepsilon} \cdot \frac{\partial q_1}{\partial t} = 0 \quad (16)$$

$$u \cdot \frac{\partial c_2}{\partial z} + \frac{\partial c_2}{\partial t} + \frac{(1-\varepsilon)}{\varepsilon} \cdot \frac{\partial q_2}{\partial t} = 0 \quad (17)$$

$$\frac{\partial q_1}{\partial t} = \frac{1}{t_m} (q_1^* - q_1) \quad \text{with } t_m = \frac{R_p}{3k_d} \quad (18)$$

Sucrose:

$$q_1^* = ac_1 + bc_1^2 + dc_1c_2 \quad (19)$$

Ash:

$$q_2 = a'c_2 + b'c_2^2 + d'c_1c_2 \quad (20)$$

Adopting the same discretization schemes as previously, a set of three equations with three unknowns is obtained and solved iteratively from boundary and initial conditions:

$$c_1(x, \tau + \Delta\tau)E + q_1(x, \tau + \Delta\tau)F + G = 0 \quad (21)$$

$$q_1(x, \tau + \Delta\tau)H + T = 0 \quad (22)$$

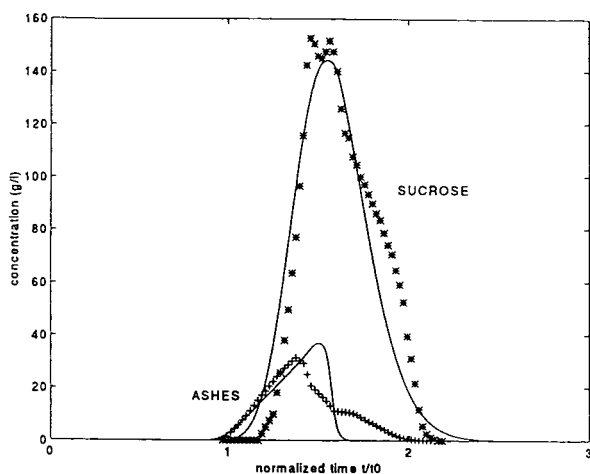


Fig. 8. Molasses elution curves (run 3): experiment (points) and best fit obtained with the mass transfer resistance model (solid line).

$$c_2(x, \tau + \Delta\tau)U + c_1(x, \tau + \Delta\tau)V + W = 0 \quad (23)$$

This model with a time constant $t_m = 50$ s improves the sucrose representation and especially the band broadening, but without accounting for the shoulder (Fig. 8). Moreover, the first coefficient of the isotherm has to be increased ($a = 0.3$ in place of 0.24) to locate the band at the correct position, suggesting that the shape of the isotherm might be more complex at these concentrations. Finally, no significant improvement to the ash band profile is observed. At high concentration, as exclusion is less effective, penetration of ash into the resin beads is no longer negligible, and kinetic limitation of transfer should probably also be considered.

5. Conclusion

For loads representing 10% of the bed volume, a simple equilibrium model based on sucrose and NaCl isotherms gives a satisfactory representation of the elution of molasses containing up to 320 g DM/l (which corresponds to a dilution ratio of about 3); a minor adjustment of parameters is necessary, however, to take into account the influence of the ionic form of the resin and the more complex nature of the medium.

For a more concentrated load, the predictions of the simple equilibrium model are far from reality. The introduction of a resistance to sucrose transfer in the form of a linear driving force allows the sucrose representation to be improved, but does not account for the shoulder on the rear side of the sucrose band and for ash tailing. In order to ensure continuity between the two models, the kinetic parameter should vary with concentration. Moreover, the necessary modification of the sucrose isotherm first parameter to locate the peak at the right position suggests that the isotherm might be more sophisticated at these concentrations.

However, as far as batch-type experiments are concerned, optimization of purity and recovery of the sucrose fraction would rather lead to the choice of a limited load with low concentration.

Symbols

a, a'	isotherm coefficient
b, b'	isotherm coefficient
c	concentration in the liquid phase
d, d'	isotherm coefficient
D_e	effective diffusivity
k_d	mass transfer coefficient
L	bed length
q	concentration in solid phase (averaged over particle volume)
q^*	concentration in the solid phase, at the particle surface
Q	flow-rate
R_p	particle radius
S	column section
t	time
t_0	mean residence time of a non-adsorbing tracer
t_m	transfer time constant
u	velocity
x	dimensionless abscissa in column
z	abscissa in column

Greek letters

ε	external porosity
τ	normalized time = t/t_0
τ_e	normalized injection time

Subscripts

1	relates to sucrose
2	relates to NaCl or ash

Abbreviations

DM	dry matter
SMB	simulated moving bed

References

- [1] M. Buckley and G. Norton, *Int. Sugar J.*, 93 (1991) 204.
- [2] K.P. Chertudi, *Int. Sugar J.*, 93 (1991) 28.
- [3] R. Gadowski, *Sugar Azucar*, (1991) 34.
- [4] M. Kearney, in *Proceedings of the Sugar Processing Research Conference, 1990*, p. 291.
- [5] G. Hotier, in *Proceedings of the 9th International Symposium on Preparative and Industrial Chromatography, Nancy, April 1992*, p. 235.
- [6] B.P. Baker, *Composition, Properties and Uses of Molasses and Related Products*, United Molasses Trading, 1971.
- [7] M. Saska, M.D. Wu, S.J. Clarke, K. Iqbal and M. Mrini, *Int. Sugar J.*, 95 (1993) 137.
- [8] R. Lewandowski and M.L. Lameloise, *Chem. Eng. Proc.*, 31 (1992) 207.
- [9] *Méthodes d'Analyses de l'I.R.I.S.*, Institut de Recherche de l'Industrie Sucrière, Villeneuve d'Ascq, 1984.
- [10] M.L. Lameloise and V. Viard, *J. Chromatogr. A*, 679 (1994) 255.
- [11] D.M. Ruthven, *Principles of Adsorption and Adsorption Processes*, Wiley, New York, 1984.
- [12] E. Glueckauf, *Trans. Faraday Soc.*, 51 (1955) 1540.

Ion chromatographic determination of fluoride in welding fumes with elimination of high contents of iron by solid-phase extraction

M. Teresa S.D. Vasconcelos*, Carlos A.R. Gomes, Adélio A.S.C. Machado

LAQUIPAI, Chemistry Department, Faculty of Science, P4000 Porto, Portugal

First received 22 March 1994; revised manuscript received 15 July 1994

Abstract

An ion chromatography (IC) procedure was developed for the determination of fluoride in fumes from arc-electric welding of steels with basic electrodes. The interference of metal ions was eliminated by passing the sample solution through an on-line pre-column of a strong cation-exchange resin. Both a strong acid (H^+ form) resin and a strong chelating (Na^+ form) resin were experimented for this purpose. Linear response was obtained from 0.02 to 1 mg of fluoride (in a 50- μ l loop), which corresponds to a concentration range from 0.15 to 7.5 mg/m³ air (6 to 300% of the threshold limit value-time weighted average), for the experimental conditions used (2-h sampling periods, air flow-rate 17 l/cm² · h, through a 1.2- μ m pore size cellulose nitrate filter, from which a 1-cm diameter disk was attacked and analysed). The short-term (within 30 min) precision of the IC determination was <3% (7 determinations). The accuracy of the procedure was evaluated by analysing both synthetic solutions and real samples. When several mixed standard solutions of fluoride, iron(III) and aluminium(III), covering the ranges and ratios of concentration levels in real samples, were analysed, practically quantitative fluoride recovery (97–101%) was found. When 13 samples with 0.6–18 mg/l of fluoride were determined in parallel by IC (0.03–0.9 μ g injected) and a well established ion-selective electrode (ISE) procedure, no bias was found: a linear regression $[IC] = 0.99 (\pm 0.12) [ISE] + 0.9 (\pm 1.4)$ (confidence limits at 95% confidence level in parentheses) was obtained.

1. Introduction

Fluoride has been identified as an important pollutant in arc-electric manual welding with basic electrodes, whose coating includes a large amount (20–40%, w/w) of salts of this anion, e.g., calcium fluoride and sodium fluoride [1–3]. In a programme developed in this Department [4,5] for studying the occupational atmosphere of a large welding plant, a large number of samples

of fumes had to be analysed and procedures to expedite the fluoride determinations were considered. Until recently, ion-selective electrode (ISE) potentiometry was the main technique used for this purpose [6–11]. In such measurements, the interferences of metal ions, of which iron(III) and aluminium(III) are usually the most important, are easily eliminated by complexation with 1,2-cyclohexylenedinitrilotetraacetic acid (CDTA), or a similar complexant included in a “total ionic strength buffer” (TISAB) [6] added to the solution. Ion chroma-

* Corresponding author.

tography (IC) with conductivity detection is a sensitive technique of increasing relevance for ionic quantification in environmental samples. It has been applied to the determination of fluoride in several types of samples including air filtrates [10–13], and can be advantageous for determinations on welding fumes provided interferences of metal ions are avoided. The same type of interferences occurs in IC with spectroscopic detection (UV–Vis, after post-column reaction [14], or fluorescence, in AlF^{2+} form [15]).

In the present case, the most frequent process in the plant was manual welding of mild steel with basic electrodes, which produces a large quantity of iron and some aluminium. Unless their interference is eliminated, those metals would provoke low results for fluoride, due to the formation of stable metal ion complexes. When IC with conductivity detection was applied to airborne particulate matter from aluminium smelters [11], no marked interference of aluminium was noted and the interference of iron was not considered. Therefore, no procedure to eliminate interferences was included in the analytical method. IC was also applied to welding fumes [10], but the procedure used to eliminate interferences was not explicitly mentioned. On the other hand, complexation of iron(III) with cyanide, used to avoid the precipitation of iron hydroxides in IC determination of anions in natural waters [16], is not convenient for IC since the large affinity of the hexacyanoferrate(III) for the resins may provoke deterioration of the columns. In addition, complexants like CDTA used in TISAB can provoke poisoning of the columns by accumulation, probably due to the high charge of the ion.

In the present study, alternative procedures for elimination of the iron(III) interference in the determination were considered. There is currently much interest in using solid-phase extraction as a preparative technique for IC when cleaning up samples prior to analysis is required and dilution or filtration are unsuitable, like in the present case, where interferences and analyte are both soluble [17,18]. In consequence, it was decided to study the use of on-line solid-phase extraction for elimination of the interfer-

ence. This paper reports the results of an evaluation study of an IC procedure, for the determination of fluoride in welding fumes, which includes elimination of iron(III) [and aluminium(III)] by solid-phase extraction. In the evaluation, IC and ISE potentiometry were used in parallel for comparison.

2. Experimental

2.1. Instrumentation and operative conditions

Cassela AFC 123 personal samplers (with flow-rates ca. $17 \text{ l/cm}^2 \cdot \text{h}$ or 2 l/min) were used to collect fumes at the breathing zone of welders on cellulose nitrate filters (Millipore RAWP 047 00, $1.2 \mu\text{m}$ pore size).

IC determinations were carried out in a Dionex 4000i ion chromatograph with a conductivity detector, equipped with a HPIC AG4A pre-column to screen foreign matter from the sample, a HPIC AS4A anion separator column and an AMMS anion micromembrane suppressor. The chromatograms were recorded and manipulated in a Spectra-Physics SP4290 integrator (paper rate 0.5 cm/min).

A $50\text{-}\mu\text{l}$ injection loop was used. The eluent was a $0.15 \text{ mM NaHCO}_3/2.0 \text{ mM Na}_2\text{CO}_3$ solution, at a flow-rate of 2 ml/min . The suppressor regeneration reservoir was pressurized with nitrogen at 0.5 atm ($1 \text{ atm} = 101\,325 \text{ Pa}$) to maintain constant flow (ca. 5 ml/min) of regenerant ($12.5 \text{ mM H}_2\text{SO}_4$). Measurements were made on the $100 \mu\text{S/cm}$ scale.

The solutions were injected with polyethylene syringes through a cellulose acetate filter (Schleicher & Schuell FP030/3, $0.2 \mu\text{m}$ pore size) and a cation-exchange pre-column (see below), both disposable (at high levels of interferent two pre-columns were used, see below).

For ISE determinations, a fluoride ISE, a double-junction Ag/AgCl electrode (Orion 94-09-00 and 90-02-00, respectively) and a Sargent Welch 6050 pH meter were used. Measurements were carried out in a polyethylene cell, at $25.0 \pm 0.2^\circ\text{C}$, with magnetic stirring. To control the pH

of the solution, a Philips GAH110 glass electrode was used.

2.2. Solutions

All chemicals were of analytical-reagent grade, unless otherwise stated, and all solutions were prepared with deionised water of resistivity $> 14 \text{ M}\Omega \text{ cm}$.

2.3. Procedures

Filter extracts

For comparison purposes, the following four different pre-treatments of the filter discs were used: (a) ultrasonic extraction with eluent during ca. 30 min; (b) extraction with water at ca. 70°C for 2 h, with magnetic stirring; (c) similar to (b) but with TISAB (pH 5.5) as extractor, at room temperature; (d) attack with concentrated HNO_3 at ca. 80°C (the destruction of the piece of filter was complete in 10 min), the acidity of the solution was neutralized with 300 ml of 5 M sodium hydroxide and, after cooling, the flask was filled with TISAB, the final pH of the solution being 5.2. In all cases calibrated flasks of 5 ml (the minimum volume necessary for a single ISE determination) were used for wet digestion.

Procedures a and b were followed in IC and procedures c and d in ISE determinations. Extraction and analysis were carried out on the same day.

Ion chromatography

Calibrations. From a 1 g/l F^- standard stock solution prepared from NaF dried at 110°C , five or six F^- standards in the range 0.2–20 mg/l were prepared daily in eluent (or in pure water, depending on the medium used for the F^- extraction from the filters).

The IC system was calibrated at the beginning of each run with a blank (matrix of the standards) and the standards. To control within-run sensitivity changes, the highest concentrated standard was analysed after each group of five samples (i.e., after ca. 30 min) and the system was re-calibrated (one-point calibration). F^-

concentrations were obtained automatically from calibration graphs based on peak height. Each determination took about 6 min (because samples also contain NO_3^- and SO_4^{2-} , see Fig. 1).

Metal ion interferences. The metal ion interferences were eliminated by passing the sample solution through on-line pre-columns of styrene-based resin in strong acid H^+ form, with 1.8–2 mequiv. of cation exchange capacity (Dionex "On Guard H"). One unit was found to be enough up to ca. 10 mg/l of iron(III) [in the present case the aluminium(III) concentration is low enough to be ignored], but two serial units were necessary to obtain quantitative fluoride recovery for higher levels of interferent (see discussion below). Alternatively, an on-line pre-column of styrene–divinylbenzene-based chelating resin in Na^+ form (Chelex-100, Bio-Rad) was used. One column with a bed (0.3–0.5 g) equal to an On Guard H (0.18–0.3 mequiv. of cation-exchange capacity) was enough in all situations.

To check the precision and the accuracy of the results, mixed standard solutions of fluoride, iron(III) and aluminium(III), with concentrations in the ranges of 0.5–20 mg/l, 0.5–20 mg/l, and 0.5 mg/l, respectively, were analysed.

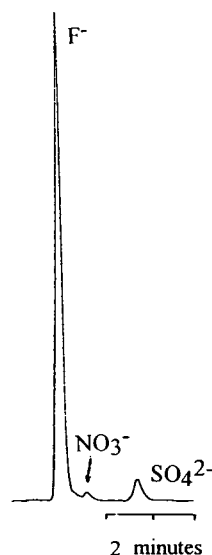


Fig. 1. A real-sample chromatogram obtained for 17.4 mg/l F^- in welding fumes by IC.

ISE potentiometry

For ISE determinations a literature procedure [6–10] was followed.

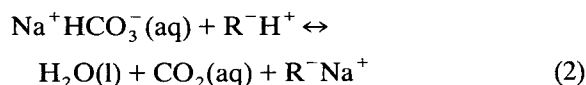
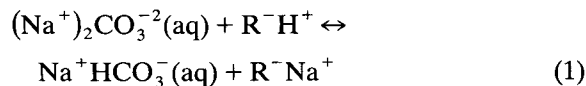
Calibrations. Five standards covering the range of 0.2–200 mg/l were prepared as above but in TISAB. The TISAB was prepared as described in the literature [6] but with 5 g/l of CDTA. The adjustment by linear regression analysis showed no bias and a near theoretical slope down to 0.2 mg/l, with high correlation coefficient ($R > 0.9999$). This value was considered as the practical detection limit for measurements. The F^- electrode was calibrated at the beginning of each working day.

3. Results and discussion

3.1. Baseline perturbation

When the eluent was injected through a on-line On Guard H pre-column (H^+ form), a small baseline perturbation at the beginning of the chromatogram was observed, which may overlap the peak of F^- for low concentrations of the analyte. However, the injection of eluent through a sodium-saturated On Guard H pre-column gave no baseline perturbation.

These results suggest that when the eluent passes through the On Guard H pre-column, hydrogen ion is displaced out of the resin (R^-) by the sodium ion from the eluent, which makes the solution acid (pH 4.5 at the exit of the On Guard H pre-column),



The loss of cations in the acid form of the eluent makes it a comparatively poor conductor, and this is the cause of the negative peak, similar to that found for water injection.

These results showed that when an on-line On Guard H pre-column is included in the system to remove metal ion interferences in the determination of anions, the use of the eluent matrix does not completely prevent the occurrence of a baseline perturbation at the beginning of the chromatogram, which disturbs the F^- peak. Therefore, the influence of this perturbation on the limit of detection of the procedure was investigated. For this purpose, calibrations (blank and six standards in the range 0.2–20 mg/l) without (C1 calibration) and with blank correction (i.e., with the chromatogram of the blank deducted from each standard chromatogram) (C2 calibration) were carried out. The relative errors associated to each standard peak height (h) in C1 calibration were calculated by the equation

$$(h_{C2} - h_{C1}) \cdot 100/h_{C2} \quad (3)$$

It was found (Table 1) that the C1 procedure introduced an error of 43% for the lower standard. The error decreased progressively for the more concentrated standards, and lost significance (<2.5%) for F^- concentrations higher than 10 mg/l. Therefore, a blank correction is required for F^- concentrations lower than 10 mg/L. In the present work, the C2 procedure was used instead of C1.

When the eluent was injected through a on-line Chelex-100 pre-column, no baseline perturbation at the beginning of the chromatogram was observed. This was expected because the resin was in Na^+ form. A typical real-sample chromatogram obtained under these experimental conditions is presented in Fig. 1.

Table 1
Relative errors associated with peak height in calibration without blank corrections (C1 procedure)

Standard (mg/l)	0.2	1.0	2.0	5.0	10	20
Error (%)	43	18	8.8	3.5	2.5	0.7

3.2. Metal interferences

The efficiency of On Guard H and Chelex-100 pre-columns to avoid metal interferences in F^- determinations was evaluated by measurements of the anion concentrations in mixed standard solutions of F^- , Fe(III) and Al(III), in which the concentrations of interferent ions (magnitudes and interferent/ F^- ratios) were similar to or higher than those expected in welding fume samples.

Recovery percentages (Table 2) between 97 and 101% were found for the whole fluoride working concentration range, if a single Chelex-100 pre-column or two On Guard H pre-columns in series were used. A single On Guard H pre-column provided complete recovery only up to 10 mg/l of both F^- and Fe(III) and 0.5 mg/l Al(III). The results also suggest that a Chelex-100 pre-column allows better recovery (98–99%) than two On Guard H pre-columns for the higher levels of concentrations.

3.3. Calibration behaviour and limit of detection

It has been demonstrated [19–22] that careful calibration over a wide range of concentration (\geq two orders of magnitude) in anionic IC with conductivity detection involving background suppression of a weakly basic eluent, reveals that the signal may be not a perfect linear function of the sample concentration (or, more precisely, of

the injected mass of analyte). Deviations from linearity occur caused by the hydrogen ions in the sample band passing the detector. These hydrogen ions will influence the dissociation equilibrium of the carbonic acid. Therefore, the conductance of the baseline during sample elution will be lower than the background level corresponding to the eluent alone. Therefore, reliable results require calibrations and measurements in a narrow range of analyte concentration. However, as environmental samples often show concentration levels dispersed in quite broad ranges, calibration in a narrow range reduces the practical interest of the method.

In the present work, linear regression was applied to a seven-point (six standards and blank) calibration in the range 0.2–20 mg/l of F^- , and perfect linearity was obtained. Therefore, none of the procedures suggested by Midgley and Parker [21] in order to reduce errors was applied to the calibration data. From the intercept and standard deviation of a typical calibration curve, peak height = 40.1 (\pm 0.8) [F^-] – 3.5 (\pm 6.8) (95% confidence limits in parentheses), the detection limit of the procedure was calculated [23]. A value of 0.4 mg/l or 0.02 μ g F^- was found, which corresponds to 4 μ g for each filter disc (or 0.15 μ g/ m^3 air, for a 2-h sample).

The range of concentrations 0.4–20 mg/l F^- was found to be satisfactory for the majority of samples. When samples with higher F^- concen-

Table 2

Mean percentage of fluoride recovery obtained with and without interferents (6 measurements in 30 min)

[F^-] (mg/l)	Recovery \pm S.D. (% , $n = 6$)			
	On Guard H			Chelex 100
	1 pre-column, [Fe^{3+}] = [Al^{3+}] = 0	1 pre-column, [Fe^{3+}] = [F^-], [Al^{3+}] = 0.5 mg/l	2 pre-columns, [Fe^{3+}] = [F^-], [Al^{3+}] = 0.5 mg/l	1 pre-column, [Fe^{3+}] = [F^-], [Al^{3+}] = 0.5 mg/l
0.5	99.2 \pm 1.12	101 \pm 1.44		
5.0	101 \pm 0.68	99.2 \pm 1.31		
10.0	101 \pm 0.17	97.6 \pm 1.20	97.2 \pm 0.41	98.7 \pm 0.19
15.0	99.9 \pm 0.41	93.6 \pm 2.26	97.0 \pm 2.56	97.6 \pm 0.46
20.0	106 \pm 0.35	95.8 \pm 0.80	96.7 \pm 5.63	99.4 \pm 0.33

trations were measured, accuracy was preserved by dilution of the sample solution. For lower F^- concentrations a more sensitive conductivity scale can be employed in the detector (see below).

The chromatographic system must be re-calibrated periodically during the working day, because the precision usually diminishes along the run, as discussed below. For this purpose, to save time, one-point (blank and one standard) calibrations are recommended [24]. In this work the highest standard (20 mg/l F^-) was used for these one-point re-calibrations. To ensure that this procedure preserved the response characteristics of the system, the reference factor, $F_r = \text{peak height}/[F^-] = 39.5 \text{ mS} \cdot \text{l}/\text{mg}$, was compared with the slope of the calibration curve ($40.1 \pm 0.8 \text{ mS} \cdot \text{l}/\text{mg}$). As both values were identical at 95% confidence level, the one-point calibration was considered acceptable.

3.4. Precision

Homogeneity of fume deposition on the filter

As found in a previous work [5], the homogeneity of particle deposition on the filters allows determination on discs of 1 cm diameter.

Analytical signal

The precision of the chromatographic response was evaluated by repeated measurements (six measurements in 30 min) on mixed standard solutions, at different levels of F^- and interferents. The results (Table 2) show that the precision was generally less than 3% when On Guard H pre-columns were used and up to 0.5% for a Chelex-100 pre-column.

3.5. Accuracy

Filter blanks

To check whether the filters used for sampling contributed with F^- , twelve discs cut at random from several blank filters were treated by procedure (a) and measured by IC. For this purpose, a more expanded conductivity scale, $10 \mu\text{S}/\text{cm}$, and calibrations in the range 0.05–1.0 mg/l F^- concentrations were used. For these experimental conditions, the practical detection

limit [23] was 0.03 mg/l (or 1.5 ng) of F^- . Levels of F^- in the range 0.03–0.09 mg/l, with mean $0.06 \pm 0.02 \text{ mg}/\text{l}$ (or $0.6 \pm 0.2 \mu\text{g}$ for each filter disc), were obtained. These values correspond to 15% of the detection limit value and 0.3% of the maximum concentration determined by the present procedure. Similar studies were carried out for both ISE procedures, but in consequence of the relatively higher detection limit of the ISE technique, ca. 0.2 mg/l, F^- was not found. It was concluded that the contribution to F^- from filters was negligible.

Comparison of procedures

As the sample pre-treatment depended on the analytical technique used for measurement, the final results could depend on both stages of the procedure, and therefore it was decided to investigate them separately.

Extractions. To extract welding fumes from filters, HCl solutions have been recommended for ISE determination of F^- [9]. However, acid solutions are unacceptable for IC determination of F^- , because the eluent is alkaline. Besides, with HCl as extractor [9], a large Cl^- peak would occur overlapping the F^- peak, because their retention times are similar.

To evaluate the influence of wet digestion on the amount of fluoride extracted, pairs of discs cut from six filters were treated in parallel by procedures a and b (see above) and measured by IC. The same procedure was applied to compare the fraction of fluoride extracted by procedures c and d for ISE determinations, but sixteen samples were used. The fluoride concentrations in solution were in the ranges 1.1–20 mg/l (IC) or 0.6–23 mg/l (ISE). Linear least-squares adjustment of each set of results yielded the following equations (95% confidence limits in parentheses [25]), [(a)IC] = $0.938(\pm 0.092) \cdot [(b)\text{IC}] + 0.41(\pm 0.93)$, $R = 0.998$, and [(c)ISE] = $1.067(\pm 0.093) \cdot [(d)\text{ISE}] - 0.3(\pm 1.3)$, $R = 0.989$. These results show no evidence of relative or fixed bias in the measured range, which means that the two extraction procedures used for each type of determination yielded the same fraction of fluoride.

IC vs. ISE. The F^- contents of the thirteen samples, in the range 0.6–18 mg/l, were de-

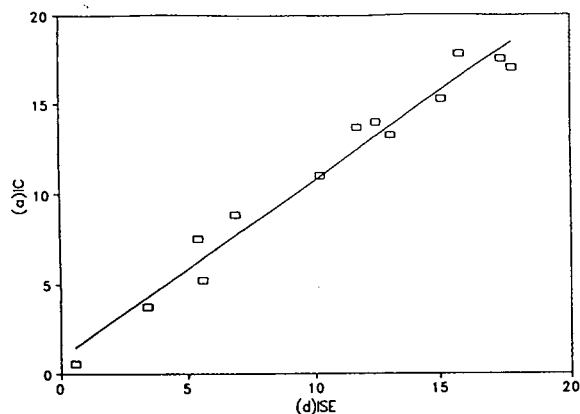


Fig. 2. Comparison of (a)IC vs. (d)ISE methods for F^- determination from welding fumes (see details in the text). Values along axes in mg/l.

terminated in parallel by the (d)ISE procedure (attack with HNO_3) and by the (a)IC method (eluent extraction). A linear regression of IC vs. ISE results (Fig. 2) yielded the equation (95% confidence limits in parentheses) $[(a)IC] = 0.99(\pm 0.12) \cdot [(d)ISE] + 0.9(\pm 1.4)$, with $R = 0.983$. These results show no relative or fixed bias at the measured concentration level. Therefore, the proposed IC procedure is considered to be acceptable for determination of F^- from welding fumes of the present type.

Moreover, these last results together with those obtained in the comparison of the extraction procedures, which showed that (a)IC and (b)IC as well as (c)ISE and (d)ISE were equivalent, show that the fraction of F^- extracted from the filter was independent of pH and of the composition of the solution. These results show that no significant losses of volatile HF occurred during the digestion with HNO_3 . They also suggest that all the F^- in the welding fumes under monitoring was water soluble.

4. Conclusions

The present results show that interferences of metal ions in the IC determination of F^- in welding fumes can be effectively avoided by passing sample solutions through On Guard H or Chelex-100 in Na^+ form on-line pre-columns. The latter seems more convenient since it allows

better precision and accuracy and does not cause any baseline perturbation when samples with eluent as matrix are injected. It was shown that the fraction of F^- extracted was not affected by pH variation over a broad range ($< 0-10.5$) and that mild extraction conditions to aqueous solutions required by IC are adequate.

IC is preferred to ISE when maximum sensitivity and/or speed is required. IC is also more versatile as a measurement technique. Although the ISE technique can be used in a large range of fluoride concentration (0.2–200 mg/l), this range cannot be modified by altering experimental conditions, since both the filter area and dilution volume were fixed. In contrast, IC has a narrower range of linear response (0.4–20 mg/l F^- in the proposed procedure), but the operational range can be moved to higher or lower concentration levels by changing operational parameters, e.g. loop capacity, eluent concentration, the sensitivity of the detector, etc. For instance, a detection limit for the IC procedure one or two orders of magnitude lower than for ISE potentiometry can be obtained, which is particularly suitable for determinations at low concentrations of fluoride in air or for short periods of sampling (grab samples). These are useful for measurement of concentration fluctuations during the working day.

In conclusion, the IC approach provides a sensitive procedure of measuring F^- from welding fumes. Moreover, the technique has considerable potential for the simultaneous measurement of other of inorganic anions in the sample.

Acknowledgement

Financial support from JNICT (Lisbon)-PROGRAMA CIÊNCIA, project M-27/9/20, for acquisition of the Dionex ionic chromatograph is gratefully acknowledged.

References

- [1] N. Jenking, J. Moreton, P.J. Oakley and S.M. Stevens, *Welding Fume, a Critical Literature Review*, Vol. 2, Welding Institute, Cambridge, 1981, p. 278.

- [2] J. Moreton, *Welding Fume, a Critical Literature Review*, Vol. 3, Welding Institute, Cambridge, 1983, p. 38.
- [3] A. Mayer, S. Salsi, A. Peltier, M. Demange, F. Diebold and E. Kanper, *Cah. Notes Doc.*, No. 101 (1980) Note 1281-101-80.
- [4] M.T.S.D. Vasconcelos, M.S. Barbosa, A.A.S.C. Machado and P.H.P. Silva, presented at the *1st International Scientific Conference of the International Occupational Hygiene Association, Brussels, 1992*, abstracts, p. 75.
- [5] M.T.S.D. Vasconcelos, A.A.S.C. Machado and P.A.P. Silva, in preparation.
- [6] P.L. Bailey, *Analysis with Ion-Selective Electrodes*, Heyden, London, 1976, p. 104.
- [7] J. Vesely, D. Weiss and K. Stulik, *Analysis with Ion-Selective Electrodes*, Ellis Horwood, London, 1978, pp. 125–138.
- [8] L.A. Elfers and C.E. Decker, *Anal. Chem.*, 40 (1968) 1659.
- [9] *British Standard Part 1: Guide to Methods for the Sampling and Analysis of Particulate Matter*, British Standard Institution, Linford Wood, 1986, p. 6.
- [10] R.K. Tandon, J. Ellis, P.T. Crisp, R.S. Baker and B.E. Chenhall, *Welding Res. J. Suppl.*, September (1986) 231.
- [11] M. Oehme and H. Stray, *Fresenius' Z. Anal. Chem.*, 306 (1981) 356.
- [12] S.A. Bouyoucos, R.G. Melcher and J.R. Vaccaro, *Am. Ind. Hyg. Assoc.*, 44 (1983) 57.
- [13] P.K. Muller, B.V. Mendoza, J.C. Collins and E.S. Wilgus, in E. Sawicki, J.D. Mulik and E. Wittgenstein (Editors), *Ion Chromatographic Analysis of Environmental Pollutants*, Vol. 1, Ann Arbor Sci. Publ., Ann Arbor, MI, 1978, Ch. 7.
- [14] N.W. Barnett, P. Jones and H.W. Handley, *Anal. Lett.*, 26 (1993) 2525.
- [15] P. Jones, *Anal. Chim. Acta*, 258 (1992) 123.
- [16] N.S. Simon, *Anal. Lett.*, 22 (1988) 319.
- [17] M. Ichikuni and M. Tsurumi, *Anal. Sci.*, 6 (1990) 111.
- [18] Y. Michigami, Y. Kuroda, K. Ueda and Y. Yanamoto, *Anal. Chim. Acta*, 274 (1993) 299.
- [19] M.J. Van Os, J. Slanina, C.L. de Ligny and J. Agterdenbos, *Anal. Chim. Acta*, 156 (1984) 169.
- [20] M. Doury-Berthod, P. Giampaoli, H. Pitsch, C. Sella and C. Pointreud, *Anal. Chem.*, 57 (1985) 2257.
- [21] D. Midgley and R.L. Parker, *Talanta*, 36 (1989) 1277.
- [22] P.F. Lindgren and P.K. Dasgupta, *Anal. Chem.*, 61 (1989) 19.
- [23] J.N. Miller, *Analyst*, 116 (1991) 3.
- [24] L.N. Polite, H.M. McNair and R.D. Rocklin, *J. Liq. Chromatogr.*, 10 (1987) 829.
- [25] J.C. Miller and J.N. Miller, *Statistics for Analytical Chemistry*, Wiley, New York, 1984, pp. 96–100.



ELSEVIER

Journal of Chromatography A, 685 (1994) 61–78

JOURNAL OF
CHROMATOGRAPHY A

Preparation of deactivated metal capillary for gas chromatography

Y. Takayama*, T. Takeichi

School of Materials Science, Toyohashi University of Technology, Toyohashi 441, Japan

First received 31 January 1994; revised manuscript received 21 June 1994

Abstract

Research was conducted to prepare a deactivated metal (stainless-steel) capillary that is physically tough and thermally stable compared with a fused-silica capillary. A key step in the preparation is the formation of a silicon layer by the thermal decomposition of monosilane. The silicon formed on the metal surface is assumed to exist as large grains compared with that on the glass surface. Activation of metal capillary was observed, which is assumed to be due to the migration of silicon grains on the metal surface during the heating test of the capillary, thus exposing the metal surface. Such a phenomenon was not found with a glass capillary treated with monosilane. These observations suggest that the problem comes from the wettability of the metal surface with silicon. The problem was solved by oxidizing the metal surface prior to the monosilane treatment. As a consequence, it became possible to prepare a deactivated metal capillary (DMC) thermally stable even above 400°C. A column coated with a commercially available gum-like liquid phase could not withstand continuous heating at 280°C. On the other hand, a column coated with dimethylpolysiloxane by the in situ (in the capillary) condensation of oligomer prepared from dimethyldichlorosilane showed excellent thermal stability: the column withstood continuous heating above 400°C and also repeated heating by programming up to 450°C. Various advantages of DMC over a fused-silica capillary (FSC) were also made clear. Hence DMC, as a metal capillary of the second generation, should replace FSC.

1. Introduction

Capillary column (capillary column signifies, in this article, a tube coated with liquid stationary phase to differentiate it from a capillary that signifies a tube that is not coated) was invented by Golay in 1957 [1]. At first, a metal was used as the material for the capillary. Handling was easy, but the application range was very limited because of the highly active inner surface.

Metal capillaries as columns for GC were

given up in 1960, and glass capillaries became used. It was found, however, that glass capillaries also possess considerable activity and that homogeneous coating of a medium-polarity or polar liquid phase is difficult. These problems were overcome with great effort and, at the end of 1970s, capillary GC finally came into bloom with the use of deactivated glass capillaries.

Just at this time, fused-silica capillaries (FSC) were reported [2]. FSC are as inert as deactivated glass capillaries and, further, they are flexible. Therefore, FSC completely replaced glass capillaries, which were no longer consid-

* Corresponding author.

ered. As an FSC is covered with a polyimide thin film, we thought that FSC could not be used at high temperatures (above 350°C), and that, even when used below 350°C, FSC is unexpectedly easily damaged owing to the polyimide, which forms cracks and becomes brittle by losing small amounts of volatiles, which cause a notch effect.

In 1980, we started a project to develop a metal capillary of the second generation that is as inert as FSC. With the same purpose, Pretorius's group [3–7] reported results on this aspect for several years after 1981. They started with a stainless-steel capillary and subsequently shifted to a nickel capillary, with which they reported that they succeeded in the preparation of a deactivated metal capillary. As they did not report on the application of the capillary, we doubt if they accomplished the technology successfully. Our methodology is similar to theirs in that thermal decomposition of monosilane is used, but the decomposition conditions are very different. Our conditions are superior, from the industrial point of view, in that the productivity is much better. Further, we introduced an oxidation process of the inner surface of the metal capillary prior to the monosilane treatment, with which it became possible to make a metal capillary that is thermally stable for continuous use above 400°C. We found that *in situ* (in the capillary) synthesis [8,9] of liquid phase by thermal condensation of a diol-type oligomer enabled us to realize columns that withstand repeated use by programming up to 450°C and holding at that temperature for 10 min. We applied the metal capillary or the column where FSC or glass capillaries are difficult to use [10–15]. We also prepared enantiomer separation columns where breakage of the columns is costly [16].

In the 5-year period since 1986, we asked a company to produce and sell the deactivated metal capillary columns (DMCC), and checked possible problems in manufacturing and claims against quality. As a result, it was found out that, although the production of DMC takes time, the productivity is good enough for industrial use, and we received no claim against ca. commercialized 150 columns. Hence it was made

clear that our DMC, taking advantage of the excellent thermal stability and the lack of fear of breakage, is more useful than FSC. Although the manufacturing technology of our DMC needs to be studied further, theoretically, we considered it useful to present the results of our efforts so far.

2. Preparation of deactivated metal capillary

The following description is for a commercial stainless-steel capillary of 0.25 mm I.D. and 0.6–0.7 mm O.D.

2.1. Acid washing of metal capillary

Per 25 m of capillary, 10 ml of chloroform, 10 ml of methanol and then 10 ml of distilled water were passed through at the rate of 1 ml/min. The capillary was filled with concentrated HNO₃ and kept standing at 80°C for 1 h. After cooling, HNO₃ was removed from the capillary, which was then washed by passing 10 ml of distilled water, 10 ml of methanol and then 10 ml of chloroform at the rate of 1 ml/min. Chloroform was removed by a flow of nitrogen gas. The flow-rate was then adjusted to 10–20 ml/min, and the capillary was dried at 200°C for 1 h.

2.2. Oxidation of capillary

Under a continuous oxygen flow at 98.6 kPa, the above-treated capillary was heated to 250°C and then maintained at that temperature for 1 h.

2.3. Treatment with monosilane

Using the apparatus shown in Fig. 1, treatment of the inner surface of the capillary with monosilane (SiH₄), was performed. Monosilane was sealed in the capillary (14) at 295.7 kPa (3 kg/cm²) and valves V1 and V2 were shut. Thermal decomposition of the sealed monosilane was conducted at 530°C for 15 min, after which the capillary was evacuated. Monosilane was sealed again at 295.7 kPa and thermally de-

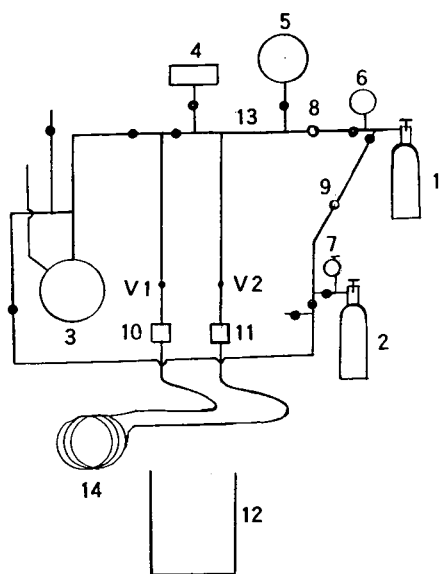


Fig. 1. Apparatus for treating capillary with monosilane. 1 = Monosilane gas cylinder; 2 = nitrogen gas cylinder; 3 = vacuum pump; 4 = Pirani gauge; 5–7 = pressure gauges; 8, 9 = needle valves; 10, 11 = joints; 12 = electric furnace; 13 = stainless-steel manifold line (I.D. 2 mm); 14 = metal capillary; ● = stop valve.

composed similarly. The capillary was evacuated and removed from the apparatus.

2.4. Polarity test for the capillary treated with monosilane

A polarity test was performed following the Grob's polarity test [17,18]. As a precolumn we employed a deactivated non-polar capillary column such as OV-1, $d_i = 0.2$ mm, $20 \text{ m} \times 0.25$ mm I.D. The test mixture was a heptane solution of 0.5 mg/ml of each solute shown in Table 1. The test parameters were as follows: nitrogen flow-rate; 40 cm/s; initial temperature, 60°C ; pro-

gramming rate, $3^\circ\text{C}/\text{min}$; sample volume, 1 ml; and splitting ratio, 1:100.

We can use the following two criteria to evaluate the capillary treated with monosilane: (1) the shape of tailing for each peak of hydrocarbon should be the same as that obtained with the precolumn alone, and (2) tailing of 2,6-dimethylphenol should be only slightly larger than that obtained with the precolumn alone. In this case, 1-decanol generally does not appear, and the peak height of 2,6-dimethylaniline is low.

2.5. Treatment with octamethyltetrasiloxane or other compounds to deactivate the capillary treated with monosilane

For preparation of non-polar column

Prior to the coating of a liquid phase, treatment with octamethyltetrasiloxane was performed. When the oligomer of a non-polar liquid phase terminated with hydroxyl groups is to be coated, octamethyltetrasiloxane treatment can often be omitted. For the easily tailing solutes, octamethyltetrasiloxane treatment should be done prior to the coating.

Octamethyltetrasiloxane treatment was performed as follows. A plug of 100% octamethyltetrasiloxane was inserted into the capillary treated with monosilane so that the length of the plug was ca. 10% of the capillary, and dynamic coating was conducted. The rate of movement of the plug was ca. 2 cm/s. After passing the plug, the capillary was dried with a nitrogen flow for 1 h. Both ends of the capillary were sealed under vacuum. The capillary was treated at 400°C for 10 h in an oven. After being

Table 1
Test mixture

Solute	Abbreviation	Solute	Abbreviation
2,3-Butanediol	D	1-Decanol	ol
<i>n</i> -Butyric acid	Ba	<i>n</i> -Tridecane	C ₁₃
2,6-Dimethylphenol	P	<i>n</i> -Tetradecane	C ₁₄
2,6-Dimethylaniline	A	<i>n</i> -Heptadecane	C ₁₇

cooled, the capillary was opened and rinsed with dichloromethane [19].

For preparation of polar column

Although treatment depends on the liquid phase to be coated later, 1,3-diphenyl-1,1,3,3-tetramethyldisilazane (DPTMDS) [20] was generally used instead of octamethyltetrasiloxane. The procedure was similar to that with octamethyltetrasiloxane. When Carbowax (CW) is to be used as a liquid phase, Aue et al.'s ageing method [21] was conducted as a further treatment of the capillary treated with monosilane. That is, a plug of a 5% dichloromethane solution of CW was inserted into the capillary so that the length of the plug was ca. 20% of the capillary, and dynamically coated at the rate of 2 cm/s. After drying with a nitrogen flow, both ends were sealed and heated at 280°C for 3 h. The seal was opened and the capillary was rinsed with dichloromethane. For the coating of Silar 5CP as a liquid phase, a plug of a 7% solution of 5CP in dichloromethane was used as further treatment of the capillary instead of CW mentioned above. Other details can be found elsewhere [20,22–25].

2.6. Polarity test for the capillary treated with the process in Section 2.5

Quality evaluation was performed under the same test parameters as mentioned in Section 2.4, using a precolumn coated with the liquid phase intended to be coated, and at a programming rate of 1°C/min if necessary. The aim is to obtain a chromatogram the same as that with the precolumn, except for retention time.

3. Results and discussion

3.1. Research on treatment of glass capillary with monosilane

A study was conducted to obtain operating parameters for monosilane (SiH_4) treatment. A Pyrex glass capillary with an untreated inner surface was submitted to monosilane treatment

using the apparatus shown in Fig. 1, and a chromatogram of the monosilane-treated capillary was obtained to evaluate the degree of deactivation following the procedure in Section 2.4. In Sections 3.1 and 3.2, columns coated dynamically with CW20M or 40M were used as precolumns unless mentioned otherwise. The test mixture often did not include 2,6-dimethylphenol and 2,6-dimethylaniline. Although the amounts of solutes in the test mixture are not perfectly accurate, they are sufficient as the relative retention and shape of each peak are discussed in this paper. The following results were obtained.

(i) When ca. 10 m of capillary was used, it is difficult to recognize the difference in the relative retention of solutes between the chromatogram and that using the precolumn alone. When a longer capillary is used, however, the late elution of hydrocarbons compared with other solutes becomes substantial (Figs. 2–4).

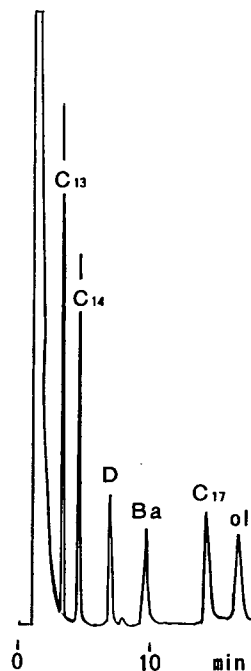


Fig. 2. Chromatogram of test mixture on precolumn coated with CW20M alone. Precolumn, 30 m \times 0.28 mm I.D. Test parameters: initial oven temperature, 80°C; programming rate, 1°C/min; N_2 flow-rate, 0.5 m/s. Test mixture and abbreviations: see Table 1, but not containing P and A.

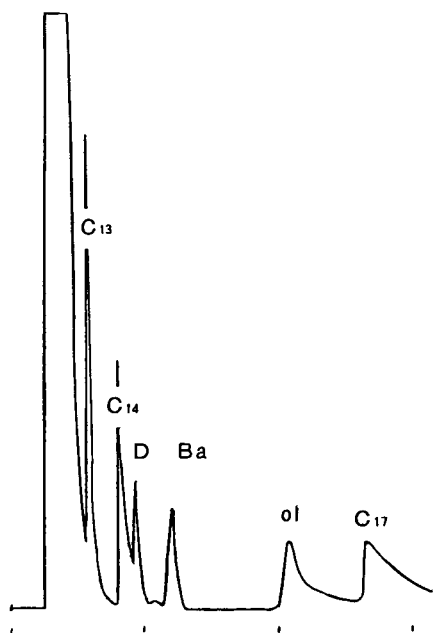


Fig. 3. Polarity test chromatogram of monosilane-treated glass capillary with precolumn of CW20M. Capillary size, 60 m \times 0.28 mm I.D. Parameters for monosilane treatment: monosilane seal pressure, 98.6 kPa; thermal decomposition, 375°C for 15 min. Test parameters: see Fig. 2.

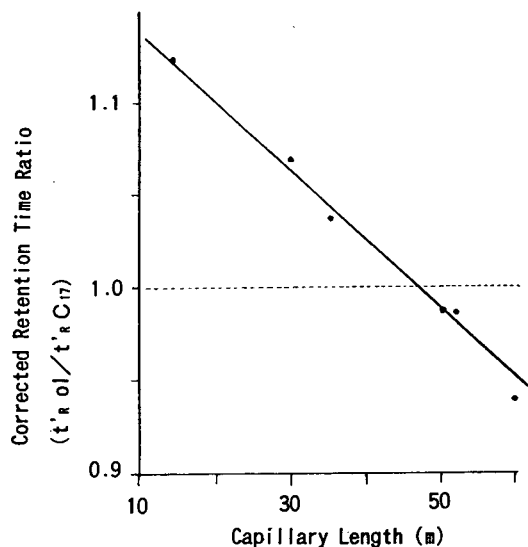


Fig. 4. Elution order of 1-decanol and C₁₇ depending on capillary length. Glass capillary, I.D. 0.28 mm. Parameters for monosilane treatment: 98.6 kPa, 400°C, 15 min. Test parameters: see Fig. 2.

(ii) As the decomposition temperature of monosilane is elevated from 375 to 550°C (softening temperature of the capillary), the peaks of hydrocarbons become narrower, keeping a triangular shape with sharp front, and tend to show leading in shape at 500–550°C (Fig. 5). The retention times of solutes, however, are almost constant independent of the decomposition temperature.

(iii) The peak of 1-decanol is higher when the decomposition temperature of monosilane is low than when the decomposition temperature is high, as shown in Figs. 3 and 5. When the decomposition temperature exceeds 500°C, the peak of 1-decanol becomes very small or is absent.

(iv) At decomposition temperatures between 400 and 550°C, the chromatograms obtained were independent of the decomposition time period during 5–60 min at each temperature.

(v) For the capillary of 0.28 mm I.D., the seal pressure of monosilane should be above ca. 50

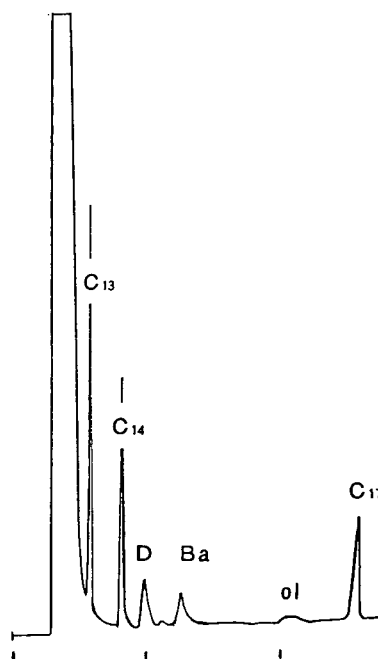


Fig. 5. Polarity test chromatogram on monosilane-treated glass capillary with precolumn of CW20M. Capillary size as in Fig. 3. Parameters for monosilane treatment: 98.6 kPa, 550°C, 15 min. Test parameters: see Fig. 2.

kPa, which corresponds to a thickness of silicon of 178 Å. The capillary treated in that way, when further treated with octamethyltetrasiloxane, gives a chromatogram the same as that in Fig. 2, except for the time needed for each solute to pass through the capillary.

The results in (i) suggest that the silicon is formed inside the glass capillary not as a homogeneous film but as piled small grains. Piled grains have small cavities, and linear hydrocarbons that have a small cross-section are assumed to be retained there temporarily, thus delaying elution. On the other hand, other solutes such as 2,3-butanediol, *n*-butyric acid, 1-decanol and also 2,6-dimethylphenol and 2,6-dimethylaniline, as will be shown later in Fig. 7, do not enter the cavity and elute without delay. As seen from the shapes of the peaks, gas–solid chromatography is assumed to be working with hydrocarbons. The effect of octamethyltetrasiloxane treatment in (v) is that octamethyltetrasiloxane reacted with silanol on the grains to block the cavities, thus acting as a so-called tailing reducer. The liquid phase also should play a role as a tailing reducer [26]. Hence it was clear that broad operation conditions are effective for monosilane treatment as described in (iv) and (v).

3.2. Research on treatment of metal capillary with monosilane

The stainless-steel (SUS 316) capillary washed with water and then with acetone was treated with monosilane as was done with the glass capillary. Evaluation was also conducted similarly. The results are described below.

(i) When the metal capillary was used, even as short as 10 m, an extraordinary chromatogram (Fig. 7a) compared with that of the precolumn (Fig. 6) was obtained. When the metal capillary was replaced with a glass capillary having the same silicon thickness, the chromatogram shown in Fig. 7b was obtained. Even when the metal capillary was used, after the octamethyltetrasiloxane treatment, the chromatogram obtained was same as that in Fig. 6.

(ii) When a column coated with OV-1 was used

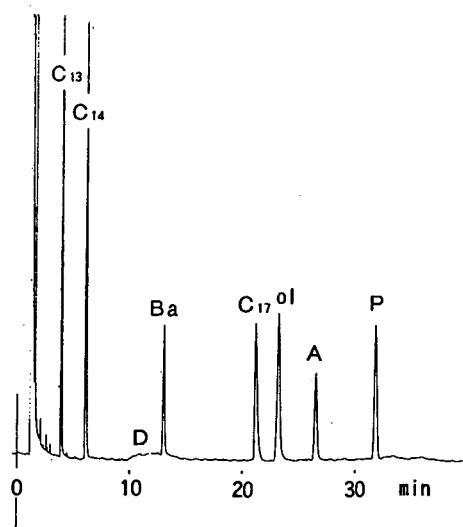


Fig. 6. Chromatogram of test mixture on precolumn of CW40M alone. Precolumn, 20 m \times 0.25 mm I.D. Test parameters: initial oven temperature, 60°C; programming rate, 1°C/min; N₂ flow-rate, 0.28 m/s. Test mixture: see Table 1.

as a precolumn, even with the metal capillary, an extraordinary elution order in the chromatogram was not observed (Figs. 8 and 9)

(iii) Aspects (ii)–(iv) in Section 3.1 was also observed in the case of a 10-m metal capillary.

The results in (i) are considered to arise from the difference in the state of deposited silicon grains depending on the capillary material. With glass, the silicon grains are small and there are few cavities to capture hydrocarbons. With a metal (in this instance stainless covered with very thin layer of naturally grown oxide), the wettability with the silicon is poor and the grains become large, thus increasing the cavities to trap hydrocarbons.

Concerning (ii), taking C₁₇ as an example, as seen from Figs. 6 and 8, C₁₇ enters the capillary at 81 and 144°C in the case of CW40M and OV-1 as precolumns, respectively. The temperature difference is assumed to determine the degree of capture of hydrocarbons.

The requirement of silicon thickness, (v) in Section 3.1, was not ascertained with the metal capillary. When octamethyltetrasiloxane was

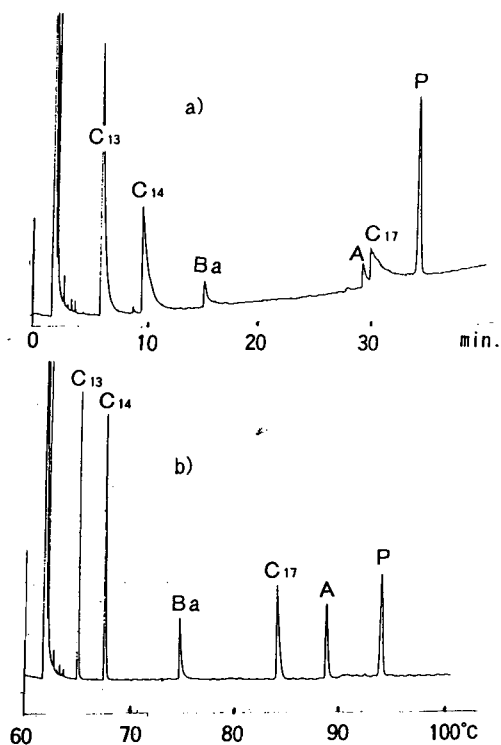


Fig. 7. Polarity test chromatograms on monosilane-treated capillaries with precolumn of CW40M. (a) Metal capillary, 10 m \times 0.25 mm I.D. Parameters for monosilane treatment: 98.6 kPa, 530°C, 15 min. (b) Glass capillary, 10 m \times 0.28 mm I.D. Parameters for monosilane treatment: 98.6 kPa, 500°C, 15 min. Test parameters: see Fig. 6.

used to treat the capillary used for the measurements in Fig. 9, and subjected to the same measurements as in Figs. 7a and 9, the chromatograms were almost the same as that with the precolumn alone. The thickness of silicon at that time was calculated to be ca. 320 Å. Hence, in the case of metal capillary, it seems that there is no necessity to deposit silicon as thick as ca. 3000 Å [4].

The inner surface of the metal capillary is uneven, however. Therefore, to obtain a reliable metal capillary treated with monosilane, the silicon layer should be sufficiently thick. For the purpose of increasing the thickness of silicon, the seal pressure of monosilane was increased and monosilane treatment was repeated three times.

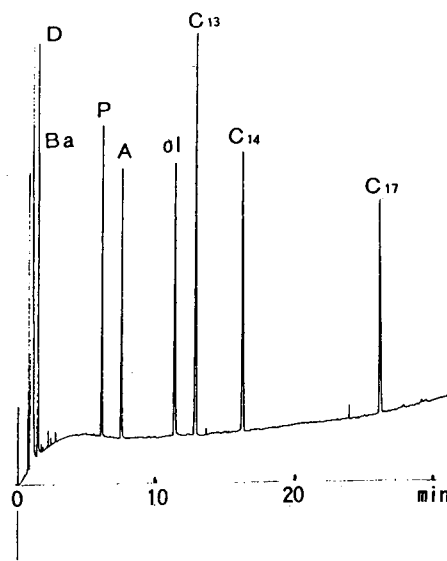


Fig. 8. Chromatogram of test mixture on precolumn of OV-1 alone. Precolumn, 25 m \times 0.25 mm I.D., OV-1, d_f = 0.4 μ m. Test parameters: initial oven temperature, 60°C; programming rate, 3°C/min; N₂ flow-rate, 0.49 m/s. Test mixture: see Table 1.

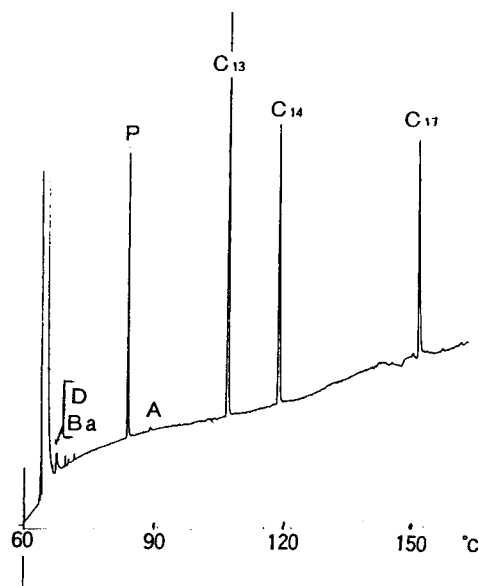


Fig. 9. Polarity test chromatogram on monosilane-treated metal capillary shown in Fig. 7a with precolumn of OV-1. Test parameters: see Fig. 8.

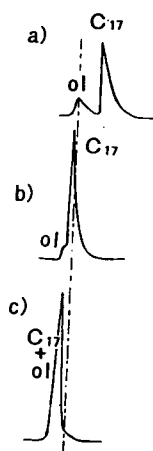


Fig. 10. Influence of repeated monosilane treatment. Column: precolumn of CW20M + metal capillary (6 m \times 0.35 mm I.D.) treated with monosilane. Parameters for monosilane treatment: 197.2 kPa, 450°C, 15 min. Number of repetitions of monosilane treatment: (a) 1, (b) 2, (c) 3. Test parameters: N₂ flow-rate, 0.4 m/s; for other parameters see Fig. 2.

When the capillary was connected to a precolumn of CW20M, as shown in Fig. 10, the reversed peak order of 1-decanol and C₁₇ was gradually improved. The thickness of the silicon layer was 890 Å/cycle. Fig. 10 shows that, although the wettability between the silicon grains and the newly deposited silicon is better than that between the metal capillary and silicon, the cavity of grains does not become sufficiently small so as not to trap hydrocarbons owing to the geometry formed by the initial silicon grains. As the uneven inner surface of the capillary can cause a smaller column plate number, it is preferable to lessen the roughness, and also to lessen the degree of capture of hydrocarbons by the cavity of grains before the octamethyltetrasiloxane treatment. Therefore, we set the standard conditions for monosilane treatment of the capillary of 0.25 mm I.D. as follows: the monosilane seal pressure was 295.3 kPa (3 kg/cm²), thermal decomposition was applied at 530°C for 15 min and the process was repeated twice. The calculated thickness of the silicon layer was 1914 Å.

3.3. Thermal stability of metal capillary column coated with commercial dimethylpolysiloxane gum

It was found out that a metal capillary column that was treated with monosilane and octamethyltetrasiloxane after washing with water and acetone was, contrary to expectation, thermally very unstable. Details are described below.

From a metal capillary treated with monosilane and octamethyltetrasiloxane, column (1) was prepared by coating with extensively used commercial dimethylpolysiloxane (DMPS) gum, X1. A cross-linked column (2) was also prepared by coating X1 with 1% of dicumyl peroxide (DCUP) [27]. A glass capillary column X1 (3) and cross-linked X1 column (4) were prepared for comparison. The thermal stability of the columns was tested at a column temperature of 250–260°C under a nitrogen flow of 0.45–0.48 m/s. The test was performed at each time period under the conditions described in Fig. 8 except for the flow-rate of carrier gas. We observed peak tailing of 1-decanol and C₁₇ as representatives for an easily tailing solute and a hardly tailing solute. The results are summarized in Table 2.

The column made by cross-linking with DCUP, as seen with column (4), showed slight tailing of 1-decanol. As the degree of the tailing does not change during the heat treatment, the glass capillary columns (4) and (3) are good enough for this kind of thermal test. On the other hand, column (1) degraded with heat treatment until not only 1-decanol but also C₁₇ started to show tailing (Fig. 11). Column (2) was not good enough from the time it was made, and showed severe degradation even after 12 h of heating. It is not clear why the column cross-linked with DCUP tend to degrade severely. The same was true with a column crosslinked with AZO [28]. It should be noted that column (1) showed tailing with hydrocarbons. The poor wettability of metal with silicon in the metal capillary has been mentioned before. If the assumption is correct, on continuous heating part of the silicon grains move from the surface and migrate or grow into larger grains, thus exposing

Table 2

Thermal stability test of metal and glass capillary columns coated with commercial dimethylpolysiloxane gum, X1

No.	Column ^a	Heating time (h)										Heating temperature (°C)
		0		12		24		50		74		
		ol	C ₁₇	ol	C ₁₇	ol	C ₁₇	ol	C ₁₇	ol	C ₁₇	
1	Metal, 10 m, NC	○	○ ^b	△	○	×	△	×	×	×	○	250
2	Metal, 15 m, C	×	△	×	×	×	×	×	×	×	○	260
3	Glass, 15 m, NC	○	○	○	○	○	○	○	○	○	○	260
4	Glass, 15 m, C	△	○	△	○	△	○	△	○	△	○	260

Symbols: ○ = no tailing, △ = slight tailing, × = tailing, ×× = severe tailing.

^a NC, non-cross-linked; C, cross-linked. I.D. of the columns is 0.25 mm.

^b See Fig. 11a.

^c See Fig. 11b.

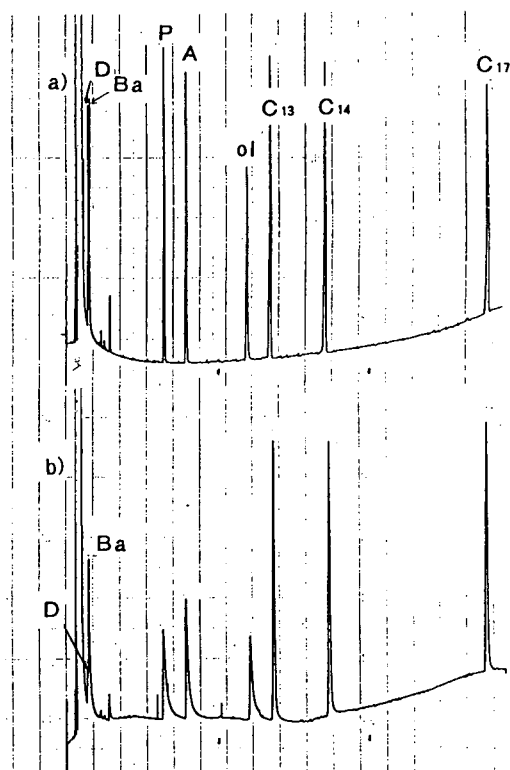


Fig. 11. Heat treatment of metal capillary column of X1: (a) before heat treatment; (b) after heat treatment at 250°C for 50 h. Column, 10 m × 0.25 mm I.D., X1, $d_r = 0.4 \mu\text{m}$. Parameters for monosilane treatment: 197.2 kPa, 530°C, 15 min, twice. Test parameters: N₂ flow-rate, 0.25 m/s; for other parameters see Fig. 8.

the metal surface and adsorbing hydrocarbons to show tailing. Polar solutes are assumed to show tailing ahead of hydrocarbons, as polar solutes are susceptible to the polarizing field [4] of a metal. Hence the tailing of polar solutes in columns (1) and (2) is due to the foregoing phenomenon of tailing of hydrocarbons, and different from the often observed tailing due to the hydroxyl groups on the surface of the support phase.

How to improve the wettability between the inner surface of the metal capillary and silicon is made clear in the following section.

3.4. Properties of the metal capillary treated with monosilane after acid washing of the inner surface

A commercially available metal capillary can, in many instances, be successfully processed into metal capillary as shown in Fig. 9. Consistency of the quality, however, was not expected, and often resulted in a capillary of poor quality. Therefore, the inner surface was acid washed as described in Section 2.1 to give a constant state for monosilane treatment. A green or black liquid results from acid washing, but it changes to a clear, colourless liquid after washing with distilled water. The capillary was then treated

with monosilane and was evaluated under the same condition as in Fig. 9.

As a result, an extremely poor chromatogram was obtained, as shown in Fig. 12a. It is similar to that with an untreated metal capillary. The reason is considered to be as follows. Acid washing of the inner surface exposed the bare metal surface, which made the wettability with silicon worse. As a consequence, silicon was deposited as larger grains and metal was exposed between the grains, thus giving a poor chromatogram. The phenomenon must be the same as that which Bertsch and Pretorius [4] experienced using a copper capillary. This experiment made

it clear that the oxide layer on the metal surface plays an important role in the wettability between the metal surface and silicon.

3.5. Oxidation of inner surface of acid-washed metal capillary

Oxygen oxidation was conducted on the inner surface of the metal capillary acid washed using the procedure in Section 2.1. It was then treated with monosilane and subjected to the evaluation. An excellent chromatogram, as a capillary prior to the octamethyltetrasiloxane procedure, in which tailing was a minimum not only with hydrocarbons but also with 2,6-dimethylphenol, was obtained, as shown in Fig. 12b. The result suggests that the troublesome acid washing procedure can be omitted because the oxidation procedure follows. However, from the point of view of quality control, we considered it necessary to start each procedure at a constant state of the inner surface of the capillary, and did not omit the procedure.

3.6. Thermal stability of deactivated metal capillary

Thermal stability was examined for the metal capillary prepared following the procedure in Section 3.5 and then treating with octamethyltetrasiloxane and also for the glass capillary treated with monosilane and octamethyltetrasiloxane. The capillaries were thermally treated in an oven as described in Table 3, under a nitrogen flow of 1 ml/min (linear velocity 0.34 m/s). After each thermal treatment, they were evaluated using a precolumn of OV-1. As shown in Table 3, the thermal stability of the metal capillary before the coating of a non-polar liquid phase, the so-called pretreated capillary, is, although slightly less than that of the glass capillary, excellent at 400°C for 50 h, and it survives heating at 450°C for several hours. This suggests that the column coated with dimethylpolysiloxane whose thermal stability is estimated to be ca. 400°C [29] from thermo-

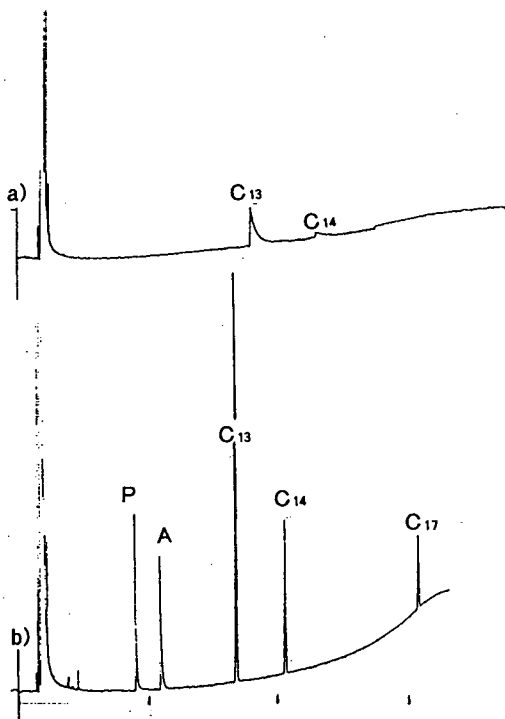


Fig. 12. Polarity test chromatograms on monosilane-treated metal capillaries (10 m × 0.25 mm I.D.) with precolumn of OV-1. (a) Capillary acid washed followed by monosilane treatment; (b) capillary acid washed and oxidized followed by monosilane treatment. Oxidation parameters: oxygen stream, 500°C, 1 h. Parameters for monosilane treatment: 295.3 kPa, 530°C, 15 min. Test parameters: N₂ flow-rate, 0.4 m/s; for other parameters see Fig. 8. Test mixture: see Table 1, except C₁₃ concentration was increased.

Table 3
Thermal stability test of deactivated metal and glass capillaries

No.	Capillary ^a	Heat treatment									
		280°C, 50 h		400°C, 50 h		450°C, 12.5 h		450°C, 25 h		450°C, 50 h	
		ol	C ₁₇	ol	C ₁₇	ol	C ₁₇	ol	C ₁₇	ol	C ₁₇
1	Metal ^b , 30 m	○	○	△	○	×	○	– ^d	○ ^e		
2	Glass ^c , 10 m	○	○	○	○	○	○	○	○	○	○

Symbols as in Table 2; ol and C₁₇: see Table 1.

^a I.D. of capillaries is 0.25 mm.

^b Capillary was prepared under conditions described in Section 2, but oxidation was conducted at 250°C for 0.5 h.

^c Parameters for monosilane treatment: 98.6 kPa, 530°C, 15 min.

^d No peak observed.

^e See Fig. 13a.

gravimetric analysis can be used with a programming mode such as heating to 450°C and holding that temperature for a while. It also shows that inertness of the pretreated surface is maintained until the liquid phase breaks down. Hence the thermal stability of the capillary showed a remarkable improvement on introducing an oxidation process prior to the monosilane treatment, and the highly thermally stable nature of the material, metal, has come to be fully utilized. Now, for the first time, we can call such a prepared capillary a deactivated metal capillary (DMC).

What should be noted in Table 3 is that, after the heat treatment of the metal capillary at 450°C for 25 h, a peak of ol did not appear but the peak shape of C₁₇ did not change at all. This suggests that, during the heat treatment, hydroxyl groups are formed on the surface of the silicon grains, and metal is not exposed between the grains. Hence, after the heat treatment, the capillary that gave the chromatogram shown in Fig. 13a was treated with octamethyltetrasiloxane again. The chromatogram, as shown in Fig. 13b, was restored to that before the heat treatment. Although it is possible to consider that the chromatogram in Fig. 13a is due to the dispersion of octamethyltetrasiloxane from the silicon layer, this possibility is denied by the fact that thermal degradation is not recognized from capillary (2) in Table 3.

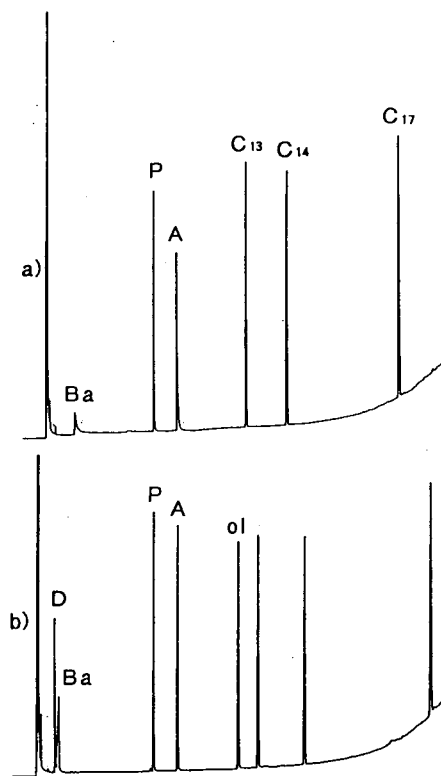


Fig. 13. Effect of repeated octamethyltetrasiloxane treatment on 1-decanol peaks: (a) before and (b) after octamethyltetrasiloxane retreatment on DMC that was heated at 450°C for 25 h. Precolumn: as in Fig. 8. Metal capillary: see Table 3. Test parameters: N₂ flow-rate, 0.34 m/s; for other parameters see Fig. 8.

3.7. Thermal stability of deactivated metal capillary column: part 1

As it is clear from Table 3 that the thermal stability of DMC is above 400°C, X1 columns (Nos. 11–15) were prepared and were tested along with the reference columns 21–31 in a similar way to that shown in Table 2. As shown in Table 4, the difference between metal and glass was not appreciable, and the thermal stability even at 280°C was not satisfactory. The major difference is that C₁₇ did not show tailing in Table 4 compared with the tailing in Table 2. With the metal capillary column that was cross-linked with peroxide, although tailing of 1-decanol was observed before the heat treatment, the degree of change in the chromatogram was almost the same as that with the non-cross-linked column. It is clear that these effects are due to the oxidation process prior to the monosilane treatment. The reason for the poor performance of the X1 columns is not clear. As there is no difference in the degradation between the metal and glass columns in Table 4, it was estimated that degradation of the columns is due to X1.

According to column 31 in Table 4, FSCC cannot withstand continuous heating at 280°C and begins to show activity towards polar solutes. This FSCC is a commercial column coated with a gum-like liquid phase X2 corresponding to X1. Although it is not yet clear whether the poor performance is due to the gum-like liquid phase, the results show that the columns coated with it acquire activity even in a moderate temperature range such as 250–350°C.

3.8. Thermal stability of deactivated metal capillary column: part 2

Thermal stability was tested again by preparing a column coated with characterized dimethylpolysiloxane (DMPS) instead of the commercially available X1. A DMPS column was prepared by thermally condensing, in a capillary, the liquid oligomer that was prepared by hydrolysing dimethyldichlorosilane with aqueous ammonia [8,9]. A 20% solution of oligomer in dichloromethane was dynamically coated in a metal capillary treated with the procedure in Sections 2.1–2.3. At the stage of condensation,

Table 4
Thermal stability test of deactivated metal capillary columns coated with X1 (see Table 2) compared with glass capillary columns coated with the same liquid phase

No.	Column ^a	Carrier gas		Heating time at 280°C (h)							
				0		25		50		75	
				ol	C ₁₇	ol	C ₁₇	ol	C ₁₇	ol	C ₁₇
11	Metal ^b , 30 m, <i>d_t</i> = 0.1 μm	C	N ₂	Δ	○	Δ	○	×	○	×	○
12	Metal ^b , 30 m, <i>d_t</i> = 0.4 μm	C	N ₂	Δ	○	Δ	○	×	○		
13	Metal ^b , 30 m, <i>d_t</i> = 0.25 μm	NC	N ₂	○	○	Δ	○	×	○		
14	Metal ^b , 30 m, <i>d_t</i> = 0.4 μm	NC	H ₂	○	○	○	○	Δ	○	Δ	○
15	Metal ^b , 30 m, <i>d_t</i> = 0.4 μm	C	H ₂	Δ	○	Δ	○	×	○		
21	Glass ^c , 25 m, <i>d_t</i> = 0.25 μm	C	N ₂	Δ	○	Δ	○	×	○		
22	Glass ^c , 25 m, <i>d_t</i> = 0.25 μm	NC	N ₂	○	○	○	○	Δ	○	Δ	○
23	Glass ^c , 30 m, <i>d_t</i> = 0.25 μm	C	N ₂	Δ	○	Δ	○	×	○		
31	FSCC ^d , 30 m, <i>d_t</i> = 0.25 μm	C	N ₂	○	○	○	○	×	○	×	○

Abbreviations and symbols as in Table 2; ol and C₁₇: see Table 1.

^a I.D. of columns is 0.25 mm.

^b These were prepared under conditions described in Section 2.

^c Parameters for monosilane treatment: see Table 3.

^d Commercial column coated with liquid phase X2 corresponding to X1.

the carrier gas flow-rate was maintained at ca. 0.1 m/s so as not to disperse the oligomer. The column was maintained at 250°C for 20 h, then at 300, 330, 350 and 370°C each for 15 h and finally at 390°C for 10 h. The results of the thermal test of the obtained DMCC at 440°C for 20 h are shown in Fig. 14. The chromatogram seems reasonable considering the results in Table 3. Although 1-decanol shows slight tailing, it must be due to the ring opening of siloxane, as will be mentioned in Section 3.9.

A column was prepared similarly to that mentioned above, except that it was coated statically with a 2% solution of the oligomer. Assuming programming up to a high temperature range, the column was heat treated twelve times by heating, holding and then cooling. A Grob test [18] was conducted with the column, and it was further confirmed from the chromato-

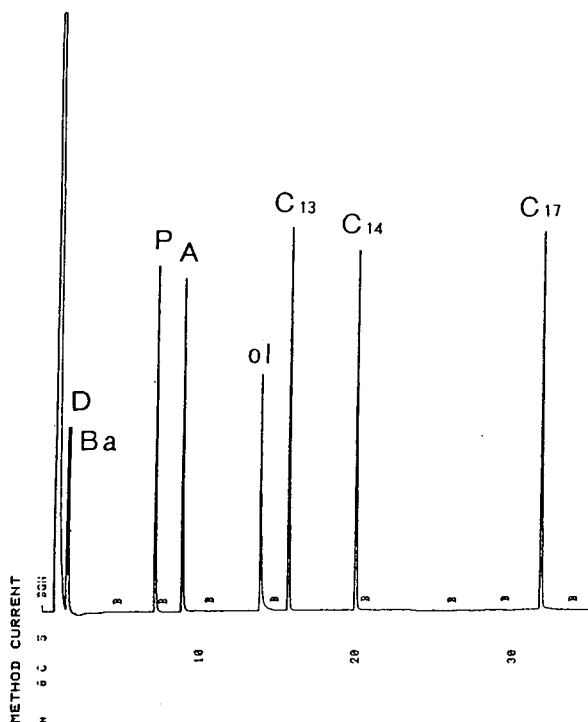


Fig. 14. Thermal test of deactivated dimethylpolysiloxane [8,9] metal capillary column. Thermal test: 440°C, 20 h, N_2 flow-rate, 0.34 m/s. Column, 15 m \times 0.25 mm I.D., $d_i = 0.25 \mu\text{m}$. Original metal capillary: as in Table 3. Test parameters: as in Fig. 13.

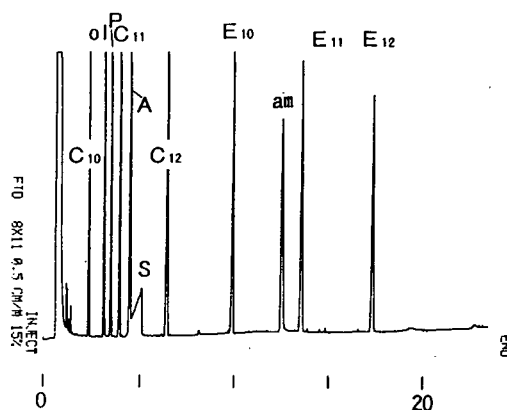


Fig. 15. Grob's test of deactivated dimethylpolysiloxane [8,9] metal capillary column after a total time of 120 min at 450°C in heat cycle test. Heat cycle test: 250–450°C at a programming rate of 10°C/min, held for 10 min at 450°C; N_2 flow-rate, 0.34 m/s. Column, 15 m \times 0.25 mm I.D., $d_i = 0.13 \mu\text{m}$, metal capillary oxidized at 250°C, 1 h. Parameters for monosilane treatment: 295.3 kPa, 530°C, 15 min, twice. Test parameters: as in Fig. 13. Sample: P = 2,6-dimethylphenol; A = 2,6-dimethylaniline; ol = 1-octanol; s = ethylhexanoic acid; am = dicyclohexylamine; C_{10} = *n*-decane; C_{11} = *n*-undecane; C_{12} = *n*-dodecane; E_{10} = methyl caprate; E_{11} = methyl undecanoate; E_{12} = methyl laurate.

gram (Fig. 15) that an extremely thermally stable column was prepared using the DMC and thermally stable liquid phase. The capacity factor (k') of C_{13} after the test was 8.68, which is 88.6% of that before the test. The theoretical plate number (N) was 23 878, which means that 87.3% of the initial performance was maintained.

3.9. Silanol and siloxane groups on the surface of the deactivated metal capillary

From Fig. 12b, a large number of silanol groups are assumed to be present on the metal capillary treated with oxidation and monosilane. From this supposition and also from the above-mentioned effectiveness of the repeated octamethyltetrasiloxane treatment, the presence of siloxane is also assumed. This is supported from the changes in a series of chromatograms, shown in Fig. 16a–c, after leaching and also after further treatment with octamethyltetrasiloxane. From the above results, it was concluded that,

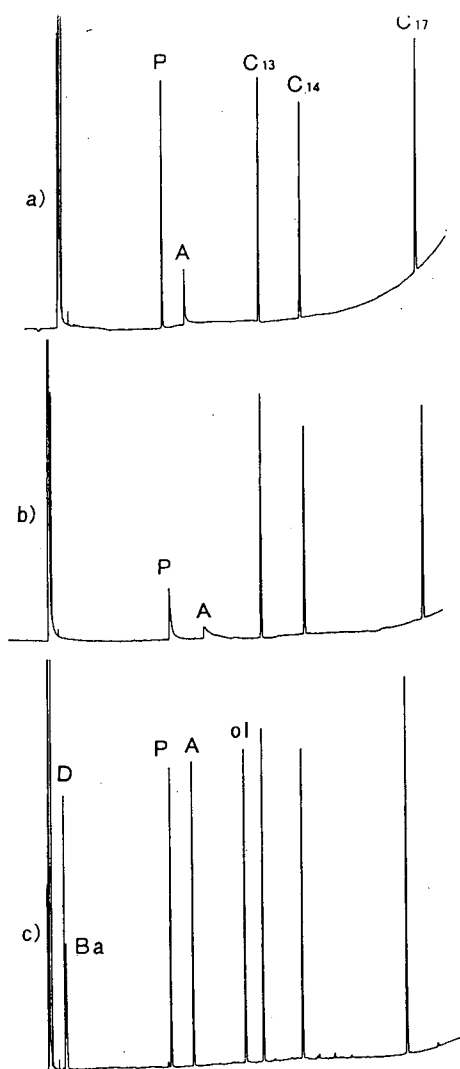


Fig. 16. Chromatogram of test mixture on metal capillary: (a) before leaching; (b) after leaching with 1% aqueous HCl for 1 h; (c) octamethyltetrasiloxane treated after leaching. Precolumn: as in Fig. 8. Metal capillary: as in Table 3. Test parameters: as in Fig. 13.

during the deactivation of the metal capillary, it is preferable to adopt a leaching process between monosilane treatment and octamethyltetrasiloxane or the corresponding treatment. Such a leaching process is considered also to be preferable from the point of view of increasing the sites for the direct reaction between an oligomeric liquid phase having hydroxyl end-groups and

the inner surface of the capillary, or for the indirect reaction through octamethyltetrasiloxane or 1,3,5-trimethyl-1,3,5-triphenylcyclotrisiloxane (TMTPCTS). The process can be neglected if the columns are operated in the isothermal mode below 400°C or in the temperature-programmed mode up to 450°C (see Table 3 and Fig. 15).

In the monosilane treatment described in Section 2, silicon is assumed to take oxygen away from the undercoated oxide to become silanol or siloxane. The reaction looks similar to the reduction of iron oxide with carbon. Undercoated oxide, however, is estimated not to be reduced completely to the oxygen-free state. Preparation of a glass capillary does not include an oxidation process. Hence oxygen is not abundant at the stage of monosilane treatment, and the formation of siloxane is almost negligible. It was confirmed that the chromatogram does not change before and after the leaching process.

3.10. Advantages of deactivated metal capillary (DMC) over fused-silica capillary (FSC)

The degree of deactivation of DMC is the same as that of FSC, as shown in Figs. 14 and 15. Naturally, DMC is easier to handle, has no problems of degradation and breakage and shows excellent thermal stability. There are some other advantages, as follows.

(i) It is easy to coat. As already pointed out, even polar liquid phases are easy to coat [3] owing to the silicon's high surface free energy. DMC has an uneven inner surface corresponding to the uneven original surface. Silicon is assumed to exist as fine grains on the uneven surface, which helps to make coating easy, as was found with PLOT columns. Hence, in addition to CW and OV-17, a highly polar liquid phase such as 5CP can be easily coated. In contrast, the inner surfaces of FSC and glass capillary are extremely flat, and it is very difficult to coat polar liquid phases without some treatment. With FSC, even if the coating looks successful, the liquid phases tend to aggregate to oily droplets during use.

(ii) The thermal stability of liquid phase can be fully utilized without worrying about degra-

dation of the physical and chemical performances of capillary during high-temperature use. An example is shown in Fig. 17. The baseline shifts upwards at around 400°C, which means that partial thermal degradation [29] of DMPS is occurring. When thermally stable liquid phases are used, DMCC can be used continuously at or above 450°C.

(iii) DMCC can be prepared by thermally condensing oligomers having hydroxyl end-groups in the capillary. In the case of cyanosilicon, FSC can be used [24] because the liquid phase can be prepared below 300°C. In other cases, however, FSC cannot be used. In such cases, glass capillaries have been used [20,22,23,25]. We have already shown in Section 3.8 that DMC can be used in those cases. Especially, thus prepared DMCC coated with DMPS keeps a superior deactivated state to the

FSC coated with a gum-like liquid phase such as X2 even at moderate temperatures.

(iv) Capillaries of large bore can be prepared. FSC exceeding 0.6 mm I.D. cannot be wound into a coil shape. A metal capillary even with 1 mm I.D. can be coiled easily. Hence a capillary column that can replace the ordinarily used packed column can be prepared. As capillary columns of wide bore can be prepared and used without problems by utilizing DMC, the age of capillary gas chromatography with thermal conductivity detection can at last begin. An example is shown in Fig. 18.

(v) The time necessary to remove the solvent with static coating is short. This is probably due to the better heat conductivity of the metal capillary over the polyimide-coated FSC. The time needed for evaporation is about 70% of that for the FSC.

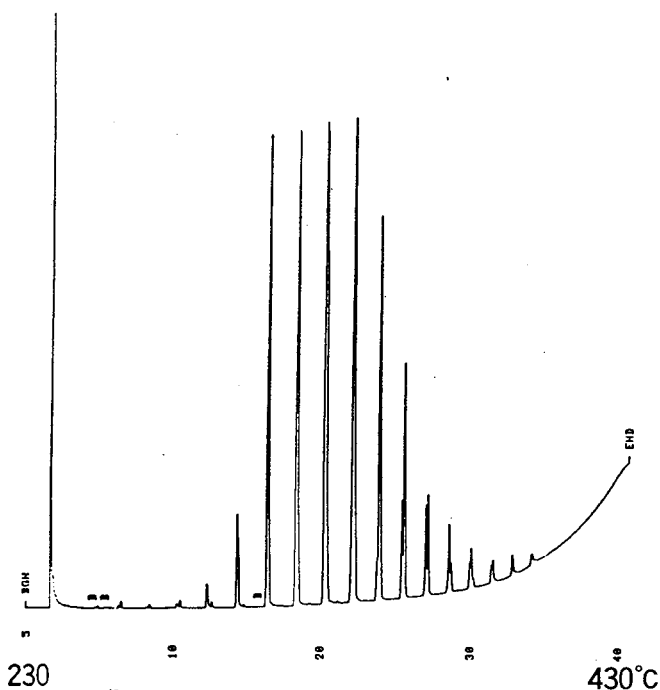


Fig. 17. High-temperature chromatogram on deactivated metal capillary column. Column, 30 m \times 0.25 mm I.D., dimethylpolysiloxane, $d_t = 0.3 \mu\text{m}$. Sample, palm oil. Test parameters: 230–430°C; programming rate, 5°C/min; N_2 flow-rate, 0.34 m/s.

3.11. Auger depth profile of deactivated metal capillary

It was difficult to prepare a sample of stainless-steel capillary of 0.25 mm I.D. whose inner surface is exposed for Auger analysis. Therefore, a stainless-steel capillary of 2 mm I.D. was treated with monosilane and was cut vertically for Auger measurement. The seal pressure of monosilane for 0.25 and 2 mm I.D. capillaries was set to give a silicon layer of the same thickness; 295.3 kPa (3 kg/cm²) and 36.5 kPa for 0.25 and 2 mm I.D., respectively, to give a 950 Å thick silicon layer.

Fig. 19a is a profile pattern of a capillary corresponding to the capillary that gave Fig. 12b. Assuming all the oxygen atoms present at the surface of silicon are bonded with silicon, the Si:O atomic ratio is 1:1.3. When monosilane was applied twice, the ratio was 1:0.8. The corresponding capillary of 0.25 mm I.D. was treated with octamethyltetrasiloxane and the chromatogram obtained was the same as that with the precolumn alone. Hence it was concluded that it is not necessary for the silicon surface to become SiO_2 [7]. The characteristic of the profile pattern of the capillary treated with monosilane after the

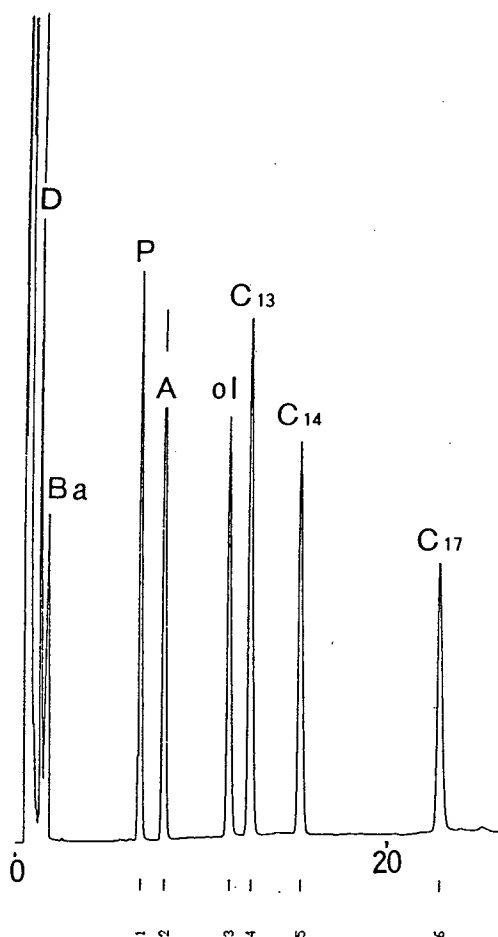


Fig. 18. Chromatogram of test mixture on large-bore deactivated metal capillary column. Column, 20 m \times 0.8 mm I.D., cross-linked X1, $d_f = 1 \mu\text{m}$. Test parameters: initial oven temperature, 60°C; programming rate, 5°C/min; N_2 flow-rate, 20 ml/min. Test mixture: see Table 1.

oxidation process is that a clear peak appears showing oxygen at the interface of the stainless steel and silicon layer. A capillary that was oxidized at 250°C for 1 h showed a smaller peak of oxygen, ca. one third in width and ca. half in height, but significantly larger than that in Fig. 19b, which omitted the oxidation process. Fig. 19b is a profile pattern of a capillary corresponding to the capillary that gave Fig. 12a. It

was not concluded that the capillary that gave Fig. 19b gives an unsatisfactory chromatogram. If we assume that the reason for Fig. 12a is partial exposure of stainless steel beneath the silicon layer, it is impossible to estimate the quality of the capillary from one Auger analysis.

4. Conclusions

The key procedure necessary to obtain a capillary that retains its inertness at moderate and high temperatures for long periods is to perform an oxidation process prior to the monosilane treatment of the capillary. Fairly broad conditions can be used for oxidation and monosilane treatment. The conditions described in Section 2 are some that we have used frequently, and it is only a recommended example. The oxidation of the metal capillary plays an important role in stabilizing and preventing coagulation of the silicon grains formed from monosilane on the metal capillary. This is the key point for the successful development of DMC. Treatment such as with octamethyltetrasiloxane prior to the coating of liquid phase to DMC can be done with various procedures being carried out with FSC or glass capillaries.

Thermal condensation in the capillary using the oligomer with hydroxyl end-groups at above 300°C has been used only in the case of glass capillaries. The know-how thus obtained can be fully used for DMC. It is of great significance that a high-performance flexible column for medium- to high-temperature gas chromatography is possible for the first time. The quality of the liquid phase is important, and the quality has to be checked when a commercially available liquid phase is to be used. With a high-quality liquid phase, column preparation does not need such a long period as described in Section 3.8.

DMC has the merit of both glass capillary and FSC, and has no problems of breakage. We believe that DMC is the metal capillary of the second generation, and it is unnecessary to predict the future of the competition with FSC.

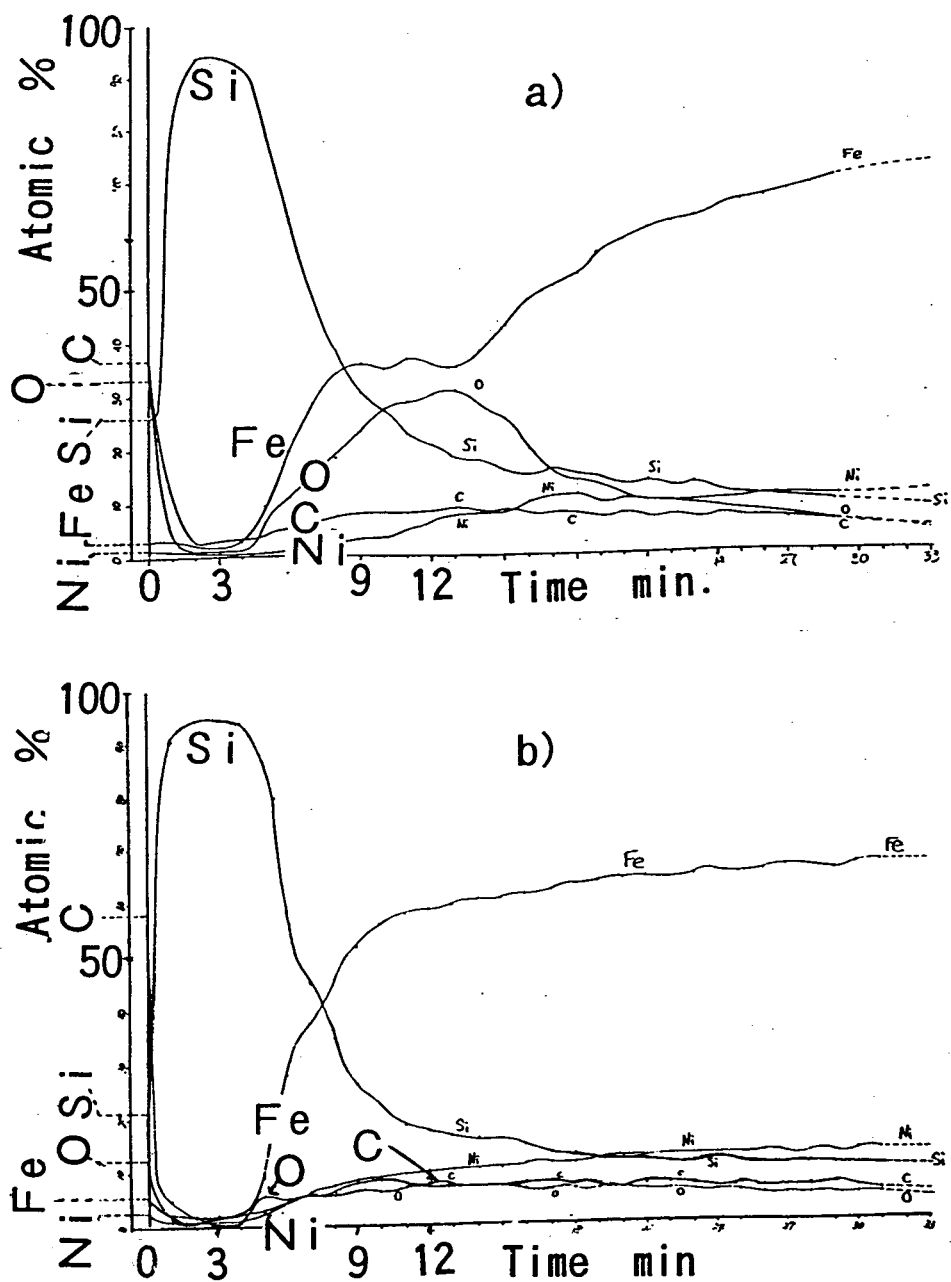


Fig. 19. Auger depth profile analysis of inner surface of metal (stainless-steel) capillaries. (a) Deactivated metal capillary, I.D. 2 mm, equivalent to that shown in Fig. 12b; (b) metal capillary, I.D. 2 mm, equivalent to that shown in Fig. 12a.

Acknowledgments

We thank students M. Mochizuki, H. Wada, S. Sato and M. Kamiyama, and the specialist Mr. M. Morikawa of Nippon Chromato Industries.

References

- [1] M.J.E. Golay, in D.H. Desty (Editor), *Gas Chromatography*, Butterworths, London, 1958, p. 67.
- [2] R.D. Dandeneneau and E.H. Zerenner, *J. High Resolut. Chromatogr. Chromatogr. Commun.*, 2(1979) 351.
- [3] V. Pretorius, J.W. du Toit and J.H. Pumell, *J. High Resolut. Chromatogr. Chromatogr. Commun.*, 4 (1981) 344.
- [4] W. Bertsch and V. Pretorius, *J. High Resolut. Chromatogr. Chromatogr. Commun.*, 5 (1982) 498.
- [5] W. Bertsch, V. Pretorius and G.C. van Niekerk, *J. High Resolut. Chromatogr. Chromatogr. Commun.*, 5 (1982) 539.
- [6] V. Pretorius, E.R. Rohwer, G.A. Hulse, K.H. Lawson and P.J. Apps, *J. High Resolut. Chromatogr. Chromatogr. Commun.*, 7 (1984) 429.
- [7] E.R. Rohwer, V. Pretorius and G.A. Hulse, *J. High Resolut. Chromatogr. Chromatogr. Commun.*, 9 (1986) 30.
- [8] C. Madani, E.M. Chamaz, M. Rigaud, P. Chebroux, J.C. Breton and F. Berthou, *Chromatographia*, 10 (1977) 466.
- [9] C. Madani, E.M. Chambaz, M. Rigaud and P. Chebroux, *J. Chromatogr.*, 126 (1976) 161.
- [10] Y. Takayama and E. Sumiya, *J. High Resolut. Chromatogr. Chromatogr. Commun.*, 9 (1986) 747.
- [11] Y. Takayama, E. Sumiya and S. Kawai, *J. High Resolut. Chromatogr. Chromatogr. Commun.*, 10 (1987) 201.
- [12] Y. Takayama, T. Yamaguchi and S. Kawai, *Bunseki Kagaku*, 36 (1987) 761.
- [13] Y. Takayama, T. Takeichi and S. Kawai, *J. High Resolut. Chromatogr. Chromatogr. Commun.*, 11 (1988) 731.
- [14] Y. Takayama, T. Takeichi and S. Kawai, *J. Chromatogr.*, 464 (1989) 172.
- [15] Y. Takayama, T. Takeichi, S. Kawai and M. Morikawa, *J. Chromatogr.*, 514 (1990) 259.
- [16] T. Takeichi, S. Shimura, H. Toriyama, Y. Takayama and M. Morikawa, *Chem. Lett.*, (1992) 1069.
- [17] K. Grob and G. Grob, *J. High Resolut. Chromatogr. Chromatogr. Commun.*, 2 (1979) 31.
- [18] K. Grob and G. Grob, *J. High Resolut. Chromatogr. Chromatogr. Commun.*, 1 (1978) 302.
- [19] L. Blomberg, K. Markides and T. Wännman, in R.E. Kaiser (Editor), *Proceedings of the 4th International Symposium on Capillary Chromatography*, Hüthig, Heidelberg, 1981, p. 73.
- [20] W. Blum, *J. High Resolut. Chromatogr. Chromatogr. Commun.*, 8 (1985) 718.
- [21] W.A. Aue, C.R. Hastings and S. Kapila, *J. Chromatogr.*, 77 (1973) 299.
- [22] W. Blum, *J. High Resolut. Chromatogr. Chromatogr. Commun.*, 9 (1986) 350.
- [23] P. Schmid and M.D. Müller, *J. High Resolut. Chromatogr. Chromatogr. Commun.*, 10 (1987) 548.
- [24] F. David, P. Sandra and G. Dirickes, *J. High Resolut. Chromatogr. Chromatogr. Commun.*, 11 (1988) 256.
- [25] R. Aichholz, *J. High Resolut. Chromatogr.*, 13 (1990) 71.
- [26] Y. Takayama, *Bunseki Kagaku, Sect. E*, 31 (1982) 231.
- [27] K. Grob and G. Grob, *J. High Resolut. Chromatogr. Chromatogr. Commun.*, 4 (1981) 491.
- [28] B.E. Richter, J.C. Kuei, N.J. Park, S.J. Crowley, J.S. Bradshaw and M.L. Lee, *J. High Resolut. Chromatogr. Chromatogr. Commun.*, 6 (1983) 371.
- [29] T.H. Thomas and T. C. Kondrick, *J. Polym. Sci., Part A-2*, 7 (1969) 537.



ELSEVIER

Journal of Chromatography A, 685 (1994) 79–94

JOURNAL OF
CHROMATOGRAPHY A

Analysis of volatile organics by supercritical fluid extraction coupled to gas chromatography

I. Optimization of chromatographic parameters

Mark D. Burford, Steven B. Hawthorne*, David J. Miller

Energy and Environmental Research Center, University of North Dakota, Grand Forks, ND 58202, USA

First received 6 April 1994; revised manuscript received 5 July 1994

Abstract

A solid-based calibration standard (consisting of several *n*-alkanes and aromatic hydrocarbons spiked onto Tenax-TA) was successfully used to optimize the chromatographic parameters for coupled supercritical fluid extraction–gas chromatography (SFE–GC). A simple and reliable split SFE–GC system was developed utilizing a commercially septumless injector installed on a split/splitless injection port. The high gaseous flow-rate generated inside the injection port during the SFE step was accommodated for by using the correct split ratio, so that high (1 ml/min liquid CO₂) SFE flow-rates could be used. The use of thick-film columns (5 μm film thickness) and cryogenic trapping temperatures in the GC oven as low as –50°C allowed efficient trapping of species as volatile as *n*-butane, acetone and methylene chloride. The chromatograms obtained using the optimized SFE–GC technique showed good peak shapes (comparable to those obtained using a conventional split injection) and peak area reproducibilities typically <5% relative standard deviation.

1. Introduction

Directly coupling sample extraction techniques with sample analysis has recently received a significant amount of attention due to the potential of the “coupled technique” to achieve very rapid, sensitive and cost effective analysis. Coupled or on-line extraction/analysis methods generally reduce the time required for sample extraction, analyte collection and analyte concentration. Since sample preparation and handling steps are minimized, the potential for analyte loss, degradation, and/or contamination is reduced and more sensitive analyses can be

achieved. Sample throughput can also be improved because the extraction and analysis occur in the same step, and on-line methods requiring less than 1 h for both extraction and gas chromatographic (GC) analysis have been reported [1–3].

Supercritical fluid extraction (SFE) is an ideal extraction technique to directly couple with capillary GC, since the gaseous effluent obtained in SFE after depressurization is compatible with GC analysis. Furthermore, using CO₂ as the supercritical fluid allows the direct use of flame ionization detection (FID) as the CO₂ does not have a FID response [4]. SFE also has the potential to extract a wide range of analytes that would normally require liquid solvent extraction

* Corresponding author.

[5,6], but avoids the problems related to introducing large volumes of liquid solvents onto a chromatographic column as the extracted analytes are introduced to the GC in the gas phase.

To achieve quantitative SFE–GC a number of experimental conditions need to be established. First, the target analyte must be efficiently extracted from the sample matrix; then the analytes must be quantitatively transferred from the SFE system to the GC; and finally, the analytes need to be chromatographically separated. The main limitation of the directly coupled SFE–GC system is with the collection and focusing of the extracted analytes and this, in turn, is related to the high gas flow-rate generated from the depressurization of the supercritical fluid. For example, using the common extraction flow of 1 ml/min of liquid CO₂ results, upon depressurization, in a CO₂ gas flow of ca. 500 ml/min. At such high gas flow-rates, poor refocusing of the analytes can occur resulting in poor peak shapes [2]. Conversely, if a low SFE flow-rate is used that results in good peak shapes, very long times might be required to completely extract the analytes from the sample [7]. An additional problem is that the analytes are extracted over a relatively long period of time (typically 10 to 30 min) compared to a typical capillary GC peak which is only about 1 s wide.

The aim of this work is to determine and optimize the experimental parameters which affect the collection and focusing of extracted analytes at the head of the chromatographic column during the extraction step in SFE–GC–FID analysis. The development and testing of a simple and reliable technique for performing split SFE–GC that utilizes a commercially available septumless injector installed on a split/splitless injection port is described. Only minor modifications to the GC instrumentation are required, and the same GC injection port can be used for liquid solvent injections or SFE–GC without conversion. A calibration mixture of *n*-alkanes and BTEX (benzene, toluene, ethylbenzene, *m*-xylene and *o*-xylene) spiked onto Tenax-TA is used to optimize the “coupling” of the SFE system to the GC system. Comparisons of peak shapes and quantitative results between

split SFE–GC and conventional split injections are also presented.

2. Experimental

2.1. Instrumentation and methods

SFE–GC–FID analysis was performed using a Hewlett-Packard 5890 gas chromatograph with helium as the carrier gas. A detailed schematic of the equipment is seen in Fig. 1. Three fused-silica capillary columns were investigated for use with SFE–GC; namely, a wide-bore (30 m × 0.32 mm I.D., 5 μm film thickness) DB-1 column, a wide-bore (30 m × 0.32 mm I.D., 1 μm film thickness) DB-5 column, or a narrow-bore (20 m × 0.25 mm I.D., 0.25 μm film thickness) DB-5 column, all supplied by J & W Scientific, Folsom, CA, USA. The septum and septum cap supplied with the conventional split/splitless injection port were replaced with a septumless injector (Model SLI-M) and installed according to the manufacturer's instructions (SGE, Austin, TX, USA). The injection port and the flame ionization detector were both operated at 300°C.

Initially, the mass flow controller supplied with the GC instrument controlled the carrier gas flow-rate. However, (as discussed later) the high gas flow-rates generated during SFE–GC proved unsuitable for use with the mass flow controller (and the back-pressure regulator supplied with the 5890 GC system). The GC system was modified so that the carrier gas flow-rate was controlled by a head pressure regulator situated on the carrier gas cylinder (see Fig. 1). The column head pressure was measured with a pressure gauge installed on the carrier gas line. A toggle shut-off valve was installed on the carrier gas supply line between the head pressure regulator and the injection port to allow the carrier gas line to be closed during the SFE step. The septum purge on the injection port was also closed by installing a cap nut on the septum purge outlet. Note, no bleed from the silicone seal or O-ring situated inside the septumless injector was detected during the SFE–GC study.

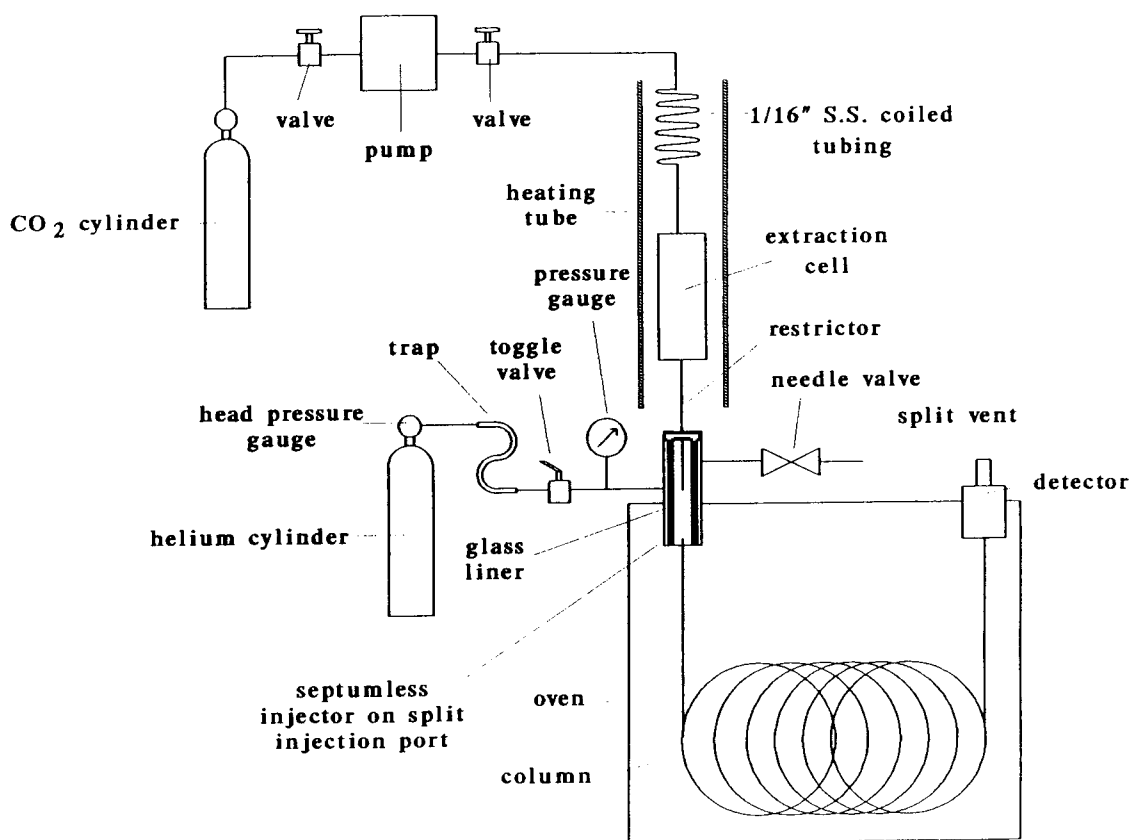


Fig. 1. Schematic diagram of the split SFE-GC-FID system. S.S. = Stainless steel; " = in. (1 in. = 2.54 cm).

The split ratio was controlled with a needle valve on the split line outlet (see Fig. 1).

Supercritical fluid extractions were performed with CO₂ (supercritical fluid grade, Scott Specialty Gases, Plumsteadville, PA, USA) and an ISCO Model 260D syringe pump (ISCO, Lincoln, NE, USA). Samples were placed in a 2.5-ml extraction cell from Keystone Scientific (Bellefonte, PA, USA). The flow-rate of the supercritical fluid through the extraction cell was controlled by 9-cm-long restrictors (15, 22, 26 or 30 μm I.D., 150 μm O.D.) cut from fused-silica tubing (Polymicro Technologies, Phoenix, AZ, USA). During the extraction, the extraction cell and a pre-equilibration coil [1 m × 0.76 mm I.D. × 1.6 mm (1/16 in.) O.D. coiled stainless-steel tubing placed before the extraction cell to pre-warm the CO₂ to the extraction temperature] were placed inside a thermostated tube

heater which was situated directly above the injection port.

Split SFE-GC analysis was performed by inserting the extraction cell restrictor through the septumless injector into the injection port liner (8 cm × 6 mm O.D. × 3 mm I.D. glass tube) so that the end of the restrictor was about 3.5 cm above the chromatographic column's inlet. As the silicone seal inside the septumless injector provided a gas-tight seal around the restrictor and, as the injector septum purge was closed, the supercritical fluid effluent exiting the restrictor either went into the chromatographic column or out the split line. The split ratio used during the extraction was, therefore, controlled by simply adjusting the needle valve on the split line.

The steps used for split SFE-GC analysis were as follows: (1) the GC oven was cooled to the appropriate cryogenic trapping temperature

(from -50 to 25°C for this study); (2) the assembled extraction cell was placed inside the tube heater, the GC carrier gas supply was shut off with the toggle valve, and the extraction cell restrictor was inserted into the injection port through the septumless injector; (3) the extraction cell was pressurized with 400 atm (1 atm = 101 325 Pa) CO_2 at 60°C and the sample was extracted for 10 min (during the extraction, the CO_2 effluent was depressurized in the injection port and the analytes were trapped on the chromatographic column); (4) the extraction cell restrictor was withdrawn from the injection port and the CO_2 effluent was allowed to dissipate from the injection port and column (this usually took about 1 min). After the CO_2 had dissipated, the carrier gas was turned on and the GC analysis begun with the GC oven rapidly heated to 40°C then at $8^{\circ}\text{C}/\text{min}$ to 300°C .

2.2. Samples and standards

A neat mixture of BTEX and C_4 – C_{20} *n*-alkanes (ca. 0.5 g each) was prepared in a vial and stored at -10°C . All the hydrocarbons were supplied by Aldrich (Milwaukee, WI, USA). Note, since *n*-butane (C_4) is a gas at room temperature and pressure, it had to be cooled to a liquid to enable the analyte to be accurately added to the neat hydrocarbon mixture. To obtain liquid *n*-butane, the compressed *n*-butane gas was passed through a coiled stainless-steel tube immersed in a dewar of methanol and ice at -15°C . The liquid exiting the coiled tube was collected in a cold (ca. -15°C) 25-ml “pressure-lok” gas syringe (Supelco, Bellefonte, PA, USA) with the plunger removed for ease of fill. After ca. 10 ml of liquid *n*-butane had been collected, the plunger was reinstalled on the syringe, and ca. 0.5 g of the liquid was injected into the neat hydrocarbon mixture.

The neat hydrocarbon mixture was spiked onto several matrices, including 70–80-mesh (180–200 μm) silanized glass beads (Analab, Norwalk, CT, USA) or the sorbent resins, 60–80-mesh Tenax-TA, 60–80-mesh (180–250 μm) XAD-2, 60–80-mesh Carbosieve S-III or 20–40-mesh (420–850 μm) Carbotrap C (Supelco). The

silanized glass beads were used as supplied. The sorbent resins were prepared by weighing 1 g of the sorbent resin into a 3.5-ml extraction cell, and preextracting for 30 min with 400 atm CO_2 (60°C) to remove contaminants. Each clean sorbent (400 mg) was placed inside a 2.5-ml extraction cell on a bed of 70–80-mesh silanized glass beads (100 mg), and 0.2 μl of the neat hydrocarbon mixture (ca. 9 μg of each analyte) were injected into the middle of the sorbent. The extraction cell was then sealed and either immediately connected to the SFE–GC apparatus or left for 24 h at room temperature and pressure. Once the extraction cell was connected to the apparatus, the cell was equilibrated at 60°C for 5 min, and then extracted by SFE–GC as described in the *Instrumentation and methods* section.

To quantify the recovery of the hydrocarbons from the matrices two internal standards were used depending on the matrix. For the majority of matrices *n*-decane (C_{10}) was used as the internal standard. However, occasionally the C_{10} *n*-alkane was irreversibly retained on the matrix (e.g., Carbosieve S-III) or evaporated from the matrix when aged 24 h (e.g., silanized glass beads) and, in these instances, an alternative internal standard, octahydroanthracene was used. A solution of octahydroanthracene (18 mg/ml) was prepared in methylene chloride and stored at -10°C . A 0.5- μl aliquot of the internal standard solution (9 μg of analyte) was injected onto a bed of glass beads (100 mg) situated inside a 2.5-ml extraction cell. The glass beads were then left exposed to the atmosphere for 10 min to allow the methylene chloride solvent to evaporate. Once the solvent had evaporated, the glass beads were covered with 400 mg of sorbent resin or with more glass beads, onto which was spiked the hydrocarbon mixture (9 μg of each analyte). The extraction cell was then sealed and analyzed by SFE–GC as described above. Analyte recovery was determined by comparing the split SFE–GC results to a conventional split injection, with the same amount of analytes that were spiked onto the matrices for SFE–GC analysis being injected directly into the GC–FID system.

The SFE–GC technique was further evaluated using several organic solvents including ethanol (Fisher Scientific, Fair Lawn, NJ, USA); acetone (Fisher Scientific); diethyl ether (J.T. Baker, Phillipsburg, NJ, USA); methylene chloride (Fisher Scientific); trichlorotrifluoroethane (Freon 113; Fisher Scientific); chloroform (Fisher Scientific); tetrahydrofuran (J.T. Baker); trichloroethylene (Aldrich); tetrachloroethylene (Aldrich); and chlorobenzene (Fisher Scientific). A mixture of the solvents (ca. 1 g each) and 1 g of the internal standard *n*-heptane was prepared in a brown vial and stored at -10°C . A 0.2- μl aliquot of the mixture (ca. 18 μg of each analyte) was spiked into the middle of 400 mg of Tenax-TA situated inside a 2.5-ml extraction cell. The extraction cell was then sealed, connected to the SFE–GC apparatus, and analyzed as described in the *Instrumentation and methods* section.

3. Results and discussion

3.1. Instrumental modifications required to perform SFE–GC

Split SFE–GC deposits the extracted analytes inside a conventional split injection port and, analogous to a conventional split injection, a fraction of the extracted analytes enters the chromatographic column for focusing in the stationary phase, while the remainder is flushed out the split vent [8–10]. While this approach is simple, reproducible qualitative and quantitative results require a few simple instrumental modifications. The SFE effluent can expand backwards into the carrier gas line during the extraction, because the internal volume of the vaporizing chamber (i.e., glass liner) inside the injection port is relatively small (ca. 0.5 ml) compared to the gaseous flow of the supercritical fluid (ca. 8 ml/s of gaseous CO_2 at a typical liquid CO_2 flow-rate of 1 ml/min), and the pressure generated inside the injection port during extraction can be higher than the carrier gas head pressure. To avoid the extracted analytes contaminating the carrier gas line a shut-off

valve was placed near the injection port to block the GC carrier gas flow during the SFE step (Fig. 1). Even though the majority of the SFE effluent (usually ca. 95–99%) was vented out of the injection port through the split vent during the SFE–GC extraction step, the gas flow through the chromatographic column was still sometimes sufficient to extinguish the FID flame. To maintain the FID signal the flame's hydrogen flow was slightly increased, and CO_2 gas flow-rates through the GC column of 10–15 ml/min have been used without quenching the FID flame [11].

The most important modification to the normal configuration of the Hewlett-Packard 5890 GC system was the addition of a needle valve installed onto the split line to control the split flow during the SFE step. In the normal configuration of the 5890 GC system, the split flow exits through the back-pressure regulator (which opens and closes to maintain constant pressure); and, the split ratio is controlled by the amount of carrier gas supplied by the mass flow controller (which is isolated from the GC flows by the toggle shut-off valve during the SFE step). In an unmodified 5890 GC system, the high CO_2 gas flow-rate which enters the injection port during SFE causes the head pressure regulator to open (in an attempt to maintain its set-point pressure) thus, varying the split ratio during the SFE step. While this does not affect the qualitative peak shapes, the change in split ratio which can occur during the SFE step can yield poor quantitative results. Therefore, to assure a constant split ratio during the SFE step, the gas chromatograph was modified so that the split was controlled by a needle valve placed in the split outlet line rather than the normal configuration where the split flow exits through the back-pressure regulator. During the GC analysis, the column head pressure was maintained by the head-pressure regulator situated on the carrier gas inlet line (Fig. 1). This simplified system resulted in good peak area reproducibility (as discussed below) and was also easier to maintain because if the split vent became contaminated during the extraction of very dirty samples, the tubing and needle valve could be easily removed and flushed with solvent.

Because of the good sensitivity possible with SFE–GC, the purity of the entire SFE–GC system had to be rigorously controlled. Minimal valving and other devices in the lines between the carrier gas cylinder, the pump and the extraction cell were used to avoid contamination. The apparatus used in this study (Fig. 1) utilized only three valves, two of which were situated on the inlet and outlet of the pump and the third, a toggle valve, was used to cut off the carrier gas supply during the extraction. The valves were packless to avoid contamination by lubricants and extractable species from components such as O-rings. A high-purity supercritical fluid (supercritical-grade CO₂) was also used because previous studies had found that impurities in the fluid can cause artifact peaks in SFE–GC generated chromatograms [12–14]. The lack of any transfer lines between the SFE cell and the GC injection port also eliminated any carryover between samples.

Several other minor modifications were made to the SFE–GC system. The bottom of the injection port protruding into the GC oven was insulated with a lined cover (as supplied by the manufacturer) so that a sharp temperature boundary could exist between the hot injection port and cold chromatographic column. This distinct temperature gradient helped focus the analytes as a band on the top of the chromatographic column during SFE; and, without the insulated cover, chromatographic peak fronting was observed. The position of the extraction cell restrictor inside the conventional split injection port also proved to be important. The best results were obtained with the tip of the restrictor situated about half way down the glass liner (which is the same position as the tip of a conventional syringe needle). If the restrictor outlet was placed a few millimeters from the chromatographic column inlet then poor peak shapes were obtained. Conversely, if the restrictor was situated just inside the injection port, poor recoveries of high-molecular-mass analytes resulted. Since the injection port was heated to 300°C, the restrictor plugging that commonly occurs with off-line SFE [15] was eliminated entirely.

3.2. Optimizing SFE–GC peak shapes

The ability of the split SFE–GC system to yield good peak shapes was investigated by comparing conventional split injections of a test mix with SFE–GC analysis of the same quantity of test mix from the Tenax-TA resin (selected for a solid-based calibration standard as described below). The test mix contained several *n*-alkanes ranging from a gas (butane) to a solid (eicosane) and BTEX aromatics. The test mix represented the major components present in gasoline and/or diesel fuel, and was seen as an ideal mixture to use to determine the experimental parameters which affected the collection and focusing of extracted analytes on the chromatographic column during the extraction step in SFE–GC. Three experimental factors were investigated: SFE flow-rate, cryogenic trapping temperature and chromatographic column stationary phase thickness.

Previous reports have shown that successful SFE–GC is dependent on the extraction flow-rate and the extraction time [2,3,8]. High extraction flow-rates may be desirable as the potential sample size can be increased, and the extraction time decreased [2,8], though additional factors such as the kinetics and mechanisms of the extraction may also affect the extraction rate [16]. Fig. 2 shows the effect of the SFE flow-rate on the peak shapes generated by SFE–GC which was performed under identical conditions using a wide-bore thick-phase (30 m × 0.32 mm I.D., 5 μm film thickness) chromatographic column at a trapping temperature of –50°C. SFE–GC analysis using extraction flow-rates as high as 0.6 ml/min (measured as liquid CO₂ at the pump, and corresponding to a restrictor with an internal diameter of 26 μm) yielded good peak shapes. The relative peak distribution (peak ratios) obtained using extraction flow-rates up to 0.6 ml/min were essentially identical to the peak distribution from split injection, indicating that the SFE–GC did not introduce any significant splitter discrimination (Fig. 2). However, differences in the absolute peak intensities occurred based on changes in the split ratio with different SFE flow-rates as discussed below.

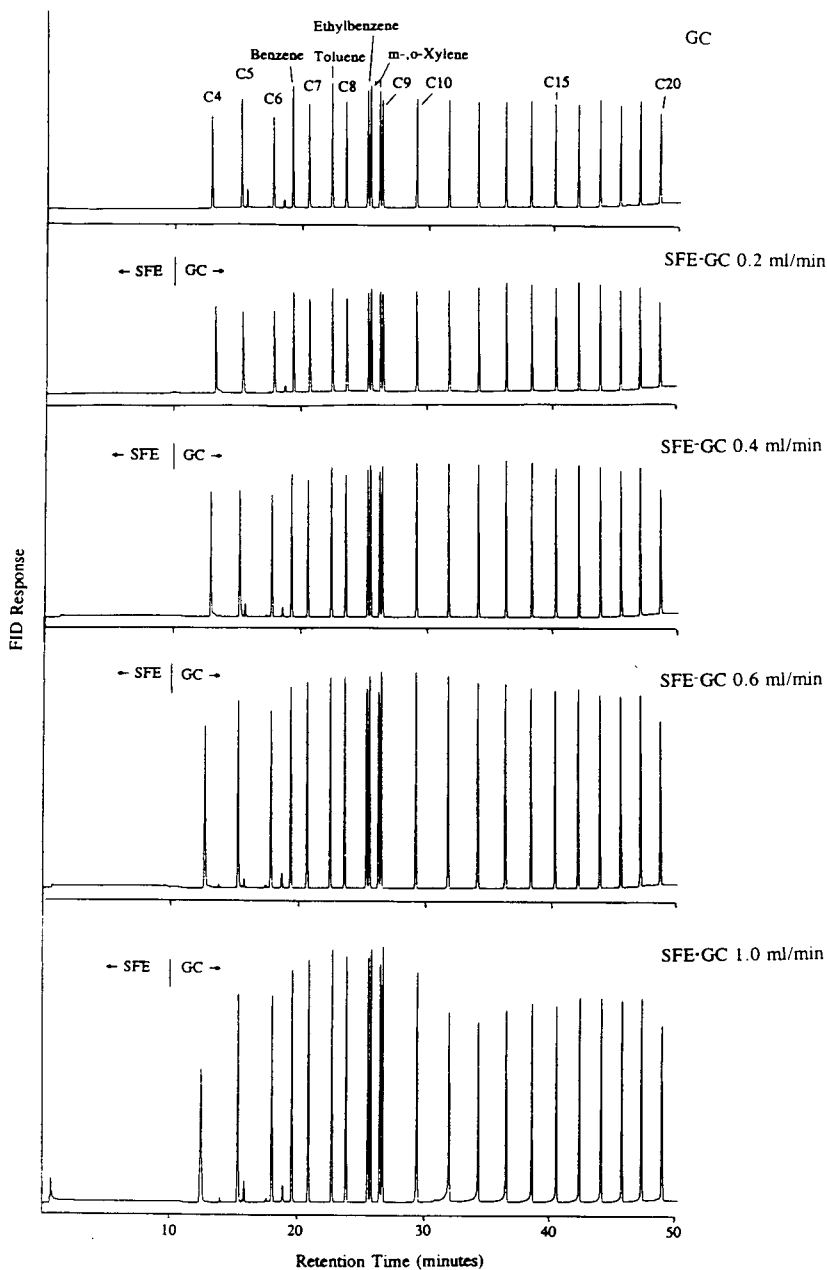


Fig. 2. Effect of SFE flow-rate on the peak shapes of BTEX and C_4 – C_{20} *n*-alkanes obtained by split SFE–GC–FID. A neat BTEX–*n*-alkane mixture ($0.2 \mu\text{l}$) was either injected onto the capillary column (top chromatogram) or the mixture was spiked onto 400-mg Tenax-TA and extracted “on-line” for 10 min with 400 atm, 60°C CO_2 at an extraction flow-rate of 0.2 ml/min ($9 \text{ cm} \times 15 \mu\text{m}$ I.D. restrictor); 0.4 ml/min ($9 \text{ cm} \times 22 \mu\text{m}$ I.D. restrictor); 0.6 ml/min ($9 \text{ cm} \times 26 \mu\text{m}$ I.D. restrictor); or 1.0 ml/min ($9 \text{ cm} \times 30 \mu\text{m}$ I.D. restrictor). For the corresponding split ratios at the various extraction flow-rates see Table 1. The $30 \text{ m} \times 0.32 \text{ mm}$ I.D. ($5\text{-}\mu\text{m}$ film) DB-1 capillary column was kept at -50°C during the injection or extraction step. After each extraction or 10 min after the injection the GC oven was heated at ca. $50^\circ\text{C}/\text{min}$ to 40°C then at $8^\circ\text{C}/\text{min}$ to 300°C .

The peak widths at half-height for both the relatively volatile (*n*-butane) and non-volatile (*n*-eicosane) alkanes generated by SFE–GC were essentially identical to those obtained by split injection. The only exception was the peak widths obtained by SFE–GC at the high (1.0 ml/min) extraction flow-rate, where the volatile (*n*-butane and *n*-pentane) and the semivolatile (C_{10} – C_{20}) peak widths are about a third and a fifth (respectively) wider than those obtained by split injection. The slight peak broadening of the early eluting analytes at the high extraction flow-rate is to be expected, as these are the most volatile analytes and are, therefore, the hardest to trap. The peak broadening of the later eluting peaks is discussed below.

The symmetry or shape of the chromatographic peaks obtained by SFE–GC at moderate extraction flow-rates (0.2 to 0.6 ml/min) also compared favorably with those obtained by split injection. However, at the high extraction flow-rate (1.0 ml/min liquid CO_2) poor peak shapes were obtained for the C_{10} to C_{20} *n*-alkanes (Fig. 2). The inefficient focusing of the analytes on the chromatographic column was related to the high gas flow (ca. 590 ml/min, Table 1) resulting from the depressurization of the supercritical fluid inside the injection port. The limiting factor was

not the high total volumetric flow-rate passing through the injection port, as higher injection port flow-rates could be tolerated under normal GC conditions (Table 1); instead, the poor peak shapes were associated with the high volumetric flow-rate through the chromatographic column. Peak fronting occurred when the gaseous CO_2 flow-rate through the GC column during SFE–GC exceeded ca. 9 ml/min (Table 1, Fig. 2). By increasing the split ratio so that more of the CO_2 was vented through the split vent and less entered the column, peak fronting was eliminated at the 1 ml/min extraction flow (even though the total gas flow through the injection port was still ca. 590 ml/min using the 30 μ m I.D. restrictor). Therefore, the maximum possible SFE flow that can be used and still obtain good peak shapes will depend on the split ratio, that is, higher split ratios (and thus lower columns flows) allow higher SFE flow-rates.

The cryogenic trapping temperature used during the extraction step also affects the ability of SFE–GC to efficiently focus volatile analytes. Fig. 3 shows the effect of the cryogenic trapping temperature on the chromatographic peak shape generated by SFE–GC which was performed under identical conditions with a 26 μ m I.D. restrictor (0.6 ml/min liquid CO_2 flow-rate) and

Table 1
Split ratio measured under GC and split SFE–GC conditions

	SFE flow-rate (ml/min) ^a	Column head pressure (p.s.i.)	Column volumetric flow (ml/min) ^b	Split vent volumetric flow (ml/min) ^b	Split ratio (column/split)
GC	–	15	5.1	789	1:155
SFE 15 μ m I.D. restrictor ^c	0.18	1	0.8	86	1:107
SFE 22 μ m I.D. restrictor ^c	0.38	4	2.8	267	1:95
SFE 25 μ m I.D. restrictor ^c	0.58	9	5.0	400	1:80
SFE 30 μ m I.D. restrictor ^c	0.96	16	9.2	577	1:63

See Fig. 2 for chromatographic results. 1 p.s.i. = 6894.76 Pa.

^a Flow-rate measured as liquid CO_2 at pump.

^b Flow-rate measured as volume of gas using a bubble flow meter. Column flow was measured at the detector end of the column.

^c SFE–GC conditions: 400 atm, 60°C CO_2 , wide-bore, thick-phase (30 m \times 0.32 mm I.D., 5 μ m film thickness), chromatographic column at –50°C.

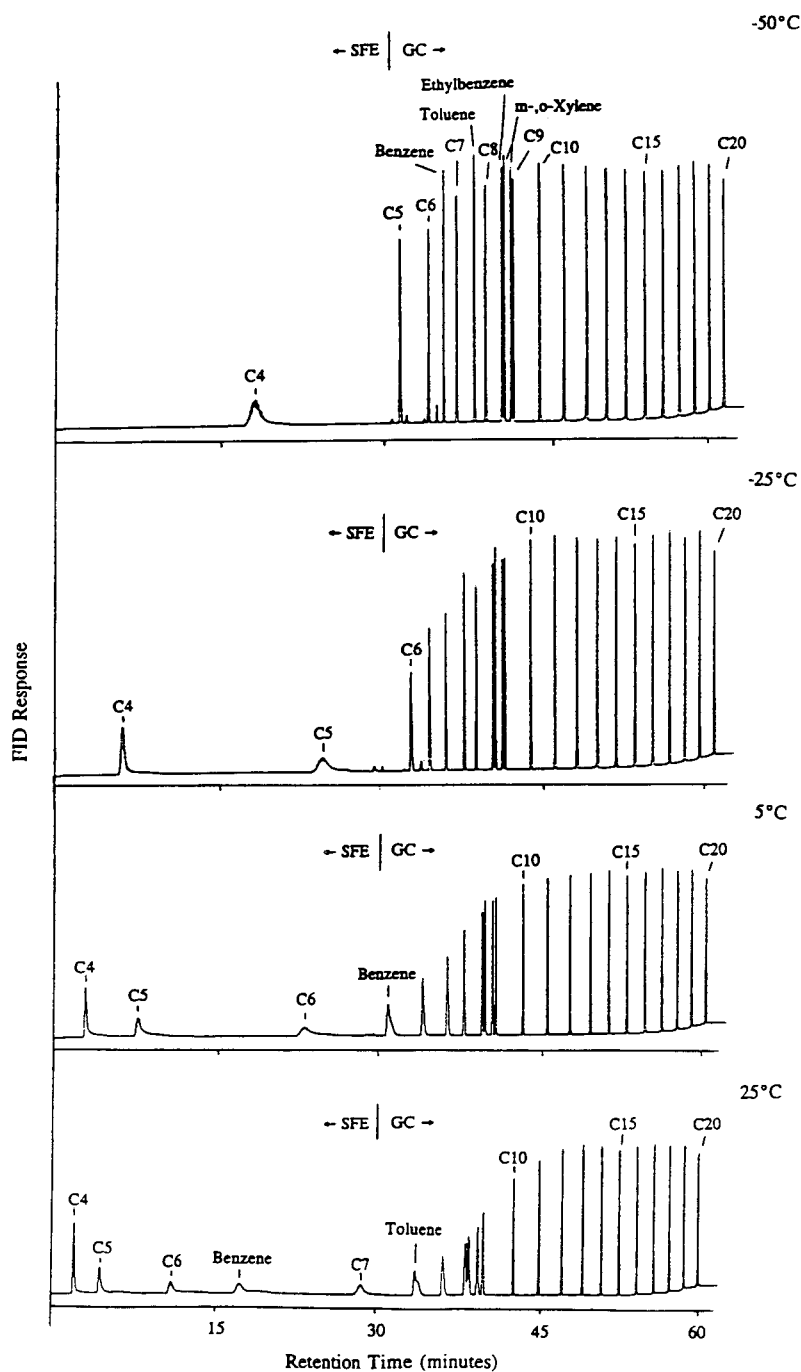


Fig. 3. Effect of the cryogenic trapping temperature on the retention of BTEX and C_4 – C_{20} *n*-alkanes on a thick-film ($5\ \mu\text{m}$) $30\ \text{m} \times 0.32\ \text{mm}$ I.D. DB-1 capillary column during SFE–GC–FID. A neat mixture ($0.2\ \mu\text{l}$) of BTEX and *n*-alkanes was extracted from Tenax-TA (400 mg) using 400 atm, 60°C CO_2 at 0.6 ml/min for 30 min. During the extraction the capillary column was maintained at a temperature of -50 , -25 , 5 or 25°C . After each extraction the GC oven was heated at ca. $50^\circ\text{C}/\text{min}$ to 40°C then at $8^\circ\text{C}/\text{min}$ to 300°C .

a wide-bore thick-phase (30 m × 0.32 mm I.D., 5 μm film thickness) chromatographic column. The coldest temperature investigated (−50°C) yielded chromatograms with the best peak shapes. However, as the SFE time was increased from 10 (Fig. 2) to 30 min (Fig. 3), the *n*-butane peak was broadened and eluted through the GC column during the SFE step. Colder trapping temperatures were not investigated as a means of increasing the trapping efficiency of *n*-butane because at lower temperatures (< −60°C) the chromatographic column stationary phase behaves as a solid [17,18]. When the cryogenic trapping temperature was raised to −25, 5 or 25°C, the trapping efficiency of the chromatographic column correspondingly decreased, and an increasing number of analytes eluted as discrete peaks through the column during the extraction step (Fig. 3). However, even with no cryogenic cooling and the column at room temperature (25°C) during the extraction step, analytes as volatile as *n*-decane could still be efficiently retained. The peak shape of the retained analytes tended to be broader for the more volatile species, but the less volatile C₁₀–C₂₀ *n*-alkanes had good peak shapes at all the trapping temperatures investigated.

Finally, the effect of the capillary column stationary phase film thickness on the chromatographic peak shape was investigated (Fig. 4). Each SFE–GC analysis was performed under identical conditions with a 26 μm I.D. restrictor (0.6 ml/min liquid CO₂ flow-rate) and a cryogenic trapping temperature of −50°C. Three chromatographic columns were investigated including the wide-bore (320 μm I.D., 5 μm film thickness) DB-1 column used in the previous studies, a wide-bore (320 μm I.D., 1 μm film thickness) DB-5 column, and a narrow-bore (250 μm I.D., 0.25 μm film thickness) DB-5 column. The column with the thickest stationary phase (5 μm film thickness) was the most efficient in focusing and retaining the analytes during the extraction step (Fig. 4). The 5- μm column was able to give good peak shapes for *n*-alkanes as volatile as pentane even after 60 min of SFE. When chromatographic columns were used with thinner stationary phase thicknesses the trapping

efficiency of the SFE–GC decreased, and more analytes eluted through the column during the SFE step. However, the advantage of using a thinner stationary phase is that higher-boiling components can be eluted at reasonable chromatographic temperatures. For example, the thick-film 5- μm column could resolve *n*-alkanes up to ca. C₂₅ in a typical GC run, but the thin-film 0.25- μm column could resolve *n*-alkanes up to ca. C₄₀ in the same analysis time. Therefore, a trade-off exists when choosing a column film thickness between the ability to efficiently trap very volatile analytes and to elute high-boiling point analytes.

3.3. Quantitative considerations for SFE–GC

The feasibility of directly coupling the SFE step with the GC analysis required the development of a calibration standard to be used to determine when quantitative SFE–GC had been achieved. A solid calibration standard was required whereby the test analytes could be easily and quantitatively spiked onto a solid matrix and then easily and quantitatively extracted from the matrix by SFE–GC, so that only the SFE–GC collection parameters were investigated, and not the SFE extraction efficiencies. To fully evaluate the potential of the on-line technique the *n*-alkane–BTEX test mixture was used. Based on the results of the peak shape studies described above, all subsequent SFE–GC analyses were performed using the 5- μm film thickness DB-1 column, a flow-rate (liquid CO₂) of 0.6 ml/min, a 10-min extraction time, and a cryogenic trapping temperature of −50°C.

Previous off-line SFE collection efficiency studies were based on the extraction of test analytes that were spiked onto relatively inert matrices [15,16]. However, unretentive matrices such as silanized glass beads proved unsuitable for use with the test mix, since a proportion of all of the more volatile analytes were lost from volatilization during the spiking process (Table 2). Thus, a more retentive matrix was required and a number of commercially available sorbent resins were investigated. Sorbent resins were seen as an ideal means of preparing a solid

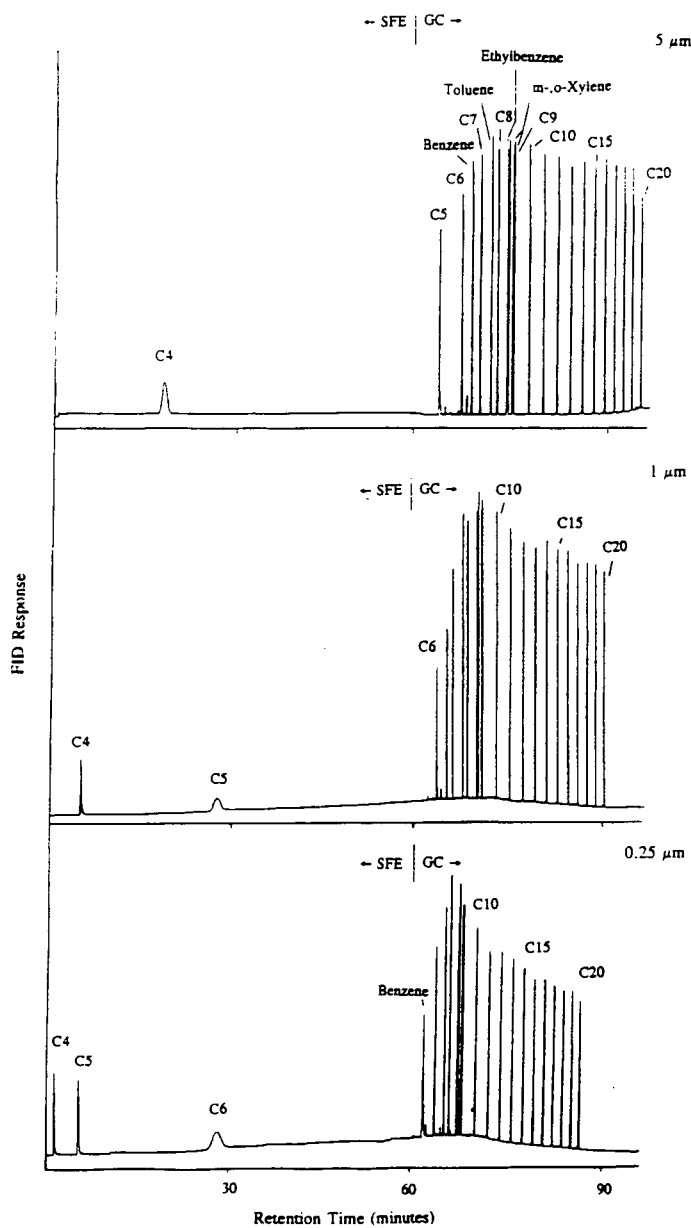


Fig. 4. Effect of capillary column stationary phase thickness on the chromatographic peak shape of BTEX and *n*-alkanes during SFE–GC–FID. A neat mixture of BTEX and C_4 – C_{20} *n*-alkanes ($0.2 \mu\text{l}$) was extracted from Tenax-TA (400 mg) using 400 atm, 60°C CO_2 at 0.6 ml/min for 60 min. The extracted analytes were cryogenically focused onto a 5- μm film DB-1 capillary column ($30 \text{ m} \times 0.32 \text{ mm}$ I.D.); a 1- μm film DB-5 capillary column ($30 \text{ m} \times 0.32 \text{ mm}$ I.D.); or a 0.25- μm film DB-5 capillary column ($20 \text{ m} \times 250 \text{ mm}$ I.D.). After each extraction the GC oven was heated at ca. $50^\circ\text{C}/\text{min}$ to 40°C then at $8^\circ\text{C}/\text{min}$ to 300°C .

calibration standard since volatile and semivolatile analytes have large gas retention volumes on the resins at ambient conditions

[19,20]. Furthermore, quantitative recovery of analytes from several sorbent resins has been achieved by SFE [7,21–23].

Table 2
Recovery of BTEX and C₄–C₂₀ *n*-alkanes from sorbent resins using 400 atm 60°C CO₂

Analyte	Recovery (%) (R.S.D., %) ^a				
	Glass beads ^b	Carbosieve S-III ^c	Carbotrap C ^b	Tenax-TA ^b	XAD-2 ^b
<i>n</i> -Butane (C ₄)	61 (20)	49 (20)	104 (3)	109 (6)	96 (3)
<i>n</i> -Pentane (C ₅)	69 (18)	44 (25)	96 (5)	105 (4)	91 (4)
<i>n</i> -Hexane (C ₆)	91 (9)	30 (20)	96 (6)	103 (3)	92 (3)
Benzene	93 (8)	26 (15)	96 (6)	97 (3)	94 (2)
<i>n</i> -Heptane (C ₇)	98 (6)	18 (12)	97 (4)	102 (3)	94 (3)
Toluene	97 (8)	6 (22)	97 (4)	97 (2)	94 (3)
<i>n</i> -Octane (C ₈)	98 (8)	8 (23)	97 (2)	100 (3)	95 (4)
Ethylbenzene	101 (4)	4 (21)	98 (2)	96 (1)	95 (3)
<i>m</i> -Xylene	101 (3)	3 (12)	97 (1)	96 (1)	95 (2)
<i>o</i> -Xylene	101 (3)	2 (13)	98 (2)	98 (3)	94 (3)
<i>n</i> -Nonane (C ₉)	101 (2)	3 (15)	100 (4)	101 (1)	96 (4)
<i>n</i> -Undecane (C ₁₁)	97 (5)	ND	102 (7)	102 (4)	103 (3)
<i>n</i> -Dodecane (C ₁₂)	95 (4)	ND	103 (6)	96 (4)	102 (3)
<i>n</i> -Tridecane (C ₁₃)	94 (6)	ND	88 (9)	97 (3)	97 (5)
<i>n</i> -Tetradecane (C ₁₄)	95 (4)	ND	81 (4)	97 (4)	100 (4)
<i>n</i> -Pentadecane (C ₁₅)	100 (5)	ND	83 (9)	98 (2)	93 (4)
<i>n</i> -Hexadecane (C ₁₆)	101 (5)	ND	57 (23)	95 (3)	90 (4)
<i>n</i> -Heptadecane (C ₁₇)	101 (5)	ND	31 (41)	95 (4)	95 (4)
<i>n</i> -Octadecane (C ₁₈)	100 (3)	ND	16 (39)	100 (4)	96 (10)
<i>n</i> -Nonadecane (C ₁₉)	101 (2)	ND	4 (16)	92 (7)	98 (7)
<i>n</i> -Eicosane (C ₂₀)	100 (2)	ND	2 (21)	99 (5)	95 (8)

ND = Not detected.

^a Values in parentheses are the percent relative standard deviations of triplicate 10-min extractions.

^b The internal standard is *n*-decane.

^c The internal standard is octahydroanthracene.

As shown in Table 2, SFE–GC recoveries with pure CO₂ were very low from the most retentive sorbent, Carbosieve S-III. For the slightly weaker sorbent, Carbotrap C, recoveries were quantitative for all BTEX compounds and for all of the alkanes up to *n*-dodecane, but not for the more highly retained (less volatile) alkanes. The poor recoveries from the Carbotrap resins were in part related to the short, 10-min extraction times. Longer (20-min) extractions resulted in nearly quantitative recovery of all the analytes from Carbotrap C and marginally improved recoveries for Carbosieve S-III. However, the goal was to develop a solid calibration standard that could be quantitatively extracted in 10 min. Fortunately, Tenax-TA and the XAD-2 resins were ideal calibration matrices since all the test analytes (including *n*-butane) could be quantita-

tively spiked into the middle of the sorbent resins at room temperature and pressure without loss of the volatile compounds, and then quantitatively recovered within 10 min using SFE–GC (Table 2).

The “shelf-life” of the spiked sorbent resins was also determined, since routine use of SFE–GC for volatile hydrocarbons would be simpler if several solid calibration standards could be made at one time and stored for use throughout the working day. As shown in Table 3, if the test *n*-alkanes and BTEX components were spiked onto an inert matrix such as glass beads, over a third of the most volatile analytes were completely lost after 24 h storage inside a closed extraction cell at room temperature. The most volatile analytes (*n*-butane and *n*-pentane) also evaporated from the Carbotrap C resin, which

Table 3
Recovery of BTEX and C₄–C₂₀ *n*-alkanes from sorbent resins 24 h after spiking

Analyte	Recovery (%) (R.S.D., %) ^a			
	Glass beads ^b	Carbotrap C ^c	Tenax-TA ^c	XAD-2 ^c
<i>n</i> -Butane (C ₄)	ND	ND	94 (5)	90 (6)
<i>n</i> -Pentane (C ₅)	ND	69 (7)	109 (4)	103 (6)
<i>n</i> -Hexane (C ₆)	ND	95 (3)	107 (3)	98 (5)
Benzene	ND	92 (4)	100 (4)	97 (4)
<i>n</i> -Heptane (C ₇)	ND	98 (5)	98 (5)	98 (4)
Toluene	ND	100 (2)	96 (6)	98 (5)
<i>n</i> -Octane (C ₈)	ND	98 (3)	99 (3)	99 (3)
Ethylbenzene	5 (59)	101 (3)	95 (5)	98 (4)
<i>m</i> -Xylene	7 (65)	101 (3)	95 (4)	98 (4)
<i>o</i> -Xylene	8 (69)	102 (2)	95 (4)	97 (4)
<i>n</i> -Nonane (C ₉)	13 (71)	98 (2)	99 (1)	100 (2)
<i>n</i> -Decane (C ₁₀)	52 (53)	100 (0)	100 (0)	100 (0)
<i>n</i> -Undecane (C ₁₁)	82 (24)	102 (4)	102 (3)	102 (3)
<i>n</i> -Dodecane (C ₁₂)	95 (8)	102 (5)	100 (4)	101 (3)
<i>n</i> -Tridecane (C ₁₃)	96 (4)	101 (6)	101 (7)	98 (7)
<i>n</i> -Tetradecane (C ₁₄)	96 (6)	97 (10)	102 (9)	98 (7)
<i>n</i> -Pentadecane (C ₁₅)	94 (7)	77 (24)	102 (9)	95 (9)
<i>n</i> -Hexadecane (C ₁₆)	95 (6)	49 (25)	101 (9)	100 (7)
<i>n</i> -Heptadecane (C ₁₇)	101 (3)	28 (26)	97 (9)	103 (8)
<i>n</i> -Octadecane (C ₁₈)	95 (4)	17 (33)	98 (9)	98 (8)
<i>n</i> -Nonadecane (C ₁₉)	98 (5)	9 (38)	99 (9)	97 (9)
<i>n</i> -Eicosane (C ₂₀)	97 (7)	5 (46)	100 (11)	97 (7)

ND = Not detected.

^a Values in parentheses are the percent relative standard deviations of triplicate 10-min extractions.

^b The internal standard is octahydroanthracene.

^c The internal standard is *n*-decane.

might be expected as the sorbent resin was designed to trap heavier hydrocarbons with volatilities similar to, or greater than C₈ [24]. However, the Tenax-TA and XAD-2 resins gave quantitative recoveries of the test mix after 24 h of storage, and replicate SFE–GC analysis of the aged sorbent standards produced low (1 to 11%) relative standard deviations (R.S.D.s) considering the R.S.D.s included all the possible errors associated with the spiking procedure, the storage, SFE–GC and the chromatographic peak integration. Both the spiked Tenax and XAD resins were, therefore, reliable calibration standards, but for convenience, only Tenax-TA was used to further investigate the SFE–GC collection parameters. Tenax-TA also proved to be a robust and reusable matrix, with no degradation

of the sorbent observed during the study even after 30 extractions, and less than 1 ppm of detectable impurities were found by SFE–GC in the SFE-cleaned resin.

For these sorbent studies, analyte recovery was determined by comparing conventional split injections of the *n*-alkane and BTEX test mix with SFE–GC analysis of the same quantity of test mix from the sorbents. Initially, analyte recoveries were calculated by comparing the raw chromatographic peak areas from the injection and SFE–GC methods, but this proved to be unreliable as the split ratio changed between the GC and SFE–GC analysis because of the changes in total gas flow introduced into the GC injection port (Table 1) [25]. For example, a split ratio of ca. 155:1 under normal GC con-

ditions decreased to ca. 65:1 under SFE–GC conditions, even though the needle valve (which controlled the split) had not been adjusted (Table 1) and the pressure in the injection port was similar. Furthermore, the split ratio during SFE–GC increased as the SFE flow-rate decreased (Table 1). At a constant SFE flow-rate, replicate SFE–GC analyses showed good quantitative reproducibility of raw peak areas; thus, demonstrating that the split ratio remains constant under constant flow conditions and that external standardization can be used for quantitation as long as the solid calibration standards (e.g., spiked sorbents) are extracted and analyzed under identical SFE–GC conditions. However, a better approach is to use an internal standard which is added to the environmental sample (and solid calibration sorbents) since any variations in split ratio that may occur at different SFE flow conditions should not affect the ratio of analyte to internal standard peak areas. Therefore, all the analyses in this study were performed with an internal standard (e.g., decane or octahydroanthracene, depending on the sorbent) added to the sample prior to SFE.

3.4. SFE–GC analysis of common solvents

In addition to the alkane–BTEX organics used for the optimization studies, the potential application of SFE–GC for determining several volatile and semivolatile hazardous organic solvents from solid samples was also investigated. A mixture of the test solvents (ca. 18 μg of each component and 18 μg of the internal standard *n*-heptane) was spiked onto Tenax-TA, extracted at 0.6 ml/min using a 80:1 split ratio (resulting in ca. 5 ml/min flow of gaseous CO_2 through the GC column), the 5- μm film thickness DB-1 GC column, and a cryogenic trapping temperature of -50°C . Fig. 5 shows that the SFE–GC chromatograms generated using these optimized experimental parameters compared favorably with those generated by using the conventional split injection technique and the peak widths and peak symmetry of the test solvents yielded by SFE–GC were similar to those obtained by the

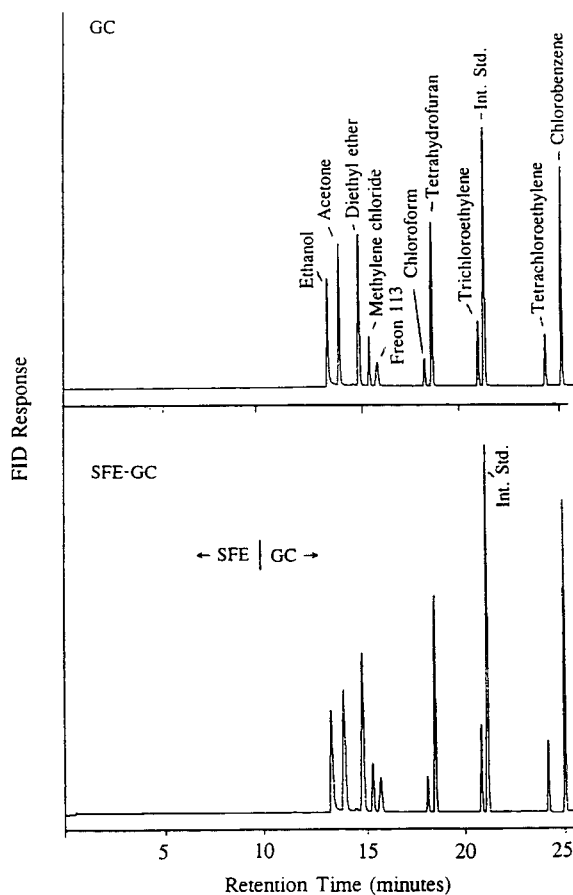


Fig. 5. Comparison of peak shapes generated using conventional GC injection of a mixture of organic solvents with those obtained using SFE–GC–FID. A mixture (0.2 μl) was either injected onto a capillary column or spiked onto Tenax-TA (400 mg) and extracted “on-line” for 10 min with 400 atm, 60°C CO_2 at 0.6 ml/min. The 30 m \times 0.32 I.D. (5- μm film) DB-1 capillary column was kept at -50°C during the injection or extraction step. After the extraction or 10 min after the injection the GC oven was heated at ca. $50^\circ\text{C}/\text{min}$ to 40°C then at $8^\circ\text{C}/\text{min}$ to 300°C .

split injection. All the solvents were quantitatively recovered from the sorbent resin, and replicate SFE–GC analyses produced very low relative standard deviations (Table 4). SFE–GC required ca. 30 min to complete including spiking the matrix, assembling the extraction cell and performing the extraction and gas chromatographic separation.

Table 4
Recovery of volatile organic compounds from Tenax-TA using 400 atm 60°C CO₂

Analyte	Recovery (%) (R.S.D., %) ^a
Ethanol	105 (1.3)
Acetone	101 (0.2)
Diethyl ether	102 (0.4)
Methylene chloride	98 (0.1)
Freon 113	111 (0.6)
Chloroform	96 (0.3)
Tetrahydrofuran	96 (0.3)
Trichloroethylene	97 (0.5)
Tetrachloroethylene	99 (0.7)
Chlorobenzene	101 (0.9)

See Fig. 5 for chromatographic results.

^a Values in parentheses are the percent relative standard deviations of triplicate 10-min extractions.

4. Conclusions

A simple and reliable method has been developed for performing split SFE–GC–FID using standard GC instrumentation which has undergone minor modifications. A solid-phase calibration standard (consisting of several *n*-alkanes and BTEX spiked onto Tenax-TA) was successfully used to determine and optimize the collection efficiency and focusing of extracted analytes on the chromatographic column during the extraction step in SFE–GC analysis. The most important experimental parameters to be optimized are the cryogenic trapping temperature, the SFE flow-rate, and the column stationary phase thickness. Cooling the chromatographic column to –50°C enables analytes as volatile as *n*-butane to be focused and retained during the SFE step, and then resolved as a sharp gaussian peak in the GC analysis. The high gaseous flow-rates generated during the SFE step can be accommodated for by using the correct split ratio so a suitable column volumetric flow-rate can be obtained, and thus, 1 ml/min liquid CO₂ SFE flow-rates can routinely be used for SFE–GC analysis. Since the results of this study demonstrate that SFE–GC has the potential to determine both volatile and semi-volatile organics, a single SFE–GC analysis has good potential

to replace two analyses (e.g., purge and trap for volatiles, and liquid solvent extraction for semivolatiles) when quantitative information is desired for organics having a wide range of volatility.

Acknowledgements

The financial support of the American Petroleum Institute, the US Department of Energy and the US Environmental Protection Agency, EMSL-LV (Las Vegas) are gratefully acknowledged, as are instrumental loans from ISCO.

References

- [1] J.M. Levy, R.A. Cavalier, T.N. Bosch, A.M. Rynaski and W.E. Huhak, *J. Chromatogr. Sci.*, 27 (1989) 341.
- [2] S.B. Hawthorne and D.J. Miller, *J. Chromatogr.*, 403 (1987) 63.
- [3] S.B. Hawthorne, D.J. Miller and M.S. Krieger, *J. Chromatogr. Sci.*, 27 (1989) 347.
- [4] J.M. Levy and A.C. Rosselli, *Chromatographia*, 28 (1989) 613.
- [5] F.I. Onuska and K.A. Terry, *J. High Resolut. Chromatogr.*, 12 (1989) 527.
- [6] S.B. Hawthorne, J.J. Langenfeld, D.J. Miller and M.D. Burford, *Anal. Chem.*, 64 (1992) 1614.
- [7] J.H. Raymer and G.R. Velez, *J. Chromatogr. Sci.*, 29 (1991) 467.
- [8] S.B. Hawthorne, D.J. Miller and J.J. Langenfeld, *J. Chromatogr. Sci.*, 28 (1990) 2.
- [9] J.M. Levy, E. Storozynsky and R.M. Ravey, *J. High Resolut. Chromatogr.*, 14 (1991) 661.
- [10] S.A. Liebman, E.J. Levy, S. Lurcott, S. O'Niel, J. Guthrie, T. Ryan and S. Yocklovich, *J. Chromatogr. Sci.*, 27 (1989) 118.
- [11] L. Baner, T. Bücherl, J. Ewender and R. Franz, *J. Supercritical Fluids*, 5 (1992) 213.
- [12] J.C. Wallace, M.S. Krieger and R.A. Hites, *Anal. Chem.*, 64 (1992) 2655.
- [13] M.W.F. Nielen, J.A. Stäb, H. Lingeman and U.A.Th. Brinkman, *Chromatographia*, 32 (1991) 543.
- [14] M.W.F. Nielen, J.T. Sanderson, R.W. Frei and U.A.Th. Brinkman, *J. Chromatogr.*, 474 (1989) 388.
- [15] M.D. Burford, S.B. Hawthorne and D.J. Miller, *J. Chromatogr.*, 609 (1992) 321.
- [16] J.J. Langenfeld, M.D. Burford, S.B. Hawthorne and D.J. Miller, *J. Chromatogr.*, 594 (1992) 297.
- [17] A. Hagman and S. Jacobsson, *J. Chromatogr.*, 448 (1988) 117.

- [18] J.W. Graydon and K. Grob, *J. Chromatogr.*, 254 (1983) 265.
- [19] J.K. Pankow, *Anal. Chem.*, 60 (1988) 950.
- [20] *GC Bulletin 846C*, Supelco, Bellefonte, PA, 1986.
- [21] B.W. Wright, C.W. Wright, R.W. Gale and R.D. Smith, *Anal. Chem.*, 59 (1987) 38.
- [22] J.M. Wong, N.Y. Kado, P.A. Kuzmicky, H.-S. Ning, J.E. Woodrow, D.P.H. Hsieh and J.N. Seiber, *Anal. Chem.*, 63 (1991) 1644.
- [23] S.B. Hawthorne and D.J. Miller, *J. Chromatogr. Sci.*, 24 (1986) 258.
- [24] *Sample Handling Bulletin 850*, Supelco, Bellefonte, PA, 1987.
- [25] X. Lou, H-G Janssen and C.A. Cramers, *J. High Resolut. Chromatogr.*, 16 (1993) 425.



ELSEVIER

Journal of Chromatography A, 685 (1994) 95–111

JOURNAL OF
CHROMATOGRAPHY A

Analysis of volatile organics by supercritical fluid extraction coupled to gas chromatography

II. Quantitation of petroleum hydrocarbons from environmental sample

Mark D. Burford, Steven B. Hawthorne*, David J. Miller

Energy and Environmental Research Center, University of North Dakota, Grand Forks, ND 58202, USA

First received 6 April 1994; revised manuscript received 5 July 1994

Abstract

A coupled supercritical fluid extraction–gas chromatography (SFE–GC) method has been developed for the quantitative extraction and analysis of gasoline and diesel range organics from real world environmental samples. Petroleum-contaminated samples containing gasoline- to diesel- and motor oil-range hydrocarbons (total hydrocarbon content typically ranging from 2 to 26 mg/g) could be quantitatively extracted by a 15-min SFE–GC extraction using 400 atm (1 atm = 101 325 Pa), 60°C CO₂. The SFE–GC hydrocarbon recoveries from real-world samples were comparable to those obtained by sonicating the samples in methylene chloride for 14 h, except for the gasoline recovery which was higher by SFE–GC analysis due to the more efficient collection of the more volatile analytes. Reproducibilities for replicate SFE–GC extractions and analyses were typically <5% (R.S.D.) for the quantitation of both individual organics and total hydrocarbon content. Gasoline- to diesel-range organics (as volatile as *n*-pentane) could be quantitatively retained during the SFE step of the SFE–GC analysis using a thick-film (30 m × 0.32 mm I.D., 5 μm film thickness) DB-1 column operated at a cryogenic trapping temperature of –25°C. Using split SFE–GC operated at a high split ratio (100:1) relatively large 1-g sample sizes could be extracted, and by using a drying agent (molecular sieve 3A) very wet (25%, w/w, water) samples could be analyzed without extracted water freezing and plugging in the GC column during the SFE step.

1. Introduction

Contamination of the environment by fuel leaks from underground storage tanks and by fuel spills during production and transport has become a major environmental issue which has prompted routine soil monitoring for TPH (total petroleum hydrocarbons) and BTEX components (benzene, toluene, ethylbenzene, *m*-xylene

and *o*-xylene). Head space [1] or purge and trap [2–4] techniques are typically used for the recovery of volatile petroleum hydrocarbons such as the gasoline range organics (defined as compounds in the C₆–C₁₀ boiling point range [1]). However, samples containing less volatile hydrocarbons such as diesel range organics (C₁₀–C₂₅ boiling point range) require more rigorous extraction conditions using organic solvents such as Freon-113 (trichlorofluoroethane) [5,6], methylene chloride [7,8], or alkalized methanol [9].

* Corresponding author.

Although both purge-and-trap and liquid solvent techniques are valuable methods for the extraction and recovery of petroleum hydrocarbons, each method has its limitations. For example, the suitability of head space and purge-and-trap analysis is severely limited by the volatility of the analyte species; thus, moderately volatile samples such as kerosene and diesel fuel are virtually non-detectable by these techniques [1,4]. Conversely, liquid solvent extraction may yield low recoveries for the volatile gasoline range organics due to sample losses during processing, and can require several hours to perform, generating large volumes of hazardous waste solvent [10]. Furthermore, one of the most common organic solvents used for petroleum hydrocarbon analysis, namely Freon-113, is being phased out of production in accordance with the Montreal Protocol on Substances that Deplete the Ozone Layer [10,11].

A recent alternative to these established extraction techniques is the use of supercritical fluid extraction (SFE). The most commonly used supercritical fluid, carbon dioxide, can extract polycyclic aromatic hydrocarbons [12–14], and alkyl and aromatic hydrocarbons [10,11,15,16] with recoveries that are comparable to liquid solvent extraction. Under SFE conditions carbon dioxide has a solvent strength that approaches that of a liquid enabling the solvent to extract analytes from the gasoline- to diesel-range organics, which is desirable as petroleum hydrocarbon contamination in the environment often involves a mixture of fuels. Another advantage of carbon dioxide is that at ambient conditions the solvent is a gas, which greatly simplifies the concentration of extracted analytes and, most importantly for this paper, allows the direct coupling of SFE with capillary gas chromatography (GC) without introducing large volumes of liquid solvent onto the chromatographic column [12,16–20].

Coupled (on-line) SFE with capillary GC is very attractive, as the extracted analytes are deposited directly into the gas chromatograph, greatly reducing sample preparation and handling steps and minimizing the potential for analyte loss. On-line SFE is, therefore, very suitable

for petroleum hydrocarbon analysis as the technique can efficiently extract and collect very volatile analytes such as the gasoline-range organics. For example, on-line SFE can recover analytes as volatile as *n*-butane [21] compared to off-line SFE (analyte collected in an organic solvent) which is only suitable for analytes as volatile as *n*-octane [22]. Furthermore, as no organic solvent is used in the on-line SFE technique, there is no solvent peak present which can chromatographically co-elute with the volatile analytes.

The aim of this study is to develop a simple and reliable coupled SFE–GC method for the analysis of petroleum hydrocarbons from a variety of environmental samples without the need for any pre-preparation (e.g., air drying). The method uses a conventional split/splitless injection port operated at the optimized SFE–GC conditions developed in the first part of this study [21]. Only slight modifications need to be made to the gas chromatographic equipment as previously described [21] and a drying agent is used to enable very wet samples to be analyzed. The quantitative recovery of gasoline- and diesel-range organics (including BTEX) from real world environmental samples using SFE–GC analysis are reported and compared to the recoveries obtained by a conventional organic solvent extraction.

2. Experimental

2.1. Instrumentation and methods

Coupled SFE–GC analysis with flame ionization detection (FID) was performed using a Hewlett-Packard 5890 gas chromatograph modified as described in Part I of this study [21] with helium as the carrier gas and a wide-bore (30 m × 0.32 mm I.D., 5 μm film thickness) DB-1 column supplied by J & W Scientific, Folsom, CA, USA. The injection port and FID system were both operated at 300°C. The split ratio (under SFE–GC conditions) was maintained at 100:1 [21].

Supercritical fluid extractions were performed

with CO₂ (supercritical-fluid grade, Scott Specialty Gases, Plumsteadville, PA, USA) and an ISCO Model 260D syringe pump (ISCO, Lincoln, NE, USA). Samples were placed in a 3.5-ml extraction cell from Keystone Scientific (Bellefonte, PA, USA). The flow-rate of the supercritical fluid through the extraction cell was controlled at 0.6 ml/min (as liquid CO₂ measured at the pump) by a 9-cm-long restrictor (26 μm I.D. × 150 μm O.D.) cut from fused-silica tubing (Polymicro Technologies, Phoenix, AZ, USA). During the extraction, the extraction cell and a pre-equilibration coil were placed inside a thermostated tube heater which was situated directly above the injection port.

To avoid the loss of volatile hydrocarbon components, sample handling and processing during SFE–GC was kept to a minimum and the contaminated samples were analyzed without drying. Prior to weighing the sample into the extraction cell, the internal standard (octahydroanthracene in methylene chloride) was spiked onto an 8-mm O.D. circular piece of Whatman No. 1 filter paper (Maidstone, UK). The methylene chloride was then allowed to completely evaporate as determined by weighing the filter paper. The 3.5-ml extraction cell was filled with 2 g of drying agent, molecular sieve 3A (Alltech, Deerfield, IL, USA). With the internal standard spiked on the filter paper and the drying agent loaded inside the extraction cell, the sample (1 g) was quickly placed on top of the drying agent, the spiked filter paper was placed on top of the sample, and the cell immediately sealed and extracted so that the SFE flow went sequentially through the filter paper, sample, and drying agent (from top to bottom). The extraction effluent was depressurized inside the split/splitless injection port (split set at 100:1) and the analytes were cryogenically trapped (–50 or –25°C depending on the sample) in the chromatographic column as previously described [21]. During SFE the GC carrier gas was then shut off with a toggle valve and the sample extracted for 15 min with 400 atm (1 atm = 101 325 Pa), 60°C CO₂. At the end of the extraction the restrictor was withdrawn from the injection port, the carrier gas was turned on, and

analysis begun by rapidly heating the GC oven to 40°C, then at 8°C/min to 300°C.

After SFE–GC analysis, the sample residue was either re-extracted by SFE–GC, or the sample, drying agent and filter paper were removed from the extraction cell and sonicated in 10 ml of methylene chloride for 14 h. After sonication, the extract was centrifuged at 300 g for 10 min to remove debris, the solvent was evaporated to 1 ml (for samples containing volatile components) or 100 μl (for samples containing less volatile components) and an internal standard (octahydroanthracene) added for GC–FID analysis. Fresh samples (1 g) were also extracted by sonicating in 10 ml methylene chloride for 14 h. The solvent extract was centrifuged and evaporated to 1 ml and an internal standard (octahydroanthracene) added for GC–FID analysis. The methylene chloride extracts were analyzed using the same GC column as the SFE–GC analysis but operated in the GC mode by injecting 1 μl of the extract into the split/splitless injection port in the splitless mode.

Since on-line SFE–GC introduces all of the extracted organics into the injection port (while this is not possible with the methylene chloride extract), SFE–GC can yield much larger peak areas than conventional solvent injections which could, in turn, lead to integration errors in comparing the two methods. This was not a problem with the samples using individual peak integration (i.e., the samples with the more volatile fuel components). Therefore, the methylene chloride extracts from these samples were concentrated only to 1 ml to avoid any unnecessary loss of volatiles. However, many of the components of the diesel- and motor oil-contaminated samples were poorly resolved (Figs. 5 and 6). Therefore, integration using an extended baseline was required for accurate determination of TPH. For these samples it was necessary to introduce equivalent quantities of extracted hydrocarbons into the GC column, both by SFE–GC and by conventional injection of the methylene chloride extracts, to allow accurate comparisons of the extraction efficiencies. To accomplish this, the SFE–GC analyses were performed with a 100:1 split ratio, and the

methylene chloride extracts were concentrated to 100 μl before injection of 1 μl in the splitless mode. Therefore, a comparable amount (1%) of the total extracted analytes were injected by both methods, and the peak areas were equivalent for the two techniques (assuming equivalent extraction efficiencies). To further ensure that the quantitative comparisons were valid, all quantitative results for all of the samples used in this study were based on the internal standard (octahydroanthracene).

2.2. Samples and standards

Six environmental samples contaminated with petroleum hydrocarbons, but with varying organic and water contents, were collected locally (North Dakota, USA), sieved to <2 mm to remove any sticks and other debris, and stored at -10°C until analyzed. The type of hydrocarbon contamination was confirmed by GC–mass spectrometry (MS) analysis using a Hewlett-Packard Model 5988 with electron impact ionization (70 eV). Scan range was 50–400 u.

Contaminated sediment was collected from an aquifer under an oil refinery at about a 2 m depth and contained ca. 5.0% (w/w) water and 0.8% (w/w) organic matter (determined by thermogravimetric analysis). A second sediment was obtained from an aquifer near underground fuel storage tanks. Two sandy soil samples were collected, each containing 0.4% organic matter and 25% (w/w) and 17% (w/w) water, respectively. A top soil collected next to an above ground diesel storage tank contained ca. 1.0% (w/w) water and 7.1% (w/w) organic matter. A motor oil-contaminated soil was taken from a railroad embankment and contained ca. 1.6% (w/w) water and 7.4% (w/w) organics. A gasoline-contaminated charcoal filter was obtained from a 1974 Chevette automobile. The filter was situated between the gasoline tank and carburetor and consisted of 1-mm O.D. carbon particles which contained ca. 3.4% (w/w) water.

The final sample was a “clean” agricultural top soil which contained ca. 16% (w/w) water and 4.7% (w/w) organic matter. This soil was spiked

with gasoline by placing the unspiked soil on top of a bed of drying agent inside a 3.5-ml extraction cell (as discussed in the *Instrumentation and methods* section) and then injecting 1 μl of fresh unleaded gasoline into the middle of the 1-g sample. A piece of filter paper containing the internal standard was placed on top of the sample (as discussed in the *Instrumentation and methods* section) and the cell was then immediately sealed and connected to the SFE–GC apparatus.

For all samples, the internal standard, octahydroanthracene, was spiked onto filter paper or into the methylene chloride sonication extract at a concentration similar to that of the native analytes in the environmental samples, namely: 53 μg (contaminated sediment from an oil refinery), 214 μg (sediment from near the underground storage tanks), 428 μg (diesel contaminated soil), 107 μg (motor oil contaminated soil), 535 μg (gasoline contaminated charcoal filter) and 53 μg (soil spiked with gasoline). Quantitation of well-resolved individual species was based on peak areas (compared to the internal standard). For poorly resolved species (e.g., motor oil organics), quantitation of total petroleum hydrocarbons was based on a total integrated FID area using an extended baseline compared to the peak area of the internal standard [11]. Quantitative recovery of the spiked gasoline sample was determined by comparing the SFE–GC recoveries to a conventional split injection of the neat gasoline containing octahydroanthracene (53 mg/ml).

To determine the detection limit of the SFE–GC system a neat mixture of BTEX and C_4 – C_{20} *n*-alkanes (ca. 0.5 g each) was prepared and diluted in ethanol (1 mg neat mixture/ml) [21]. A sorbent resin, Tenax-TA (Supelco, Bellefonte, PA, USA) was prepared by weighing 400 mg of the 60–80 mesh (180–250 μm) resin into a 2.5-ml extraction cell, and pre-extracting for 30 min with 400 atm CO_2 (60°C) to remove contaminants. The hydrocarbon–ethanol solution (1, 0.4 or 0.2 μl) was injected into the center of the clean Tenax-TA. The spiked sorbent resin was flushed with dry helium for 10 min at 300 ml/min to remove the ethanol. The sample was then

analyzed under identical SFE–GC conditions as the environmental samples using the 100:1 split ratio.

3. Results and discussion

3.1. Quantitative SFE–GC

The success of SFE–GC is dependent upon the correct choice of the SFE flow-rate, the GC column stationary phase thickness, and the oven temperature used for the cryogenic trapping of extracted analytes as optimized in the first part of this study [21] and as now used for the analysis of petroleum-contaminated environmental samples. The samples were extracted at a suitable extraction flow-rate (0.6 ml/min CO₂ as liquid CO₂ measured at the pump) using the appropriate split ratio (100:1), chromatographic column (5 μm film thickness), and cryogenic trapping temperature (–50 or –25°C).

The ability of split SFE–GC analysis to quantitatively extract and recover petroleum hydrocarbons from environmental samples was first investigated by analyzing replicate 1-g samples of agricultural soil spiked with neat gasoline. Complete extraction and trapping of the spiked soil should yield the same quantity of gasoline (1 μl spike) as 1 μl of gasoline injected into the gas chromatograph. Initially, analyte recoveries were calculated by comparing the raw chromatographic areas obtained by the SFE–GC and conventional injection techniques. However, this proved to be unreliable because the split ratio changed between the SFE–GC and GC analysis [21,23]. Therefore, to determine the recoveries internal standardization was used as this quantitative method is independent of the split ratio. The analyte response factors (area ratio of analyte to internal standard, octahydroanthracene) produced from the SFE–GC method were compared with those generated from the conventional split injection of the gasoline spike and internal standard.

The SFE–GC technique gave chromatograms with virtually identical peak shapes as those generated by a conventional split injection of

neat gasoline, demonstrating that the use of coupled SFE–GC did not cause any loss in the quality of the chromatographic separations (Fig. 1). Furthermore, no peak tailing or split peaks associated with poor trapping were observed, as

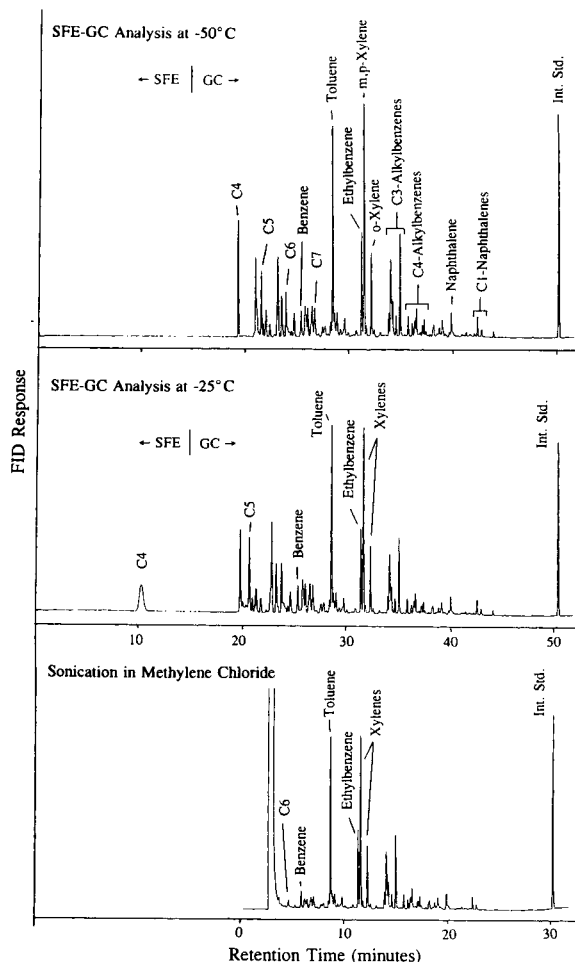


Fig. 1. Analysis of a 1-g soil sample spiked with 1-μl of neat gasoline using split SFE–GC–FID (split ratio ca. 1:100) and sonication in methylene chloride. The contaminated sample and a piece of filter paper spiked with the internal standard octahydroanthracene were placed on a bed of drying agent (molecular sieve 3A) inside an extraction cell and extracted for 15 min with 400 atm, 60°C, CO₂ at 0.6 ml/min. The extracted analytes were trapped onto a thick-film (5 μm) 30 m × 320 μm I.D. DB-1 capillary column at either –50 or –25°C (see top and middle chromatogram). After each extraction, the GC oven was heated at ca. 50°C/min to 40°C then at 8°C/min to 300°C. For comparison, the contaminated sample was also sonicated in 10-ml methylene chloride for 14 h (see lower chromatogram).

the peak width at half-height for both the volatile (pentane) and semivolatile (methylnaphthalene) analytes generated by the SFE–GC analysis were comparable to a conventional injection of the solvent extract. Raising the cryogenic temperature of the column from -50 to -25°C during SFE–GC analysis decreased the trapping efficiency of the column, as butane was eluted as a broad peak during the SFE step (Fig. 1). However, all the analytes could still be chromatographically resolved and quantified. Conversely, sonicating the sample in methylene chloride caused chromatographic problems as some of the volatile analytes (e.g., butane and pentane) could not be resolved from the solvent (Fig. 1) and, therefore, could not be quantified.

The extraction and recovery efficiencies obtained using the coupled SFE–GC techniques are shown in Table 1. The SFE–GC recovery of the gasoline was essentially quantitative at both the -50 and -25°C column trapping tempera-

tures, except for the very volatile species (e.g., butane, pentane, hexane and benzene) which had recoveries as low as ca. 74%. The low recoveries are probably due to volatilization losses that occurred during the spiking of the soil, since SFE–GC yielded quantitative recovery of all of these species when gasoline range organics were extracted from Tenax-TA and XAD-2 sorbent resins [21]. To further ensure that quantitative recoveries were achieved the spiked soil sample was either re-extracted by SFE–GC or sonicated in methylene chloride. Both extraction techniques failed to recover additional analytes from the sample, confirming a quantitative recovery.

For comparison, the spiked soil was also analyzed by a conventional extraction method, namely sonication in methylene chloride (Table 1). Using the organic extraction method a non-quantitative or partial recovery of the gasoline was obtained. In this instance analyte losses

Table 1
Recovery of spiked gasoline from soil using split SFE–GC and sonication in methylene chloride

Analyte	Recovery (%) (R.S.D., %) ^a		
	Sonication ^b	SFE–GC (-50°C) ^c	SFE–GC (-25°C) ^d
Butane	ND	85 (13)	93 (12)
Pentane	ND	75 (12)	77 (9)
Hexane	11 (33)	74 (11)	85 (9)
Benzene	46 (26)	77 (10)	81 (12)
Heptane	39 (18)	89 (11)	94 (10)
Toluene	101 (8)	97 (9)	98 (8)
Ethylbenzene	103 (8)	102 (8)	104 (8)
<i>m</i> -, <i>p</i> -Xylene	103 (9)	102 (8)	104 (7)
<i>o</i> -Xylene	99 (8)	107 (8)	107 (9)
C ₃ -Alkylbenzene	107 (9)	107 (7)	106 (5)
C ₃ -Alkylbenzene	112 (11)	109 (7)	111 (3)
Naphthalene	103 (6)	115 (7)	109 (5)
C ₁ -Naphthalene	104 (7)	111 (8)	115 (6)
Total petroleum hydrocarbon	63 (10)	95 (9)	103 (6)

See Fig. 1 for chromatographic results. ND = Not detected.

^a Recovery relative to values obtained from a neat injection of the gasoline spike. Values in parentheses are the relative standard deviations (%) of triplicate extractions and GC analyses.

^b Spiked 1-g sample sonicated in 10-ml methylene chloride for 14 h.

^c Spiked 1-g sample analyzed by SFE–GC–FID, the column temperature during the extraction was -50°C .

^d Spiked 1-g sample analyzed by SFE–GC–FID, the column temperature during the extraction was -25°C .

occurred due to the sample handling, which included the sonication, centrifugation and evaporation of the extract from 10 to 1 ml (note that the methylene chloride extracts were never evaporated lower than 1 ml). These losses were most severe for the volatile analytes (e.g., *n*-butane to *n*-heptane) which were either not detected (as the organic solvent co-eluted with the analyte, Fig. 1) or had very low recoveries of 11 to 46% (Table 1). The loss of the volatiles during the extraction had a significant impact on the overall recovery of the gasoline, which was only in the region of ca. 63%. Sonication was, therefore, an unsuitable extraction method for gasoline analysis because of the loss of volatiles.

The reproducibility of both extraction techniques is indicated by the relative standard deviation which ranged from 6 to 33% for sonication extraction and from 3 to 13% for the SFE–GC analysis (Table 1). As expected, the recovery of the volatile analytes was more reproducible by the SFE–GC technique than by the sonication method as the coupled technique had far fewer sample handling steps. Furthermore, the online technique only required approximately 80 min analysis time, including sample weighing and loading the SFE cell, extraction, analyte collection and GC separation, compared to 18 h for the sonication analysis.

The analysis of such a relatively wet sample (16%, w/w, for the spiked soil) by SFE–GC can be a problem, as water is not very amenable to GC analysis since it causes band broadening [24]. Furthermore, the extracted water may freeze and plug in the column during the extraction and cryogenic trapping step of the SFE–GC analysis [16,25]; thus, preventing any additional analytes being introduced into the column (i.e., all analytes extracted after column plugging go out the split vent). Wet samples have previously been analyzed by SFE–GC by maintaining the GC column cryogenic trapping temperature above 0°C [25]. However, this approach was unsuitable for the analysis of gasoline range organics as volatile analytes in the C₄–C₆ range can not be efficiently retained on the column at this temperature [21]. In this study, column plugging by frozen water was avoided by placing the sample

on a bed of drying agent (molecular sieve 3A) situated inside the extraction cell. Molecular sieve 3A is one of the most effective drying agents for SFE analysis [26] and proved ideally suited for the SFE–GC technique as a constant flow was maintained through the cryogenically cooled (–50°C) column during the entire extraction of the wet (16%, w/w, water) sample. Furthermore, the molecular sieve 3A selectively retained only the water during the extraction step, as demonstrated by the quantitative recoveries in Table 1 (except for the very volatile species lost during spiking), as well as the fact that no petroleum hydrocarbons were recovered by sonicating the drying agent in methylene chloride after the SFE–GC analysis.

Besides water, matrix components (e.g., non-volatile organics present in the soil samples) may potentially be co-extracted with the target analytes of interest and may cause a degradation of the chromatographic column performance. However, by using a split injection port with a high split ratio (100:1), the amount of non-“GC-able” components transferred into the chromatographic column was greatly reduced as the majority of these co-extracted compounds were deposited on the injection port liner. The use of molecular sieve 3A with the sample may also help reduce column contamination, as the drying agent can retain high-molecular-mass polar compounds. Therefore, the drying agent was used for all of the samples analyzed by SFE–GC, regardless of water or organic content.

3.2. SFE–GC detection limit

Coupled SFE–GC is often perceived as a technique that is limited to very small sample sizes typically in the order of < 100 mg [16,19]. While this is an advantage when the sample is difficult to collect in large quantities (e.g., air particulates or some samples collected at the scene of a crime), some analyses may require the use of larger sample sizes in order to ensure adequate sensitivity or sample homogeneity. In an attempt to work with a more realistic sample size, 1-g samples were used in this study. The final sensitivity of the SFE–GC method then

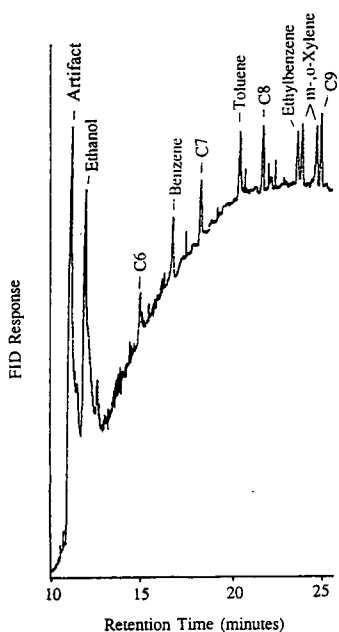


Fig. 2. Detection limit of the split SFE–GC–FID system. Approximately 9 ng each of the *n*-alkane and BTEX analytes were spiked onto Tenax-TA sorbent resin, and analyzed by SFE–GC at a split ratio of 1:100.

Table 2

Comparison of split SFE–GC and sonication in methylene chloride for the quantitation of petroleum hydrocarbons in a fuel-contaminated sediment from an oil refinery

Analyte	Concentration ($\mu\text{g/g}$) (R.S.D., %) ^a			
	Sonication ^b	SFE–GC (-50°C) ^c	SFE–GC (-25°C) ^d	SFE residue ^e
<i>n</i> -Nonane	7.6 (1)	6.6 (7)	7.3 (6)	ND
<i>n</i> -Decane	34 (6)	29 (4)	31 (5)	1.3 (19)
<i>n</i> -Undecane	68 (5)	55 (3)	67 (4)	2.4 (15)
<i>n</i> -Dodecane	107 (3)	87 (3)	95 (4)	2.7 (13)
<i>C</i> ₁ -Naphthalene	91 (2)	73 (3)	87 (3)	ND
<i>C</i> ₁ -Naphthalene	53 (2)	45 (4)	51 (4)	ND
Naphthalene	36 (2)	32 (2)	35 (7)	ND
<i>C</i> ₂ -Naphthalene	20 (0)	17 (2)	18 (7)	ND
Phenanthrene	12 (3)	15 (3)	16 (5)	ND
Total petroleum hydrocarbon	1429 (6)	1700 (10)	1582 (14)	7.1 (17)

See Fig. 3 for chromatographic results. ND = Not detected.

^a Values in parentheses are the relative standard deviations (%) of triplicate extractions and GC analyses.

^b Sample sonicated in 10-ml methylene chloride for 14 h.

^c Sample extracted with 400 atm 60°C CO_2 for 15 min, the column temperature during the extraction was -50°C .

^d Sample extracted with 400 atm 60°C CO_2 for 15 min, the column temperature during the extraction was -25°C .

^e SFE–GC sample residue re-extracted by sonicating in 10-ml methylene chloride for 14 h.

depends on the split ratio used during SFE and the FID detection limit. Selection of the split ratio depends on several factors. As previously described, higher split ratios during the SFE step allow faster extraction flow rates without causing distortion of the chromatographic peaks [21]; however, a higher split ratio also reduces the sensitivity of the analysis. In addition, many real-world samples are highly contaminated, so a relatively high split ratio is desirable to avoid overloading the GC column stationary phase. The goal of this study was to develop SFE–GC conditions that yielded low ppb (ng/g soil) detection limits for individual fuel components, while also being able to accommodate 1-g samples that were contaminated at widely varying concentrations. Therefore, a split ratio of 100:1 and a SFE extraction flow of 0.6 ml/min were chosen as standard conditions.

The detection limit of these SFE–GC conditions was determined using a hydrocarbon calibration standard spiked onto Tenax-TA [21] as described in the Experimental section. The resultant chromatogram for a spike of 9 ng each

of BTEX compounds and *n*-alkanes ranging from *n*-hexane to *n*-nonane is shown in Fig. 2. Each of the fuel components showed a signal-to-noise ratio of >5:1, demonstrating that very low ppb detection limits were achieved, even with the 100:1 split ratio used during the SFE step. Note also that artifacts from the Tenax-TA resin were very low compared to the low ppb quantities of the test analytes.

3.3. SFE–GC analysis of real-world environmental samples

With quantitative SFE–GC collection recoveries having been established and the coupled SFE–GC having sufficient sensitivity, five real-world samples were investigated. The ability of SFE–GC to yield reproducible quantitative results from real-world samples (1 g) was assessed by comparing the SFE–GC petroleum hydro-

carbon recoveries to those obtained by a conventional organic solvent extraction. Table 2 shows the hydrocarbon recoveries from a fuel-contaminated sediment obtained from an oil refinery using SFE–GC and sonication in methylene chloride. The 15-min SFE–GC extraction was able to achieve similar quantitative recoveries as the 14 h sonication extraction, yet it did not need any of the intervening sample handling steps required by the organic extraction method. The SFE–GC technique also showed good reproducibilities with relative standard deviations for the individual species ranging from 2 to 7%, thus demonstrating the ability of the technique to yield both rapid and reproducible determinations of the extractable petroleum hydrocarbons. The low relative standard deviations also suggest that the 1-g sample is representative of the bulk sample.

To ensure that quantitative recoveries were

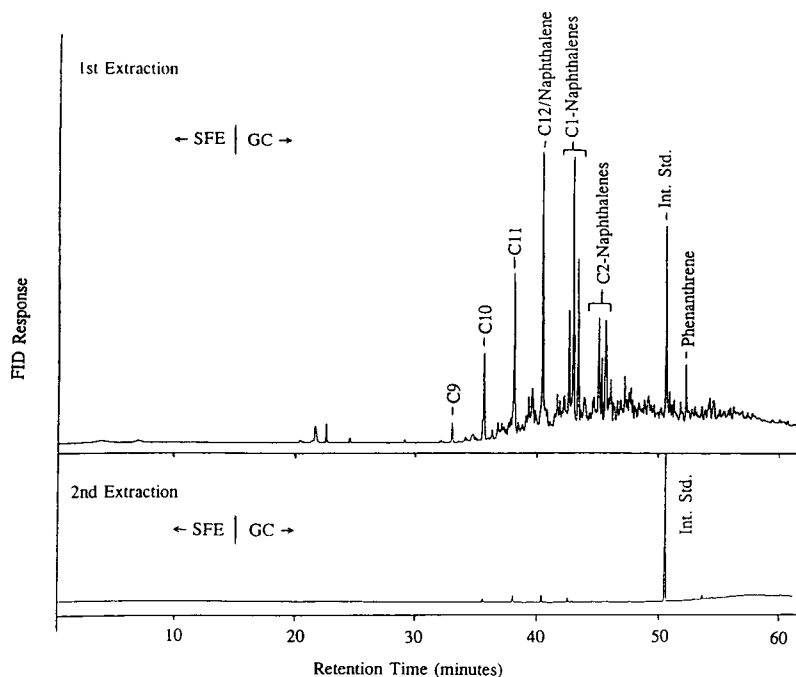


Fig. 3. Analysis of fuel-contaminated sediment from an oil refinery using split SFE–GC–FID analysis (split ratio ca. 1:100). A 1-g sample and a piece of filter paper spiked with the internal standard octahydroanthracene were placed on a bed of drying agent (molecular sieve 3A) inside an extraction cell and extracted for 15 min with 400 atm, 60°C, CO₂ at 0.6 ml/min. The extracted analytes were trapped onto a thick-film (5 μm) 30 m × 320 μm I.D. DB-1 capillary column at –25°C. After the extraction, the GC oven was heated at ca. 50°C/min to 40°C, then at 8°C/min to 300°C (top chromatogram). The sample was then extracted a second time under identical conditions as the first extraction (lower chromatogram).

obtained by SFE–GC the sample residue was either re-extracted by SFE–GC (Fig. 3) or sonicated in methylene chloride (Table 2). A second independent extraction method (e.g. sonication) was used as previous work had shown that simply re-extracting a real world sample under the same conditions as the first SFE extraction often failed to recover the more strongly bound analytes [27]. However, both extraction methods recovered less than 1% of the total hydrocarbon content from the SFE residues, indicating that the 15-min SFE was sufficient to quantitatively extract the fuel from the sediment. The SFE–GC quantitative recoveries also confirmed that the 0.6 ml/min CO₂ extraction flow-rate used during this study was an appropriate flow, both in terms of the requirements of the extraction (i.e., adequate flow to sweep the void volume and solubilize the analytes) and of the chromatography (i.e., produced Gaussian chromatographic peak shapes).

The quality of the SFE–GC chromatograms generated with a cryogenic trapping temperature of –50 or –25°C compared favorably with those generated by using the conventional split injection of the methylene chloride extract. Both trapping temperatures were suitable for the efficient retention of the extracted analytes on the column during the SFE step, as the recoveries at –50 and –25°C were similar (Table 2). Furthermore, no deterioration in the column performance or chromatographic peak shape was observed from analyzing the environmental sample in its native state [e.g., 5.0% (w/w) water and 0.8% (w/w) organic matter] demonstrating the effectiveness of using a high 100:1 split ratio and a drying agent in the SFE–GC analysis.

A second fuel-contaminated sediment obtained from an aquifer near underground fuel storage tanks contained analytes in the gasoline to kerosene range (Fig. 4). Two samples were collected, a water logged sediment from a poorly drained area (ca. 25% w/w, water) and a wet sediment from a well drained area (ca. 17% w/w, water). Both samples were placed on a bed of drying agent and analyzed by SFE–GC, but the recoveries obtained were significantly different (Tables 3 and 4). For the well drained

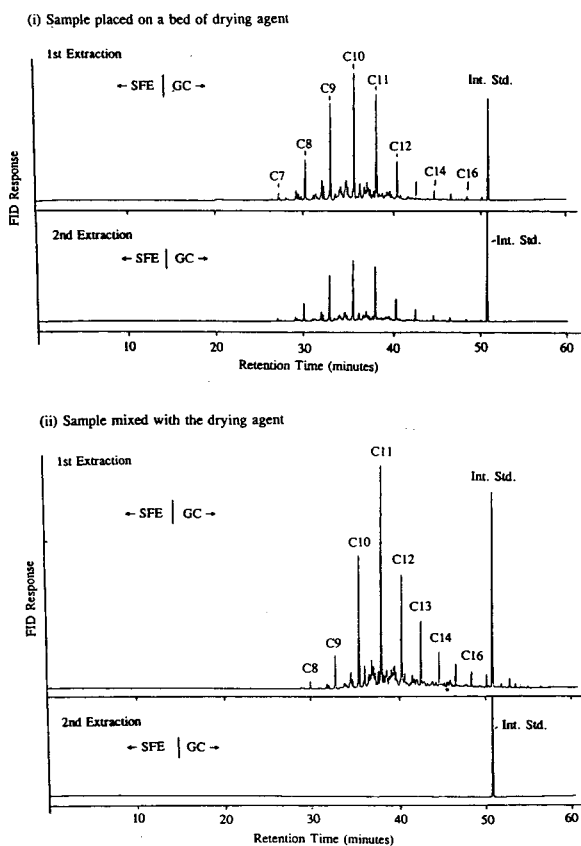


Fig. 4. Analysis of contaminated sediment near underground fuel storage tanks using split SFE–GC–FID (split ratio ca. 1:100). The water logged (25% w/w, water) 1-g sample and a piece of filter paper spiked with the internal standard octahydroanthracene were either (i) placed on a bed of drying agent (molecular sieve 3A) inside the extraction cell or (ii) mixed with the drying agent (molecular sieve 3A) and then placed inside the extraction cell. The sediment, drying agent and internal standard were extracted for 15 min with 400 atm, 60°C, CO₂ at 0.6 ml/min. The extracted analytes were trapped onto a thick-film (5 μm) 30 m × 320 μm I.D. DB-1 capillary column at –25°C. After the extraction, the GC oven was heated at ca. 50°C/min to 40°C, then at 8°C/min to 300°C. The samples were then extracted a second time under identical conditions as the first extract.

sediment (17% w/w, water) quantitative fuel recoveries were possible using the SFE–GC technique, as the hydrocarbon recoveries from the 15-min SFE–GC extraction were comparable to those obtained by sonicating the sediment in methylene chloride for 14 h (Table 3) whether the cryogenic trapping temperature was –25 or

Table 3

Comparison of split SFE–GC and sonication in methylene chloride for the quantitation of petroleum hydrocarbons in a contaminated sediment near underground storage tanks: wet sample (17%, w/w, water) placed on a bed of drying agent

Analyte	Concentration ($\mu\text{g/g}$) (R.S.D., %) ^a		
	Sonication ^b	SFE–GC ^c	SFE residue ^d
<i>n</i> -Hexane (C ₆)	ND	26 (18)	ND
<i>n</i> -Heptane (C ₇)	73 (15)	134 (12)	1.4 (32)
<i>n</i> -Octane (C ₈)	306 (12)	297 (8)	10 (43)
<i>n</i> -Nonane (C ₉)	505 (9)	428 (4)	24 (50)
<i>n</i> -Decane (C ₁₀)	486 (7)	422 (3)	31 (43)
<i>n</i> -Undecane (C ₁₁)	354 (6)	280 (4)	34 (38)
<i>n</i> -Dodecane (C ₁₂)	110 (5)	92 (3)	16 (35)
<i>n</i> -Tridecane (C ₁₃)	50 (7)	42 (4)	8.4 (34)
<i>n</i> -Tetradecane (C ₁₄)	24 (5)	21 (4)	4.4 (35)
<i>n</i> -Pentadecane (C ₁₅)	18 (7)	15 (4)	2.8 (35)
<i>n</i> -Hexadecane (C ₁₆)	12 (5)	10 (2)	1.8 (31)
<i>n</i> -Heptadecane (C ₁₇)	10 (5)	7.7 (5)	1.3 (26)
Total petroleum hydrocarbon	4415 (8)	4071 (5)	116 (2)

^a Values in parentheses are the relative standard deviations (%) of triplicate extractions and GC analyses.

^b Sample sonicated in 10-ml methylene chloride for 14 h; ND = not detected.

^c Sample and bed of drying agent (molecular sieve 3A) extracted with 400 atm 60°C CO₂ for 15 min, the column temperature during the extraction was –25°C.

^d SFE–GC sample residue re-extracted by sonicating in 10-ml methylene chloride for 14 h.

–50°C. The drying agent also efficiently retained the water from the 17% (w/w) sample as a continuous CO₂ flow was maintained through the cryogenically cooled column during the entire SFE step.

For the 25% (w/w) water sediment SFE–GC recovered only ca. 60% of the fuel in a 15-min extraction [Table 4, Fig. 4 (i)]. As the only measurable difference between the wet (17%, w/w, water) and water logged sediments (25%, w/w, water) was the water content, it appeared that the presence of a large amount of water was interfering with the SFE–GC analysis. There were two potential reasons for the low recoveries from the water logged sample, namely: (i) the water was inhibiting the column trapping efficiency despite the fact that a bed of drying agent was present; or (ii) the large amount of water present in the sediment was inhibiting the extraction, a similar phenomenon having been reported for the SFE analysis of a wet petroleum waste sludge [28]. To determine which hypoth-

esis was correct the SFE–GC sample residue was re-extracted by sonicating in methylene chloride (Table 4). The combined recoveries of the SFE–GC and sonication extraction were comparable to the conventional extraction method of sonicating the sediment in methylene chloride, demonstrating that the low recoveries obtained from the 15-min SFE step were due to the slow extraction rate of the hydrocarbons from the 25% (w/w) water sample rather than due to poor trapping. Mixing the sample with the drying agent was partially successful in that all the extractable hydrocarbons present in the sample could be recovered by a 15-min SFE–GC extraction [Fig. 4 (ii)]. No additional fuel was recovered either by a second SFE–GC extraction or by re-extracting the sample with methylene chloride (Table 4). However, the sample–drying agent mixture approach also failed since significant volatile analyte losses (C₆–C₁₂ n-alkanes) occurred during the mixing process because the molecular sieve 3A is an exothermic drying agent

Table 4

Comparison of split SFE–GC and sonication in methylene chloride for the quantitation of petroleum hydrocarbons in a contaminated sediment near underground storage tanks: water logged sample (25%, w/w, water) placed on a bed of drying agent or mixed with the drying agent

Analyte	Concentration ($\mu\text{g/g}$) (R.S.D., %) ^a				
	Sonication ^b	Sample on a bed of drying agent ^c		Sample mixed with a drying agent ^d	
		SFE–GC	SFE residue	SFE–GC	SFE residue
<i>n</i> -Hexane (C ₆)	ND	2.2 (13)	ND	ND	ND
<i>n</i> -Heptane (C ₇)	13 (31)	18 (19)	2.3 (34)	2.1 (43)	ND
<i>n</i> -Octane (C ₈)	93 (19)	73 (9)	24 (15)	13 (37)	ND
<i>n</i> -Nonane (C ₉)	218 (13)	148 (4)	67 (8)	46 (35)	ND
<i>n</i> -Decane (C ₁₀)	275 (10)	170 (2)	91 (9)	116 (24)	ND
<i>n</i> -Undecane (C ₁₁)	248 (7)	140 (1)	91 (12)	162 (12)	ND
<i>n</i> -Dodecane (C ₁₂)	88 (6)	47 (1)	34 (10)	63 (6)	ND
<i>n</i> -Tridecane (C ₁₃)	41 (3)	24 (7)	15 (8)	37 (9)	ND
<i>n</i> -Tetradecane (C ₁₄)	20 (4)	12 (0)	7.0 (9)	18 (5)	ND
<i>n</i> -Pentadecane (C ₁₅)	12 (0)	8.1 (1)	4.5 (5)	12 (7)	ND
<i>n</i> -Hexadecane (C ₁₆)	8.1 (6)	5.4 (2)	2.8 (5)	8.7 (7)	ND
<i>n</i> -Heptadecane (C ₁₇)	6.0 (3)	4.5 (10)	2.1 (4)	6.4 (5)	ND
Total petroleum hydrocarbon	2686 (11)	1551 (9)	1089 (8)	1109 (12)	ND

See Fig. 4 for chromatographic results. ND = Not detected.

^a Values in parentheses are the relative standard deviations (%) of triplicate extractions and GC analyses.

^b Sample sonicated in 10-ml methylene chloride for 14 h.

^c Sample placed on a bed of drying agent (molecular sieve 3A) inside an extraction cell and extracted with 400 atm 60°C CO₂ for 15 min. Column temperature during the extraction was –25°C.

^d Sample and drying agent (molecular sieve 3A) mixed together and then placed inside the extraction cell and extracted with 400 atm 60°C CO₂ for 15 min. Column temperature during the extraction was –25°C.

and produces heat upon hydration (Table 4). Similar losses have previously been reported for other wet samples mixed directly with drying agents [26].

SFE–GC analysis of the soil contaminated with diesel-range organics was quantitative as no additional hydrocarbons were recovered from either re-extracting the sample by SFE–GC (Fig. 5) or sonicating the sample residue in methylene chloride (Table 5). The 15-min SFE–GC extraction gave good quantitative agreement with the 14-h sonication extraction and both extraction methods had low relative standard deviations of replicate extractions in the region of 1 to 8%. The exception was the *n*-decane recovery by sonication, which had a lower recovery than that achieved by SFE–GC, which is a result of

volatilization losses occurring during the sonication extraction process. The previous samples contained gasoline to kerosene range organics which could be analyzed by SFE–GC using a column cryogenic trapping temperature of –50 or –25°C. However, the –50°C column trapping temperature was unsuitable for the diesel-contaminated sample as the supercritical flow through the column quickly decreased upon commencing the extraction and within 5 min the GC column had plugged. The column plugging did not appear to be related to the water content of the soil as the sample only contained ca. 1.0% (w/w) water. Furthermore, the drying agent had previously enabled much wetter samples (e.g., spiked gasoline sample with 16%, w/w, water) to be analyzed at the –50°C cryogenic trapping

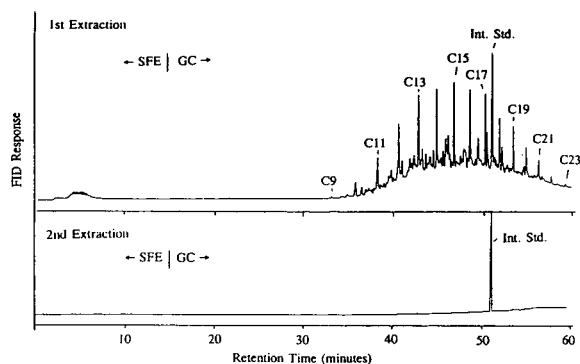


Fig. 5. Analysis of diesel contaminated soil using split SFE–GC–FID (split ratio ca. 1:100). A 1-g sample and a piece of filter paper spiked with the internal standard octahydroanthracene were placed on a bed of drying agent (molecular sieve 3A) inside an extraction cell and extracted for 15 min with 400 atm, 60°C, CO₂ at 0.6 ml/min. The extracted analytes were trapped onto a thick-film (5 μm) 30 m × 320 μm I.D. DB-1 capillary column at –25°C. After the extraction, the GC oven was heated at ca. 50°C/min to 40°C, then at 8°C/min to 300°C (top chromatogram). The sample was then extracted a second time under identical conditions as the first extract (lower chromatogram).

temperature. It was, therefore, envisaged that the problem was related to the nature of the extracted hydrocarbons, the diesel extract having a “waxy” consistency at –50°C which caused the column to become plugged. However, when the diesel extract was analyzed at the –25°C trapping temperature a continuous supercritical flow was obtained through the column during the entire SFE step, enabling quantitative recoveries (Table 5) and good chromatographic analysis (Fig. 5) to be achieved. As shown in Tables 1–5, using the –25°C column trapping temperature would enable both gasoline- and diesel-range organics to be extracted and analyzed by SFE–GC.

To assess the range of petroleum hydrocarbons which could be analyzed by the SFE–GC technique a motor oil-contaminated sample was also analyzed. SFE–GC gave good quantitative agreement with sonicating the sample in methylene chloride for 14 h (Table 6). This sample (like the diesel sample) had to be analyzed with a cryogenic trapping temperature of –25°C to avoid column plugging, but this did not affect the

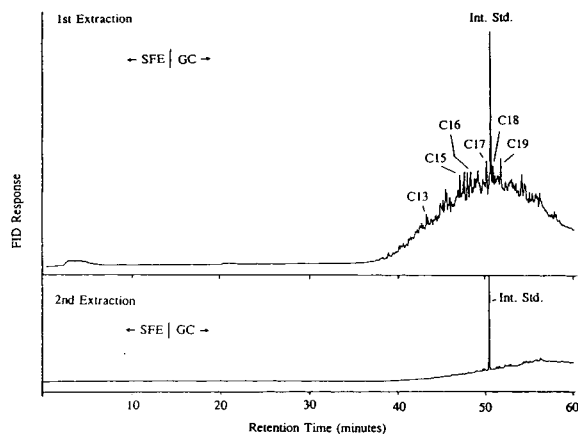


Fig. 6. Analysis of motor oil-contaminated soil from railroad embankment using split SFE–GC–FID (split ratio ca. 1:100). A 1-g sample and a piece of filter paper spiked with the internal standard octahydroanthracene were placed on a bed of drying agent (molecular sieve 3A) inside an extraction cell and extracted for 15 min with 400 atm, 60°C, CO₂ at 0.6 ml/min. The extracted analytes were trapped onto a thick-film (5 μm) 30 m × 320 μm I.D. DB-1 capillary column at –25°C. After the extraction, the GC oven was heated at ca. 50°C/min to 40°C, then at 8°C/min to 300°C (top chromatogram). The sample was then extracted a second time under identical conditions as the first extract (lower chromatogram).

chromatographic peak shapes, as the chromatograms generated by the SFE–GC (Fig. 6) were comparable to those generated by using a split injection of the methylene chloride extract. However, not all the analytes extracted from the soil by either SFE or by sonicating in methylene chloride could be easily eluted from the 5-μm thick-film capillary column, as the less volatile analytes had a tendency to accumulate on the column to produce a shift in the baseline during the GC analysis (Fig. 6, second extraction). The motor oil components could have been fully eluted using a 0.25-μm film column but this would result in lower trapping efficiency of volatile components [21]. Fortunately, the gradual degradation of the thick-film column’s chromatographic performance could easily be rectified by simply trimming off ca. 15 cm of the injection end of the column. The thick-film capillary column was, therefore, the appropriate column to use for the analysis of gasoline- and diesel-contaminated soils, and the motor oil

Table 5

Comparison of split SFE–GC and sonication in methylene chloride for the quantitation of petroleum hydrocarbons in a diesel-contaminated soil

Analyte	Concentration ($\mu\text{g/g}$) (R.S.D., %) ^a		
	Sonication ^b	SFE–GC ^c	SFE residue ^d
<i>n</i> -Decane (C ₁₀)	41 (19)	91 (2)	ND
<i>n</i> -Undecane (C ₁₁)	151 (2)	190 (4)	ND
<i>n</i> -Dodecane (C ₁₂)	288 (2)	294 (3)	ND
<i>n</i> -Tridecane (C ₁₃)	318 (2)	277 (1)	ND
<i>n</i> -Tetradecane (C ₁₄)	311 (1)	301 (1)	ND
<i>n</i> -Pentadecane (C ₁₅)	313 (2)	319 (2)	ND
<i>n</i> -Hexadecane (C ₁₆)	339 (1)	252 (5)	ND
<i>n</i> -Heptadecane (C ₁₇)	249 (5)	261 (3)	ND
<i>n</i> -Octadecane (C ₁₈)	172 (0)	187 (4)	ND
<i>n</i> -Nonadecane (C ₁₉)	160 (2)	150 (5)	ND
<i>n</i> -Eicosane (C ₂₀)	85 (1)	98 (7)	ND
<i>n</i> -Heneicosane (C ₂₁)	59 (2)	64 (8)	ND
<i>n</i> -Docosane (C ₂₂)	31 (1)	30 (3)	ND
Total petroleum hydrocarbon	24 319 (2)	26544 (1)	ND

See Fig. 5 for chromatographic results.

^a Values in parentheses are the relative standard deviations (%) of triplicate extractions and GC analyses.

^b Sample sonicated in 10-ml methylene chloride for 14 h.

^c Sample extracted with 400 atm 60°C CO₂ for 15 min, the column temperature during the extraction was –25°C.

^d SFE–GC sample residue re-extracted by sonicating in 10-ml methylene chloride for 14 h; ND = not detected.

Table 6

Comparison of split SFE–GC and sonication in methylene chloride for the quantitation of petroleum hydrocarbons in a motor oil-contaminated soil

Analyte	Concentration ($\mu\text{g/g}$) (R.S.D., %) ^a		
	Sonication ^b	SFE–GC ^c	SFE residue ^d
<i>n</i> -Tridecane (C ₁₃)	13 (13)	13 (18)	ND
<i>n</i> -Pentadecane (C ₁₆)	23 (11)	23 (14)	ND
<i>n</i> -Hexadecane (C ₁₆)	37 (4)	34 (14)	ND
<i>n</i> -Heptadecane (C ₁₇)	30 (6)	30 (6)	ND
<i>n</i> -Octadecane (C ₁₈)	14 (6)	16 (6)	ND
<i>n</i> -Nonadecane (C ₁₉)	25 (28)	30 (12)	ND
Total petroleum hydrocarbon	9747 (10)	10413 (7)	173 (4)

See Fig. 6 for chromatographic results.

^a Values in parentheses are the relative standard deviations (%) of triplicate extractions and GC analyses.

^b Sample sonicated in 10-ml methylene chloride for 14 h.

^c Sample extracted with 400 atm 60°C CO₂ for 15 min, the column temperature during the extraction was –25°C.

^d SFE–GC sample residue re-extracted by sonicating in 10-ml methylene chloride for 14 h; ND = not detected.

sample was realistically the limit of the petroleum hydrocarbon range that could be analyzed using this column.

The final real-world sample was a gasoline-contaminated charcoal filter obtained from a 1974 Chevette automobile. Since this sample was contaminated with ca. 17% extractable hydrocarbons, the sample size had to be reduced to 50 mg to avoid gross overloading of the GC column stationary phase. The 15-min SFE–GC extraction again yielded recoveries comparable to those obtained by sonicating the sample in methylene chloride for 14 h (Table 7), though the SFE–GC recoveries of naphthalene and methylnaphthalene were slightly lower than the values obtained by the sonication method. However, by re-extracting the sample for an additional 15 min by SFE–GC (Fig. 7), or sonicating the sample residue in methylene chloride (Table 7), quantitative polynuclear aromatic hydrocarbon recoveries were achieved. Both the SFE–GC and sonication extraction methods were reproducible (e.g., relative standard deviations from ca. 1 to 7%) demonstrating that the small

50-mg sample size was representative of the bulk sample.

4. Conclusions

Split SFE–GC is a rapidly developing technique which can quickly and quantitatively extract and analyze petroleum hydrocarbons from real-world environmental samples. SFE–GC analysis typically requires less than 80 min per sample to perform since no concentration and sample handling procedures are needed between the SFE and GC steps. The SFE–GC hydrocarbon recoveries are comparable to those obtained by a conventional organic extraction method which requires ca. 18 h to perform including the extraction, centrifugation, evaporation and GC analysis. A simple and reliable method has been developed to analyze the petroleum-contaminated samples in their native state (without any pre-preparation such as air drying) by using split SFE–GC operated at a high split ratio (e.g., 100:1) to avoid overloading

Table 7

Comparison of split SFE–GC and sonication in methylene chloride for the quantitation of petroleum hydrocarbons in a charcoal filter from a vehicle gasoline tank

Analyte	Concentration (mg/g) (R.S.D., %) ^a		
	Sonication ^b	SFE–GC ^c	SFE residue ^d
Toluene	1.2 (6.9)	1.2 (4.9)	ND
Ethylbenzene	4.8 (5.3)	4.4 (6.3)	ND
<i>m</i> -, <i>p</i> -Xylene	22.6 (5.9)	24.0 (2.2)	0.2 (41)
<i>o</i> -Xylene	12.2 (6.5)	12.2 (1.6)	0.2 (29)
C ₃ -Alkylbenzene	16.6 (5.0)	17.1 (2.0)	0.2 (7.1)
C ₃ -Alkylbenzene	23.8 (4.6)	25.5 (2.4)	0.6 (10)
C ₃ -Alkylbenzene	6.7 (4.0)	6.2 (4.2)	0.3 (9.3)
C ₄ -Alkylbenzene	5.8 (4.3)	5.6 (2.3)	0.2 (19)
Naphthalene	3.5 (3.9)	2.8 (2.8)	0.7 (11)
C ₁ -Naphthalene	2.2 (6.3)	1.2 (5.7)	0.9 (15)
Total petroleum hydrocarbon	169.7 (3.6)	167.9 (2.6)	6.0 (6.1)

See Fig. 7 for chromatographic results.

^a Values in parentheses are the relative standard deviations (%) of triplicate extractions and GC analyses.

^b Sample sonicated in 10-ml methylene chloride for 14 h.

^c Sample extracted with 400 atm 60°C CO₂ for 15 min, the column temperature during the extraction was –25°C.

^d SFE–GC sample residue re-extracted by sonicating in 10-ml methylene chloride for 14 h; ND = not detected.

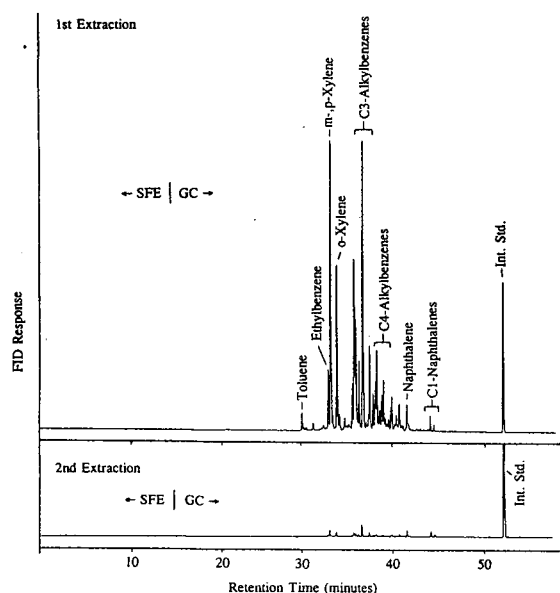


Fig. 7. Split SFE-GC-FID analysis of a gasoline-contaminated charcoal filter from a 1974 Chevette automobile. A 50-mg sample and a piece of filter paper spiked with the internal standard octahydroanthracene were placed on a bed of drying agent (molecular sieve 3A) inside an extraction cell and extracted for 15 min with 400 atm, 60°C, CO₂ at 0.6 ml/min. The extracted analytes were trapped onto a thick-film (5 μm) 30 m × 320 μm I.D. DB-1 capillary column at -25°C. After the extraction, the GC oven was heated to ca. 50°C/min to 40°C, then at 8°C/min to 300°C (top chromatogram). To ensure quantitative recoveries the sample was then extracted a second time under identical conditions as the first extract (lower chromatogram).

the GC column, and by using a drying agent to retain the extracted water from the sample so that column plugging could be eliminated. Furthermore, by using a thick-film (5 μm) column with a cryogenic trapping temperature of -25°C gasoline- to diesel-range organics can be determined by SFE-GC analysis using the same extraction and chromatography conditions with detection limits for individual compounds in the low ppb range. Good quantitative reproducibilities (R.S.D.s typically <5%) demonstrate that the SFE-GC technique is reproducible and that 1-g samples are representative of the bulk samples.

Acknowledgements

The financial support of the American Petroleum Institute, the US Department of Energy and the US Environmental Protection Agency (EMSL, Las Vegas), are gratefully acknowledged, as are instrument loans from ISCO.

References

- [1] J.L. Parr, G. Walters and M. Hoffman, *Hydrocarbon Contaminated Soils and Groundwater*, Enseco, Arvada, CO, 1991, Ch. 8.
- [2] *Test Methods for Evaluating Solid Waste: Physical and Chemical Methods*; SW-846, US Environmental Protection Agency, Office of Emergency Response, Washington, DC, 3rd ed., 1986.
- [3] T.A. Bellar and J.J. Lichtenberg, *J. Am. Water Works Assoc.*, 66 (1974) 739.
- [4] *Tekmar Technical Bulletin, Tek/Dat B021082*, Tekmar, Cincinnati, OH, 1982.
- [5] *Methods for Chemical Analyses of Water and Wastes*; EPA 600/14-79/020, US Environmental Protection Agency, Washington, DC, 1979 revised 1983.
- [6] State Water Resources Control Board, *Leaking Underground Fuel Tank (LUFT) Field Manual*, State of California, Sacramento, CA, 1988.
- [7] *Analytical Chemistry Manual for the Petroleum Products in the Environment*, Department of Environmental Protection and Energy, State of New Jersey, Trenton, NJ, December 1991.
- [8] M. Hiatt and T. Jones, *J. High Resolut. Chromatogr. Chromatogr. Commun.*, 8 (1985) 4.
- [9] J. Albaiges and J. Grimalt, *Int. J. Environ. Anal. Chem.*, 31 (1987) 281.
- [10] V. Lopez-Avila, J. Benedicto, N.S. Dodhiwala, R. Young and W.F. Beckert, *J. Chromatogr. Sci.*, 30 (1992) 335.
- [11] S.E. Eckert-Tilotta, S.B. Hawthorne and D.J. Miller, *Fuel*, 72 (1993) 1015.
- [12] S.B. Hawthorne and D.J. Miller, *J. Chromatogr. Sci.*, 24 (1986) 258.
- [13] S.B. Hawthorne and D.J. Miller, *Anal. Chem.*, 59 (1987) 1705.
- [14] B.W. Wright, C.W. Wright and J.S. Fruchter, *Energy Fuels*, 3 (1989) 474.
- [15] J.C. Monin, D. Barth, M. Perrut, M. Espitalie and B. Durand, *Adv. Org. Geochem.*, 13 (1988) 1079.
- [16] S.B. Hawthorne, D.J. Miller and M.S. Krieger, *J. Chromatogr. Sci.*, 27 (1989) 347.
- [17] B.W. Wright, S.R. Frye, D.G. McMinn and R.D. Smith, *Anal. Chem.*, 59 (1987) 640.

- [18] I.L. Davies, M.W. Raynor, J.P. Kithinji, K.D. Bartle, P.T. Williams and G.E. Andrews, *Anal. Chem.*, 60 (1988) 683A.
- [19] J.M. Levy, R.A. Cavalier, T.N. Bosch, A.M. Rynaski and W.E. Huhak, *J. Chromatogr. Sci.*, 27 (1989) 341.
- [20] M.R. Andersen, J.T. Swanson, N.L. Porter and B.E. Richter, *J. Chromatogr. Sci.*, 27 (1989) 371.
- [21] M.D. Burford, S.B. Hawthorne and D.J. Miller, *J. Chromatogr. A*, 685 (1994) 79.
- [22] M.D. Burford, S.B. Hawthorne, D.J. Miller and T.J. Braggins, *J. Chromatogr.*, 609 (1992) 321.
- [23] X. Lou, H.-G. Janssen and C.A. Cramers, *J. High Resolut. Chromatogr.*, 16 (1993) 425.
- [24] K. Grob and D. Fröhlich, *J. High Resolut. Chromatogr.*, 16 (1993) 224.
- [25] S.B. Hawthorne, D.J. Miller and J.J. Langenfeld, *J. Chromatogr. Sci.*, 28 (1990) 2.
- [26] M.D. Burford, S.B. Hawthorne and D.J. Miller, *J. Chromatogr. A*, 657 (1993) 413.
- [27] M.D. Burford, S.B. Hawthorne and D.J. Miller, *Anal. Chem.*, 65 (1993) 1497.
- [28] S.B. Hawthorne, J.J. Langenfeld, D.J. Miller and M.D. Burford, *Anal. Chem.*, 64 (1992) 1614.



ELSEVIER

Journal of Chromatography A, 685 (1994) 113–119

JOURNAL OF
CHROMATOGRAPHY A

Solute collection after off-line supercritical fluid extraction into a moving liquid layer

Jiří Vejrosta^{a,*}, Josef Planeta^a, Milena Mikešová^a, Alena Ansorgová^a,
Pavel Karásek^a, Jaromír Fanta^b, Václav Janda^{b,*}

^a*Institute of Analytical Chemistry, Academy of Sciences of the Czech Republic, Veveří 97, 611 42 Brno, Czech Republic*

^b*Institute of Chemical Technology, Department of Water Technology and Environmental Engineering, Technická 5, 166 28 Prague 6, Czech Republic*

First received 29 April 1994; revised manuscript received 22 July 1994

Abstract

A solute collection method after off-line supercritical fluid extraction using a moving layer of liquid organic solvent flowing down through a fused-silica capillary (0.5 mm I.D.) is proposed. Recoveries of over 90% were measured for selected polycyclic aromatic hydrocarbons (acenaphthene, phenanthrene, fluoranthene, pyrene and benzo[a]pyrene) and *s*-triazine herbicides when methanol was used as a trapping solvent.

1. Introduction

To establish supercritical fluid extraction (SFE) as a routine sample preparation method, three distinctive features need to be studied [1]. Whereas the extraction process itself is and will be unremittingly studied mainly from the viewpoint of new SFE applications, the problems connected with solute transport from the extractor and efficient analyte collection from the expanding supercritical fluid must be unambiguously solved. Transport of solutes from the extractor into a suitable collection device depends on restrictor selection and also on problems connected with restrictor plugging and its mechanical stability. Plugging is often encountered when real sample matrices contain large amounts of water or other co-extractable com-

ponents. As pure or modified CO₂ is predominantly used in SFE, elimination and/or suppression of the Joule–Thompson cooling effect complicates solution of the plugging problem.

Three basic approaches have been proposed and used to collect solutes effectively from an expanding stream of gaseous fluid: direct trapping in a liquid solvent [2–8], use of a solid sorbent trap [9–15] and trapping on a cooled solid surface [16,17] (other methods such as solventless collection in an empty vial [18] are used more rarely).

The third method mentioned above is rarely used, owing to the properties of an expanding fluid mixture, where the formation of aerosols and solute clustering can occur. The use of a fused-silica capillary (0.5 mm I.D.) as a trapping element seems to be a promising method [19].

When solid sorbent traps are used, rinsing of adsorbed solutes by liquid solvent adds a further

* Corresponding author.

step to the overall analytical process, the recovery of which must be taken into account. Another problem is connected with a higher modifier concentration, which is a liquid under ambient conditions. Its partial condensation on the sorbent surface can lead to serious losses of solutes caused by their washing out from the sorbent trap [14].

The simplest and the most commonly used collection method consists of depressurizing a supercritical fluid into an organic solvent. The tip of the restrictor is simply immersed in liquid solvent in a vial. In spite of its obvious simplicity, this collection method offers a high degree of experimental variability and flexibility, especially from the point of view of method optimization.

Selection of the organic solvent is of primary importance. Langenfeld et al. [5] found the collection solvent polarity and temperature to be more important than the solvent volume and the height of its level in a vial. Based on the recoveries of 66 compounds, the best overall collection efficiency was found for methylene chloride and chloroform. Methanol failed to collect 35–50% of each test compound. The results for acetone were similar to those for methylene chloride; hexane exhibited the poorest collection capability for the most volatile species, but better than that of methanol for the less volatile components.

Thompson et al. [6] evaluated the collection efficiency of various solvents and solvent mixtures. A polarity test mixture consisting of acetophenone, *N,N*-dimethylaniline, naphthalene, decanoic acid, 2-naphthol and tetracosane (the same as in the work by Mulcahey and Taylor [14]) was added to a sand matrix and extracted with supercritical carbon dioxide. In addition to all the commonly used collection solvents, cyclohexane and perchloroethylene were used. The lowest recoveries and the highest R.S.D.s were found for decanoic acid and, in some solvents (CHCl_3 , CH_2Cl_2 and perchloroethylene), for *N,N*-dimethylaniline. The recovery data indicate no correlation between any of the solvent physical property (i.e., boiling point, density, viscosity, surface tension and/or Hildebrand solubility parameter) and

analyte recovery. Perchloroethylene, despite having the highest viscosity [8], exhibited the lowest overall trapping efficiency for all the analytes studied. Use of a multi-component collection solvent [hexane–trichloromethane–methanol (1:1:1)] increased all the individual analyte recoveries to above 92%.

Such extensive studies reflect well the influence of the solvent physico-chemical properties only if all other parameters are kept constant (the same value in all experiments). The reproducibility of results obtained in another laboratory, especially if commercial devices are used [20], is questionable.

Our experience leads us to the opinion that direct bubbling into the bulk liquid is not as an efficient trapping process as is commonly believed. If the analyte recoveries are over 90%, usually relatively high volumes of organic liquid solvents are necessary, and the resulting sample volumes are sometimes the same as from Soxhlet or sonication methods.

We believe that it is necessary to focus on the development of more sophisticated (efficient) processes to facilitate analyte mass transfer from an expanding supercritical mixture into an organic liquid solvent. In a recent study, Burford et al. [7] used the constant delivery of organic solvent just after the restrictor tip. The stream of expanding supercritical fluid nebulized the added solvent, forming a fine mist. A glass tube (61 mm \times 3 mm I.D.) was used to sweep it into the bulk of the collection solvent. The substantial increase in collection efficiency was attributed to enhanced solvent contact with the analytes in the depressurized extract. Although the method was proposed as one of the possibilities to remove restrictor plugging, and the authors found a certain solution, this method was unfortunately not investigated further.

Mulcahey and Taylor [14] found enhanced recoveries in the presence of liquid methanol in an ODS trap when 1–2% methanol-modified carbon dioxide was used. Also, Howard and Taylor [21] obtained nearly quantitative recoveries of sulphonylurea herbicides at 45°C on stainless steel beads when 2% methanol-modified carbon dioxide was employed. They con-

cluded that the presence of liquid methanol on the stainless-steel surface enhances analyte trapping. In both studies the main problem was to find conditions under which the modifier condensation is diminished and analytes are trapped only on the solid surface. Hence the conclusion that larger amounts of liquid modifier decrease the trapping efficiency is correct only from the viewpoint of the amount of analyte deposited on the solid sorbent.

As for analyte trapping in a liquid organic solvent, the above-mentioned facts indicate much more effective trapping than in the case of bubbling through a bulk liquid. A solid trap, where particles are covered with a dew of condensed modifier, resembles a multi-capillary with small internal diameters, coated with liquid solvent.

This mode of trapping was simulated using a capillary for the collection of flufenoxurone by Vejrosta et al. [22]. Carbon dioxide containing 10 vol.-% of methanol and a fused-silica capillary (30 cm \times 0.5 mm I.D.) equipped with a cryofocusing unit as a trapping device were used for the SFE of a spike. The condensed methanol from the methanol-modified CO₂ was used as the trapping liquid. The amount of liquid methanol was controlled by the temperature of the cryofocuser. Recoveries of over 90% were found at a CO₂ flow-rate of ca. 100 ml/min (under ambient conditions).

It seems probable that in the above experiments the transfer of flufenoxurone into condensing methanol was enhanced by mutual clustering of flufenoxurone and methanol molecules during expansion of the methanol-modified supercritical CO₂.

Trapping of analytes leaving the flow restrictor combining flowing water with a solid sorbent (reversed C₁₈ phase) has also been described [23].

In this work, for the SFE of a polycyclic aromatic hydrocarbon (PAH) mixture we used pure CO₂, and a continuous stream of methanol was pumped into the trapping capillary (fused silica, 0.5 mm I.D.) during extraction. Acenaphthene, phenanthrene, fluoranthene, pyrene and benzo[*a*]pyrene were selected

because of their lower recoveries [5] when bubbling through liquid methanol was used as a collection method. A similar system was used for the collection of *s*-triazine herbicides. In addition, a new principle of liquid solvent recirculation through the trapping capillary was preliminarily tested.

2. Experimental

Samples for extraction of PAHs were prepared by spiking 20 μ l of standard PAH solution (0.25 mg of each in 1 ml) in methanol–tetrachloromethane (1:1) into an inert glass bead bed (60–80 mesh).

SFE was performed using the same device as described in previous papers [19,22]. Instead of a syringe, a linear sampling pump was connected to three-port union allowing a continuous flow of liquid solvent into the trapping capillary. In all experiments with SFE of PAHs the flow-rate of methanol fed into the trapping capillary was 50 μ l/min. A fused-silica capillary (15 cm \times 25 μ m I.D.) was used as a restrictor and the last 4-cm length of the restrictor on the outlet edge was heated to 100°C. In some instances (SFE of *s*-triazine herbicides) the restrictor tip (17 and/or 25 μ m I.D. restrictor) was not heated because methanol acted as an antifreeze, preventing blocking of the restrictor. Because of the volatility of methanol, the final sample volume deposited in a microvial at the outlet of the trapping capillary was ca. 0.3–0.75 ml (the volume depends on the restrictor parameters and the resulting flow-rate of gaseous CO₂). The time of SFE of PAHs was 15 min in all experiments (temperature 60°C and pressure 25 MPa). More than half of the methanol volume pumped into the trapping capillary evaporated during SFE. The flow-rate of gaseous CO₂ was 170 ml/min \pm 10%, measured under ambient conditions.

For all analyses a Chrom 5 gas chromatograph equipped with an OV-101 column and a flame ionization detector (Laboratory Devices, Prague, Czech Republic) was used.

For all experiments with *s*-triazines, a techni-

cal mixture of *s*-triazines (Zymazin herbicide) was used for recovery measurements. Zymazin is a product containing 93% of atrazine, 3.5% of simazine and 3.5% of propazine. As only the trapping efficiency after SFE was tested, a simple and inert matrix was used, Gas Chrom Q silanized support for gas chromatography (Alltech). The absolute amount of Zymazin spiked into the cartridge package was 40 μg . Zymazin was spiked in 20 μl of methanolic solution and allowed to dry before SFE. As *s*-triazines may not be extracted effectively by pure carbon dioxide [24], modifier (20 μl of methanol or acetonitrile) was added to the extraction cartridge before SFE of the spiked matrix. SFE using CO_2 with modifier was also tested in a recent study of the extraction of triazines from spiked soil and other environmental solids using a commercial device [25].

We did not heat the restrictor tip in this instance. Methanol delivered into the trapping capillary acted as an antifreeze and also transported a sufficient amount of heat to prevent its blocking by solid CO_2 .

s-Triazine herbicides were determined by high-performance liquid chromatography (HPLC). For all analyses an HP 1050 liquid chromatograph (Hewlett-Packard) equipped with 200 \times 4.6 mm I.D. column (Hypersil ODS, 5 μm) and a multiple-wavelength detector (MWD) was used. The signal of the MWD was monitored at 225 and 254 nm and peak identities were checked by measuring UV spectra. The mobile phase was acetonitrile–water (50:50) at a flow rate of 1 ml/min. Acenaphthene was used as an internal standard (added to the solution obtained after SFE). The capacity factors of the analytes were as follows: propazine 0.84, atrazine 1.16, simazine 1.80 and acenaphthene 6.32. The recovery of the analytes was calculated by com-

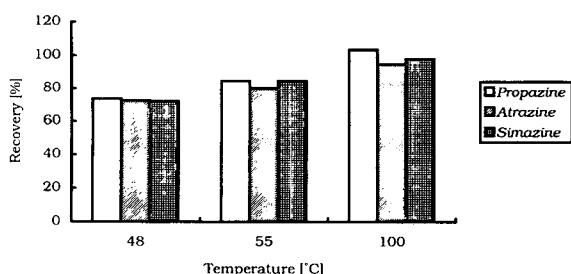


Fig. 1. Recoveries of *s*-triazines at different temperatures of extraction cartridge. Pressure of carbon dioxide, 23 MPa; restrictor, 15 cm \times 20 μm I.D.; time of SFE, 10 min; 20 μl of methanol added to the cartridge before SFE (time of SFE 25 min and 100 μl of methanol added to the cartridge for extraction temperature 48°C).

parison of peak areas obtained from the SFE extract and a reference “100% recovery” solution.

3. Results and discussion

The results of ten repeated spike experiments with the PAH mixture are summarized in Table 1. Almost quantitative trapping was achieved for all individual PAHs with reasonable R.S.D. values. Because the input of methanol was placed above the heated restrictor zone, a great deal of methanol was evaporated and condensed again after restrictor tip. This means that the nebulization effect should be taken into account.

At the start of experiments with the SFE of triazines, the conditions were optimized. This was done using trapping of analytes at the outlet of the restrictor in 2 ml of methanol. The outlet of the flow restrictor was immersed directly in the methanol. All extractions were performed at 23 MPa. The influence of the temperature of the extraction cartridge is shown in Fig. 1. It can be

Table 1
Recoveries with R.S.D.s of selected PAHs ($n = 10$)

	Acenaphthene	Phenanthrene	Fluoranthene	Pyrene	Benzo[a]pyrene
Recovery (%)	90.5	91.0	91.2	93.3	93.0
R.S.D. (%)	9.3	4.8	6.5	7.5	6.1

seen that the best recoveries were obtained at 100°C. Therefore, all further SFE with trapping of analytes into the continuously rinsed capillary was carried out at this cartridge temperature. An SFE time of 10 min was sufficient for removing of triazines from the cartridge at 100°C. The use of acetonitrile instead of methanol as a polarity modifier of carbon dioxide had no effect on the *s*-triazines recovery.

The positive influence of elevated temperature on recovery suggests that the SFE efficiency was limited by the vapour pressure of *s*-triazines and kinetic phenomena rather than by solubility in a less dense fluid (the higher the temperature of a fluid at constant pressure, the lower are its density and solvation power).

The recoveries of *s*-triazines using a trapping capillary into which methanol was continuously pumped during SFE are given in Table 2. The flow-rate of methanol during the SFE was 0.05 ml/min. This means that the whole volume of methanol in the microvial after finishing the 15-min SFE is less than 0.75 ml (a portion of methanol evaporates during SFE owing to bubbling of gaseous CO₂ through the contents of the vial). Recoveries of SFE with direct trapping of *s*-triazines in 2 ml of methanol are also given in Table 2 for comparison. It can be seen that the recovery of the analytes is the same with comparable standard deviations. However, the concentration factor is at least three times higher when using trapping in the capillary owing to the lower final volume of the solution obtained after

SFE. On the other hand, in our experimental set-up, a flow-rate of methanol through the trapping capillary of 0.05 ml/min was the minimum that prevented blocking of the restrictor unless the tip of restrictor needed to be heated. When lower flow-rates of methanol were used, the amounts of methanol and heat transported by methanol to the restrictor tip were insufficient.

A question is how to compare the efficiencies of different collection modes using liquid solvents. It might be possible to trap analytes quantitatively if greater volumes of solvent and longer paths of bubbles were used.

As a very rough parameter for mutual comparison of different solvent trapping methods, the trapping efficiency coefficient (TEC), defined as follows, can be introduced:

$$\text{TEC} = \frac{V_{\text{fr}}}{V_1} \cdot \frac{R(\%)}{100} \quad (1)$$

where V_{fr} is volume flow-rate of depressurized fluid mixture measured under ambient conditions, V_1 the resulting volume of trapping solvent and R the recovery.

All parameters, usually studied without interrelation among different workers, such as solvent nature, trapping temperature, flow-rate of expanded CO₂ and system geometry, can be compared with respect to the TEC values. In this work, for example, the TEC values were approximately 560 min⁻¹ and in the work of Howard

Table 2

Recovery of *s*-triazines by SFE and trapping in a continuously rinsed capillary (0.05 ml/min of methanol) and by SFE with direct trapping into 2 ml of methanol

<i>s</i> -Triazine	Trapping system			
	Capillary		2 ml of methanol	
	Recovery (%)	R.S.D. (%) ($n = 5$)	Recovery (%)	R.S.D. (%) ($n = 5$)
Propazine	90.9	2.5	91.5	1.8
Atrazine	90.0	2.1	90.8	1.6
Simazine	91.7	2.6	91.2	2.2

SFE conditions: temperature of extraction cartridge, 100°C; time of SFE, 15 min; restrictor, 15 cm × 17 μm I.D.; pressure, 23 MPa; 20 μl of methanol added to the extraction cartridge before commencing SFE.

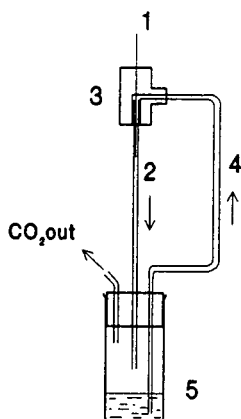


Fig. 2. Scheme of solvent trapping system with solvent recirculation. 1 = Restrictor; 2 = trapping capillary; 3 = three-port union; 4 = connecting line for solution recirculation; 5 = vial with solvent.

and Taylor [21] 83 min^{-1} . It is clear that higher values reflect more efficient collection.

One of common objections against the nebulization [7] of an expanding supercritical stream is the necessity to use another pump (a low pressure pump is sufficient) for solvent addition. In our arrangement, where the restrictor is placed in the trapping capillary (0.5 mm I.D. or less), the trapping system resembles and behaves like a water vacuum pump and a pressure lower than atmospheric is generated in the connection union above the restrictor tip. One of possibilities to utilize this suction effect is shown schematically in Fig. 2. In this arrangement, liquid solvent recirculates permanently along the restrictor and through the trapping capillary. Preliminary results are presented in Table 3. All the extraction conditions were the same as in previous experiments with PAHs. The resulting recoveries suffer from the short length of trapping capillary (10 cm), which was the maximum possible length at

which solvent recirculation functioned. No heating of the restrictor tip is necessary because of the sufficient heat flow from liquid methanol passing around the flow restrictor and its anti-freeze properties.

As the device used was not specially designed for this trapping method, dead volumes and also the use of PTFE tubing for the recirculation line could be sources of possible analyte losses. A more suitable device for utilization in this trapping method is under development.

4. Conclusions

Solvent trapping of analytes after off-line SFE can be a source of potential analyte losses that may be incorrectly interpreted as a poor SFE efficiency. In addition to parameters usually studied such as solvent nature, temperature, volume and height, the trapping efficiency depends strongly on the method of mutual treatment of both phases. From this point of view, bubbling through the bulk liquid seems to be the process with the lowest efficiency. When the average distance from the precipitated analyte molecules to the liquid surface is shortened and/or the expanding mixture is nebulized with solvent, the trapping efficiency increases substantially. As a result, quantitative trapping can be obtained with lower solvent volumes.

This was demonstrated by means of the proposed trapping mode, where analyte transfer into the liquid solvent is realized in a capillary (0.5 mm I.D.) and a liquid layer flows down along the inner capillary wall.

For solvent supply to the trapping capillary, which can simultaneously compensate for the losses of trapping liquid solvent, the suction

Table 3
Recoveries with R.S.D.s of selected PAHs (experiment with methanol recirculation; $n = 5$)

	Acenaphthene	Phenanthrene	Fluoranthene	Pyrene	Benzo[a]pyrene
Recovery (%)	79.5	83.0	85.8	81.1	89.7
R.S.D. (%)	4.6	1.9	1.4	2.0	19.2

effect resulting from the restrictor location in a narrow capillary can be employed.

References

- [1] S.B. Hawthorne, D.J. Miller, M.D. Burford, J.J. Langenfeld, S. Eckert-Tilotta and P.K. Louie, *J. Chromatogr.*, 642 (1993) 301.
- [2] S.B. Hawthorne and D.J. Miller, *Anal. Chem.*, 59 (1987) 1705.
- [3] V. Lopez-Avila, N.S. Dodhiwala and W.S. Beckert, *J. Chromatogr. Sci.*, 28 (1990) 468.
- [4] N. Alexandrou and J. Pawliszyn, *Anal. Chem.*, 61 (1989) 2770.
- [5] J.J. Langenfeld, M.D. Burford, S.B. Hawthorne and D.J. Miller, *J. Chromatogr.*, 594 (1992) 297.
- [6] P.G. Thomson, L.T. Taylor, B.E. Richter, N.L. Porter and J.L. Ezzell, *J. High Resolut. Chromatogr.*, 16 (1993) 713.
- [7] M.D. Burford, S.B. Hawthorne, D.J. Miller and T.J. Braggins, *J. Chromatogr.*, 609 (1992) 321.
- [8] N.L. Porter, A.F. Rynaski, E.R. Campbell, M. Saunders, B.E. Richter, J.T. Swanson, R.B. Nielsen and B.J. Murphy, *J. Chromatogr. Sci.*, 30 (1992) 367.
- [9] M.M. Schantz and S.N. Chesler, *J. Chromatogr. Sci.*, 363 (1986) 401.
- [10] J.L. Hedrick and L.T. Taylor, *J. High Resolut. Chromatogr.*, 13 (1990) 312.
- [11] L.J. Mulcahey, J.L. Hedrick and L.T. Taylor, *Anal. Chem.*, 63 (1991) 2225.
- [12] R.M. Smith and M.D. Burford, *J. Chromatogr.*, 600 (1992) 175.
- [13] J.M. Levy, R.M. Ravey, R.K. Houck and M. Ashraf-Khorassani, *Fresenius' J. Anal. Chem.*, 344 (1992) 517.
- [14] L.J. Mulcahey and L.T. Taylor, *Anal. Chem.*, 64 (1992) 2352.
- [15] S. Bowadt, B. Johansson, F. Pelusio, B.R. Larsen and C. Rovida, *J. Chromatogr. A*, 662 (1994) 424.
- [16] R.D. Smith, J.L. Fulton, R.C. Petersen, A.J. Kopriva and B.W. Wright, *Anal. Chem.*, 58 (1986) 2057.
- [17] B.W. Wright, Ch.W. Wright, R.W. Gale and R.D. Smith, *Anal. Chem.*, 59 (1987) 38.
- [18] D.J. Miller, S.B. Hawthorne and M.E.P. McNally, *Anal. Chem.*, 65 (1993) 1038.
- [19] J. Vejrosta, A. Ansorgová, M. Mikešová and K.D. Bartle, *J. Chromatogr. A*, 659 (1994) 209.
- [20] V. Lopez-Avila, N.S. Dodhiwala, J. Benedicto and W.F. Beckert, *LC·GC*, 10 (1992) 762.
- [21] A.L. Howard and L.T. Taylor, *J. High Resolut. Chromatogr.*, 16 (1993) 39.
- [22] J. Vejrosta, A. Ansorgová, J. Planeta, D.G. Breen, K.D. Bartle and A.A. Clifford, *J. Chromatogr. A*, 683 (1994) 407.
- [23] T. Greibrokk, M. Radke, M. Skurdal and H. Willsch, *Org. Geochem.*, 18 (1992) 447.
- [24] V. Janda, G. Steenbeke and P. Sandra, *J. Chromatogr.*, 479 (1989) 200.
- [25] T.R. Steinheimer, R.L. Pfeiffer and K.D. Scoggin, *Anal. Chem.* 66 (1994) 645.

Preparation of highly condensed polyacrylamide gel-filled capillaries with low detection background

Yi Chen¹, Joachim-Volker Höltje, Uli Schwarz*

Max Planck-Institut für Entwicklungsbiologie, Abteilung Biochemie, Spemannstrasse, 35/II, D-72076 Tübingen, Germany

First received 10 May 1994; revised manuscript received 25 July 1994

Abstract

A method was established for the preparation of capillaries filled partially with highly condensed polyacrylamide gels (including step gradient gels) used for separation and partially with a buffer used for detection. These novel capillaries combine the high resolution of gel-filled capillaries and the low background of buffer-filled capillaries. They can be used for more than 1 week or for more than 50 injections, as demonstrated by the separation of poly-(α,β)-D,L-aspartate. The detection limit tested with diaspertate is about two orders of magnitude lower than that with the totally gel-filled capillaries. Some problems such as baseline drifting arise when using these capillaries but can be overcome by pre-running the capillaries several times with highly concentrated samples.

1. Introduction

Capillary gel electrophoresis, suggested by Hjerten in 1983 [1], has been valued as a new method for high-speed DNA sequencing [2–8] and demonstrated to be a powerful tool for the size analysis of other substances such as oligosaccharides [9–11], polyamino acids [12] and proteins [13–16]. However, the usefulness of this method depends on whether the separated bands can be detected. Gel-filled capillaries have a strong UV background, which leads to low or poor detection sensitivity. Another problem in using this method is the difficulty in preparing the gel filled capillaries: voids develop in the immobilized cross-linked gels or the gels not

immobilized migrate in uncoated capillaries because of electroendosmosis [4,17], leading to irreproducible separation and/or re-formation of voids.

A way to overcome these problems is to use replaceable gels or entangled polymer solutions [18–24]. These solutions have a low background and/or are UV transparent [20]. They can easily be filled into a capillary and renewed whenever necessary. Nevertheless, Liu et al. [10] and Dolnik and Novotny [12] have demonstrated that highly condensed (or high-concentration) gels are essential to separate oligosaccharides and polyamino acids well. Unfortunately, condensed gels are not replaceable. To prepare capillaries which such condensed gels, special filling or polymerization methods are needed and one or two methods have been developed [17,25]. However, the high background of the capillaries remains a problem or becomes even more serious because

* Corresponding author.

¹ On leave from the Institute of Chemistry, Chinese Academy of Science, Beijing, China.

the condensed gels such as polyacrylamide have a much stronger UV absorption than the low-percentage gels. Although laser-induced fluorescence (LIF) detection is an excellent way to overcome the detection problem [9–12], the samples should be fluorescent or must be labelled with fluorescent agents, which more or less influences the structure of the samples. It might also be questionable whether or not all the samples can be labelled or can be homogeneously labelled. In addition, the construction of the detector is much more expensive than for a UV detector. UV spectrophotometry therefore preferred as an inexpensive, universal detection method but low-background gel-filled capillaries should be available.

In this paper, we discuss a method for the preparation of such low-background capillaries. These capillaries are filled partially with polyacrylamide gels used for separation and partially with buffer used for detection. To eliminate voids, the separation gels are not immobilized but blocked by two plugs of immobilized gels to overcome the gel migration problem. With this method, capillaries with more than one step of separation gels can also be prepared. The detection sensitivity, stability and performance of the resulting capillaries were tested by the separation of polyaspartate and diaspertate. Some problems in using the resulting capillaries were found and are discussed, but the peak identities are not discussed because the elution standards available are insufficient.

2. Experimental

2.1. Materials

Tricine [N-tris(hydroxymethyl)methylglycine], bicine [N,N-bis(2-hydroxyethyl)glycine], γ -methacryloxypropyltrimethoxysilane, poly(Asp) [poly-(α,β)-D,L-aspartate Na⁺, M_r (average molecular mass detected by viscosity) = 6850], aspartic acid and diaspertate were purchased from Sigma (St. Louis, MO, USA). Acrylamide and Bis [N,N'-methylenebis(acrylamide)], electrophoretically pure, were obtained from Bio-Rad

Labs. (Richmond, CA, USA). Tris [tris(hydroxymethyl)aminomethane], TEMED (N,N,N',N'-tetramethylethylenediamine), APS (ammonium peroxydisulfate), TEA (triethanolamine) and other chemicals were of analytical-reagent grade from Merck (Darmstadt, Germany). Fused-silica capillaries of O.D. 375 μ m and a wide-bore capillary of 0.53 mm I.D. were obtained from Composite Metal Services (Worcestershire, UK). The water used was purified with a Millipore Super Q system.

2.2. Filling principle

There are at least three principles that can be used for filling solutions into capillaries: (1) capillary surface tension or capillary force, that is, when a capillary is dipped into a solution, the solution will automatically flow into the capillary; (2) vacuum; (3) pressure. For filling solutions with low viscosity, using the capillary force is very convenient. The filling can be speeded up by lowering the other end of the capillary. For filling viscous liquids such as gelling solutions, using the capillary force combined with slight pressure is adopted for easy manipulation.

There are several ways to pressurize a solution slightly, of which only one way is described, that is, using sealed glass vials as micro-pumps [25]. A glass vial (Beckman, part No. 358807) is sealed using a modified screw-cap (Beckman, part No. 360004) with a rubber septum and a PTFE septum (Millipore, part No. 73005) as shown in Fig. 1A. The vial is pressurized by injection of air or solution into it and can also be evacuated by drawing the air out of the vial (Fig. 1B). These sealed vials are also used for polymerizing the acrylamide under slight pressure (Fig. 1C), for degassing a solution (after evacuation) and for drying a capillary (by injection of >10 ml of air into the vial; see Fig. 1B).

2.3. Partial silanization of capillaries [3,4,25,26]

One end of a new capillary is dipped into a 0.5% (v/v) solution of γ -methacryloxypropyl-trimethoxysilane in acetic acid-methanol (1:250, v/v) until the solution inside the capillary

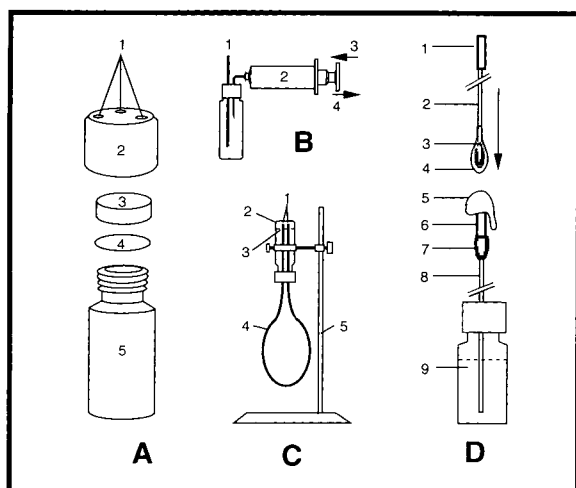


Fig. 1. (A) Structure of a sealed vial. 1 = 1.5 mm diameter holes, two used for plugging capillaries and one for syringe needle; 2 = screw-cap; 3 = rubber septum (2–3 mm thick); 4 = PTFE septum; 5 = glass vial. (B) Sealed vial with a capillary (1), pressurized (3) or evacuated (4) using a syringe (2). (C) Capillary filled with gelling solutions pressurized using a sealed vial. 1 = Capillary tips; 2 = sealed vial, pressurized by injection of 3.5–4 ml of ice-cooled water; 3 = water level; 4 = filled capillary; 5 = hanging device. (D) An important step for coupling a gel-filled capillary with a buffer-filled capillary where the arrow shows that the gel-filled capillary is being plugged into the connector against the buffer flow. 1 = Buffer-filled casing tube; 2 = gel-filled capillary; 3 = Pattex sealing membrane; 4 = a drop of buffer to prevent the polyacrylamide gel from drying out; 5 = buffer flow; 6 = connector; 7 = fixative; 8 = buffer-filled capillary; 9 = sealed vial with buffer, pressurized by injection of about 5 ml of air into the vial.

reaches the height required (measured from the dipped end). The capillary is removed from the solution and laid on a table at room temperature for 10–20 min, during which the solution filled in it will evaporate naturally. To compensate for the evaporation, the capillary end should be re-dipped into the silane solution every 2–5 min. The capillary is then washed for 5 min by drawing water into the not yet modified end and dried for 10–15 min (see Section 2.2 and Fig. 1B). It is critical to dry capillary completely, otherwise the filling speed cannot be controlled further. The other end of the capillary is modified and dried in the same way except that the water for washing is drawn in from the first modified end.

All the parts filled with the silane solution are considered to be completely silanized.

2.4. Preparation of partially coated capillaries

A partially silanized capillary is completely filled with a 3.5% (w/v) solution of acrylamide in 0.1 M Tricine–0.05 M Tris containing 0.1% (v/v) TEMED + 0.1% (w/v) APS, and kept for at least 30 min. The capillary is then washed with water for 15 min and dried for 5–10 min.

2.5. Preparation of totally coated capillaries

A new capillary is washed first with 1 M NaOH for 1 h and then with water and methanol for 30 min each. This capillary is completely filled with the silane solution mentioned above. After keeping for 1 h, the capillary is washed again with methanol and water for 30 min each and then filled with 3.5% T gelling solution and kept for 1 h. The capillary is finally washed with 0.1 M Tricine–0.05 M Tris buffer for 30 min and dried for more than 10 min. This coated capillary can be stored at room temperature for more than 5 months.

2.6. Gelling solutions

All the gelling solutions are prepared in 0.1 M (final concentration) Tricine–0.05 M Tris from stock solutions of 40% T + X% C ($X \geq 0$), where %T is the grams of the total monomers in 100 ml of water solution and %C the grams Bis in 100 g of the total monomers. The solutions are placed inside evacuated glass vials and degassed for about 10 s by ultrasonic shocking [25]. Just before filling, TEMED and APS are added to a final concentration of 0.04–0.05% each. The solutions, after addition of APS and TEMED, should be filled into the capillary at 15–20°C within 8 min.

2.7. Preparation of partially or step gradient gel-filled capillaries

A general structure of the partially gel-filled capillaries, described with the positions of the

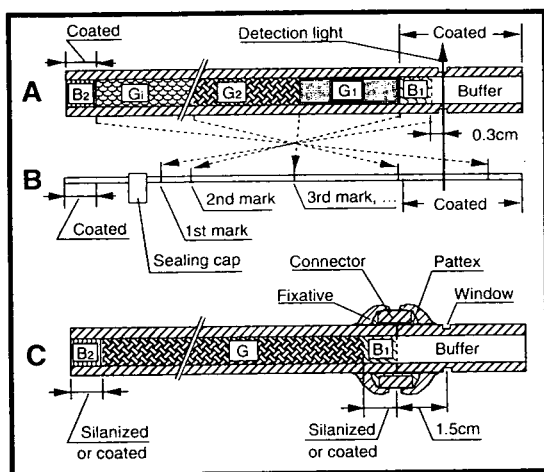


Fig. 2. Schematic configurations of (A) a partially or step gradient gel-filled capillary and (C) a coupled capillary where the boundaries between the different gels are defined by the positions of the initial solutions. (B) Capillary ready for filling gelling solutions. B_1 = immobilized cross-linked gels ($<20\%T$); B_2 = immobilized linear gels ($\geq 10\%T$) or cross-linked gels at the injection end of the capillary; G_1 – G_i and G = gels used for separation.

initial gelling solutions, is shown schematically in Fig. 2A, where G_1 – G_i ($i \geq 1$) are the gels used for separation and their concentrations are arranged as $G_1 > G_2 > \dots > G_i$. B_1 and B_2 are a short plug (≥ 1 cm) of immobilized cross-linked gels ($\leq 15\%T + 5\%C$) or linear gels ($\geq 10\%T$) used for preventing the separation gels from migrating. When $G_1 < 20\%T (+5\%C)$ and $G_i \leq 10\%T (+5\%C)$, B_1 can be replaced by a portion of immobilized G_1 and B_2 by a portion of immobilized G_i .

To prepare such a capillary, the buffer portion is generally first filled into the capillary to create a clean detection environment; it is then followed by solutions of B_1 , G_1 , \dots , G_i . B_2 is filled into the capillary at the final step. If this filling sequence is reversed, that is, B_2 is first filled in and the buffer is filled in after all the gelling solutions, the detection background of the resulting capillaries may not clear because the buffer may be seriously contaminated by the gelling solutions remaining at the capillary wall. In this case, more than 2 h of equilibration (see below) are required to clean the background.

The buffer portion can also be filled in between the gels, for instance, the capillary can be filled first with a portion of B_1 and then with a portion of the buffer followed by B_1 and other gelling solutions.

It is clear that, to fill different solutions into one capillary, the capillary should be transferred from solution to solution several times, and how the tube is transferred is critical. To prevent air bubbles from being introduced into the capillary, the transfer time should be less than 2 s, which is especially important when transferring a capillary from a buffer to other solutions because most of the buffers have low viscosity. Whenever a bubble is observed during filling, the capillary should be re-washed with water for 10 min and then dried for re-filling. A more detailed filling procedure is as follows.

(1) One end of a new capillary is coated (see above) for 3–5 cm and the other end for 10 cm (2 cm for immobilization of gel and 8 cm for buffer). The buffer part of the capillary is coated in order to reduce electroosmosis.

(2) The capillary is marked from the shorter coated end as shown in Fig. 2B and then mounted with a sealing cap, which will be used for speeding up the filling when necessary.

(3) The shorter coated end is dipped into a newly degassed buffer of 0.1 M Tricine–0.05 M Tris until the buffer level inside the capillary reaches the first mark.

(4) The capillary is vertically and quickly removed from the buffer and immediately dipped into B_1 solution until the buffer level reaches the second mark.

(5) As in (4), the capillary is transferred to the vial with G_1 solution until the buffer reaches the third mark. This step is repeated until G_i and B_2 are filled in. The buffer level should, at this point, reach the other end of the capillary. The filling, if too slow, is speeded up by sealing the vial, which is then injected with less than 2 ml of air (see also Fig. 1B).

(6) For polymerization, both ends of the filled capillary are plugged into one sealed vial and about 3.5–4 ml of ice-cooled water are then injected into the vial to build up a slight pressure of 5–7 atm and to lower the polymerization

speed at the ends of the capillary [25]. The tips of the capillary are set at a higher level than the water in the vial (Fig. 1C) so that the empty space at the ends, a result of gel shrinkage, can be measured after polymerization. The capillary is hung for about 4 h in a windless and shockless location at 15–20°C. After hanging, at least 0.5 cm of both ends of the capillary are cut off to remove the empty ends.

(7) The resulting capillary is equilibrated with 0.1 M Tricine–0.05 M Tris buffer at 200 V/cm and 25°C for at least 1 h and then stored at room temperature with both ends dipped into the buffer. The capillaries can be stored for more than 3 months.

(8) The detection window is opened just before using the capillary for the separation of samples. About 2 mm of the over-coating at the buffer part of the capillary (0.3 cm from the boundary of the buffer, Fig. 2A) are manually removed using a scalpel and further cleaned with methanol.

2.8. Preparation of capillaries totally filled with gels

Such capillaries can be prepared by cutting off the buffer part of the partially gel-filled capillaries or by the following method. A partially silanized capillary (3–5 cm of silanization from both tips) is filled with 3–5 cm of B₁ solution followed by sections of separation gelling solutions and then by 3–5 cm of B₂ solution. This capillary is pressurized for 4 h and then equilibrated with 0.1 M Tricine–0.05 M Tris buffer as described in section 2.6.

2.9. Coupling of a gel-filled capillary with a buffer-filled capillary

The structure of a coupled capillary is shown in Fig. 2C. Such capillaries are prepared as follows.

(1) One end of a totally coated capillary (ca. 10 cm) is pasted with Pattex (Henkel, Düsseldorf, Germany) and kept for 5 min. This end is then slipped into a buffer-filled connector (1 cm × 0.53 mm I.D., cut from a coated, wide-

bore, fused-silica capillary) and fixed by pasting a quick-drying glue (a cyanoacrylate from UHU Vertrieb, Bühl, Baden, Germany) outside the joint. This fixative takes about 2–5 min to dry. Because a wide connector is used for each manipulation, the gap between the walls of the capillary and the connector is fairly large and should be sealed. This is achieved by pasting the capillary tip with the Pattex before coupling. The gap also retains air bubbles, which are eliminated by pre-filling the connector with a buffer. The suggested buffer is 0.1 M Tricine–0.05 M Tris. Some buffers, such as borate, dramatically reduce the adherence of the fixative.

(2) The B₁-end of a gel-filled capillary prepared in as in Section 2.7 is quickly pasted with the Pattex as in (1). To prevent the gel tips from drying out, a drop of buffer is put on the Pattex-pasted tip and the other end is slipped into a casing tube filled with buffer (Fig. 1D, upper).

(3) The capillary prepared in (1) is continuously filled with newly degassed buffer of 0.1 M Tricine–0.05 M Tris using a sealed and pressurized vial (Fig. 1D, lower). Against the buffer flow (Fig. 1D, upper), the pasted tip of the gel-filled capillary is plugged into the connector until both ends of the capillaries meet.

(4) The new joint is held manually and the filling pressure is then released by plugging a syringe needle through the cap (do not pull the capillary out of the vial at this moment!).

(5) After the buffer outside has been cleaned with a filter paper, the new joint is fixed by pasting the quick-drying glue over it and kept for more than 2 min (the capillary can now be pulled out for further treatment).

(6) The resulting capillary is equilibrated with buffer and stored as in Section 2.6. The detection window is opened at the buffer part of the capillary, 1.5 cm from the gel tip.

2.10. Electrophoresis

Electrophoresis was performed at 25°C using a Beckman P/ACE System 5500 and 2100, controlled by an IBM SP/2 computer with System Gold software. The cartridges used were modified so that the coupled capillaries could be

mounted without breakage. For detection, the 100×200 (axial direction) μm apertures were mounted and, except where stated otherwise, the data were collected with a PMT (photomultiplier tube). The data sampling rate was 1 Hz and the rise time 1 s. When a diode-array detector was used, the detection band width was 6 nm. The running buffer (0.1 M Tricine–0.05 M Tris) was degassed just before use and renewed every five runs. The sample was introduced into the negative end of the capillary by dipping it into a sample solution for 30 s (diffusing injection [27]). To carry out the diffusing injection, the run method should be started 16 s after the capillary has been dipped into the sample solution because the response time of the software or the CE system is 14 s.

3. Results and discussion

3.1. Detection sensitivity

The most important advantage of the partially gel-filled capillaries is that they retain the high performance of gel-filled capillaries and the low detection background of buffer-filled capillaries. When using totally gel-filled capillaries to separate polyamino acids, the detection sensitivity is too low even at the optimum wavelength of 200 nm [12] and no peaks can be detected at 200 nm (Fig. 3A and B). A simple way to increase the detection sensitivity is to couple the gel-filled capillaries with a piece of buffer-filled capillary as a detection cell. Fig. 3C and E show that the peak height is doubled at 220 nm and further improved, at 200 nm, more than five-fold by using a buffer-filled detection capillary with the same inner diameter. However, the resolution is dramatically reduced. To improve the resolution, fairly condensed gels ($\geq 20\%T + 5\%C$) are required, leading to a greatly increased separation time. In contrast, when using the partially gel-filled capillaries, a $15\%T + 5\%C$ gel can yield a good separation of poly(Asp), the resolution is the same as with the totally gel-filled capillaries (Fig. 4A and C) and the detection sensitivity is similar to that of coupled

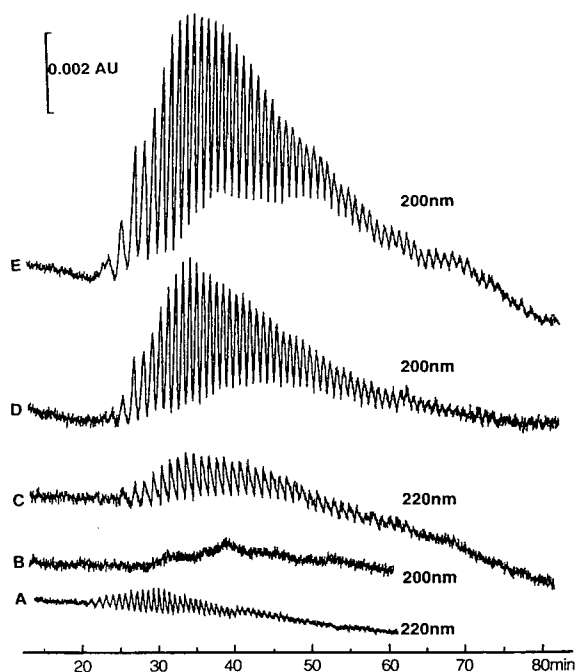


Fig. 3. Comparison of detection sensitivity between a gel-filled capillary (A and B) and a coupled capillary (C–E). Electrophoresis was performed at constant current of $3.5 \mu\text{A}$ (ca. 6.4 kV for A–B and 5.7 kV for C–E) by using the P/ACE System 2100. Capillary: A–B, 25/32 cm (separation/total lengths) $\times 50 \mu\text{m}$ I.D.; C–E, 25 cm $\times 50 \mu\text{m}$ I.D. (gel) + 8.5 cm $\times 50 \mu\text{m}$ I.D. (buffer). Gel: G = 20%T + 5%C; B₁ = 10%T + 5%C (2 cm solution); B₂ = 1 cm of 20%T. Sample: A–C and E, 100 mg/ml poly(Asp); D, 50 mg/ml poly(Asp)

capillaries (Fig. 4C and D). Further studies showed that the detection limit of the partially gel-filled capillaries was about two orders of magnitude lower than that of the total gel-filled capillaries. The testing was carried out with the P/ACE System 5500 as follows. Capillaries with a dimension of 32/37 cm (gel/total lengths) $\times 75 \mu\text{m}$ I.D. were filled totally or partially with a separation gel of 15%T + 5%C (B₂ = 1 cm of 10%T and B₁ = 2 cm of the immobilized separation gel) and run with diaspertate at an average electric field of 400 V/cm. The concentration of diaspertate was decreased until a signal-to-noise ratio of 3. The detection limit for the totally gel-filled capillary was 850 $\mu\text{g/ml}$. For a partially gel-filled capillary with the buffer not inserted between the gels, the detection limit was

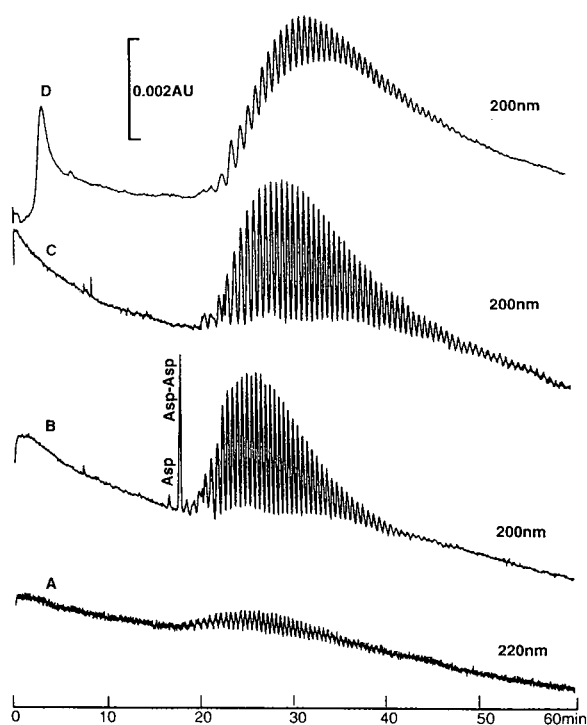


Fig. 4. Comparison of resolution between (A) a gel-filled capillary, (B and C) partially gel-filled capillaries and (D) a coupled capillary. The aspartate and diaspartate in (B) were added at concentrations of 20 and 100 $\mu\text{g}/\text{ml}$ each. All the capillaries were run at 6.5 μA (ca. 7.4, 6, 7 and 7.1 kV from A to E) by using the P/ACE System 5500. Capillary: A–C, 32/39 $\text{cm} \times 75 \mu\text{m}$ I.D.; D, 32 $\text{cm} \times 75 \mu\text{m}$ I.D. (gel) + 8.5 $\text{cm} \times 75 \mu\text{m}$ (buffer). Gel: A, G = 15%T + 5%C, B₁ = 2 cm of the immobilized G, B₂ = 1 cm of 10%T; B, G₁ to G₅ (6 cm each) are 15%T + 5%C, 14%T + 5%C, 13%T + 5%C, 11.5%T + 5%C and 10%T + 5%C, respectively, B₁ = 2 cm of G₁, B₂ = 2 cm of 10%T; C–D, G = 15%T + 5%C, B₁ = 2 cm of G, B₂ = 2 cm of 10%T. Sample: 50 mg/ml poly (Asp).

20 $\mu\text{g}/\text{ml}$; if the buffer was inserted between the gels, the detection limit increased to 50 $\mu\text{g}/\text{ml}$, which might result from the buffer being slightly compressed in this instance. It is therefore better to use the former kind of partially gel-filled capillaries.

Similarly to the coupled capillaries, partially gel-filled capillaries also increase the separation time (compare Fig. 4A and C), but this can easily be overcome by using capillaries with step gradient separation gels (compare Fig. 4A and B). The resolution is only slightly affected.

These kinds of capillaries may also be useful in the separation of complicated samples such as natural proteins or oligosaccharides, but further investigation is required.

3.2. Voids and gel migration

We found that the voids in immobilized linear gels (up to 35%T) can easily be prevented and that the voids in a short section of immobilized cross-linked gel (<20%T + 5%C) or in a long section of condensed cross-linked gel that is not immobilized can also be eliminated without too much difficulty [25]. This implies that we can establish a new method to prepare void-free and stable capillaries, that is, using the non-immobilized cross-linked gels as separation media to eliminate the voids and prevent them from migrating with two plugs of immobilized linear gels and/or cross-linked gels. It would seem difficult to introduce two plugs of immobilized gels at the ends of the separation gels, but it is actually easy to do so or at least not too difficult. The success rate of the preparation with the described method is higher than 90%. The resulting capillaries can be used continuously for more than 1 week or for more than 50 injections of poly(Asp) at about 200 V/cm (Fig. 4). This stability seems to be comparable to that of istachophoretically prepared capillaries [17].

It is essential that the gel plugs at the capillary ends (B₁ and/or B₂, Fig. 2A) should be formed at a lower speed than the separation gels, otherwise several large voids may develop in the separation gels. There are two options to control the gelatinization speed: (1) adding a larger amount of TEMED and/or APS to the separation gelling solutions than to the B₁ and B₂ solutions so that the gelatinization of the former solutions will start at least 5 min ahead of the latter; inside a capillary, it is difficult to measure the starting point of the gelatinization, and an easy way is to measure the starting point in a vial and use the measured values as a reference; (2) cooling the ends of the capillaries as described under Experimental, which is easier in practice than the first method. To eliminate voids com-

pletely, a slight pressure should be applied to the capillary during polymerization [25].

Any linear gels with concentrations higher than 4.5%T can be used as the plugs, but higher percentage linear gels such as 10%T are suggested for preparing stable capillaries. For the preparation of partially gel-filled capillaries, we suggest using a cross-linked gel as the plug in front of buffer (B_1). Linear gel plugs may sometimes cause a low detection sensitivity after several runs with the capillaries. The main reason might be that some part of the linear gels which do not bind to the capillary wall gradually dissolve into the buffer.

Interestingly, when any of the gel plugs (B_1 and B_2) is omitted, the stability of the resulting capillaries will be influenced by the direction of the applied electric field. For instance, without B_2 , the capillaries may be unstable (observed by a current drop) if a positive voltage is applied to the injection end (gel end), although they are stable if a negative voltage is applied to the injection end. When B_1 is omitted, the situation is reversed.

3.3. Reproducibility and problems

The main problem in using the suggested method is that, because the flexible capillaries are generally protected by a polyimide over-coating, it is difficult to measure the correct positions of the gels after polymerization as they are different from those of the solutions, owing to the gel shrinkage during polymerization. In order to measure the gel positions photometrically, the over-coating should be removed but then the capillaries become too fragile. We therefore use the solution lengths or positions to describe the capillaries (Fig. 2A). Clearly, if the lengths of the solutions cannot be controlled correctly, irreproducible capillaries will result. To investigate the reproducibility, five capillaries with 1 cm of 10%T gel (solution) in the injection end followed by 29 cm of 10%T + 5%C separation gel (2 cm = B_1) and 7 cm of buffer were prepared and run at 400 V/cm. Each capillary was used for ten injections of diaspertate. The average elution time \pm the relative standard de-

viation from run-to-run for each capillary were 10.65 ± 0.82 , 10.78 ± 0.43 , 10.96 ± 0.55 , 10.77 ± 0.21 and $10.89 \pm 0.37\%$, respectively. For capillary to capillary, the elution times of the tenth injection of each capillary were averaged, the result being $10.76 \pm 1.61\%$. The reproducibility was not too bad. To obtain higher reproducibility, the capillaries should be run at a constant current or a constant power.

Special phenomena are observed when using the partially gel-filled capillaries and also the totally gel-filled capillaries for the separation of poly(Asp). (1) the baseline of the capillaries drifts negatively. For partially gel-filled capillaries, the drift in the first several runs may be larger than -0.01 absorbance per hour at 200 nm but is reduced to about -0.003 absorbance after about ten runs. Interestingly, the baseline drift depends on the detector and on the detection wavelength, as shown in Fig. 5. With a PMT detector, we found that different buffers or buffer components yield different drifts. Compared with Tricine-Tris, Bicine-Tris and Tricine-TEA buffers increase the drift by ca. 10%. (2) When using newly prepared capillaries, the first several separations are generally not ideal, and are accompanied by a current decrease. The current will become stable at a value lower than that without the injection of the sample. This is not due to the re-formation of voids in the gels, which can be checked under a microscope. A possible interpretation is that some pores of the gels are blocked by some large solutes because the current can be recovered by applying a reversed electric field to the capillaries (positive voltage at the injection end) for more than 1 h after separation. The separation is improved after the capillaries have been stored for 2–5 days or run more than three times with a highly concentrated sample [100 mg/ml poly(Asp)], which is a way to overcome the problems.

4. Conclusion

The described method and the resulting capillaries offer a new approach to overcoming some of the problems in capillary gel electrophoresis.

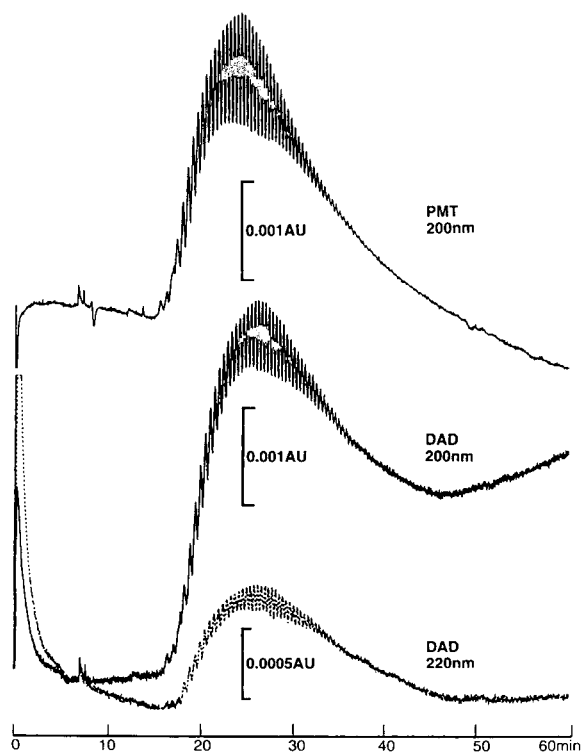


Fig. 5. Electrophoresis using a 30/37 cm \times 75 μ m I.D. capillary filled with 30 cm of 10%T + 5%C gel (B_1 and $B_2 = 2$ cm of the immobilized gel) as separation medium and with 7 cm of buffer as detection background. The capillary was run with 50 mg/ml poly(Asp) at 7.5 μ A (ca. 6.7 kV) by using the P/ACE System 5500. The lower two electropherograms were generated in one run.

It is clear that the partially or gradient gel-filled capillaries will also increase the detection sensitivity of LIF or other absorption-dependent detection methods. After modification, this method could be used for the production of capillaries with different kinds of polymers, not only polyacrylamide. Polymers with stability independent of temperature, voltage and pH are highly desirable.

Acknowledgements

We thank Victoria Kastner for improving the English of the manuscript, and the financial support of the Alexander von Humboldt foundation is gratefully acknowledged by Y.C.

References

- [1] S. Hjerten, *Chromatogr.*, 270 (1983) 1–6.
- [2] L.M. Smith, *Nature*, 349 (1991) 812–813.
- [3] J.A. Luckey, H. Drossman, A.J. Kostichka, D.A. Mead, J. D’Cunha, T.B. Norris and L.M. Smith, *Nucleic Acids Res.*, 18 (1990) 4417–4421.
- [4] D.Y. Chen, H.P. Swerdlow, H.R. Harke, J.Z. Zhang and N.J. Dovichi, *J. Chromatogr.*, 559 (1991) 237–246.
- [5] M.-J. Rocheleau and N.J. Dovichi, *J. Microcol. Sep.*, 4 (1992) 449–453.
- [6] H. Swerdlow and R. Gesteland, *Nucleic Acids Res.*, 18 (1990) 1415–1419.
- [7] H. Swerdlow, S. Wu, H. Harke and N.J. Dovichi, *J. Chromatogr.*, 516 (1990) 61–67.
- [8] G.L. Trainor, *Anal. Chem.*, 62 (1990) 418–426.
- [9] J. Liu, O. Shirota and M. Novotny, *J. Chromatogr.*, 559 (1991) 223–235.
- [10] J. Liu, O. Shirota and M. Novotny, *Anal. Chem.*, 64 (1992) 973–975.
- [11] J. Liu, V. Dolnik, Y.-Z. Hsieh and M. Novotny, *Anal. Chem.*, 64 (1992) 1328–1336.
- [12] V. Dolnik and M. Novotny, *Anal. Chem.*, 65 (1993) 563–567.
- [13] D. Wu and F.E. Regnier, *J. Chromatogr.*, 608 (1992) 349–356.
- [14] K. Tsuji, *J. Chromatogr.*, 550 (1991) 823–830.
- [15] A.S. Cohen and B.L. Karger, *J. Chromatogr.*, 397 (1987) 409–417.
- [16] K. Hebenbrock, K. Schugerl and R. Freitag, *Electrophoresis*, 14 (1993) 753–758.
- [17] V. Dolnik, K.A. Cobb and M. Novotny, *J. Microcol. Sep.*, 3 (1991) 155–159.
- [18] D.N. Heiger, A.S. Cohen and B.L. Karger, *J. Chromatogr.*, 526 (1990) 33–48.
- [19] P.D. Grossman and D.S. Soane, *J. Chromatogr.*, 559 (1991) 257–226.
- [20] K. Ganzler, K.S. Greve, A.S. Cohen, B.L. Karger, A. Guttman and N.C. Cooke, *Anal. Chem.*, 64 (1992) 2665–2671.
- [21] P. Bocek and A. Chrambach, *Electrophoresis*, 13 (1992) 31–34.
- [22] M.H. Kleemiss, M. Gilges and C. Schomburg, *Electrophoresis*, 14 (1993) 515–522.
- [23] M.C. Ruizmartinez, J. Berka, A. Belenkii, F. Foret, A.W. Miller and B.L. Karger, *Anal. Chem.*, 65 (1993) 2851–2858.
- [24] W.E. Werner, D.M. Demorest, J. Stevens and J.E. Wiktorowicz, *Anal. Biochem.*, 212 (1993) 253–258.
- [25] Y. Chen, J.-V. Hölftje and U. Schwarz, *J. Chromatogr. A*, 680 (1994) 63–71.
- [26] S. Hjerten, *J. Chromatogr.*, 347 (1985) 191–198.
- [27] Y. Chen and A. Zhu, *Sepu (Chin. J. Chromatogr.)*, 7 (1990) 5–10.

Micellar electrokinetic capillary chromatography with in situ charged micelles

IV. Influence of the nature of the alkylglycoside surfactant

Joel T. Smith, Ziad El Rassi*

Department of Chemistry, Oklahoma State University, Stillwater, OK 74078-0447, USA

First received 25 April 1994; revised manuscript received 12 July 1994

Abstract

Four different in situ charged micellar phases were evaluated in micellar electrokinetic capillary chromatography (MECC) of neutral and acidic herbicides, and other aromatic compounds. In situ charged micelles refer to dynamically charged entities that are formed via the complexation of borate with surfactants having sugar head groups. These dynamically charged surfactants yield micelles with adjustable surface charge densities which can be conveniently manipulated by changing borate concentration and pH of the running electrolyte. The four surfactants, namely octanoylsucrose (OS), octyl- β -D-glucopyranoside (OG), octyl- β -D-maltopyranoside (OM) and nonanoyl-N-methylglucamide (MEGA 9), in the presence of alkaline borate yielded micelles characterized by migration time windows of varying width. The width of the migration time window was largely influenced by the nature of the sugar head group of the polyolic surfactant. The electrochromatographic behavior of OS, OM, OG and MEGA 9 was influenced by both the nature of the sugar head group and the length of the alkyl tail. OS, which differed from the other surfactants by having an alkyl tail with one fewer carbon atom, exhibited the lowest retention. MEGA 9 with its acyclic sugar head group and the presence of a polar amide linkage between the sugar and the alkyl tail showed a medium retentivity towards the various solutes under investigation. OG and OM, which differed from each other by the nature of the sugar head group, exhibited more or less similar retention behavior. Overall, due to differences in their migration time windows and retention behaviors, the four micellar phases afforded different selectivities toward charged and neutral solutes. The separation efficiencies achieved with in situ charged micelles, which exceeded 750 000 plates/m, appear to be superior to those achieved with traditionally used micellar phases.

1. Introduction

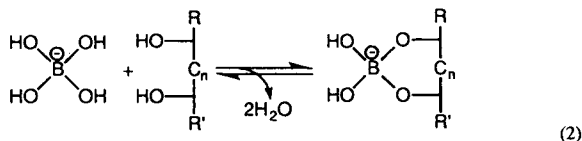
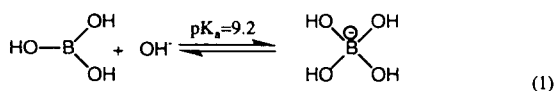
Over the last decade, capillary electrophoresis (CE) has developed rapidly and became an important analytical separation technique [1,2] of unsurpassed resolving power. The technique

has found applications in the separation of almost all types of compounds. This universal use of CE has been facilitated in part by the fact that a given separation can be performed in several modes thus permitting the achievement of different selectivities. An important development of CE has been the introduction of micellar electrokinetic capillary chromatography (MECC) by

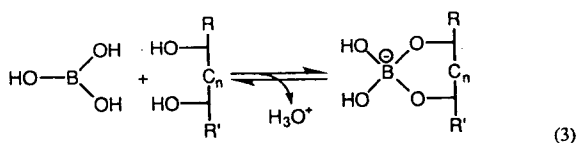
* Corresponding author.

Terabe et al. in 1984 [3], a technique that allows the separation of neutral species under the influence of an electrical field. MECC has shown great promises in the separation of both neutral and charged species [4–8]. The separation is achieved via the differential partitioning of the analytes between an aqueous phase and a charged micellar phase. The basic operational principles and the applications of MECC have recently been reviewed [9,10].

Recently, our laboratory has introduced the concept of in situ charged micelles [11–14] to MECC of neutral and charged species. In situ charged micelles are dynamically charged entities via complexation of a diol group of a polyol surfactant with borate or boronate ion. The generalized reaction scheme of a diol with the borate ion is shown in equilibria 1 and 2 below.



Equilibrium 1 represents the ionization of boric acid ($\text{p}K_a = 9.2$) to the tetrahydroxy borate ion, i.e., borate. Equilibrium 2 represents complexation between the borate ion and a diol. It is well known that a polyol possessing vicinal diols of the proper geometry can undergo complexation with borate to form an ionized complex upon the loss of two molecules of water [15–17]. In equilibrium 2, n is either 0 or 1, which corresponds to a 1,2- or 1,3-diol, respectively. The 1,2-diol forms a five-membered ring upon complexation and is more stable than the 1,3-diol complex which forms a six-membered ring. Boric acid, in the neutral form, can also complex with diols and is illustrated below in equilibrium 3.



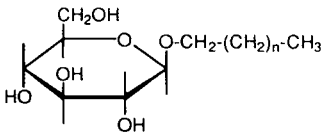
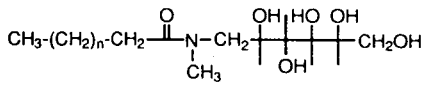
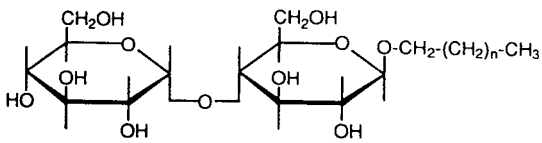
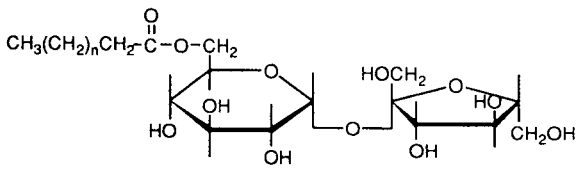
In this reaction, the complex is formed upon the loss of one water molecule and a proton. It is well known that the stability constant of equilibrium 2 is much greater than that of equilibrium 3. The forward rate constant for the complexation (equilibrium 2) is at least 3 orders of magnitude greater than the rate constant for the trigonal boric acid (equilibrium 3) for some polyols [18]. Equilibrium 3, whose rate constants are largely dependent on the geometrical arrangement of diols, is currently being exploited in our laboratory with in situ charged micelles at neutral pH. At alkaline pH, the formation of diol–borate complex is primarily the result of equilibrium 2.

According to the above equilibria, the surface charge density of an alkylglycoside micelle can be easily manipulated by altering the borate concentration, the surfactant concentration, and/or the pH of the running electrolyte. As a result, the migration time window of the in situ charged MECC system can be tailored to suit a given separation problem.

We have examined several polyol surfactants as possible in situ charged micellar phases including a series of four alkyl- β -D-glucopyranosides [12], a series of three *N*-D-glucosyl-*N*-methylalkanamides (MEGA) [14], octyl- β -D-maltopyranoside and octanoylsucrose [13]. The structures of these surfactants are listed in Table 1. Fig. 1 illustrates our view of the idealized structure of the alkylglycoside–borate micelle. The micelle consists primarily of the hydrophobic core with hydrophilic sugar residues facing outwards towards the aqueous phase. Borate can complex with the diols of the proper geometry at the surface of the micelle. Since the degree of complexation can be readily controlled, the surface charge density is therefore adjustable.

Due to the nature of the hydrophilic sugar head group, different surfactants have different affinities towards borate. ^{11}B NMR studies [13] have shown that the alkyl- β -D-glucopyranoside surfactants complex through O-4 and O-6 of the glucose residue as suggested by Foster [15]. Similarly, octanoylsucrose and octyl- β -D-maltopyranoside complex with borate primarily via the nonreducing glucose residue and have bind-

Table 1
Structures and CMCs of surfactants used in our studies

Identification	Name	Abbreviation	CMC (mM) ^a
<i>Alkylglucosides</i>			
			
$n = 5$	Heptyl- β -D-glucopyranoside	HG	79
$n = 6$	Octyl- β -D-glucopyranoside	OG	25
$n = 7$	Nonyl- β -D-glucopyranoside	NG	6.5
$n = 8$	Decyl- β -D-glucopyranoside	DG	2–3
<i>Alkylglucamides</i>			
			
$n = 5$	Octanoyl- <i>N</i> -methylglucamide	MEGA 8	58
$n = 6$	Nonanoyl- <i>N</i> -methylglucamide	MEGA 9	19–25
$n = 7$	Decanoyl- <i>N</i> -methylglucamide	MEGA 10	6–7
<i>Alkylmaltosides</i>			
			
$n = 6$	Octyl- β -D-maltopyranoside	OM	23.4
<i>Alkanoylsucrose</i>			
			
$n = 5$	<i>n</i> -Octanoylsucrose	OS	24.4

^a Obtained from Ref. [19]

ing affinities very similar to that of the alkyl- β -D-glucopyranosides [14]. The MEGA surfactants possess an acyclic sugar residue which allows the hydroxyl groups to change their conformation freely. This freedom in changing conformation

allows the MEGA surfactants to have a much higher affinity towards borate. Previous ¹¹B studies have indicated that the surfactants with acyclic sugar head groups have at least a three-fold higher affinity for borate than surfactants

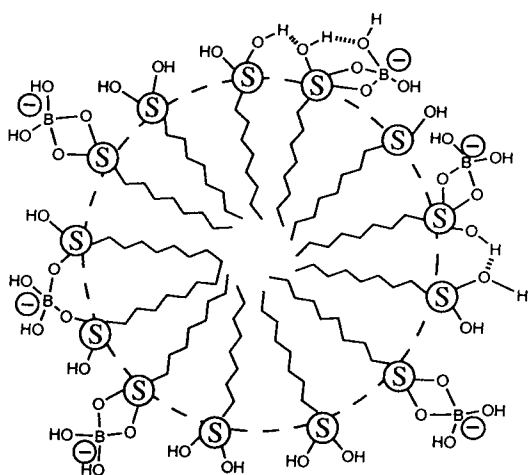


Fig. 1. Idealized structure of alkylglycoside–borate micelle showing borate complexation and hydrogen bonding on the outer surface of the micelle. Circled-S stands for the sugar head group of the surfactant.

possessing a cyclic sugar head group [13]. This feature allows the MEGA micellar phases to form a larger migration time window under similar electrophoretic conditions.

As can be seen in Table 1, the alkylglycoside surfactants under investigation possess a straight chain alkyl tail and a sugar polar head group. We have previously evaluated the influence of the length of the alkyl tail with various types of analytes [12,13], and demonstrated that the differences in hydrophobic character among surfactants with different tails are useful in optimizing selectivity for a given separation.

The aim of this report is to investigate the influence of the nature of the alkylsaccharide surfactant on the electrochromatographic properties of the in situ charged micelles. To achieve this goal, surfactants having different types of sugar head groups and hydrocarbonaceous tails were evaluated, namely, octanoylsucrose (OS), octyl- β -D-maltopyranoside (OM), octyl- β -D-glucopyranoside (OG) and nonanoyl-*N*-methylglucamide (MEGA 9). As can be seen in Table 1, all four of the surfactants have similar CMCs. Three of the surfactants differ in the nature of the sugar head group and have in common an eight-carbon lipophilic tail (i.e., OM, OG and MEGA 9) while the fourth surfactant has a

different alkyl tail (a seven-carbon alkyl tail) and sugar head group, i.e., OS. The surfactants were compared in terms of the migration time window, peak capacity, efficiency, retention energetics and selectivity as a function of the nature of the surfactant. The micellar phases were applied to MECC of mixtures of both neutral and acidic herbicides as well as very hydrophobic aromatic compounds.

2. Experimental

2.1. Instrumentation

This work was performed on a capillary electrophoresis system Model HP ^{3D}CE from Hewlett Packard (Waldbronn, Germany) equipped with a real time UV–visible diode array detector (DAD) and accompanying data analysis software. The column temperature was maintained at 30°C. The detection wavelength was set at 240 nm for the detection of herbicides, and at 254 nm for the detection of aromatics and alkyl phenyl ketones. In all the experiments, the electrical field strength was 187.5 V/cm.

Fused-silica capillaries having an inner diameter of 50 μ m and an outer diameter of 375 μ m were obtained from Polymicro Technology (Phoenix, AZ, USA). The total length of the capillary was 64.0 cm with an effective length of 56.0 cm, i.e., from the injection end to the detection point.

2.2. Reagents

Octyl- β -D-glucopyranoside (OG) was obtained from Sigma Chemical Co. (St. Louis, MO, USA). *n*-Octanoylsucrose (OS), octyl- β -D-maltopyranoside (OM) and nonanoyl-*N*-methylglucamide (MEGA 9) were purchased from Calbiochem (San Diego, CA, U.S.A.). For the structures and the critical micelle concentrations (CMCs) of the surfactants, see Table 1. It should be noted that the CMC values given in Table 1 are those obtained in low ionic strength buffer solutions, i.e., 0–0.05 M Na⁺. All herbicides used in this study were purchased from Chem

Service (West Chester, PA, USA). The series of alkyl phenyl ketones (APK) was purchased from Aldrich Chemical Co. (Milwaukee, WI, USA). Aniline, 2-naphthylamine, naphthalene, biphenyl, 1-chloronaphthalene and anthracene were purchased from Eastman Kodak Co. (Rochester, NY, USA). All chemicals for the preparation of electrolytes were purchased from Fisher Scientific (Pittsburgh, PA, USA). Methanol was purchased from EM Science (Cherry Hill, NJ, USA). All electrolyte solutions were prepared with deionized water and filtered with 0.2 μm Uniprep Syringeless filters from Fisher Scientific to avoid capillary plugging.

2.3. Methods

The running electrolyte was prepared by dissolving proper amounts of boric acid and surfactant in water, and adjusting the pH to the desired value with sodium hydroxide. For all experiments, the running electrolyte was composed of 100 mM of the surfactant and 200 mM borate at pH 10.0. All sample stock solutions were made by first dissolving pure compounds in methanol. Sample solutions for injection were made by dissolving the proper amount of stock solution in the running electrolyte and adjusting the total volume of methanol in the sample to 20% (v/v). Sample injection was performed by pressurizing the sample reservoir for an appropriate length of time (50–100 mbar · s). Between runs, the capillary was rinsed consecutively with water, 1.0 M NaOH, 0.10 M NaOH, water and the running electrolyte.

In all calculations involving efficiency, the plate count was estimated from peak standard deviation taken as the half peak width at 0.607 of peak height (i.e., the inflection point) and was reported as the average of at least three runs. Mobilities were determined from average migration times, and again a minimum of three runs were used to calculate the average. The migration time of an unretained species, t_0 , was determined by the deflection peak of methanol. The migration time of the micelle, t_{mc} , was determined by the iterative method of a homologous series [8]. Anthracene was used as a marker

to visualize t_{mc} but was not used in the calculation of the capacity factor, k' .

3. Results and discussion

3.1. Migration time window

As we have described in previous studies involving in situ charged micellar systems, i.e., alkylglycoside–borate or –boronate micelles [11,13,14], the migration time window can be adjusted over a wide range by adjusting the pH, borate (or boronate) concentration and/or the surfactant concentration. This is because these parameters affect the surface charge density of the micelle.

To provide a meaningful comparison for the results pertaining to the migration time window, the four surfactants, OG, OS, OM and MEGA 9, were evaluated under conditions of constant micellized surfactant concentration. Constant micellized surfactant concentration corresponds to keeping the concentration of surfactant [S] minus the CMC constant, i.e., $[S] - \text{CMC} = \text{constant}$. Since the four surfactants all have similar CMC values, all electrolyte solutions used in the present studies contained the same surfactant concentration. All running electrolytes were composed of 100 mM surfactant and 200 mM borate at pH 10.0. Table 2 lists the migration times for the unretained species, t_0 , and those of the micelle, t_{mc} . The elution range parameters (t_0/t_{mc}) were calculated to be 0.65, 0.60, 0.55 and 0.31 for OM, OS, OG and MEGA micellar phases, respectively. The width of migration time window was the smallest for OM–borate micelle (7.70 min) and the highest for MEGA 9 (28.30 min). The value of the width of the migration time window for OS (9.96 min) and OG (10.67 min) was slightly larger than that observed with OM but much smaller than the one exhibited by MEGA 9. These results corroborate well those previously reported with ^{11}B NMR studies [13] in the sense that the MEGA surfactants have two- to three-fold greater affinity for borate than the alkylglucoside surfactants. This translates into a greater electrophoretic

Table 2
Comparison of migration time window, mobility, efficiency and peak capacity for the various micellar phases

Micellar phase	t_o	t_{mc}	$\mu_{ep(mc)}$ ($\text{cm}^2\text{V}^{-1}\text{s}^{-1}$)	N_{av}	n
OS	14.65	24.61	-1.38×10^{-4}	253 960	65
OM	14.27	21.97	-1.22×10^{-4}	337 230	63
OG	12.91	23.58	-1.75×10^{-4}	429 850	99
MEGA 9	12.47	40.77	-2.77×10^{-4}	301 500	163

Conditions: running electrolyte, 200 mM borate containing 100 mM surfactant, pH 10.0; capillary, untreated fused-silica, 56.0 cm (to detection point), 64.0 cm (total length) \times 50 μm I.D.; voltage 15 kV.

mobility, $\mu_{ep(mc)}$, for MEGA–borate micelle, and in turn to a wider migration time window. Also, the small differences in the width of the migration time windows among OS, OM and OG agree with ^{11}B NMR results which revealed that these surfactants have similar affinities for borate [14]. As can be seen in Table 2, the values of t_o were different among the various micellar phases which may due to slight differences in the viscosity of their running electrolyte solutions.

Furthermore, Table 2 lists the $\mu_{ep(mc)}$ for the four surfactant–borate micellar phases under investigation. The $\mu_{ep(mc)}$ is a direct indication of the degree of complexation between borate and the micelle. OS, OM and OG have a somewhat lower $\mu_{ep(mc)}$ as reflected by the migration time window. The larger $\mu_{ep(mc)}$ observed with MEGA 9 is a result of the acyclic nature of the sugar head group of the surfactant. This is because the hydroxyl groups of acyclic sugars, which are not held in a fixed position, are free to move into more favorable binding positions. Due to this conformational freedom found in acyclic sugars, they can possess up to a ten-fold greater affinity for borate than cyclic sugars [20].

The differences in borate affinity for the different surfactants offer a variety of migration time windows. It should be emphasized that the $\mu_{ep(mc)}$ for OS, OM and OG can be increased up to $\approx -2.5 \times 10^{-4} \text{ cm}^2\text{V}^{-1}\text{s}^{-1}$ by increasing the borate concentration and/or the pH because the surface charge density of the micelle is increased. The MEGA surfactants exhibit a relatively high $\mu_{ep(mc)}$ that can be varied over a wide range with an upper limit approaching that achieved with

SDS. A micellar phase consisting of 43 mM MEGA 9 and 400 mM borate at pH 10.0 produced an $\mu_{ep(mc)}$ of $-3.6 \times 10^{-4} \text{ cm}^2\text{V}^{-1}\text{s}^{-1}$ [13] while that of 100 mM SDS is reported to be $-4.2 \times 10^{-4} \text{ cm}^2\text{V}^{-1}\text{s}^{-1}$ [21]. Many separations do not require a large migration time window in order to separate completely all of the components of a given mixture. If a large retention time window is not required, OS, OM or OG could possibly provide the best results in terms of throughput, but if a complex sample is to be analyzed, a larger migration time window will probably be beneficial and the use of MEGA–borate or –boronate is recommended in this case.

3.2. Efficiency and peak capacity

The separation efficiencies exhibited by the in situ charged micellar phases under investigation are listed in Table 2 in terms of average plate count for the APK homologous series. OG offers the highest separation efficiency with an average plate count of 430 000. The lowest plate count was observed with OS which on the average was 254 000 plates. According to Terabe et al. [22], the dominant intracolumn contributions to band broadening are longitudinal diffusion, sorption–desorption kinetics and electrophoretic homogeneity of the micelles. Since OS–borate micellar phase was the least retentive towards the APKs (see below), the solutes would spend less time associated with the OS micelle than with the other micelles, a condition that would lead to more longitudinal diffusion. This would explain in part the lower separation efficiency obtained

with OS. With the other three alkylglycoside–borate micellar phases under consideration, the contributions to band broadening arising from longitudinal molecular diffusion or electrophoretic homogeneity can be considered to be similar. The observed differences in separation efficiencies among OM, OG and MEGA 9 suggest that the contributions to band spreading arising from sorption–desorption kinetics are different from one micellar phase to another. Davis [23] suggested that nonequilibrium band broadening can be reduced by decreasing the micelles' mobility. In fact, the OM and OG micelles, having the lowest electrophoretic mobilities, yielded higher separation efficiencies than that exhibited by MEGA 9 which is characterized by a higher electrophoretic mobility. Overall, the in situ charged micellar phases produced higher separation efficiencies than those reported with SDS [3,22] or alkyltrimethylammonium halide micelles [24]. The conditions under which these measurements were made produced micelles with mobilities significantly lower than those obtained with SDS and alkyltrimethylammonium halide micelles which, among other things, could explain the higher efficiencies obtained with in situ charged micelles.

As a result of the high plate counts, the number of peaks that can be resolved in a certain time frame is very high as shown in Table 2. The peak capacity, n , is defined as the number of peaks that will fit in a given elution time interval with a resolution of unity. The peak capacity can be calculated experimentally from the values of t_o , t_{mc} and the average plate count [5]. Both OS and OM demonstrated peak capacities greater than 60, but these separations were achieved in a short time frame, i.e., less than 25 min. The peak capacities for OG approached 100 while that of MEGA 9 was in excess of 160. These peak capacities illustrate the tremendous resolving power of MECC in a short time period.

3.3. Retention energetics

To evaluate the influence of the nature of the surfactant on the retention behavior of the various alkylglycoside–borate micellar phases, a

series of alkyl phenyl ketone (APK) homologous solutes, ranging from acetophenone to heptanophenone, were electrochromatographed under the above mentioned conditions. In all cases, the six homologous solutes were well resolved, and typical electropherograms obtained with OG– and MEGA 9–borate micellar phases are illustrated in Fig. 2. The last peak is that of anthracene which was used to visualize the migration time window. Table 3 lists the capacity factors, k' , of the APK homologous solutes with each micellar phase. As expected, the k' values were the smallest for OS. This surfactant has one fewer carbon atom in its alkyl chain than the other three surfactants, see Table 1. The k' values observed with MEGA 9 were significantly higher than those obtained with OS. OM showed higher retention than any of the other micellar phases for the first three solutes of the homologous series ($n_c = 1$ to 3, where n_c is the number of carbon atoms in the alkyl chain of the solute) while OG was the most retentive for the solutes having $n_c = 4$ to 6.

The retention data of Table 3 were further exploited by plotting logarithmic capacity factor versus n_c for the homologous APKs which yielded a straight line on each micellar phase. This is in agreement with our previous studies [12–14, 24] in which we demonstrated that the relationship between $\log k'$ and n_c follows the expression normally found in reversed-phase chromatography:

$$\log k' = (\log \alpha)n_c + \log \beta$$

where the slope ($\log \alpha$) is a measure of the methylene group selectivity which characterizes nonspecific hydrophobic interactions, while the intercept ($\log \beta$) reflects the specific interactions between the residue of the molecule (i.e., benzaldehyde group) and the aqueous and micellar phase. For an in-depth discussion of this data treatment the reader is referred to previous reports from our laboratory [13,24].

Table 4 lists the results of linear regression for plots of $\log k'$ versus n_c for the different micellar phases. The R values obtained with the four plots were either 0.999 or 1.000. The methylene

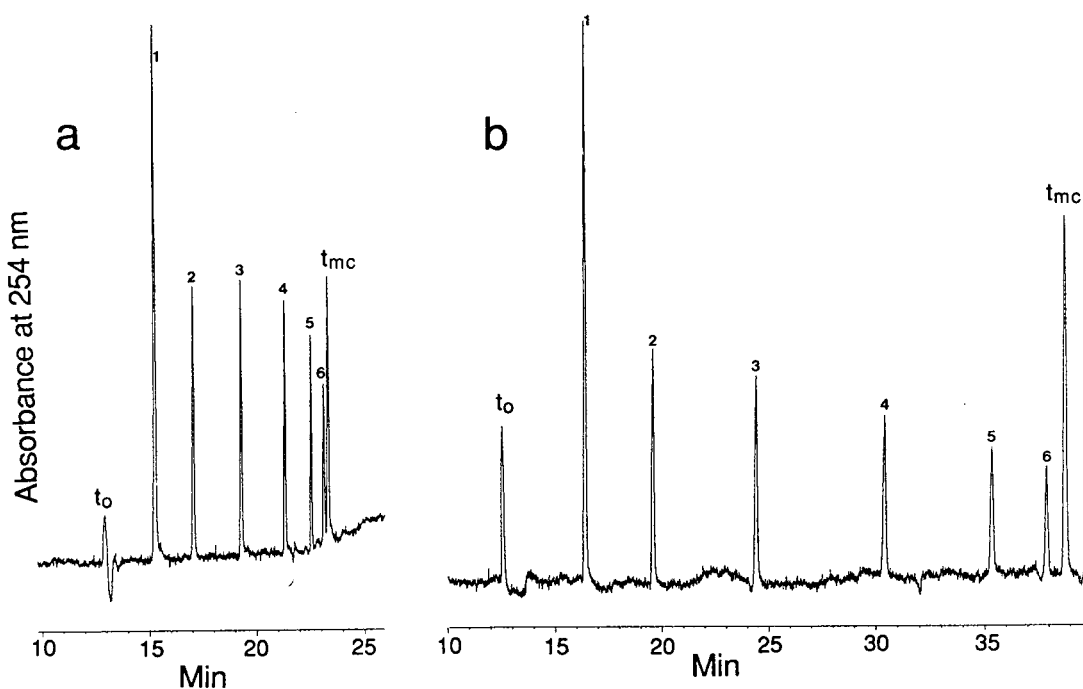


Fig. 2. Electropherograms of APK homologous series. Experimental conditions: running electrolytes, 200 mM borate containing 100 mM OG in (a) or 100 mM MEGA 9 in (b), pH 10.0; capillary, untreated fused silica, 64.0 cm (total length) \times 50 μ m I.D., 56.0 cm to detection point; voltage, 15 kV. Analytes: 1, acetophenone; 2, propiophenone; 3, butyrophenone; 4, valerophenone; 5, hexanophenone; 6, heptanophenone; t_{mc} , anthracene.

group selectivity for the two surfactants having disaccharide head groups, i.e., OS and OM, are very similar. Both OG and MEGA 9 yielded higher methylene group selectivities, with OG being the highest. On the other hand, there is a significant difference between OS and OM in the magnitude of their specific interactions (i.e., log β values), whereas the specific interactions ex-

hibited by OG and MEGA 9 are similar. OS showed the lowest specific interactions (i.e., the highest negative value for log β) followed by OG and MEGA 9, while OM exhibited the highest specific interactions (i.e., the lowest negative value for log β) with the APK series. These retention behaviors reflect the fact that OM is more retentive towards the smallest

Table 3
Comparison of capacity factors obtained with the various micellar phases

Micellar phase	k'					
	$n_c = 1$	$n_c = 2$	$n_c = 3$	$n_c = 4$	$n_c = 5$	$n_c = 6$
OS	0.37	0.70	1.44	3.17	7.94	15.6
MEGA 9	0.52	1.08	2.37	5.67	14.1	30.4
OM	0.67	1.37	2.90	6.47	14.1	29.7
OG	0.51	1.14	2.69	6.65	16.1	37.2

Conditions as in Table 2. Analytes: $n_c = 1$, acetophenone; $n_c = 2$, propiophenone; $n_c = 3$, butyrophenone; $n_c = 4$, valerophenone; $n_c = 5$, hexanophenone; $n_c = 6$, heptanophenone.

Table 4
Correlation between $\log k'$ and n_c of APK homologous series for various micellar phases

Micellar phase	$\log \beta$	$\log \alpha$	R
OS	-0.805	0.333	0.999
OM	-0.517	0.332	1.000
OG	-0.681	0.375	1.000
MEGA 9	-0.673	0.359	0.999

Conditions as in Table 2.

solutes in the homologous series (i.e., $n_c = 1$ to 3) where the specific interactions are predominant, and OG exhibits the highest retention toward the solutes with $n_c = 4$ to 6 where the effect of the hydrophobic chain of the solute becomes increasingly more significant.

To gain further insight into the retention behavior of the various micellar phases, the retention energetics of these phases were compared by plotting $\log k'$ of the APK homologous series obtained with a given micellar phase versus the $\log k'$ of the same solutes obtained with a reference micellar phase. Usually, such plots yield straight lines for homologous solutes. If the slope is unity, the differences in Gibbs retention energies of the two micellar phases is zero for all solutes and the retention is termed *homeoenergetic* [25]. In this case, the intercept of the line is equal to the logarithm of the quotient of the phase ratios of the two micellar phases. The quotient of the phase ratios can then be obtained from the antilog of the intercept. If the slope is not unity, then the Gibbs retention energies are proportional by a constant that is equivalent to the slope, and the retention is

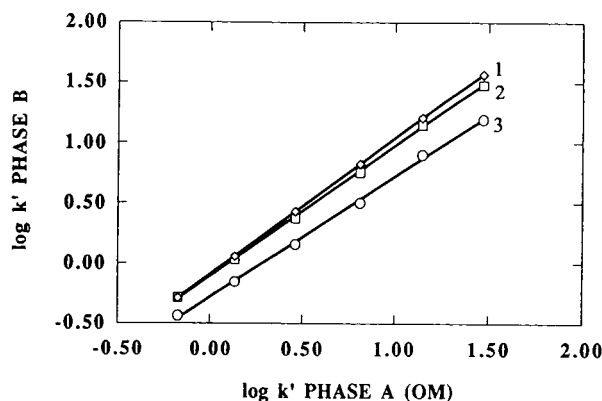


Fig. 3. Plots of $\log k' - \log k'$ of APK homologous series obtained on one micellar phase versus another reference micellar phase at constant micellized surfactant concentration. Lines: 1, OG micellar phase versus OM micellar phase; 2, MEGA 9 micellar phase versus OM micellar phase; 3, OS micellar phase versus OM micellar phase. Experimental conditions: running electrolytes, 200 mM borate containing 100 mM surfactant, pH 10.0; other conditions as in Fig. 2.

termed *homeoenergetic* [25]. We have previously reported this approach in the characterization of numerous micellar systems [12–14, 24]. Fig. 3 shows plots of $\log k'$ for micellar phase B versus $\log k'$ of a reference micellar phase A for the APK homologous series. In these plots, the OM–borate system was chosen as the reference micellar phase, i.e., micellar phase A. The six data points for each line in Fig. 3 are the $\log k'$ obtained with the six APK solutes. The slopes, intercepts, and antilog of the intercepts of the $\log k' - \log k'$ of these plots are listed in Table 5. The R values from the linear regression were all 0.999 or greater. The slope of $\log k' - \log k'$ plot for OS versus OM was close to unity, thus

Table 5
Slopes, intercepts and antilog of intercepts of $\log k' - \log k'$ plots for APK homologous series obtained with different micellar phases

Phase A / phase B	Slope	Intercept	R	φ_B/φ_A
OS / OM	1.005	-0.286	0.999	0.52
MEGA 9 / OM	1.084	-0.112	1.000	0.77
OG / OM	1.132	-0.095	1.000	0.80
OM / OM	1.000	0.000	1.000	1.00

Conditions as in Table 2.

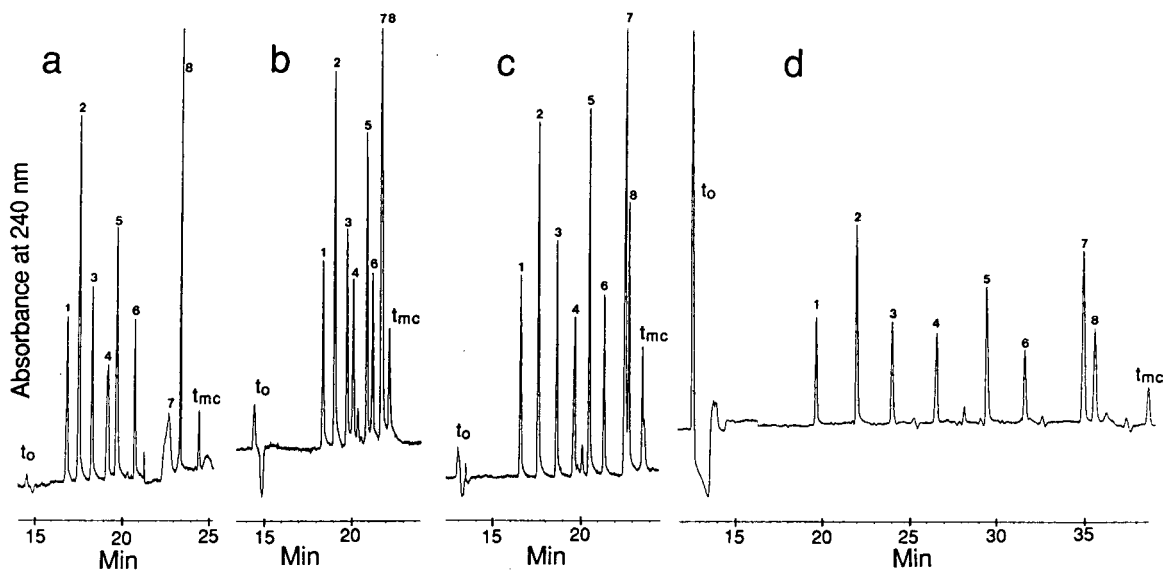


Fig. 4. Electropherograms of urea herbicides obtained with each of the various micellar phases. Experimental conditions: running electrolytes, 200 mM borate containing 100 mM OS in (a) or 100 mM OM (b) or 100 mM OG (c) or 100 mM MEGA 9 in (d), pH 10.0. Other conditions as in Fig. 2. Solutes: 1, monuron; 2, fluometuron; 3, metobromuron; 4, siduron; 5, diuron; 6, linuron; 7, neburon; 8, chloroxuron; t_{mc} , anthracene.

indicating homoenergetic retention behavior between the two micellar phases, and is consistent with previously reported data [14]. The $\log k' - \log k'$ plots for MEGA 9/OM and OG/OM have slopes near unity indicating quasi-homoenergetic behaviors between these surfactants. The net influence of the nature of the surfactant (i.e., different hydrophilic sugar head groups and hydrocarbonaceous moieties) is realized by examining the quotient of the phase ratios, φ_B/φ_A . The phase ratio of the OM micellar phase is double that of the OS micellar phase. The phase ratios of MEGA 9 and OG micellar phases are 77% and 80%, respectively, of that obtained on the OM micellar phase.

This method of data treatment has proven to be very useful in the characterization of new micellar phases. The in situ micellar phases we have introduced differ significantly in hydrophobic character. These different characteristics are of great value when selecting a micellar system to perform a given separation. The differences in hydrophobic character allow each micelle to have slightly different selectivities as will be discussed in the following section.

3.4. Selectivity

Fig. 4 illustrates the separation of a mixture of eight closely related urea herbicides obtained on each of the four micellar phases. The structures of the herbicides are listed below.

	R ₁	R ₂	R ₃	R ₄
(1) Monuron	Cl	H	CH ₃	CH ₃
(2) Fluometuron	H	CF ₃	CH ₃	CH ₃
(3) Metobromuron	Br	H	CH ₃	OCH ₃
(4) Siduron	H	H	H	*
(5) Diuron	Cl	Cl	CH ₃	CH ₃
(6) Linuron	Cl	Cl	CH ₃	OCH ₃
(7) Neburon	Cl	Cl	CH ₃	C ₄ H ₉
(8) Chloroxuron	**	H	CH ₃	CH ₃

* 2-methylcyclohexyl
** 4-chlorophenoxy

The average plate counts were 297 360, 329 840, 388 080 and 283 920 for OS, OM, OG and MEGA 9 micellar phases, respectively. The distorted peak shape of neburon obtained with the OS micellar phase (Fig. 4a) may be due to the presence of an impurity.

To examine the influence of the nature of the

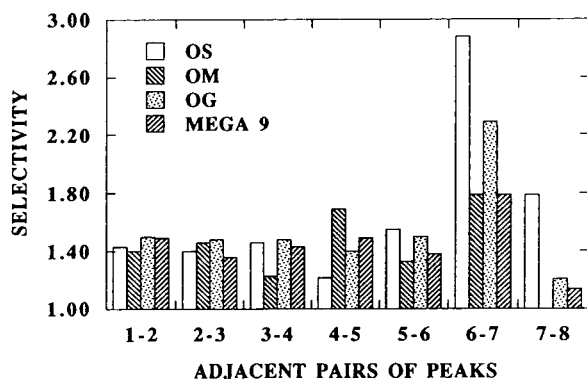


Fig. 5. Bar graphs of the selectivity factor for the urea herbicides with each micellar phase. Experimental conditions as in Fig. 4.

surfactant on the separation of these urea herbicides, the selectivity, $\alpha = k_2'/k_1'$, between adjacent peaks was calculated. Fig. 5 shows bar graphs for the selectivity between each adjacent pair of urea herbicides obtained on each of the four micellar phases. The only case an adjacent pair of peaks is not resolved is with the OM micellar phase where the last two herbicides, neburon and chloroxuron, co-elute. This is attributed to the increased hydrophobic character of OM when compared to the other micellar phases. The selectivities of the first five adjacent pairs are very similar, but with the last two

adjacent pairs OS provides notably higher selectivity. This is due to the weaker hydrophobic character of OS when compared to the other three surfactants.

To illustrate further the influence of the nature of the surfactant, a mixture of neutral and acidic herbicides was analyzed. This mixture contained three s-triazine herbicides (i.e., prometon, propazine and prometryne), three chlorinated phenoxy acid herbicides (i.e., silvex, 2,4,5-T and 2,4-D), one organophosphorous pesticide (i.e., parathion) and one sulfur-carbamate herbicide (i.e., aldicarb). The structures of these herbicides are shown below.

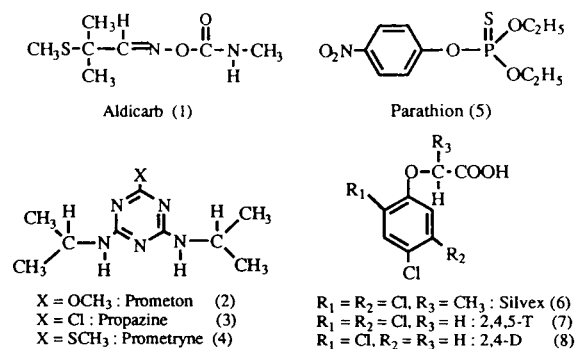


Fig. 6 shows typical electropherograms obtained with 200 mM borate and 100 mM of

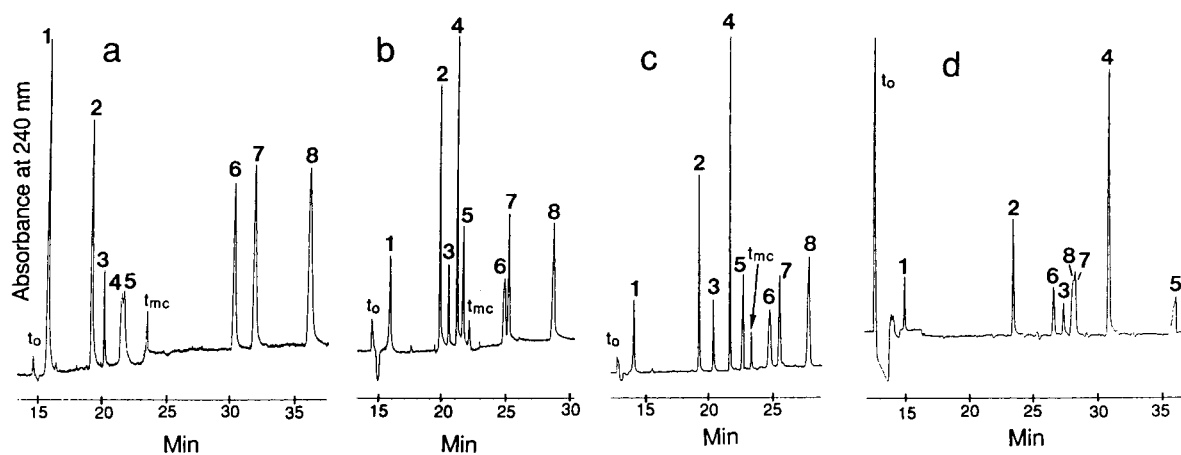


Fig. 6. Electropherograms of neutral and acidic herbicides obtained with each of the various micellar phases. Experimental conditions: running electrolytes, 200 mM borate containing 100 mM OS in (a) or 100 mM OM (b) or 100 mM OG (c) or 100 mM MEGA 9 in (d), pH 10.0. Other condition as in Fig. 2. Solutes: 1, aldicarb; 2, prometon; 3, propazine; 4, prometryne; 5, parathion; 6, silvex; 7, 2,4,5-T; 8, 2,4-D; t_{mc} , anthracene.

surfactant at pH 10.0. At this pH, the acidic herbicides are fully ionized and are migrating primarily by their own electrophoretic mobility. These acidic herbicides elute after t_{mc} with OS, OM and OG micellar phases, but elute within the migration time window with the MEGA 9 micellar phase. In this aspect, the narrower migration time window is advantageous since the neutral components are removed from the acidic components. The average theoretical plates were 176 400 for OS, 257 040 for OM, 283 920 for OG and 222 880 for MEGA 9. The lower average separation efficiencies arise from the much lower plate counts observed with the acidic species. This is because the acidic herbicides are not significantly partitioned in the micelle, a condition that leads to increased longitudinal diffusion.

Fig. 7 shows plots of the selectivities between each adjacent pair of peaks for neutral herbicides (i.e., aldicarb, prometon, propazine, prometryne and parathion) for the various micellar phases. The selectivity for pairs 2-3 and 3-4 are very similar for all the micellar phases. The selectivity of the first adjacent pair, 1-2, is the highest with OM and OG micellar phases, whereas the selectivity for the last adjacent pair, 3-4, is greatest with OG and MEGA 9 micellar phases. For this mixture of herbicides, the OG micellar phase yielded the best separation in terms of resolution and separation efficiency.

As a final illustration of the different selec-

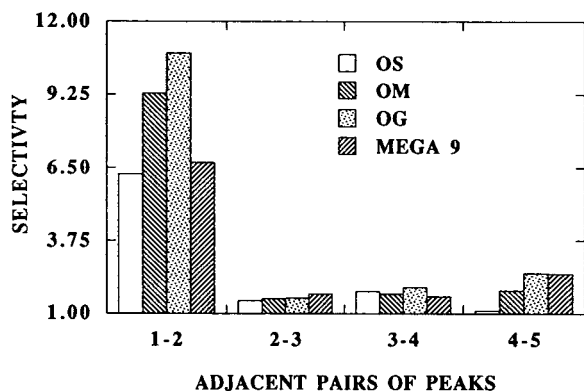


Fig. 7. Bar graphs of the selectivity factor for neutral herbicides with each micellar phase. Experimental conditions as in Fig. 6.

tivities obtained with the different micellar phases, a mixture of hydrophobic aromatic compounds containing one, two or three fused rings was electrochromatographed, see Fig. 8. The OS micellar phase provides better separation than OM or OG micellar phases, but still the most hydrophobic species are only partially resolved. The wider migration time window of the MEGA 9 micellar phase allowed the best separation of the aromatic species, but at the cost of longer analysis time. The average plate counts were 233 520, 248 080, 287 280 and 246 400 for OS, OM, OG, and MEGA 9 micellar phases, respectively.

4. Conclusions

In situ charged micellar phases have proven very effective in the separation of both neutral and acidic species. These micellar phases offer an adjustable migration time window that is largely influenced by the nature of the hydrophilic sugar head group of the individual surfactants. The acyclic sugar head group present in the MEGA 9 micellar phase provides the widest migration time window due its increased affinity to borate. Retention energetic studies show that OM micellar phase possesses the greatest hydrophobic character followed by OG and MEGA 9 micellar phases. Having one fewer carbon atom in its alkyl tail and possessing a disaccharide head group, the OS micellar phase displayed the least hydrophobic character making it most suitable for MECC of very hydrophobic species. In all cases, separation efficiencies ranged from 170 000 to 400 000 theoretical plates.

Acknowledgements

This material is based upon work supported by the Cooperative State Research Service, U.S. Department of Agriculture, under Agreement No. 92-34214-7325. JTS is the recipient of a Water Resources Presidential Fellowship from the University Center for Water Research at Oklahoma State University. The loan of the

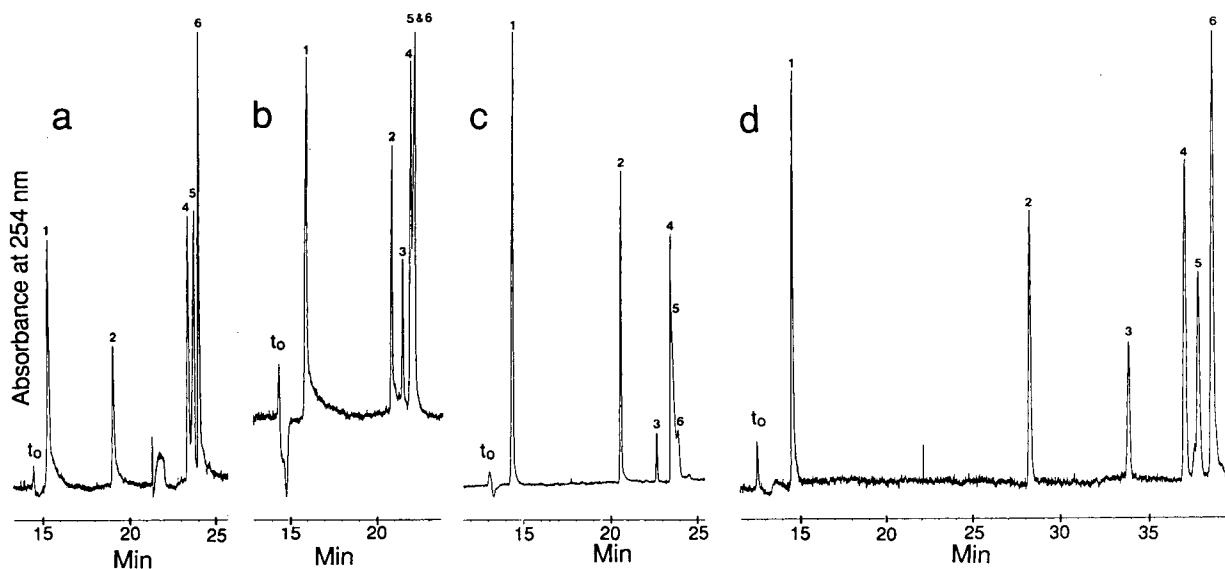


Fig. 8. Electropherograms of aromatic species obtained with each of the various micellar phases. Experimental conditions: running electrolytes, 200 mM borate containing 100 mM OS in (a) or 100 mM OM (b) or 100 mM OG (c) or 100 mM MEGA 9 in (d), pH 10.0. Other condition as in Fig. 2. Solutes: 1, aniline; 2, 1-naphthylamine; 3, naphthalene; 4, biphenyl; 5, 1-chloronaphthalene; 6, anthracene.

capillary electrophoresis instrument from Hewlett Packard is greatly appreciated.

References

- [1] B.L. Karger, *Am. Lab.*, October (1993) 23.
- [2] S.F.Y. Li, *Capillary Electrophoresis: principles, practice, and applications*, Elsevier, Amsterdam, 1992.
- [3] S. Terabe, K. Otsuka, K. Ichikama, A. Tsuchiya and T. Ando, *Anal. Chem.*, 56 (1984) 111.
- [4] A.S. Cohen, S. Terabe, J.A. Smith and B.L. Karger, *Anal. Chem.*, 59 (1987) 1021.
- [5] S. Terabe, K. Otsuka and T. Ando, *Anal. Chem.*, 57 (1985) 834.
- [6] K. Otsuka, S. Terabe and T. Ando, *J. Chromatogr.*, 332 (1985) 219.
- [7] D. Burton, M.J. Sepaniak and M. Maskarinec, *J. Chromatogr. Sci.*, 24 (1986) 347.
- [8] M.M. Bushey and J.W. Jorgenson, *J. Microcol. Sep.*, 1 (1989) 125.
- [9] S. Terabe, *Trends Anal. Chem.*, 8 (1989) 129.
- [10] G.M. Janini and H.J. Issaq, *J. Liq. Chromatogr.*, 15 (1992) 927.
- [11] J. Cai and Z. El Rassi, *J. Chromatogr.*, 608 (1992) 31.
- [12] J.T. Smith and Z. El Rassi, *Electrophoresis*, (1994) in press.
- [13] J.T. Smith, W. Nashabeh and Z. El Rassi, *Anal. Chem.*, 66 (1994) 1119.
- [14] J.T. Smith and Z. El Rassi, *J. Microcol. Sep.*, 6 (1994) 127.
- [15] A.B. Foster and M. Stacey, *J. Chem. Soc.*, (1955) 1778.
- [16] A.B. Foster, *Adv. Carbohydr. Chem.*, 12 (1957) 81.
- [17] J. Böeseken, *Adv. Carbohydr. Chem.*, 4 (1949) 189.
- [18] R. Pizer and C. Tihal, *Inorg. Chem.*, 31 (1992) 3243.
- [19] J. Neugebauer, *A Guide to the Properties and Uses of Detergents in Biology and Biochemistry*, Calbiochem-Novabiochem Corp., San Diego, 1994.
- [20] M. Makkee, A.P.G. Kieboom and H. van Bekkum, *Recl. Trav. Chim. Pays-Bas*, 104 (1985) 230.
- [21] T. Kaneta, S. Tanaka, T. Mitsuhiko and H. Yoshida, *J. Chromatogr.*, 609 (1992) 369.
- [22] S. Terabe, K. Otsuka and T. Ando, *Anal. Chem.*, 61 (1989) 251.
- [23] J.M. Davis, *Anal. Chem.*, 61 (1989) 2455.
- [24] D. Crosby and Z. El Rassi, *J. Liq. Chromatogr.*, 16 (1993) 2161.
- [25] Z. El Rassi and Cs. Horváth, *Chromatographia*, 19 (1984) 9.



ELSEVIER

Journal of Chromatography A, 685 (1994) 145–153

JOURNAL OF
CHROMATOGRAPHY A

Capillary zone electrophoresis with indirect UV detection of organic anions using 2,6-naphthalenedicarboxylic acid

Ewa Dabek-Zlotorzynska*, Joseph F. Dlouhy

Chemistry Division, Environmental Technology Centre, Environment Canada, 3439 River Road, Ottawa, Ontario K1A 0H3, Canada

First received 27 December 1993; revised manuscript received 13 June 1994

Abstract

2,6-Naphthalenedicarboxylic acid (NDC) was characterized as a carrier electrolyte for a separation of organic anions by capillary zone electrophoresis (CZE) with indirect UV detection. Parameters which influence CZE separations such as concentration of NDC, electrolyte pH and various electroosmotic flow modifiers were investigated. The sensitivity obtained with the NDC electrolyte was five times higher than with phthalate, which is commonly used for the separation of organic anions. This method was applied to the determination of organic anions in the ambient air.

1. Introduction

The analysis of inorganic and organic anions using capillary zone electrophoresis (CZE) with indirect detection continues to be of interest [1–16]. Most published work is based on the indirect absorption detection, because UV–visible absorption detectors are still the most popular due to their versatility and simplicity, and because they are supplied with every commercial CE system [17]. This method of detection has long been used in single-column ion chromatography [18].

Many investigations have been undertaken to achieve high-sensitivity detection by the selection of appropriate electrolyte composition for indirect absorption CZE [1,3–6,9,15,16]. The optimization of CZE with indirect UV detection consists of selection of a carrier electrolyte with

large molar absorptivity and effective mobility similar to that of the sample ions [1]. The correlation between peak response and carrier electrolyte molar absorptivity in capillary electrophoresis has been documented by Jandik and Jones [4]. Choice of electrolyte components must be carefully considered, because mis-matched ionic mobilities of the carrier electrolytes and sample ions produce peak fronting or tailing [1,3]. Various chromophore-containing electrolytes based on chromate, pyromellitate, benzoate, phthalate and other aromatic carboxylic acid salts have been characterized for the analysis of inorganic and organic anions by CZE in many real samples [3–15].

The characterization of 2,6-naphthalenedicarboxylic acid (NDC) as a promising carrier ion for separation of less mobile anions by CZE with indirect UV detection is reported in this paper. NDC absorbs strongly in the UV region and is suitable as an electrolyte as well, because its

* Corresponding author.

electrophoretic mobility when fully ionized closely matches many organic anions.

Application of the NDC-based electrolyte is demonstrated on organic anion analysis in the ambient air.

2. Experimental

2.1. Instrumentation

Measurements were carried out on a P/ACE 2100 capillary electrophoresis instrument (Beckman Instruments, Fullerton, CA, USA), equipped with a UV detector (filters for 200, 214, 254 and 280 nm), an autosampler and a temperature-controlled fluid-cooled capillary cartridge. An IBM computer (PS2/70) and Gold software v. 7.11 (Beckman Instruments) were used for instrument control and for data collection and processing. A 57.0 cm long (50.0 cm to the detector cell) \times 75 μ m I.D. fused-silica capillary (Beckman Instruments) was used. The temperature of a capillary was kept at $25 \pm 0.1^\circ\text{C}$. The applied voltage was 20 kV using the negative power supply and all injections were achieved by applying 0.5 p.s.i. (1 p.s.i. = 6894.76 Pa) pressure for 10 s, unless otherwise noted.

Glass vials (5 ml) and 100- μ l polyolefin microvials were used for electrolytes and samples, respectively. All vials were rinsed with deionized water and dried prior to use.

A Beckman pH meter with a combination electrode was used to measure the pH of electrolytes.

Molar absorptivities of aqueous 2,6-naphthalenedicarboxylate (sodium form) and potassium hydrogenphthalate solutions were determined using a CARY I UV-Vis spectrophotometer (Varian Australia, Springvale, Australia) with 1-cm path quartz cells.

2.2. Reagents

All chemicals were obtained from either Aldrich (Milwaukee, WI, USA) or Fisher Scientific (Ottawa, Canada) at the highest purity available, and were used without additional purification.

All solutions, electrolytes and standards were prepared using deionized water (18 M Ω cm resistance) obtained by treating the tap water using reverse osmosis and ion exchange (Millipore, Model RO 20 and Model SuperQ).

2.3. Electrolytes and procedures

All NDC-based electrolytes were prepared each day from the stock solution which contained 20 mM NDC and 50 mM NaOH, and from 10 mM solution of tetradecyltrimethylammonium bromide (TTAB) as an electroosmotic flow (EOF) modifier. Other EOF modifiers such as tetrabutylammonium hydroxide (TBAOH), dodecyltrimethylammonium bromide (DTAB) and cetyltrimethylammonium bromide (CTAB) were also tested in this study. The pH was then adjusted with NaOH or sulphuric acid as required.

The phthalate electrolyte used in this study contained 5 mM potassium hydrogenphthalate, 2.0 mM boric acid and 0.5 mM TTAB.

In order to compare mobility of NDC with respect to phthalate, both carrier electrolyte anions were injected into a 5 mM borate buffer with 0.5 mM TTAB at pH 8, and migration time of NDC relative to phthalate was measured by direct UV detection at 254 nm.

All electrolyte solutions were filtered through a 0.22- μ m syringe PTFE membrane filter (Nalgene Brand Products, Rochester, NY, USA) and degassed by creating vacuum inside the syringe.

Separations were carried out using a method that consisted of a 1 min rinse of capillary with used electrolyte immediately prior to injection. At the beginning of each experimental day, the capillary was pretreated with 0.1 M NaOH for 10 min, then rinsed with deionized water (5 min) and with the used electrolyte (2 min).

2.4. Quantitation procedure

The mixed anion stock solution was diluted to produce working standard solutions at four different concentrations within the range 0.2–10 μ g/ml. Calibration graphs were plotted based on

the linear regression analysis of the corrected peak area.

Identification of individual ions in extracts of ambient air was based on the comparison of migration times of analytes with those of standard solutions. Also, all migration times were normalized to that of carbonate or bromide in order to obtain reproducible results. Bromide was added to the CE electrolyte as TTAB (EOF modifier) and acted as a negative reference peak. Some samples were spiked with standard solution. Ion chromatography with different selectivity than CE was also used for identification of some ions.

Detection limits were defined as three times the standard deviation of 18 replicate analyses of a standard with concentration equal to about ten times the estimated detection limit, the latter being the concentration giving a signal-to-noise ratio of 3.

2.5. Ambient air extracts

Ambient air constituents (particles, liquids and gases) were sampled by using the annular denuder/filter pack system [19,20].

The gaseous inorganic and organic acids, either collected during sampling or formed by oxidation on the carbonate coated denuders were extracted with 10 ml of deionized water and analyzed by ion chromatography [20].

IC-H Solid-phase extraction (SPE) disks (Alltech, Deerfield, IL, USA) were used to reduce of amount of carbonate presented in the extract for CZE analysis. Before applying sample, the disk was pre-conditioned by passing 10-ml of deionized water. Then the sample (approximately 3 ml) was passed through the disk at a flow-rate of less than 1 ml/min. The first 1 ml of the eluate was discarded and the remaining eluate was collected for analysis [21].

3. Results and discussion

The UV absorption spectrum of the NDC solution from 220 to 350 nm shows an absorption maximum at 235 nm and 284 nm with a large

molar absorptivity at 284 nm ($\epsilon = 11\,000\text{ l mol}^{-1}\text{ cm}^{-1}$). Because of the availability of a 280-nm filter in the used CE instrument, 280 nm was chosen as a representative detection wavelength throughout this work. NDC has a molar absorptivity higher by a factor of about 8 than phthalate (NDC: $\epsilon = 7667\text{ l mol}^{-1}\text{ cm}^{-1}$ and $10\,020\text{ l mol}^{-1}\text{ cm}^{-1}$ at 254 nm and 280 nm, respectively; phthalate: $\epsilon = 1350\text{ l mol}^{-1}\text{ cm}^{-1}$ and $600\text{ l mol}^{-1}\text{ cm}^{-1}$ at 254 nm and 280 nm, respectively). Lower detection limits can be therefore achieved. The strong UV absorbance of NDC at 280 nm allows also to detect anions with absorption in the wavelength range up to 250 nm with reasonable sensitivity by the indirect detection (i.e. phthalate and benzoate). As expected, the mobility of NDC is slightly lower than the mobility of phthalate. The relative migration time of NDC with respect to phthalate obtained at pH 8 and with direct detection at 254 nm was 1.07 and indicates its suitability as an electrolyte for separation of organic anions. NDC has also little adsorptive interaction with the column walls, as indicated by its very sharp elution peak in the direct mode. Hence, this compound is suitable for indirect detection.

3.1. Optimization of separation

The effects of various parameters such as concentration of NDC, electrolyte pH and various EOF modifiers were investigated to determine the optimum conditions of CZE separation. A standard solution of anions of interest at concentration $4\text{ }\mu\text{g/ml}$ was used in this study.

The optimization of the carrier ion concentration and ionic strength of electrolyte is very crucial in CZE with indirect UV detection [5,9]. Low concentration of carrier ion results in a better signal-to-noise ratio [18], but the overloading of system occurs due to the decrease of sample ion to carrier ion concentration ratio. The linear dynamic range decreases also. As the electrolyte concentration increases and consequently electrolyte conductivity rises, baseline noise due to additional Joule heating increases as well. This effect is much more significant with the indirect UV-detection electrolyte system than

with high UV-transparent electrolytes [22]. In this study, the increase of electrolyte concentration (NDC and sodium hydroxide) caused a rise of the current from $5.9 \mu\text{A}$ at 1 mM NDC (2.5 mM NaOH) to $36.2 \mu\text{A}$ at 8 mM NDC (20 mM NaOH) at 20 kV voltage. The optimum NDC concentration was found to be 2 mM which is the best compromise between peak separation, sensitivity and acceptable baseline noise level.

To investigate the influence of pH on the separation, measurements were made for the tested anions in 2 mM NDC-based electrolyte. The pH was varied in the range 6.1 to 11. A precipitate was formed in electrolytes below pH 6. There is no significant pH dependence for most of the tested anions. A decrease in migration time is observed for hydrogencarbonate (Fig. 1). The reason for this behaviour is the full deprotonation at pH 11. The increase of charge of one unit leads to a higher electrophoretic mobility, and the migration time decreases. The carbonate often present in the natural samples may complicate the separation of methanesulphonate or other anions less mobile than carbonate (Fig. 2A). Poor resolution of methanesulphonate and hydrogencarbonate ions at pH 8 can be improved by using the electrolyte at pH 11 (Fig. 2B).

Various EOF modifiers such as TBAOH, DTAB, TTAB [23] and CTAB [24] were tested. These compounds are electrostatically attracted to the silanol groups on the inner wall of the capillary, resulting in shielding the negative charge of the silica and thus directly influences the direction and magnitude of EOF [23]. The more hydrophobic was the EOF modifier, the shorter migration times were obtained due to more effective change of the silica–water interface structure resulting in a better suppression or reversal of EOF. No significant difference in the analysis speed with the long alkyl group modifiers such as TTAB and CTAB was observed. In this study TTAB was selected as the EOF modifier to obtain separation of anions within 5 min without diminishing the resolution between the peaks. A plateau of TTAB amount adsorbed on the silica surface is reached at 0.5 mM concentration, which results in negligible change in the magnitude of the reversed EOF.

On the basis of the results reported above, the electrolyte containing the 2 mM NDC, 5 mM NaOH and 0.5 mM TTAB at pH 8 or 11 was used for separation of organic anions. Fig. 3 shows a separation of selected mono- and dicarboxylic acid anions at pH 11. The order of separation is the expected one, because migra-

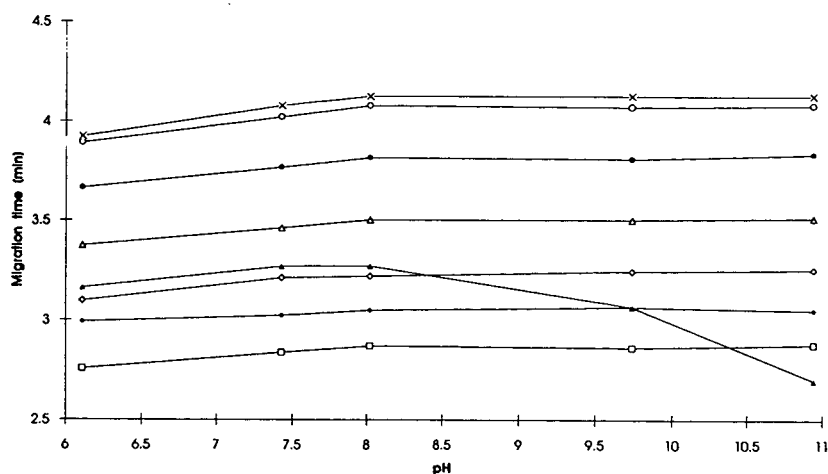


Fig. 1. Effect of the pH of the NDC electrolyte on the migration time of a $4 \mu\text{g/ml}$ anion standard mixture. □ = Formate; ◆ = phthalate; ◇ = methanesulphonate; ▲ = hydrogencarbonate; △ = acetate; ● = propionate; ○ = butyrate; × = benzoate. Electrolyte: 2 mM NDC, 5 mM NaOH, 0.5 mM TTAB. See Experimental section for more details.

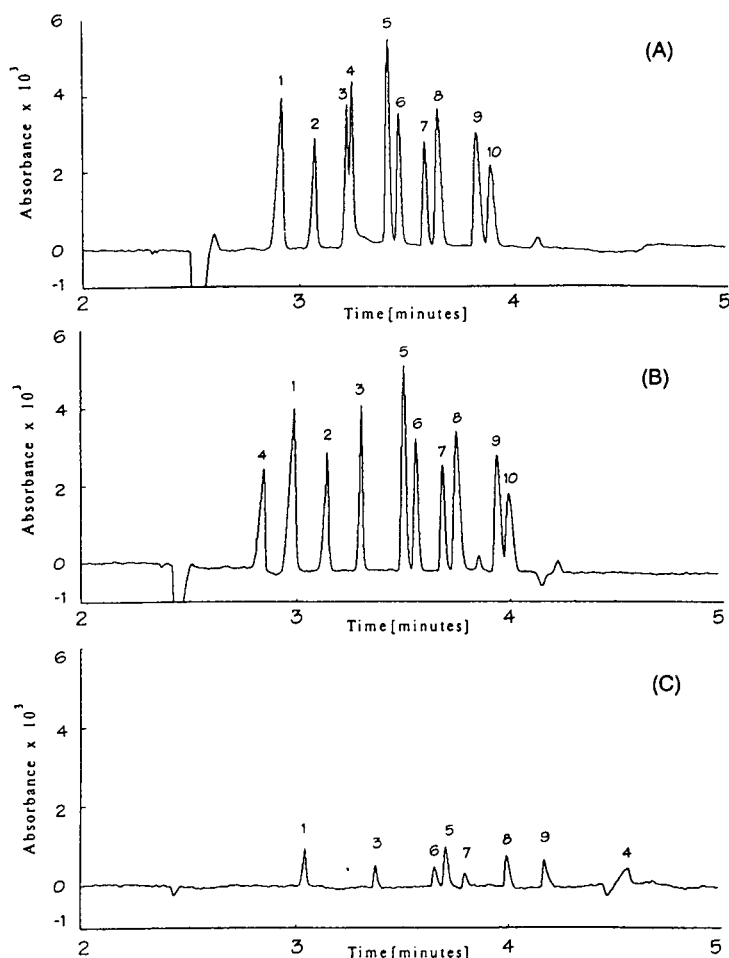


Fig. 2. Electropherograms of a 4 $\mu\text{g/ml}$ anion standard mixture obtained with the NDC electrolyte at pH 8 (A) and pH 11 (B), and with the phthalate electrolyte at pH 5.9 (C). Peaks: 1 = formate; 2 = phthalate; 3 = methanesulphonate; 4 = hydrogencarbonate or carbonate; 5 = acetate; 6 = chloroacetate; 7 = dichloroacetate; 8 = propionate; 9 = butyrate; 10 = benzoate. See Experimental section for more details.

tion time inversely relates to the equivalent conductance [5]. Another example of the capability of the NDC-based electrolyte as a powerful electrolyte is the separation of linear alkylsulfonates (Fig. 4).

3.2. Analytical performance

The precision of migration time and sample size are very important to obtain precise results in a quantitative analysis using CZE. With the electrolyte and instrument conditions estab-

lished, 18 injections of anion standard mixture at a concentration of 4 $\mu\text{g/ml}$ were made. The relative standard deviations (R.S.D.s) of migration times for the tested anions, shown in Table 1, were less than 0.5%, while the R.S.D.s of peak areas were less than 5%.

Quantitative determination using a pressure injection can be carried out on the basis of a linear relationship between peak area (or corrected peak area) and sample concentration over two orders of magnitude. Calibration graphs constructed for a mixed standard showed the

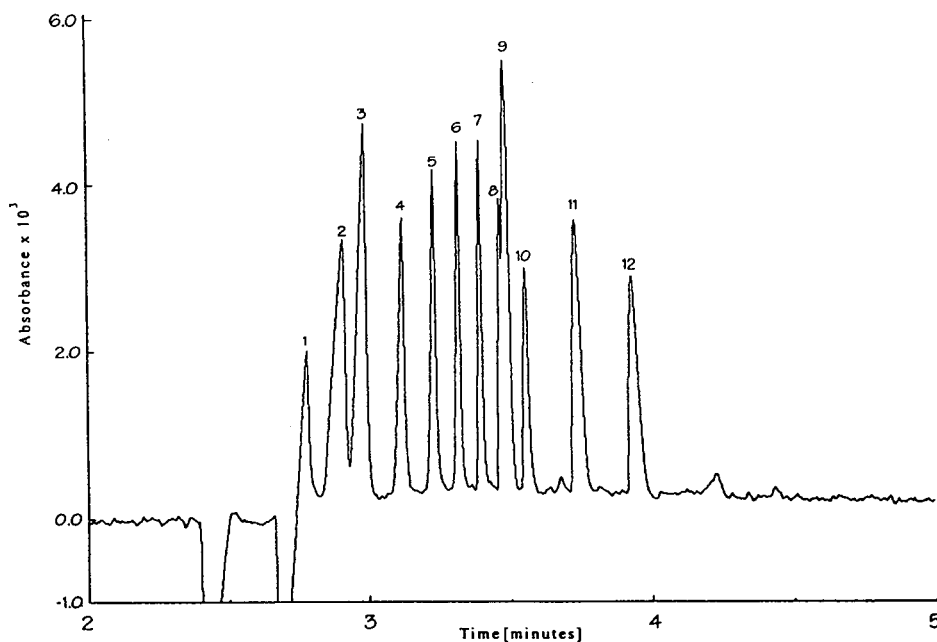


Fig. 3. Electropherogram of a 4 $\mu\text{g/ml}$ mono- and dicarboxylic anion standard mixture obtained with the NDC electrolyte at pH 11. Peaks: 1 = carbonate; 2 = fumarate; 3 = formate; 4 = glutarate; 5 = adipate; 6 = pimelate; 7 = suberate; 8 = azelate; 9 = acetate; 10 = sebacate; 11 = propionate; 12 = butyrate. See Experimental section for more details.

linear range extended from the detection limit to at least 20 $\mu\text{g/ml}$ with correlation coefficients ranging from 0.9989 to 0.9999 for all tested anions (Table 1). It should be mentioned that,

although the quantitation is possible at high sample concentration, the peak becomes broad and the resolving power is diminished. The NDC concentration should be increased when the

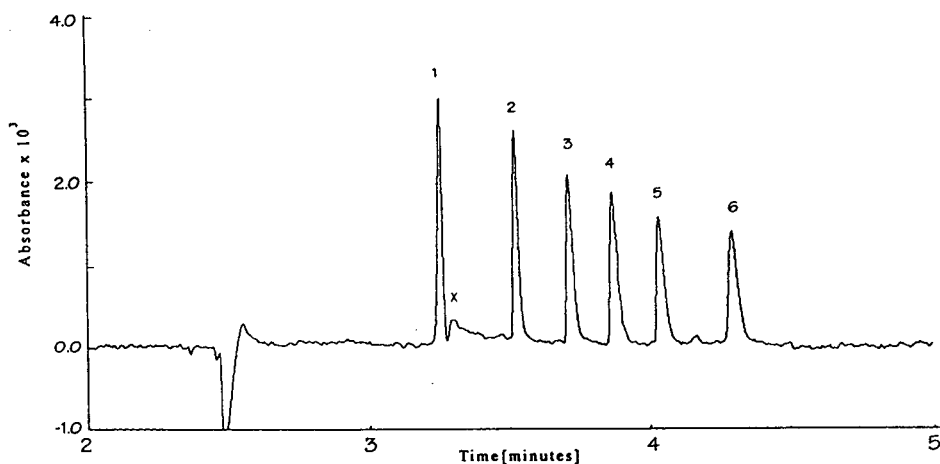


Fig. 4. Electropherogram of a 4 $\mu\text{g/ml}$ alkylsulphonate standard mixture obtained with the NDC electrolyte at pH 8. Peaks: 1 = methanesulphonate; 2 = ethanesulphonate; 3 = propanesulphonate; 4 = butanesulphonate; 5 = pentanesulphonate; 6 = hexanesulphonate; x = hydrogencarbonate. See Experimental section for more details.

Table 1
Selected parameters of CZE using NDC

	R.S.D. ^a (%)		Correlation coefficient	Sensitivity ratio (NDC:KHP) ^b	Detection limit (ng/ml)
	Migration time	Area			
Formate	0.32	4.43	0.9999	5.40	133
Phthalate	0.30	4.52	0.9998	–	168
Methanesulphonate	0.31	4.20	0.9990	5.60	143
Acetate	0.38	3.42	0.9998	4.15	102
Propionate	0.45	3.39	0.9999	4.73	102
Butyrate	0.48	3.94	0.9995	3.93	118
Benzoate	0.49	4.00	0.9989	–	159

^a Relative standard deviation of 18 replicates of anion standard mixture at concentration 4 µg/ml.

^b The ratio of sensitivities (slopes of calibration curves) obtained with the NDC- and the phthalate-based electrolytes (KHP = potassium hydrogenphthalate).

analyte concentration is high or the injection time should be decreased.

The sensitivity defined as the peak area (or corrected peak area) per unit concentration can be easily compared for each anion. The sensitivity obtained with the NDC electrolyte is about five times higher than with the phthalate electrolyte (Table 1 and Fig. 2).

The detection limits of analytes (for 10-s pressure injection) using the described method are presented in Table 1. The results indicate that the proposed method gave the same or better detection limits than ion-exclusion chromatography commonly used for the separation and the determination of carboxylic acids [25].

3.3. Application

The proposed method was demonstrated on the determination of organic anions in aqueous extracts of atmospheric aerosol collected on thin PTFE filters [15] and in the extracts of ambient air collected by using of carbonate/glycerol-coated denuders. The determination of organic acids, in addition to the other inorganic acid species more commonly measured, is of great importance for a better understanding of the nature of acidity of ambient air.

Fig. 5A shows a typical electropherogram of

an ambient air extract obtained with the NDC-based electrolyte at pH 11. However, the presence of an excessive level of carbonate (from carbonate/glycerol-coated denuders) overlaps the following peaks and causes the peak broadening. Dilution of sample or removal of the carbonate before the analysis was necessary. Fig. 5B and C represent the separation of the same extract with the NDC-based electrolytes at pH 8 and 11, after passing it through a IC-H SPE disk to reduce the amount of carbonate. Recoveries of a group of carboxylic acids (formic, acetic, propionic, butyric and benzoic acids) in the presence of 0.1% sodium carbonate after using the IC-H SPE disks were found to be greater than 97%, except for benzoic acid, where recovery was greater than 92%. This "clean up" of carbonate allows determination of formate and other anions. There are some unidentified peaks with lower mobility than propionate present when the NDC electrolyte at pH 11 was used (Fig. 5A and C). This indicates that the denuder extract contains analytes which dissociate at pH higher than 8. The identification of these peaks will be the subject of future research.

4. Conclusions

This study has shown that CZE with indirect

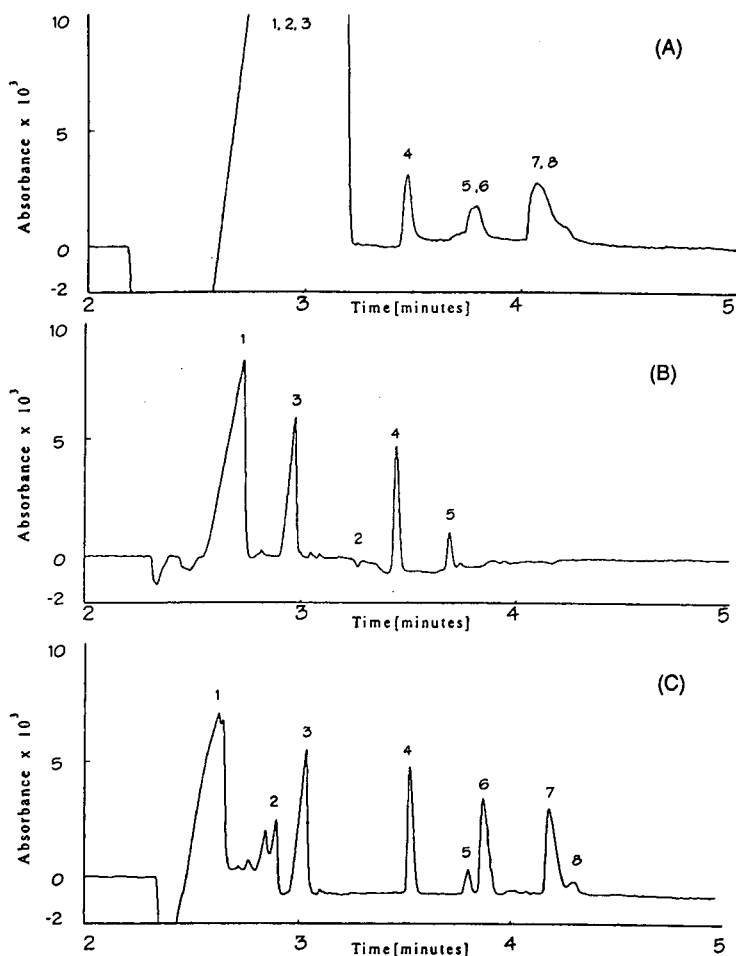


Fig. 5. Typical electropherograms of an ambient air extract collected by a carbonate/glycerol-coated annular denuder. (A) Untreated extract sample obtained with the NDC electrolyte at pH 11; (B, C) the same extract sample after treatment with IC-H SPE disk and obtained with the NDC electrolyte at pH 8 and 11, respectively. Peaks: 1 = unresolved inorganic anions; 2 = carbonate or hydrogencarbonate; 3 = formate; 4 = acetate; 5 = propionate; 6–8 = unidentified. See Experimental section for more details.

UV detection, employing NDC as the carrier electrolyte, is an effective method for the separation of organic anions.

The use of NDC as the carrier electrolyte has some advantages over other carriers such as phthalate: (i) UV absorption is at a longer wavelength (near 300 nm) and is very strong resulting in five times higher sensitivity; (ii) it allows for the detection of anions with absorption up to 250 nm by indirect detection; (iii) it

minimizes quantitation errors by reducing the interference from UV-absorbing substances, which might be present in real samples.

References

- [1] F. Foret, S. Fanali, L. Ossicini and P.J. Boček, *J. Chromatogr.*, 470 (1989) 299–308.
- [2] W.R. Jones and P. Jandik, *Am. Lab.*, 22, No. 9 (1990) 51–58.

- [3] J. Romano, P. Jandik, W.R. Jones and P. Jackson, *J. Chromatogr.*, 546 (1991) 411–421.
- [4] P. Jandik and W.R. Jones, *J. Chromatogr.*, 546 (1991) 431–443.
- [5] W.R. Jones and P. Jandik, *J. Chromatogr.*, 546 (1991) 445–458.
- [6] B.F. Kenney, *J. Chromatogr.*, 546 (1991) 423–430.
- [7] A. Nardi, M. Cristalli, C. Desiderio, L. Ossicini, S.K. Shukla and S. Fanali, *J. Microcol. Sep.*, 4 (1992) 9–11.
- [8] W. Jones, *J. Chromatogr.*, 640 (1993) 387–395.
- [9] M.P. Harold, M. Jo Wojtusik, J. Riviello and P. Henson, *J. Chromatogr.*, 640 (1993) 463–471.
- [10] P. Jandik and G. Bonn, *Capillary Electrophoresis of Small Molecules and Ions*, VCH, New York, 1993.
- [11] K.A. Hargadon and B.R. McCord, *J. Chromatogr.*, 602 (1992) 241–247.
- [12] D.L. Kelly and R.J. Nelson, *J. Liq. Chromatogr.*, 16 (1993) 2103–2112.
- [13] J.P. Romano and J. Krol, *J. Chromatogr.*, 640 (1993) 403–412.
- [14] J.B. Nair and C.G. Izzo, *J. Chromatogr.*, 640 (1993) 445–461.
- [15] E. Dabek-Zlotorzynska and J.F. Dlouhy, *J. Chromatogr. A*, 671 (1994) 389–395.
- [16] S.M. Cousins, P.R. Haddad and W. Buchberger, *J. Chromatogr. A*, 671 (1994) 397–402.
- [17] A.G. Ewing, R.A. Wallingford and T.M. Olefirowicz, *Anal. Chem.*, 61 (1989) 292A–303A.
- [18] H. Small and T.E. Miller, Jr., *Anal. Chem.*, 54 (1982) 462–469.
- [19] P. Koutrakis, J.M. Wolfson, J.L. Slater, M. Brauer, J.D. Spengler, R.K. Stevens and C.L. Stone, *Environ. Sci. Technol.*, 22 (1988) 1463–1468.
- [20] J.R. Brook, *Canadian Acid Aerosol Measurement Program, 1992–1993*, Atmospheric Environment Service, Toronto, 1993.
- [21] R. Saari-Nordhaus, L.M. Nair and J.M. Anderson, Jr., *J. Chromatogr. A*, 671 (1994) 159–163.
- [22] W. Beck and H. Engelhardt, *Fresenius' J. Anal. Chem.*, 346 (1993) 618–621.
- [23] X. Huang, J.A. Luckey, M.J. Gordon and R.Z. Zare, *Anal. Chem.*, 61 (1989) 766–770.
- [24] K. Altria and C. Simpson, *Anal. Proc.*, 23 (1986) 453–454.
- [25] V. Cheam, *Analyst*, 117 (1992) 1137–1144.

Practical aspects in chiral separation of pharmaceuticals by capillary electrophoresis

II. Quantitative separation of naproxen enantiomers[☆]

Andr s Guttman*, Nelson Cooke

Beckman Instruments, Inc., 2500 Harbor Boulevard, Fullerton, CA 92634, USA

First received 2 May 1994; revised manuscript received 5 July 1994

Abstract

In recent years, there has been considerable activity in the separation and characterization of optically active molecules. In this paper we report a new, improved and automated electrophoretic method for the separation of enantiomers in the form of high-performance capillary gel electrophoresis using hydroxypropyl- β -cyclodextrin as a chiral selector. Rapid, efficient separation of naproxen enantiomers is shown with very low detection limits and excellent detection linearity. The intra- and inter-day as well as intra- and inter-column migration time reproducibility was less than 2% R.S.D. Trace level enantiomeric contamination determination is also shown.

1. Introduction

Recently, there has been a great deal of interest in the separation and characterization of optically active compounds [1]. The problem is a challenging one since optical isomers possess identical physical characteristics and differ only slightly from another in their spatial orientation [2]. Conventionally, chiral separations were achieved by gas chromatography [3] and more recently by high-performance liquid chromatography [4]. The potential advantages of using capillary gel electrophoresis over HPLC are the higher peak efficiency attained that results in higher resolution with similar selectivities and

low buffer and chiral selector consumption [5]. It has been shown that inclusion complex equilibria using different native, α -cyclodextrin [6–9], β -cyclodextrin [6–12], γ -cyclodextrin [7,8,13,14], and chemically modified cyclodextrins such as dimethyl- β -cyclodextrin, trimethyl- β -cyclodextrin [8,13–17], hydroxypropyl- β -cyclodextrin (HP- β -CD) [18–20] as chiral selectors is very powerful in the separation of enantiomers. These natural and derivatized cyclodextrins were implemented as chiral selectors in different capillary electrophoresis (CE) separation modes such as capillary zone electrophoresis [6,13,15], micellar electrokinetic chromatography [21–23], isotachopheresis [14–17] and capillary gel electrophoresis (CGE) [7,24].

Early attempts of CGE separations employed cross-linked polyacrylamide gel filled capillaries with various native cyclodextrins (α , β and γ) that were physically entrapped into the small

* Corresponding author.

[☆] Presented at the 13th International Symposium on High-Performance Liquid Chromatography of Proteins, Peptides and Polynucleotides, San Francisco, CA, 30 November–3 December 1993.

pore size polymer matrix [7]. D and L forms of dansylated amino acids were easily separated within 10 min with these gels. The major disadvantage of cross-linked (chemical gels) compared to non-cross-linked linear polymer networks (physical gels) is that chemical gels are non-replaceable, therefore if the gel becomes contaminated or develops bubbles the gel-filled capillary must be replaced [25].

In this paper we report the use of a non-cross-linked, hydrophilic linear polymer network in conjunction with HP- β -CD for CGE of naproxen enantiomers. This polymer network is advantageous in that suppressing the ζ potential on the inside surface of the capillary substantially. Polymer networks containing chiral selectors are easily prepared and are easily replaceable in the capillary column, if necessary. Examples are shown with high resolutions under optimized separation conditions as well as the usefulness of this system in the demonstration of very low level (<1%) enantiomeric contamination determination.

2. Materials and methods

2.1. Apparatus

In all these studies, the P/ACE system 2100 CE apparatus (Beckman Instruments, Fullerton, CA, USA) was used in reversed-polarity mode (cathode on the injection side). The separations were monitored on-column at 230 nm. The temperature of the cartridge containing the polymer network-filled capillary column was thermostated at $20 \pm 0.1^\circ\text{C}$ by the liquid cooling system of the P/ACE instrument. The electropherograms were acquired and stored on an IBM 486/66 MHz computer and were evaluated with the System Gold software package (Beckman Instruments).

2.2. Procedures

In all the CE experiments a 20 cm effective length (27 cm total length) \times 375 μm O.D. \times 25 μm I.D. bare fused-silica capillary tubing was used. The use of low-viscosity polymer network

permitted replacement of the gel–buffer system in the capillary column by means of the pressure-rinse operation mode of the P/ACE apparatus (i.e., replaceable gel). It is important to note that the inside surface of the capillary column was deactivated by means of 1 M HCl rinse prior to each run in these experiments to decrease ζ potential of the inside capillary wall, thus causing further decrease in electroosmotic flow in the polymer network-filled capillary column. The samples were injected by pressure (typically: 3–20 s, 0.5 p.s.i. = 3447.4 Pa) into the replaceable gel-filled capillary column.

2.3. Chemicals

Ultrapure-grade 200 mM 2-(N-morpholino)ethanesulfonic acid (MES) buffer adjusted to pH 5.0 by tetrabutylammonium hydroxide (TBAH) was used in the experiments (ICN, Costa Mesa, CA, USA). The exact composition of all the buffers used during the pH optimization experiments (pH 3, 4, 5, 6, 7, 8 and 9) were described elsewhere [26]. The chiral selector, HP- β -CD with the average substitution rate of 4.9, was purchased from American Maise Products (Hammond, IN, USA). The racemate and S forms of Naproxen (Syntex, Palo Alto, CA, USA) were dissolved in deionized water containing 10^{-5} M TBAH, in 0.1 and 1 mg/ml concentrations, respectively. Prior to injection this mixture was diluted ten times by the running buffer, 200 mM MES/TBAH, 10 mM HP- β -CD, 0.4% polymeric additive, pH 5.0. The samples were stored at -20°C or freshly used. The internal standard of *p*-toluenesulfonic acid (pTSA) was purchased from Sigma (St. Louis, MO, USA). All buffer and gel solutions were filtered through a 0.45- μm pore size filter (Schleicher and Schuell, Keene, NH, USA) and carefully vacuum degassed before use.

3. Results and discussion

3.1. Separation optimization

CGE with chiral selectors has proven to be a powerful tool for the separation and purity

assessment of optically active molecules [7,24]. As we have shown earlier [26] in accordance to the theory of Vigh and co-workers [27,28], chiral separation method development should follow the following scheme: (1) optimization of the separation pH, (2) optimization of the chiral selector concentration, (3) optimization of the applied electric field strength and (4) optimization of the separation temperature. Following this optimization scheme [26] the subsequent separation parameters were found to be as best for the separation of the naproxen enantiomers using HP- β -CD as a chiral selector. (1) Evaluating the pH range of 3–9 by one pH unit increments [26], maximum resolution was attained employing the pH 5.0 buffer. (2) Varying the chiral selector concentration between 2 and 100 mM a concentration of 10 mM was found to be optimal for the separation of the naproxen enantiomers. (3) A maximum in enantiomeric resolution was found at 700 V/cm when the applied electric field was varied from 100 to 1000 V/cm by 100 V/cm increments. (4) Checking the effect of the temperature between 20 and 50°C on the separation of the *R* and *S* forms of naproxen, 20°C was found to give the highest resolution. As the result of this optimization, Fig. 1 shows the complete baseline separation

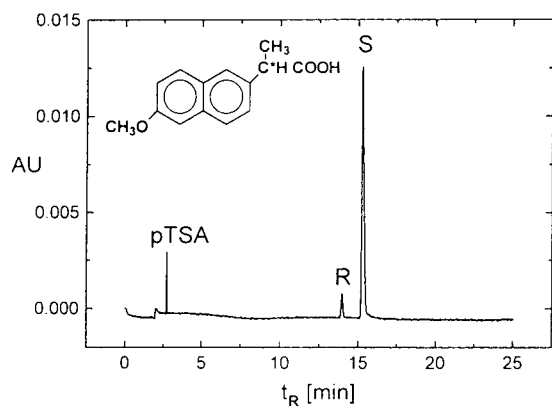


Fig. 1. CGE separation of 1:10 mixture of *R*- and *S*-naproxen. Peaks: pTSA = *p*-toluenesulfonic acid, anionic marker; R = *R*-naproxen; S = *S*-naproxen. Conditions: gel–buffer: 200 mM MES/TBAH, 10 mM HP- β -CD, 0.4% polymeric additive, pH 5.0, Injected amount: 0.1 ng *R*-naproxen and 1 ng *S*-naproxen. Effective capillary length: 20 cm, internal diameter: 25 μ m; detection: 230 nm; run temperature: 20°C; applied electric field strength: 700 V/cm; current: 3 μ A.

($R_s = 3.54$) of the 1:10 mixture of *R*- and *S*-naproxen in 15 min using these separation parameters.

3.2. Reproducibility

Initial characterization of CGE of enantiomers using HP- β -CD as a chiral selector in the gel–buffer system involved the determination of reproducibility for migration time. The uncorrected and corrected migration times and chiral selectivities (α) for the first and 100th runs of the mixture of 0.01 mg/ml *R*- and 0.1 mg/ml *S*-naproxen accompanied by the relative standard deviations are shown in Table 1. The migration times of the pTSA were used for the calculation of the corrected migration times of the naproxen enantiomers, i.e.:

$$t_M^{iR\text{-naproxen}} = t_M^{R\text{-naproxen}} / t_M^{\text{pTSA}} \quad (1)$$

This data represents two batches of capillaries and buffers that were cycled for 100 runs (intra- and inter-day variability) with a 1 M HCl wash in between each run. The good reproducibility of the results (R.S.D. < 1%) may be attributed to the ability to wash the capillary between runs and the replacement of the polymer network by means of a rinsing step after each run. If a sample containing particulates is applied to the gel, or a sample containing a contaminant too large to be analyzed in the standard run time, the replacement of the low-viscosity gel alleviates any damage to this non-cross-linked linear polymer matrix.

3.3. Detection limit and detection linearity

Employing the pressure injection mode, the injection flow was found to be 1 nl/s for this particular capillary gel–buffer system. This was calculated based on the migration velocity of the pTSA internal standard using the low-continuous-rinse mode with injection pressure of 0.5 p.s.i. (3447.4 Pa) [29]. The minimum amount detected on column with peak-to-noise ratio of 4 for *R*-naproxen was $8 \cdot 10^{-14}$ g ($0.75 \cdot 10^{-15}$ mol) that corresponds to the minimal detectable sample concentration of 300 nM. Detection mass

Table 1
Reproducibility data of the enantiomeric separation of *R*- and *S*-naproxen

	Migration time (min)			Corrected migration time		α
	<i>R</i>	<i>S</i>	pTSA	<i>R'</i>	<i>S'</i>	
<i>Batch I</i>						
Run 1	15.25	13.26	2.73	5.586	4.857	1.092
Run 100	16.07	14.71	2.87	5.599	5.125	1.092
R.S.D. (1–100) (5)	6	9.8	4.87	0.42	0.92	
<i>Batch II</i>						
Run 1	15.9	14.5	2.788	5.703	5.204	1.096
Run 100	16.31	14.87	2.88	5.663	5.163	1.096
R.S.D. (1–100) (%)	3.6	2.42	3.47	0.7	0.78	
<i>Batch-to-batch reproducibility (% change in migration time)</i>						
Run 1	4.09	3.7	2.08	2.05	1.75	
Run 100	1.47	1.07	0.35	1.13	0.73	

Separation conditions as in Fig. 1.

linearity was evaluated by pressure injection increasing amounts of solute in equal volumes onto the capillary column. The peak area was found to be a linear function of the injected amount in the sample concentration range of 1 $\mu\text{g/ml}$ ($4.3 \cdot 10^{-7}$ M) to 10 mg/ml ($4.3 \cdot 10^{-3}$ M), with 0.998 correlation coefficient:

$$\text{Peak area} = 1.3314 + 0.9754C_{\text{naproxen}} \quad (2)$$

where C_{naproxen} is the concentration of the naproxen in mg/ml. Peak area normalization to migration times and limit of detection (LOD) was calculated according to Altria et al. [30].

3.4. Enantiomeric purity assessment

For trace analysis, i.e. 1% enantiomeric contamination or below, analytical criteria are very rigorous [31]. Some of the reasons for this are unequal contributions of peak overlap, peak asymmetry, etc. For example when the trace component migrates closely, faster or slower, problems associated with mobility mismatch that causes peak asymmetry (fronting or tailing, respectively) making quantitative trace analysis difficult [32]. Since the “pure” *S*-naproxen con-

tained 1.26% *R* form, the only way to evaluate the ability to detect 0.1% excess impurity was to spike the *S* form with 0.1% *R* form (0.2% racemate). As shown in Fig. 2, the detected enantiomeric contamination level for the *R* form, by the addition of 0.2% racemate to the *S* form, increased from 1.26% to 1.37%, so that a 0.11% difference was detected in this way.

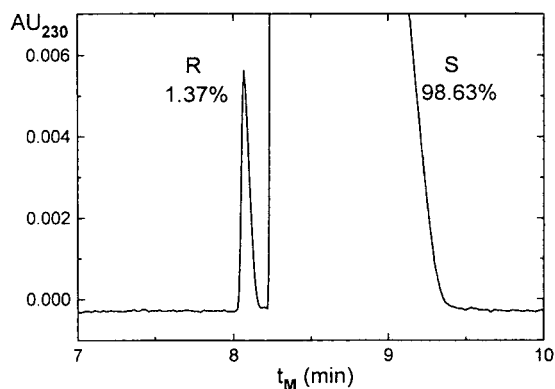


Fig. 2. Detection of 1.37% *R*-naproxen in the presence of *S*-naproxen. The “pure” *S* enantiomer containing 1.26% *R* form was spiked by 0.1% *R* form (0.2% racemate) thus 0.11% enantiomeric contamination is shown. Separation conditions as in Fig. 1.

3.5. System suitability

Doyle [31] suggests that a minimal resolution value of 2.0 is necessary for racemic mixtures as an appropriate criterion for quantitative applications. The required separation efficiency can then be easily calculated based on the resolution equation Karger and Foret [33] derived for capillaries with no electroosmotic flow:

$$R_s = 0.25N^{1/2} \cdot \frac{\alpha - 1}{\alpha} \quad (3)$$

where R_s is resolution, N is the number of theoretical plates and α is chiral selectivity. Thus, with a given chiral selectivity of the separation system a minimum separation efficiency (N_{\min}) is required to see the separation. If this minimal efficiency is not achieved trace analysis is not viable. In the instance of the naproxen example (using conditions of Fig. 1) to fulfill the above criterion of $R_s = 2$, separation efficiency should be at least $N_{\min} = 8500$ with the chiral selectivity of $\alpha = 1.095$. This becomes very important in trace analysis where the main component is usually heavily overloaded, in order to observe a detectable amount of the enantiomeric impurity. However, sample overloading in most instances causes severe peak asymmetry (peak asymmetry at 10% of the peak height, $A_{10\%} > 10$). Therefore, peak efficiency needs be large enough in enantiomeric purity analysis to enable the detection of impurities at very low (< 1%) level.

Acknowledgement

The authors gratefully acknowledge Professor Gyula Vigh for his stimulating discussions.

References

- [1] J. Snopek, I. Jelinek and E. Smolkova-Keulemansova, *J. Chromatogr.*, 609 (1992) 1.
- [2] M.M. Rogan and K.D. Altria, in *Introduction to the Theory and Applications of Chiral Capillary Electrophoresis* (Beckman Primer, Vol IV), Beckman, Fullerton, CA, 1993.
- [3] D. Stevenson and G. Williams, in D. Stevenson and I.D. Wilson (Editors), *Chiral Separations*, Plenum Press, New York, 1987.
- [4] D. Armstrong, *Anal. Chem.*, 59 (1987) 84A.
- [5] B.L. Karger, A.S. Cohen and A. Guttman, *J. Chromatogr.*, 492 (1989) 585.
- [6] M. Tanaka, S. Asano, M. Yoshinago, Y. Kawaguchi, T. Tetsumi and T. Shono, *Fresenius' Z. Anal. Chem.*, 339 (1991) 63.
- [7] A. Guttman, A. Paulus, A.S. Cohen, N. Grinberg and B.L. Karger, *J. Chromatogr.*, 448 (1988) 41.
- [8] S. Fanali and P. Boček, *Electrophoresis*, 11 (1990) 757.
- [9] R. Kuhn, F. Stoecklin and F. Erni, *Chromatographia*, 33 (1992) 32.
- [10] S. Fanali, *J. Chromatogr.*, 545 (1991) 437.
- [11] K.D. Altria, D.M. Goodall and M.M. Rogan, *Chromatographia*, 34 (1992) 19.
- [12] M.W.F. Nielen, *Anal. Chem.*, 65 (1993) 885.
- [13] J. Snopek, H. Soini, M. Novotny, E. Smolkova-Keulemansova and J. Jelinek, *J. Chromatogr.*, 559 (1991) 215.
- [14] S. Fanali, M. Flieger, M. Steinerova and A. Nardi, *Electrophoresis*, 13 (1992) 39.
- [15] S. Fanali, *J. Chromatogr.*, 474 (1989) 441.
- [16] S.A.C. Wren and R.C. Rowe, *J. Chromatogr.*, 609 (1992) 363.
- [17] S.A.C. Wren and R.C. Rowe, *J. Chromatogr.*, 635 (1993) 113.
- [18] M.J. Sepaniak, R.O. Cole and B.K. Clark, *J. Liq. Chromatogr.*, 15 (1992) 1023.
- [19] A. Pluym, W. Van Ael and M. De Smet, *Trends Anal. Chem.*, 11 (1992) 27.
- [20] T. Schmitt and H. Engelhardt, *J. High Resolut. Chromatogr.*, 16 (1993) 525.
- [21] S. Terabe, *Trends Anal. Chem.*, 8 (1989) 129.
- [22] A. Dobashi, T. Ono, S. Hara and J. Yamaguchi, *Anal. Chem.*, 61 (1989) 1986.
- [23] H. Nishi, T. Fukuyama, M. Matsuo and S. Terabe, *J. Chromatogr.*, 515 (1990) 233.
- [24] I.D. Cruzado and Gy. Vigh, *J. Chromatogr.*, 608 (1992) 421.
- [25] A. Guttman and N. Cooke, *Anal. Chem.*, 63 (1991) 2038.
- [26] A. Guttman and N. Cooke, *J. Chromatogr. A*, 680 (1994) 157.
- [27] Y.Y. Rawjee, R.L. Williams and Gy. Vigh, *J. Chromatogr. A*, 652 (1993) 233.
- [28] Y.Y. Rawjee and Gy. Vigh, *Anal. Chem.*, 66 (1994) 416.
- [29] A. Guttman, unpublished results.
- [30] K.D. Altria, A.R. Walsh and N.W. Smith, *J. Chromatogr.*, 515 (1993) 193.
- [31] T.D. Doyle, in S. Ahuja (Editor), *Chiral Separations by Liquid Chromatography*, American Chemical Society, Washington, DC, 1991, p. 27.
- [32] Y.Y. Rawjee, R.L. Williams and Gy. Vigh, *Anal. Chem.*, submitted for publication.
- [33] B.L. Karger and F. Foret, in N.A. Guzman (Editor), *Capillary Electrophoresis Technology*, Marcel Dekker, New York, 1993, p. 3.



ELSEVIER

Journal of Chromatography A, 685 (1994) 161–165

JOURNAL OF
CHROMATOGRAPHY A

Optimisation of separation selectivity in capillary zone electrophoresis of inorganic anions using binary cationic surfactant mixtures

Anthony H. Harakuwe, Paul R. Haddad*, Wolfgang Buchberger

Department of Chemistry, University of Tasmania, GPO Box 252C, Hobart, Tasmania 7001, Australia

First received 5 May 1994; revised manuscript received 18 July 1994

Abstract

Mixtures of different cationic surfactants such as dodecyltrimethylammonium bromide and tetracycltrimethylammonium bromide can be used as carrier electrolyte additives in order to manipulate separation selectivity and resolution of inorganic anions in capillary zone electrophoresis. The migration order is dependent on both the total surfactant concentration and the ratio of the two surfactants. The optimisation of separation selectivity is demonstrated for a nine-anion standard mixture as well as for complex matrices such as Bayer liquor.

1. Introduction

While the majority of applications of capillary zone electrophoresis (CZE) continue to deal with the separation of large biomolecules, this technique has also become increasingly important for the determination of inorganic and low-molecular-mass organic ions [1]. It even holds out the prospect of becoming an alternative to the well-established technique of ion chromatography.

Separation selectivity of CZE depends on differences in the effective mobilities of the species to be separated. Several ways can be exploited for manipulation of separation selectivity: changing the pH of the carrier electrolyte for species undergoing protonation or deprotonation reactions; adding ion-pairing reagents or complexing reagents in order to affect charge

and size of the species; use of organic solvents in the carrier electrolyte for changing the hydration and size of the ions; employment of pseudo-stationary phases such as micelles or polymeric ions in the carrier.

CZE of inorganic anions is generally done in a coelectroosmotic mode with injection at the cathodic side and detection at the anodic side [2–4]. This arrangement requires the reversal of the electroosmotic flow (EOF) which can be achieved by addition of cationic surfactants such as hydrophobic quaternary ammonium ions (EOF modifiers) to the carrier electrolyte [2,5]. The reversal of the EOF is caused by the formation of hemimicelles on the inner surface of the fused-silica capillary. On the other hand, EOF modifiers are potential ion-pairing reagents and can be useful for the optimisation of the separation selectivity as well.

Previous work [6] has demonstrated that different alkylammonium ions can have different

* Corresponding author.

effects on the migration order of inorganic anions. It seems that all papers published until now on the separation of inorganic anions have included the use of a single surfactant in the carrier electrolyte and the employment of mixtures of different surfactants has not yet been reported. Therefore, this study was undertaken in order to evaluate the extent to which the use of more than one cationic surfactant in the carrier electrolyte can be employed to optimise separation selectivity and resolution. Chromate was chosen as the carrier electrolyte itself because this is a well-established system allowing universal indirect UV detection [7].

2. Experimental

2.1. Instrumentation

The CZE instrument employed was a Quanta 4000 (Waters, Milford, MA, USA) interfaced to a Maxima 820 data station (Waters). Separations were carried out using a polyimide-coated fused-silica capillary (Polymicro Technologies, Phoenix, AZ, USA), measuring 60 cm \times 75 μ m I.D., effective length 52 cm. Injections were performed hydrostatically by elevating the sample at 10 cm for 30–45 s at the cathodic side of the capillary. The running voltage was -20 kV and indirect UV detection at 254 nm was used.

2.2. Reagents and procedures

The carrier electrolyte consisted of 5 mM sodium chromate (6.5 mM chromate for the Bayer liquor sample) containing varying amounts of dodecyltrimethylammonium bromide (DTAB) and tetradecyltrimethylammonium bromide (TTAB) and adjusted to pH 8.8 with potassium hydroxide. Both DTAB and TTAB were obtained from Aldrich (Milwaukee, WI, USA) and were dried at 100°C for 1 h before use. All other chemicals used were of analytical grade. All solutions were prepared in water treated with a Millipore (Bedford, MA, USA) Milli-Q water-purification apparatus. Standard anion mixtures containing 10 μ g/ml of each

anion were prepared from appropriate stock solutions.

Before starting a series of injections, the capillary was conditioned by the following flushing sequence: water, ethanol, water, 5 min each; 0.5 M potassium hydroxide, 8 min; water, 5 min; carrier electrolyte, 10 min.

3. Results and discussion

3.1. Selectivity effects in mixed EOF modifiers

The employment of two EOF modifiers such as DTAB and TTAB (as used throughout this work) leads to the necessity of optimising two variables, namely the total concentration of the quaternary ammonium salts as well as the ratio of the two different compounds. Fig. 1 shows the dependence of the electrophoretic mobilities of a series of inorganic anions on the total concentration of EOF modifier for a ratio of 1:1 between DTAB and TTAB. An interpretation of these results must take into account the critical micelle concentrations (CMCs) of DTAB and TTAB, which are 15 and 3.5 mM, respectively [8]. It might be concluded that in the range below 7 mM total concentration of the 1:1 mixture the changes in separation selectivity are mainly due to ion-pairing effects, whereas above this concentration ions establish an equilibrium between the aqueous phase and the micelles (which may include micelles formed by ions of both surfactants individually or as mixtures).

The concept of two different equilibria existing below and above the CMC has also been proposed by Kaneta et al. [9] who reported the separation of five anions with direct UV detection in a phosphate-Tris buffer containing cetyltrimethylammonium chloride. The authors also calculated ion-association constants for the equilibrium existing below the CMC as well as distribution coefficients for the concentration range above the CMC. On the other hand, it should be pointed out that the results obtained above the CMC are not necessarily to be described as a distribution of anions between the aqueous phase and the micelles but could be due

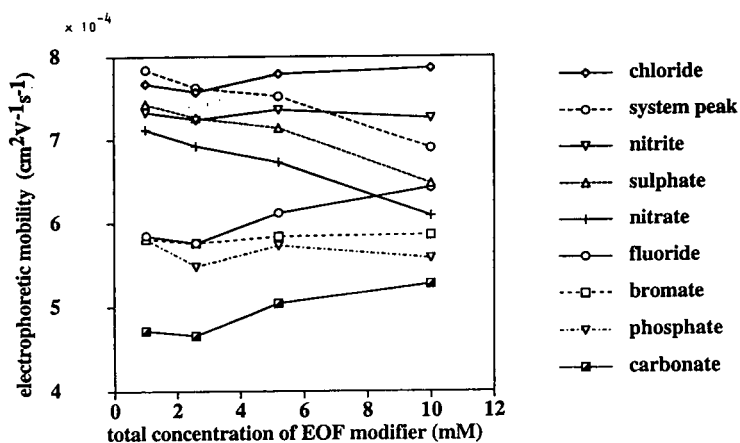


Fig. 1. Dependence of electrophoretic mobilities of anions on the total concentration of the EOF modifier using 1:1 mixtures of DTAB and TTAB.

to some ion-pairing between the anions and the micelles as well with an equilibrium constant different from that for the interaction between the anions and the monomeric surfactant. In this case, the micelles would act in the same way as polymer ions, which have been reported as additives to the buffer in order to optimise separation selectivity [10]. Whatever the detailed mechanism of these interactions might be, our results indicate that upon addition of cationic surfactants, the separation selectivity changes gradually from the migration order to be expected from consideration of the molar conduc-

tivities of the ions to a migration order resembling in part that occurring in ion-exchange chromatography.

Once an appropriate total concentration of surfactant has been chosen, variation of the TTAB:DTAB ratio can be used for fine-tuning the separation. Fig. 2 shows the dependence of electrophoretic mobilities on the ratio of TTAB and DTAB at a total concentration of 2.6 mM. A computer-assisted iterative optimisation procedure developed initially for reversed-phase chromatography [11] was found to be quite helpful for this final optimisation step. This

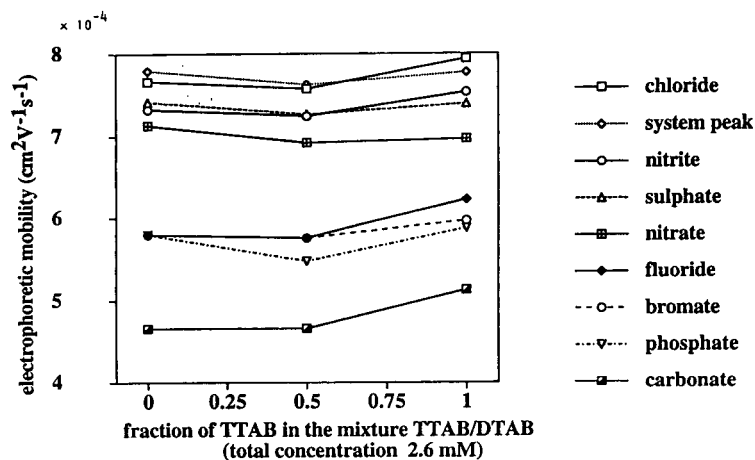


Fig. 2. Dependence of electrophoretic mobilities of anions on the ratio of TTAB and DTAB (total concentration 2.6 mM).

procedure was initiated using two experiments in which desired concentrations of TTAB and DTAB alone were used as EOF modifier. Migration times were calculated for all intermediate mixtures of linear combinations of the two limiting concentrations by assuming a linear relationship between migration time and TTAB:DTAB ratio. Using an appropriate optimisation criterion, the optimal ratio was then predicted and verified by an additional experiment. If these experimental data differed from the predicted data, the additional experimental data were used to establish an improved function for the dependence of migration times on the ratio and a new prediction performed. The optimal separation of a mixture of nine anions is shown in Fig. 3.

Besides the effects on separation selectivity, the TTAB:DTAB ratio also affects the analysis time due to its influence on the electroosmotic flow. Both salts are effective in reversing the EOF with TTAB exhibiting the predominant effect when combined with DTAB. The electroosmotic mobility calculated for a chromate carrier electrolyte containing only DTAB or TTAB at a concentration of 2.6 mM was $1.58 \cdot 10^{-4} \text{ cm}^2$

$\text{V}^{-1} \text{ s}^{-1}$ for DTAB and $2.48 \cdot 10^{-4} \text{ cm}^2 \text{ V}^{-1} \text{ s}^{-1}$ for TTAB.

As mentioned above, the reversal of the EOF is due to the formation of hemimicelles of TTAB and DTAB at the inner surface of the fused-silica capillary, which causes the ζ potential to reverse its sign. Therefore, conditioning of the capillary is crucial. Our investigations indicated that inappropriate conditioning can have serious effects not only on the EOF but also on the quantification of some ions, especially phosphate. Phosphate almost completely disappeared (especially at levels below 10 ppm) if the flushing procedure described in the experimental part did not include the final purge with the carrier electrolyte for 10 min. Apparently, phosphate tended to adsorb to the bare silica surface. If the capillary was conditioned with the carrier electrolyte, the active sites of the surface became saturated with TTAB and DTAB and phosphate was no longer lost by adsorption.

3.2. Applications of mixed EOF modifiers

The optimisation strategies described in this paper have been applied to a range of different applications including the analysis of fluoride in Bayer liquors which are alkaline, high ionic strength solutions from the Bayer process for extraction of alumina from bauxite. Initial experiments [12] had indicated that a chromate electrolyte containing 0.5 mM TTAB was incapable of resolving the fluoride peak from formate and succinate present in the complex sample. The results given above suggested the employment of higher concentrations of TTAB-DTAB mixtures which would move the fluoride to considerably shorter migration times. On the other hand, it was mentioned earlier that at higher concentrations of the EOF modifier the separation selectivity tends towards that of ion-exchange chromatography. Therefore, one would expect that the resolution between fluoride and formate would not improve considerably at higher concentrations of the surfactants, as fluoride and formate show similar retention times in ion chromatography. Nevertheless, organic acids turned out to behave in a quite

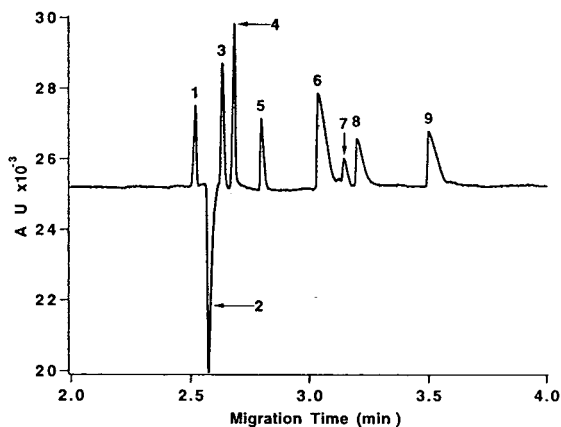


Fig. 3. Optimised separation of a mixture of nine inorganic anions. Conditions: electrolyte contained 2.35 mM TTAB, 2.65 mM DTAB and 5 mM chromate at pH 8.8. Sample was introduced by hydrostatic injection (30 s at 10 cm) and separated using 20 kV from a negative power source. Detection was in the indirect UV mode at 254 nm. Solute concentrations: 10 ppm. Peaks: 1 = chloride; 2 = system peak (bromide); 3 = nitrite; 4 = sulfate; 5 = nitrate; 6 = fluoride; 7 = bromate; 8 = phosphate; 9 = carbonate.

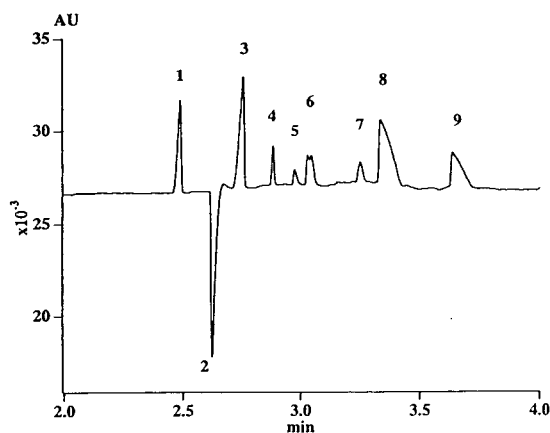


Fig. 4. Separation of 1:1000 (v/v) diluted Bayer liquor using an electrolyte comprising 5 mM TTAB and 1 mM DTAB. Other conditions: 6.5 mM chromate, pH 8.84, 45 s sampling time, -20 kV separation voltage and indirect UV detection at 254 nm. Peaks: 1 = chloride; 2 = system peak; 3 = sulfate; 4 = oxalate; 5 = fluoride; 6 = formate + malonate; 7 = succinate + tartrate; 8 = carbonate; 9 = acetate.

different way, as shown in the electropherogram given in Fig. 4. Fluoride is well separated from organic acids using 5 mM TTAB–1 mM DTAB (for this application, the chromate concentration of the carrier electrolyte had been increased from 5 to 6.5 mM in order to get a more efficient focusing of the sample components by sample stacking).

4. Conclusions

In conclusion, the use of mixtures of different quaternary ammonium salts as well as variation of the total concentration of these salts are efficient approaches to the optimisation of separation selectivity, resolution and analysis time in

the determination of inorganic and low-molecular-mass organic anions. Computer-assisted procedures are likely to gain importance in the optimisation process and require only a small number of experiments in order to find an optimum for a given separation.

Acknowledgement

Financial support from the Waters Chromatography Division of Millipore is gratefully acknowledged.

References

- [1] P. Jandik and G. Bonn, *Capillary Electrophoresis of Small Molecules and Ions*, VCH, New York, 1993.
- [2] W.R. Jones and P. Jandik, *J. Chromatogr.*, 546 (1991) 445.
- [3] W.R. Jones and P. Jandik, *J. Chromatogr.*, 608 (1992) 385.
- [4] W.R. Jones, *J. Chromatogr.*, 640 (1993) 387.
- [5] K.D. Altria and C.F. Simpson, *Chromatographia*, 24 (1987) 527.
- [6] W. Buchberger and P.R. Haddad, *J. Chromatogr.*, 608 (1992) 59.
- [7] P. Jandik and W.R. Jones, *J. Chromatogr.*, 546 (1991) 431.
- [8] E.J. Fendler and J.H. Fendler, in V. Gold (Editor), *Advances in Physical Organic Chemistry*, Academic Press, London, 1970, p. 276.
- [9] T. Kaneta, S. Tanaka, M. Taga and H. Yoshida, *Anal. Chem.*, 64 (1992) 798.
- [10] S. Terabe and T. Isemura, *Anal. Chem.*, 62 (1990) 652.
- [11] P.J. Schoenmakers, A.C.J.H. Drouen, H.A.H. Billiet and L. de Galan, *Chromatographia*, 15 (1982) 688.
- [12] S. Vanderaa and P.R. Haddad, presented at 6th International Symposium on High Performance Capillary Electrophoresis, San Diego, CA, 1994, poster P-509.



ELSEVIER

Journal of Chromatography A, 685 (1994) 166–171

JOURNAL OF
CHROMATOGRAPHY A

Short communication

Immobilization of peralkylated β -cyclodextrin on silica gel for high-performance liquid chromatography

Ionel Ciucanu*, Wilfried A. König

Institute for Organic Chemistry, Hamburg University, Martin Luther King Platz 6, D-20146 Hamburg, Germany

First received 3 March 1994; revised manuscript received 25 May 1994

Abstract

The synthesis of mono-O-5-pent-1-enyl- β -cyclodextrin was studied in order to obtain the best yield of mono-O-substitution. Permethylated mono-O-5-pent-1-enyl- β -cyclodextrin, purified by liquid chromatography, was characterized by fast atom bombardment MS and ^1H NMR spectrometry. GC-MS analysis of partially methylated alditol acetates obtained from mono-O-pent-1-enyl- β -cyclodextrin showed that the 5-pent-1-enyl ether group was in the α -D-glucopyranoside residue in the 2-OH position in a proportion of 95.9% for the O-substitution reaction in dimethyl sulfoxide and in the presence of sodium hydroxide. Silica gel with chemically bonded peralkylated(methyl or propyl)- β -cyclodextrin proved to be an efficient stationary phase for the separation of enantiomers.

1. Introduction

Cyclodextrins (CDs) are extensively used in high-performance liquid chromatography (HPLC) as stationary phases bonded to a solid support or as additives in mobile phases for the separation of various types of organic compounds and enantiomers.

CDs can be bonded to silica beads via several spacer arms [1–7] and these methods can be generally classified in three main ways. First, a spacer arm is grafted on silica gel and the CD is

reacted with the reactive terminal group of the spacer arm [5]. Second, the reactive group of the spacer arm coupled to a CD molecular is reacted with silanol groups on the surface of silica gel [6]. Third, part of the spacer arm is coupled to silica gel and another part to the CD and immobilization consists in reaction of the reactive groups of these two parts [1–4,7]. In the first and third approaches, the presence of unreacted groups of spacers exhibit complex retention properties. Moreover, thermodynamic and theoretical parameters of the inclusion complex cannot be correctly evaluated when the silica gel surface and the position of the spacer arm on the CD are not well characterized.

* Corresponding author. Present address: University of Timisoara, Department of Chemistry, str. Pestalozzi 16, RO-1900 Timisoara, Romania.

This paper described a procedure to obtain silica gel with well characterized chemically bonded peralkylated β -CDs, using the second approach for immobilization.

2. Experimental

2.1. Reagents and materials

β -Cyclodextrin, dimethoxymethylhydrosilane (DMMHS), dichloromethylhydrosilane (DCMHS), 5-bromo-1-pentene and hexachloroplatinic acid hexahydrate ($\text{H}_2\text{PtCl}_6 \cdot 6\text{H}_2\text{O}$) were obtained from Fluka (Buchs, Switzerland). Microporous spherical silica gel (LiChrosorb Si 100) with a medium particle diameter of 5 μm , a mean pore size of 110 nm and a specific surface area of 320 m^2/g , dimethyl sulfoxide (DMSO), dimethylacetamide (DMAA), dimethylformamide (DMFA), dioxane, iodomethane, 1-iodopropane and thin-layer chromatography (TLC) aluminium roll coated silica gel 60 F₂₅₄ were purchased from Merck (Darmstadt, Germany). Water was purified by means of a Milli-Q water-purification system (Millipore, Bedford, MA, USA).

2.2. Apparatus

HPLC was performed with a Spectra-Physics (Santa Clara, CA, USA) Model 8500 chromatograph equipped with a UV detector operated at 254 and 280 nm. The HPLC columns (250 mm \times 4.6 mm I.D.) were packed by the usual slurry method.

Gas chromatography (GC) was carried out on a Fractovap 2101 gas chromatograph (Carlo Erba, Milan, Italy) equipped with split injection, a flame ionization detector and a Hewlett Packard Model 3390A integrator.

Electron impact mass spectrometry (EI-MS) was performed with a Finnigan MAT Model 311 A mass spectrometer (MAT, Bremen, Germany) coupled to a Hewlett-Packard HP-5840 gas chromatograph.

Fast atom bombardment mass spectrometry (FAB-MS) was carried out on a VG mass spec-

trometer (VG Analytical, Manchester, UK) using nitrobenzyl alcohol as matrix.

Nuclear magnetic resonance (NMR) spectra were recorded on a Bruker WM 400 spectrometer operating at 400.13 MHz for proton (^1H). All measurements were carried out on solutions in deuteriochloroform and tetramethylsilane was used as the internal standard.

2.3. Preparation of stationary phases

To a solution of 1 mol of β -CD (dried in vacuum for 24 h) in dipolar aprotic solvents was added finely powdered sodium hydroxide and then 5-bromo-1-pentene under a nitrogen atmosphere. The suspension was rapidly stirred at room temperature and after 24 h the solution was evaporated under reduced pressure. For peralkylation, the reaction products dissolved in fresh dipolar aprotic solvent were stirred at room temperature for 12 h with 3 equiv. of sodium hydroxide and 3 equiv. of alkyl halide (iodomethane, 1-iodopropane) per replaceable hydrogen [8]. The reaction mixture was carefully added to 50 ml of cold water and excess of unreacted sodium hydroxide was neutralized with 1 M hydrochloric acid. The peralkylated product was extracted three times with chloroform. The combined extracts were washed with water and dried over anhydrous magnesium sulfate. The filtered chloroform solution was concentrated under reduced pressure and the residue was purified by liquid chromatography over silica gel using light petroleum and a light petroleum–acetone (1:1) as eluents.

For the hydrosilylation reaction, to 1 mol of the appropriate peralkylated mono-O-pent-1-enyl- β -CD dissolved in 150 ml of anhydrous toluene was added 1.2 mol of DMMHS or DCMHS in a 250-ml three-necked, round-bottomed flask equipped with a nitrogen inlet and reflux condenser. A few drops of a 4% solution of hexachloroplatinic acid hexahydrate in anhydrous tetrahydrofuran were added at intervals of 2 h. The reaction mixture was heated at 50–90°C with stirring. The progress of the reaction was monitored by IR spectrometry, measuring the decrease in the absorption band at 2060–

2080 cm^{-1} (Si–H), usually requiring more than 36 h. The excess of hydrosilane was removed under reduced pressure. The products were purified by liquid chromatography on silica gel using hexane–toluene (5:1) as eluent. When hydrosilylation was performed with DCMHS, the platinum catalyst was removed by stirring overnight with a drop of mercury.

2.4. Preparation of O-alkylated alditol acetates

Permethylated mono-O-pent-1-enyl- β -CD (10 mg) was hydrolysed in 1 ml of trifluoroacetic acid–80% formic acid (1:1) at 80°C for 20 h. The solution containing the hydrolysate was evaporated to dryness under reduced pressure. The reduction was carried out in water (10 ml) with sodium borohydride (100 mg) for 6 h at room temperature. After acidification with few drops of 80% formic acid and concentration to dryness in the presence of methanol, the product, dried using a high-vacuum pump, was acetylated with acetic anhydride (0.2 ml) and pyridine (0.2 ml) at 100°C for 2 h.

2.5. Immobilization of stationary phase

A 6-g amount of silica gel (dried in vacuum at 150°C for 10 h) was added to 150 ml of a 10% solution of peralkylated mono-O-5-(dimethoxymethylsilyl)pentyl- β -CD in dry toluene with gentle shaking and then the suspension was refluxed for 30 h under nitrogen without stirring. After cooling, the resulting silica gel was filtered through a membrane filter, washed successively

with toluene, methanol and diethyl ether, and then dried under vacuum at 40°C for 10 h. The amounts of bonded peralkylated- β -CD were calculated from the results of elemental analysis [9]. The values were 187 $\mu\text{mol/g}$ for permethylated- β -CD and 175 $\mu\text{mol/g}$ for perpropylated- β -CD.

3. Results and discussion

The first step of the coupling technique is to obtain a monofunctionalized derivative of β -CD. Normally this functionalization of CD is possible in one position (2-, 3- or 6-OH) or more positions as the β -CDs have 21 hydroxyl groups. Discrimination by selective reaction between the primary and secondary hydroxyl groups of a β -CD is complicated because of statistical and steric problems. It is known that 2- and 6-OH are more acidic than 3-OH in α -D-glucose [10] and for this reason the basicity of the reaction medium could affect the regioselectivity.

The reaction of β -CDs in dipolar aprotic solvents with various amounts of 5-bromo-1-pentene and powdered sodium hydroxide [8,11] was studied in order to obtain a high yield of mono-O-pent-1-enyl- β -CD. The best results were obtained with DMSO as solvent, 1.2 mol of 5-bromo-1-pentene and 2.5 mol of sodium hydroxide for 1 mol of β -CD. The reaction products showed a high yield of mono-O-pent-1-enyl- β -CD and small amounts of di- and tri-substituted derivatives (Table 1). The first control of the reaction was made by TLC using 25%

Table 1

Yields of permethylated mono-O-pent-1-enyl- β -CDs and substitution position of the 1-pentenyl group as a function of solvent (1.2 mol of 5-bromo-1-pentene per mole of β -CD and 2.5 mol of sodium hydroxide per mole of β -CD)

Solvent	Yield (%)	Relative proportion (%)		
		2-Substitution	3-Substitution	6-Substitution
DMSO	63 ± 2.1	95.9	0.6	3.5
DMAA	50 ± 2.6	73.9	1.2	24.7
DMFA	31 ± 1.8	56.8	1.7	41.5
DMSO–dioxane (1:1, v/v)	53 ± 1.9	60.7	1.7	37.6

ammonia solution–ethanol–2-propanol (2:1:1) as eluent, which separated very well monofunctionalized β -CDs with a 1-pentenyl group in the 2-OH ($R_F = 0.46$), 3-OH ($R_F = 0.42$) or 6-OH position ($R_F = 0.33$). Identification of the spots was made with standard compounds. The optimum reaction temperature was 22°C because at higher temperatures the amounts of di- and tri-substituted β -CD derivatives were larger. After 1 day at room temperature, the reaction mixture was permethylated [8] and then fractionated by liquid chromatography on silica gel.

The purity of permethylated mono-O-pent-1-enyl- β -CD was determined by FAB-MS and ^1H NMR spectrometry. Permethylated mono-O-pent-1-enyl- β -CD was analysed in a variety of FAB matrices to determine the relative sensitivity of the molecular ion. The best result was obtained with nitrobenzyl alcohol, which generated $[\text{M} + \text{H}]^+$ ion over $[\text{M} + \text{Na}]^+$ and $[\text{M} + \text{K}]^+$ ions. The loss of the methanol molecule gave an intense fragment ion $[\text{M} + \text{H} - 32]^+$ (Fig. 1). The presence of the O-pent-1-enyl group in permethylated- β -CD gave a slight modification of the proton chemical shift by comparison with the ^1H NMR spectrum of permethylated- β -CD [12]. The proton absorption at $\delta = 5.68$ – 5.83 gave a multiplet that may be ascribed to vinyl CH from the 1-pentenyl group.

In order to determine the position of the O-pent-1-enyl group in the α -D-glucopyranosyl residue, the fraction of permethylated mono-O-

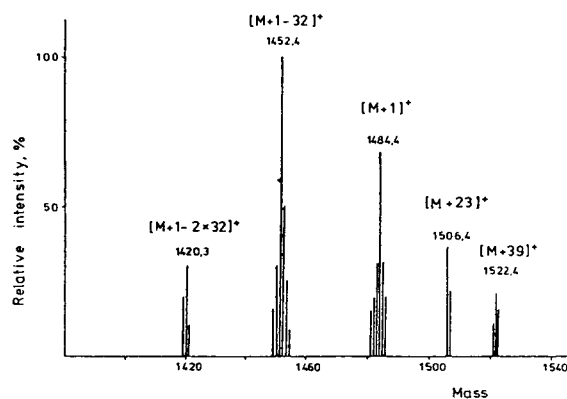


Fig. 1. Positive-ion FAB-MS of permethylated mono-O-pent-1-enyl- β -CD.

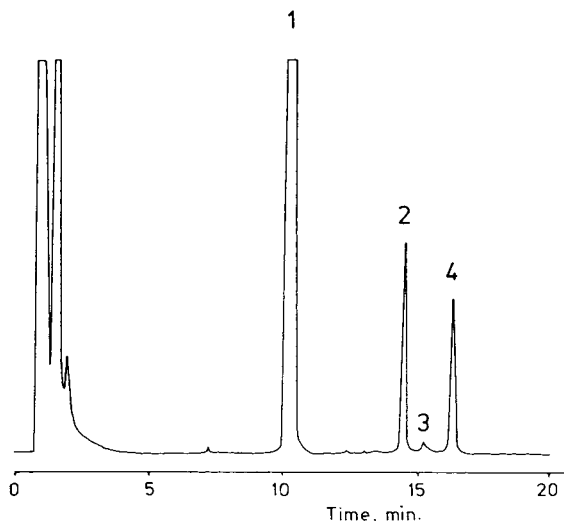


Fig. 2. Gas chromatogram of partially methylated alditol acetates from mono-O-pent-1-enyl- β -CD synthesized in DMFA. Capillary column, SE-30; column temperature increased from 140 to 200°C at 4°C/min; carrier gas, hydrogen. Peaks: 1 = 1, 4, 5-tri-O-acetyl-2, 3, 6-tri-O-methylglucitol; 2 = 1,4,5-tri-O-acetyl-3,6-di-O-methyl-2-O-pent-1-enylglucitol; 3 = 1, 4, 5-tri-O-acetyl-2, 5-di-O-methyl-3-O-pent-1-enylglucitol; 4 = 1, 4, 5-tri-O-acetyl-2, 3-di-O-methyl-6-O-pent-1-enylglucitol.

pent-1-enyl- β -CD was successively hydrolysed, reduced and acetylated, and O-methylated alditol acetates were analysed by GC (Fig. 2). The peaks were identified by EI-MS and the intensities and the characteristic fragment ions are listed in Table 2. The interpretation of the mass

Table 2

Partial EI mass spectra of derivatives obtained from permethylated mono-O-pent-1-enyl- β -CD after hydrolysis, reduction and acetylation

Peak No. ^a	<i>m/z</i> (% of base peak)
1	43(100), 101(20), 117(61), 129(10), 161(6), 173(5), 189(1), 233(20)
2	43(90), 69(100), 113(30), 117(5), 129(63), 171(9), 173(8), 215(3), 233(32), 319(3)
3	43(100), 69(87), 117(55), 167(13), 215(2), 227(6), 287(23), 319(3)
4	43(100), 69(59), 101(26), 117(81), 129(43), 161(11), 171(2), 233(3), 243(3), 287(3), 319(5)

^a See Fig. 2.

spectra was based on the known fragmentations of partially methylated alditol acetates [13,14]. All compounds with a 1-pentenyl group gave a characteristic fragment ion at m/z 69 $[\text{CH}_2\text{CH}_2\text{CH}_2\text{CH}=\text{CH}_2]^+$ and m/z 319 $[\text{M}-85]^+$. The high abundance of primary fragment ions results from fission between two methoxylated carbons in the chain and decreases when methyl is replaced with acetyl. The compounds in peak 1 gave similar mass spectrum to those reported [13,15] and was consistent with 1,4,5-tri-O-acetyl-2,3,4-tri-O-methylglucitol. The compound in peak 2 was identified as 1,4,5-tri-O-acetyl-3,6-di-O-methyl-2-O-pent-1-enylglucitol. The presence of a 1-pentenyl group on 2-OH was indicated by the absence of fragment ions at m/z 287 and 117 and by the presence of a primary intense fragment ion at m/z 233 and a secondary fragment ion at m/z 129 formed from m/z 171, due to the loss of $\text{CH}_3\text{CH}=\text{CH}_2$. The compound in peak 3 was identified as 1,4,5-tri-O-acetyl-2,6-di-O-methyl-3-O-pent-1-enylglucitol owing to the presence of intense fragment ions at m/z 287 and 117. The compound in peak 4 gave an intense fragment ion at m/z 117 and characteristic fragment ions at m/z 161 and 243. These data and the absence of fragment ions at m/z 233 and 171 indicate the compound to be 1,4,5-tri-O-acetyl-2,3-di-O-methyl-6-O-pent-1-enylglucitol.

Table 1 gives the quantitative results for the distribution of the 1-pentenyl group in the α -D-glucopyranosyl residue of mono-O-pent-1-enyl- β -CD. As expected for such base-catalysed, kinetically controlled alkylation reaction, the 2-OH position was preponderantly substituted. The formation of anions is the rate-determining step. The best yield of 2-OH substitution was obtained using DMSO as solvent. These results are not in accord with those obtained by Schurig et al. [16], which indicated the 6-OH position for substitution in this solvent. We observed that the selectivity of mono-O-substitution decreases with decreasing polarity of the dipolar aprotic solvent (DMSO > DMAA > DMFA) [17]. Similar results were obtained by adding dioxane to DMSO. The very low yield at the 3-OH position can be explained by hydrogen bonding and steric

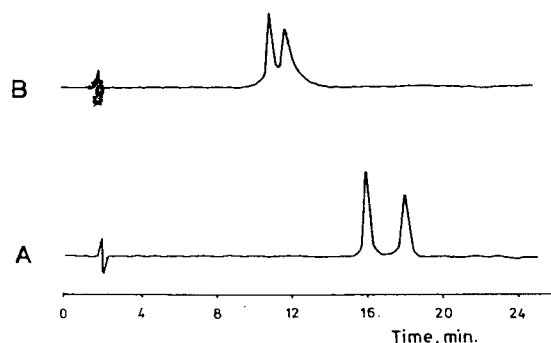


Fig. 3. Separation of enantiomers of hexobarbital on (A) permethylated β -CD and (B) perpropylylated β -CD bonded stationary phases. Mobile phase, 0.5% triethylammonium acetate buffer (pH 4.2)–methanol (70:30, v/v); flow-rate, 0.8 ml/min; detection, UV at 254 nm.

hindrance due to their direction in the cavity of the CD [18].

Preliminary chromatographic evaluation of peralkylated (methyl or propyl) chemically bonded β -CDs showed the successful separation of racemates of some drugs. Fig. 3 shows the separation of racemic hexobarbital. Comparison between columns A and B indicates a change in the retention time, selectivity and shape of the peaks. These modifications can be only attributed to the replacement of methyl with propyl groups in the β -CD. Clearly, more studies need to be done with these columns in order to give a good explanation for the mechanism of chiral recognition.

Acknowledgements

A research fellowship from Alexander von Humboldt Foundation (Bonn, Germany) to I.C. is gratefully acknowledged. We thank Annegret Meiners and Manfred Preusse for recording the spectra.

References

- [1] K. Fujimura, T. Ueda and T. Ando, *Anal. Chem.*, 55 (1983) 446–450.

- [2] Y. Kawaguchi, M. Tanaka, M. Nakae, K. Funazo and T. Shono, *Anal. Chem.*, 55 (1983) 1852–1857.
- [3] M. Tanaka, Y. Kawaguchi, M. Nakae, Y. Mizobuchi and T. Shono, *J. Chromatogr.*, 299 (1984) 341–350.
- [4] M. Tanaka, J. Okazaki, H. Ikeda and T. Shono, *J. Chromatogr.*, 370 (1986) 293–301.
- [5] D.W. Armstrong, *US Pat.*, 4539399 (1985).
- [6] K. Fujimura, S. Suzuki, K. Hagashi and S. Masuda, *Anal. Chem.*, 62 (1990) 2198–2205.
- [7] Y. Kuroda, T. Koto and H. Ogoshi, *Bull. Chem. Soc. Jpn.*, 66 (1993) 1116–1120.
- [8] I. Ciucanu and F. Kerek, *Carbohydr. Res.*, 131 (1984) 209–217.
- [9] G.E. Brendsen and L. de Galan, *J. Liq. Chromatogr.*, 1 (1978) 561–586.
- [10] R.I. Gelb, M. Schwartz and D.A. Laufer, *Bioorg. Chem.*, 11 (1982) 274–280.
- [11] I. Ciucanu, S. Negura, W. Hirschvogel and C.-t. Luca, *Rev. Roum. Chim.*, 37 (1992) 843–847.
- [12] J.R. Johnson and N. Shankland, *Tetrahedron*, 41 (1985) 3147–3152.
- [13] H. Bjoerndal, C.G. Hellerqvist, B. Lindberg and B. Svensson, *Angew. Chem.*, 16 (1970) 643–652.
- [14] J. Loenngren and S. Svensson, *Adv. Carbohydr. Chem. Biochem.*, 29 (1974) 41–106.
- [15] P.-E. Jansson, L. Kenne, H. Liedgren, B. Lindberg and J. Loenngren, *Chem. Commun.*, (1976) 1–74.
- [16] V. Schurig, D. Schmalzig, U. Muehleck, M. Jung, M. Schleimer, P. Mussche, C. Duvkot and J.C. Buyten, *J. High Resolut. Chromatogr.*, 13 (1990) 713–717.
- [17] D.W. Meek, in J.J. Langowski (Editor), *The Chemistry of Non-Aqueous Solvents*, Academic Press, New York, 1960, p. 23.
- [18] W. Saenger, *Angew. Chem.*, 92 (1980) 343–361.



ELSEVIER

Journal of Chromatography A, 685 (1994) 172–177

JOURNAL OF
CHROMATOGRAPHY A

Short communication

Determination of Stokes radii and molecular masses of sodium hyaluronates by Sephacryl gel chromatography

Eiji Shimada*, Kazuo Torii Nakamura

School of Pharmaceutical Sciences, Showa University, 1-5-8, Hatanodai, Shinagawa-ku, Tokyo 142, Japan

First received 29 March 1994; revised manuscript received 29 July 1994

Abstract

Stokes radii (R) of sodium hyaluronate fractions were estimated from their available volumes (K) by gel chromatography on a column of Sephacryl S-1000 instead of the Sepharose series previously examined. The relationships between R and K already established for the Sephadex and Sepharose series were also applicable to Sephacryl S-500 and S-1000 gels. R values were determined with the use of bovine serum albumin as a standard of known size and the average radius (5.8 nm) of fibres constructing Sephacryl gels. The molecular masses (M) of the glycosaminoglycan fractions, calculated from their intrinsic viscosities according to Mark–Houwink equations, were in the range $3.9 \cdot 10^4$ – $8.8 \cdot 10^5$. Their Stokes radii were in the range 5.9–19.6 nm. The plots of R and $M^{1/2}$ for these fractions gave $R = 0.030 M^{1/2}$ and $R = 0.016 M^{1/2} + 4.3$ with M below and above 10^5 , respectively. Although an upper limit of M for hyaluronic acid on Sepharose 2B appeared to be about $4 \cdot 10^5$, the use of Sephacryl S-1000 seems to extend this limit to about $1.5 \cdot 10^6$ under the experimental conditions

1. Introduction

A method for determining the molecular mass of sodium hyaluronate by use of its Stokes radius (R), which was calculated from its available volume (K) estimated by Sepharose gel chromatography, was given in a previous paper [1]. R of a substance B [$R(B)$], for instance, was calculated according to the following equation:

$$\log K(B)/\log K(A) = \{[R(B) + r]/[R(A) + r]\}^2 \quad (1)$$

where $K(A)$ and $K(B)$ are available volumes of substances A and B, respectively; A is a sub-

stance with known Stokes radius such as bovine serum albumin. The average fibre radius (r) constructing gel networks was 2.5 nm for the Sepharose series [1].

Molecular masses (M) of hyaluronate samples were calculated from the relationships between M and R , and an upper limit of M for the polymer measurable by gel chromatography seemed to be about $4 \cdot 10^5$ on Sepharose 2B. As hyaluronic acid with $M > 4 \cdot 10^5$ is generally found in soft tissues such as vitreous body of the eye [2] and skin [3], and Sephacryl S-1000 (Pharmacia) is said to have a larger fractionation range than that of Sepharose 2B, we tried to investigate whether the method described above is applicable to Sephacryl gels. These gels consist of the fibres produced by cross-linking dextran

* Corresponding author.

chains allylated perhaps at the position C-2 of appropriate residues with N,N'-methylenebis-acrylamide and it is assumed that their networks form stiff and hydrophilic gels. The validity of Eq. 1 was verified at least for Sephacryl S-500 and S-1000 gels by the observation that the radii of the fibres constructing both gels (5.8 nm) agreed with each other; other Sephacryl types (S-100, S-200, S-300 and S-400) were not examined, because the chief interest in this work was the molecular sizes of hyaluronate samples with $M > 4 \cdot 10^5$.

In this paper, we describe a method for determining the Stokes radii of hyaluronates by Sephacryl gel chromatography.

2. Experimental

2.1. Materials

In order to prepare hyaluronic acid fractions with molecular masses $>4 \cdot 10^5$, a sample of sodium hyaluronate (rooster comb) was further fractionated by gel filtration of Sephacryl S-1000. Part (22 mg) of the hyaluronate sample, which was included in the above gel, was dissolved in 22 ml of 0.2 M sodium chloride and 2-ml aliquots were chromatographed on a column (54.5 × 2 cm I.D.) of Sephacryl S-1000 equilibrated with the above salt solution. The eluate was divided into five fractions (I–V) in eleven identical runs. Each pooled fraction was lyophilized after dialysis against distilled water. Although each elution pattern of these fractions was still broad on the same column, further fractionation was not done.

Six hyaluronate fractions (B-1, B-3 and E-1 to 4), already characterized in a previous study [1], were also used in this experiment to determine the fibre radius of Sephacryl gels.

The viscosities of six hyaluronate samples (a–f) with different molecular masses above $M = 1.5 \cdot 10^5$ were used to examine the reliability of the Mark–Houwink equations for hyaluronic acid reported by several investigators [4–7].

2.2. Gel chromatography

Gel filtration for the determination of available volumes (K) of hyaluronate samples and bovine serum albumin (BAS) was performed on a column (54.5 × 2 cm I.D.) of Sephacryl S-500 or S-1000 (Pharmacia) at room temperature, using 0.2 M sodium chloride as the eluent. BSA (Sigma) was used as a standard having a known Stokes radius of 3.5 nm [8]. BSA (1 mg) or hyaluronate fractions (1–1.5 mg) were applied in 1 ml of 0.2 M sodium chloride. Column eluents were collected in 2-ml fractions.

Blue dextran 2000 (Pharmacia) of concentration 10 mg/ml was used to determine the void volume of a given column (54.5 × 2 cm I.D.), which was not detected as a peak, but as a small shoulder corresponding to a 75-ml elution volume.

2.3. Analytical methods

Hyaluronate in column eluates was detected by the method of Bitter and Muir [9], using glucuronolactone as a standard. Its contents in solution were calculated from the glucuronolactone value by multiplication by an experimental factor of 2.39 [5]. Bovine serum albumin and blue dextran were determined by absorbance measurements at 230 and 620 nm, respectively.

2.4. Intrinsic viscosity and molecular mass

For the determination of the mass-average molecular mass (M) of hyaluronic acid, a simple procedure is to measure its intrinsic viscosity ($[\eta]$), whose measurement was done in the same way as described previously [1], and then utilize a Mark–Houwink equation established for the polymer, $[\eta] = KM^\alpha$, where K and α are empirical constants. In a previous paper [5], we presented double logarithmic plots of $[\eta]$ and M of hyaluronate samples with M from 10^4 to $1.2 \cdot 10^6$: $[\eta]$ was measured in sodium phosphate buffer (pH 7.3) at 37°C and M was determined by sedimentation equilibrium. This graph indicated two linear regions below and above $M =$

$1.5 \cdot 10^5$. The former was represented by $[\eta] = 3.0 \cdot 10^{-4} M^{1.20}$ and the latter by $[\eta] = 5.7 \cdot 10^{-2} M^{0.76}$, in which $[\eta]$ is here expressed in ml/g instead of 100 ml/g as in the previous paper [5]. Cleland and Wang [4] also suggested such a tendency and obtained $[\eta] = 2.28 \cdot 10^{-2} M^{0.816}$ for $M > 10^5$: $[\eta]$ was measured in 0.2 M sodium chloride at 25°C and M was determined by light scattering. Cleland [10] proposed $[\eta] = 2.8 \cdot 10^{-3} M$ for low-molecular-mass samples of hyaluronate below $M = 10^5$ under the same conditions as described above. In this experiment, M was determined by using the Mark–Houwink coefficients by Cleland [10] and by Cleland and Wang [4] for hyaluronate samples below and above $M = 10^5$, respectively.

3. Results and discussion

3.1. Relationship between intrinsic viscosity and molecular mass

With the aim of examining the reliability of Mark–Houwink equations proposed for hyaluronic acid by several investigators, four equations [4–7] obtained from the various combinations of solvent and temperature were compared.

Molecular masses of six hyaluronate samples above $M = 10^5$ (a–f), whose gel chromatograms demonstrated different molecular size distributions, were calculated from their intrinsic viscosities measured under various conditions. The results are summarized in Table 1. The molecular masses calculated from four Mark–Houwink equations differed from each other. Standard deviations (S.D.), also shown in Table 1, were in the range 13–19% on the basis of each mean value. The unexpected difference may be due to the difficulty in measuring the molecular mass of these polymers, the degree of polydispersity of the samples examined, etc. As a matter of convenience, the average molecular mass of these equations will be taken as the polymer's molecular mass. It should be noted in Table 1 that the molecular masses estimated from the Mark–Houwink equation (0.2 M, 25°C) by Cleland and Wang [4] agreed well with the mean values. Based on this finding, the average molecular mass of hyaluronate above $M = 10^5$ was approximated by the mass determined by using the Mark–Houwink coefficients in 0.2 M NaCl at 25°C.

For hyaluronic acid with $M < 10^5$, there are two Mark–Houwink equations by Shimada and Matsumura [5] and Cleland [10], as described

Table 1
Molecular masses (above 10^5) of hyaluronate samples from four Mark–Houwink equations

Sample	Conditions				Mean \pm S.D.
	0.2 M NaP ^a , 37°C	0.2 M NaCl ^b , 30°C	0.2 M NaCl ^c , 25°C	0.15 M NaCl ^d , 25°C	
a	96	126	120	148	123 \pm 19
b	83	107	102	120	103 \pm 13
c	59	83	80	96	80 \pm 13
d	37	58	55	65	54 \pm 10
e	24	39	36	40	35 \pm 6
f	17	28	25	27	24 \pm 4

Molecular masses (M) of samples were calculated from their intrinsic viscosities according to Mark–Houwink equations and expressed as $M \cdot 10^{-4}$.

^a Sodium phosphate buffer (pH 7.3), $[\eta] = 0.057 M^{0.76}$ [5].

^b $[\eta] = 0.039 M^{0.77}$ [6].

^c $[\eta] = 0.0228 M^{0.816}$ [4].

^d $[\eta] = 0.0346 M^{0.779}$ [7].

Table 2
Molecular masses (below 10^5) of hyaluronate samples from two Mark–Houwink equations

Sample	0.2 M NaP, 37°C ^a		0.25 M NaCl, 25°C ^b	
	$[\eta]$	M	$[\eta]$	M
E-1	372	13	425	15
E-2	256	8.8	280	10
E-3	167	6.1	177	6.3
E-4	96	3.9	109	3.9

Molecular mass (M) is expressed as $M \cdot 10^{-4}$ and intrinsic viscosity, $[\eta]$, is given in ml/g.

^a Sodium phosphate buffer (pH 7.3), $[\eta] = 3.0 \cdot 10^{-4} M^{1.20}$ [5].

^b $[\eta] = 2.8 \cdot 10^{-3} M$ [10].

under Experimental. The intrinsic viscosities of hyaluronate samples with such low molecular masses were measured under each given conditions and are listed in Table 2 together with the molecular masses calculated by using the Mark–Houwink relationships mentioned above. Table 2 indicates that the M values for the same sample agree well with each other and therefore suggests

that both equations are suitable. For the determination of molecular masses of hyaluronate samples below $M = 10^5$, Cleland's equation was used because of the same conditions (0.2 M, 25°C) as those for $M > 10^5$.

3.2. Radii of the fibres in Sephacryl gels

An averaged radius of the fibres in Sephacryl networks was determined in a similar manner to that for agarose fibres forming Sepharose gels [1].

Six hyaluronate fractions and BSA with known Stokes radii were separately chromatographed on both columns of Sephacryl S-500 and S-1000. Their available volumes (K) on both gels are given in Table 3 and their Stokes radii (R) are given in square brackets. The values for $(-\log K)^{1/2}$ were plotted against R as shown in Fig. 1. These plots suggested two straight lines crossing at a point of -5.8 nm on the abscissa. As can be seen in Table 3, the log K ratios based on BSA are in good agreement for Sephacryl S-500 and S-1000, and the ratios of log K_{S-1000} to log K_{S-500} [0.60 ± 0.02 (mean \pm S.D.)] are considered to be constant. The observations

Table 3
Relationships between log K values on Sephacryl S-500 and S-1000 and physico-chemical data for sodium hyaluronates

Sample	K	Ratio ^a	Log $K_{S-1000}/$ log K_{S-500}	R (nm)	$[\eta]$ (ml/g)	M ($\times 10^{-4}$)
I	0.19			19.6	1611	88
II	0.26			17.1	1280	66
III	0.34			14.7	915	44
IV	0.38			13.5	732	33
B-1	0.39 (0.19)	4.2 (4.5)	0.57	13.3 [13.4]	723	33 [23.6]
B-3	0.43 (0.25)	3.8 (3.7)	0.61	12.2 [12.0]	504	21 [16.8]
V	0.46			11.6	554	24
E-1	0.48 (0.31)	3.3 (3.2)	0.63	11.0 [11.1]	425	17
E-2	0.56 (0.37)	2.6 (2.7)	0.58	9.2 [8.9]	280	10
E-3	0.63 (0.47)	2.1 (2.0)	0.61	7.6 [7.5]	177	6.3
E-4	0.70 (0.54)	1.6 (1.7)	0.58	5.9 [5.9]	109	3.9
BSA	0.80 (0.69)	1.0 (1.0)	0.60			

Chromatographic data for seven samples on a column of Sephacryl S-500 are given in parentheses. Some R and M values obtained from our previous experiments [1] are given in square brackets for comparison.

^a Log K ratio based on that of BSA.

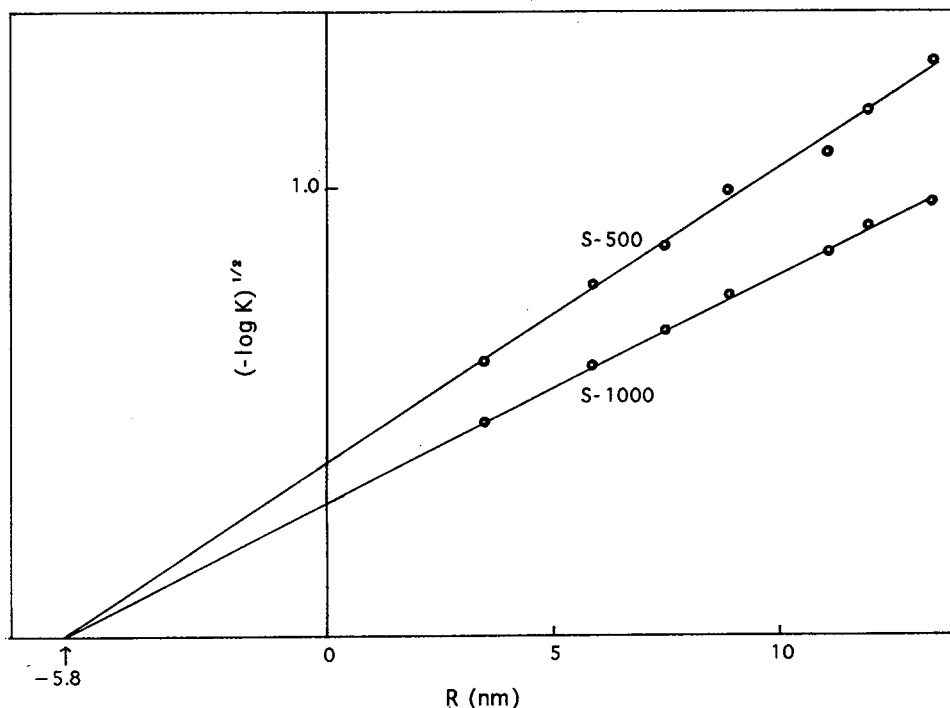


Fig. 1. Relationship between available volume (K) and Stokes radius (R) of six hyaluronate samples and BSA by gel chromatography on Sephacryl S-500 or S-1000. The plots of $(-\log K)^{1/2}$ against R are shown with the use of the K values (B-1, B-3, E-1 to 4 and BSA) in Table 3. These lines were determined by a linear least-squares method.

indicate that Eq. 1 is applicable to both types of Sephacryl gels, S-500 and S-1000.

3.3. Stokes radius and molecular mass of hyaluronic acid

Sodium hyaluronate samples were chromatographed on a column of Sephacryl S-1000 as described. Their Stokes radii (R) were calculated from Eq. 1 by use of the K values, $R(\text{BSA}) = 3.5$ nm and $r = 5.8$ nm. The molecular masses (M) of hyaluronates were calculated using the Mark-Houwink equations given by Cleland and Wang [4] and Cleland [10]; the latter equation was used for samples E-2 to E-4. The R and M values are summarized in Table 3, together with intrinsic viscosities ($[\eta]$). R was plotted against $M^{1/2}$ as shown in Fig. 2. The open circles are our previous results from Sepharose gel chromatog-

raphy [1]. It is reasonable that the open and closed circles overlap in the range of low molecular masses, because the two Mark-Houwink equations give similar values, as seen in Table 2. The equation for each line of closed circles was calculated by a linear least-squares method: $R = 0.030 M^{1/2}$ for the lower range and $R = 0.016 M^{1/2} + 4.3$ for the higher range. A line of open circles with $M > 10^5$, $R = 0.0175 M^{1/2} + 4.82$ [1], is also shown in Fig. 2 for comparison. This different line is due to the lower values of the molecular mass of hyaluronic acid calculated using the Mark-Houwink equation by Shimada and Matsumura [5].

The present method for determining the molecular mass of hyaluronic acid by use of a Sephacryl S-1000 column has the advantage that it needs only a standard of known size such as BSA. However, it is not applicable to the glycos-

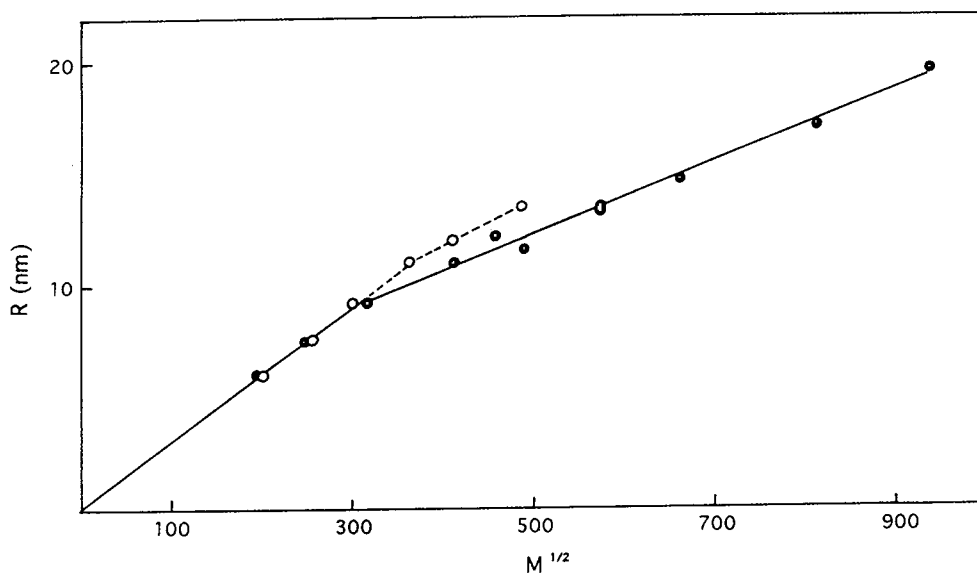


Fig. 2. Stokes radius (R) and molecular mass (M) of hyaluronate samples. The open circles are the data from Sepharose gel chromatography in a previous paper [1].

aminoglycan fraction with a very large size. An upper limit of M may be $1.5 \cdot 10^6$, by assuming $K(\text{hyaluronate}) = 0.10$ and $K(\text{BSA}) = 0.80$ in gel chromatography on Sephacryl S-1000.

Acknowledgement

We are grateful to Seikagaku Kogyo for generously supplying sodium hyaluronate preparations.

References

- [1] E. Shimada and G. Matsumura, *J. Chromatogr.*, 627 (1992) 43.
- [2] T.L. Laurent, M. Ryan and A. Pietruszkiewicz, *Biochim. Biophys. Acta*, 42 (1960) 476.
- [3] E. Shimada and G. Matsumura, *J. Biochem. (Tokyo)*, 81 (1977) 79.
- [4] R.L. Cleland and J.L. Wang, *Biopolymers*, 9 (1970) 799.
- [5] E. Shimada and G. Matsumura, *J. Biochem. (Tokyo)*, 78 (1975) 513.
- [6] Y. Ueno, Y. Tanaka, K. Horie and K. Tokuyasu, *Chem. Pharm. Bull.*, 36 (1988) 4971.
- [7] H. Bothner, T. Waaler and O. Wik, *Int. J. Biol. Macromol.*, 10 (1988) 287.
- [8] J.M. Creeth, *Biochemistry*, 51 (1952) 10.
- [9] J. Bitter and H. Muir, *Anal. Biochem.*, 4 (1962) 330.
- [10] R.L. Cleland, *Biopolymers*, 23 (1984) 647.



ELSEVIER

Journal of Chromatography A, 685 (1994) 178–181

JOURNAL OF
CHROMATOGRAPHY A

Short communication

Silver ion high-performance liquid chromatographic separation of fatty acid methyl esters labelled with deuterium atoms on the double bonds

R.O. Adlof*, E.A. Emken

US Department of Agriculture, Agricultural Research Service, National Center for Agricultural Utilization Research,
Food Quality and Safety Research, 1815 N. University Street, Peoria, IL 61604, USA

First received 30 June 1994; revised manuscript received 19 August 1994

Abstract

Silver ion HPLC (acetonitrile in hexane as solvent) was used to separate non-deuterated fatty acid methyl esters (*cis*-9-octadecenoate, *cis*-9,*cis*-12-octadecadienoate and *cis*-9,*cis*-12,*cis*-15-octadecatrienoate) from their analogues labelled with deuterium atoms on one or more of the double bonds. Placement of the deuterium atoms on the double bonds increased the retention time of the fatty acid methyl esters and could have useful applications in the analysis or isolation of deuterium-labelled fats and other metabolic products produced during the synthesis and metabolism of deuterium-labelled fatty acids. The % composition data, obtained by silver ion HPLC, can be used to evaluate isotopic purity.

1. Introduction

Silver ion high-performance liquid chromatography (Ag-HPLC) is a useful tool for separating a variety of unsaturated compounds by the number, configuration (*cis* vs. *trans*) or position of (location in the molecule) the double bonds [1–5]. Since separation by silver ion chromatography is primarily due to the interaction of the silver ion(s) with the double bond(s) π electrons of the compound, any neighboring group having an effect on the π electron density of the double bond would affect the retention of unsaturated compounds on a silver ion column. This effect

has been documented for olefins and allenes [6] utilizing a silver nitrate–ethylene glycol gas chromatography (GC) column. In addition, steric effects can be inferred during the Ag-HPLC separation of *cis*- and *trans*-pheromone isomers containing branched side-chains adjacent to the double bonds (results not shown). Placement of deuterium atoms on the double bond(s) of fatty acid methyl esters (FAMES) was therefore expected to effect retention times when compared with non-deuterated FAME analogues.

2. Experimental¹

2.1. Materials and reagents

Hexane (Allied Fisher Scientific, Orangeburg, NY, USA) and acetonitrile (ACN; E. Merck,

* Corresponding author.

¹ The mention of firm names or trade products does not imply that they are endorsed or recommended over other firms or similar products not mentioned.

Darmstadt, Germany) were HPLC grade and used as received. Isooctane (E. Merck) was ACS grade. Non-deuterated samples of methyl oleate and methyl linolenate were obtained from NuCheck Prep, Elysian, MN, USA.

2.2. Syntheses

Samples of methyl oleate (18:1; *cis*-9-octadecenoate), methyl linoleate (18:2; *cis*-9,*cis*-12-octadecadienoate) and methyl linolenate (18:3; *cis*-9,*cis*-12,*cis*-15-octadecatrienoate) were prepared with deuterium atoms on one or more of the double bonds. [9,10-²H₂]Methyl oleate (methyl oleate-9,10-d₂) was prepared [7] by reduction (Lindlar catalyst, deuterium gas) of methyl stearolate (9-octadecynoate). Methyl linoleate-12,13-d₂ was synthesized by the reduction (Lindlar catalyst, deuterium gas) of *Crepis alpina* seed oil and subsequent transesterification with HCl-methanol [8]. Since *Crepis alpina* seed oil originally contains about 14% non-deuterated linoleic acid [1.2% 14:0; 4.1% 16:0; 1.0% 18:0; 2.2% 18:1; 2.4% *cis*-9,*trans*-12-18:2; 14.3% 18:2; 74.0% crepenynic (9-*cis*-octadecen-12-ynoic acid)], the methyl linoleate isolated after reduction contained roughly an 80:20 ratio of deuterated to non-deuterated 18:2 and was used as such. Methyl linolenate-9,10,12,13,15,16-d₆ was prepared by the synthesis and subsequent reduction (Lindlar catalyst, deuterium gas) of the triacetylenic precursor [analogous to preparations described in Ref. 9]. Sample FAME mixtures were eluted with petroleum ether through a silica gel Sep-Pak (Waters Assoc., Milford, MA, USA) to remove any oxidation products and dissolved (ca. 10 mg/ml) in isooctane.

2.3. High-performance liquid chromatography

The liquid chromatography system consisted of a ChromSpher Lipids column (catalogue No. 28313; 250 mm × 4.6 mm I.D. stainless steel; 5 μm particle size; silver ion impregnated) purchased from Chrompack (Middelburg, Netherlands), a Spectra-Physics (Freemont, CA, USA) P2000 solvent-delivery system, a Rheodyne (Cotati, CA, USA) 7125 injector with a 20-μl injection loop and an ISCO (Lincoln, NE, USA)

V4 UV absorbance detector at 206 nm. A strip-chart recorder (Houston Instruments, Austin, TX, USA) was used during sample collection, etc., while a recording integrator (Model 3390A; Hewlett-Packard, Avondale, PA, USA) was included during method reproducibility studies. Samples were eluted under isocratic solvent conditions (ACN in hexane); solvent flow was standardized at 1.0 ml/min. Solvent compositions and injected sample sizes are presented in Fig. 1.

2.4. Analyses

FAME fractions were collected from the HPLC and analyzed in triplicate by GC. GC-mass spectrometry (MS) was used to determine the % deuterated and non-deuterated FAMES. Analyses were made on a Hewlett-Packard Model 5890A GC-MS system (quadrupole; positive chemical ionization mode; isobutane as ionizing gas) equipped with a 30 m × 0.25 mm Supelcowax 10 fused-silica capillary column (Supelco, Bellefonte, PA, USA). Data collection and manipulation have been described previously [10].

3. Results

Fig. 1 illustrates the Ag-HPLC elution patterns observed with deuterated and non-deuterated methyl oleate, linoleate and linolenate. In all examples, the non-deuterated isomer eluted first. Retention times of the deuterated FAME (compared to the non-deuterated analogue) increased as the number of deuterium-containing double bonds increased. The separation of the methyl oleate-d₀/-9,10-d₂ and methyl linoleate-d₀/-12,13-d₂ pairs was incomplete (Fig. 1A and B), but baseline separation of methyl linolenate-d₀ and -9,10,12,13,15,16-d₆ (Fig. 1C) was achieved.

The methyl linoleate-d₀ and -d₂ mixture used to generate Fig. 1B was analyzed in triplicate and the results were compared with composition data obtained by GC-MS. The percentages obtained by Ag-HPLC for -d₀ (20.8 ± 1.9) and -d₂ (79.1 ± 1.8) are similar (less than 2% of -d₂

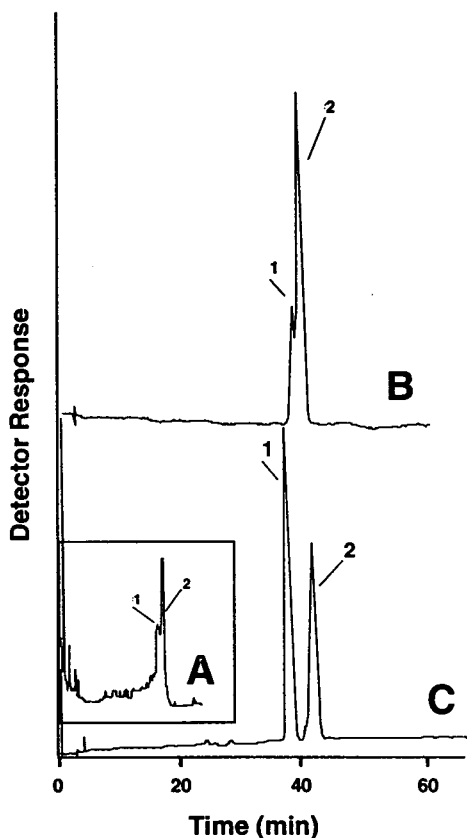


Fig. 1. Separation of deuterium-labelled and unlabelled FAMES. (A) Methyl oleate- d_0 and -9,10- d_2 ; sample injected: 5 μ l (1:3, w/w; 10 mg/ml isooctane); flow-rate: 1.0 ml/min of 0.07% ACN in hexane; UV detector at 206 nm; chart speed: 20 cm/h; peaks: 1 = oleate- d_0 ; 2 = oleate-9,10- d_2 . (B) Methyl linoleate- d_0 and -12,13- d_2 ; sample injected: 0.5 μ l (1:4, w/w; 10 mg/ml isooctane); flow-rate: 1.0 ml/min of 0.1% ACN in hexane; UV detector at 206 nm; chart speed: 10 cm/h; peaks: 1 = linoleate- d_0 ; 2 = linoleate-12,13- d_2 . (C) Methyl linolenate- d_0 and -9,10,12,13,15,16- d_6 ; sample injected: 1.0 μ l (2:1, w/w; 7 mg/ml isooctane); flow-rate: 1.0 ml/min of 0.2% ACN in hexane; UV detector at 206 nm; chart speed: 10 cm/h; peaks: 1 = linolenate- d_0 ; 2 = linolenate-9,10,12,13,15,16- d_6 .

peak area) to the results obtained by GC-MS (19.3 and 80.7, respectively).

4. Discussion

No simple theory exists to predict the influence of substituents on the stability of the

complex formed between silver ions and olefinic double bonds. Both steric effects and effects due to substituents that increase or decrease the electron density of the double bond have been suggested as explanation for observed differences in the stability of Ag-olefin complexes [6]. The fractionation of unsaturated FAMES with deuterium atoms on the double bond(s) from their non-deuterated analogues by Ag-HPLC may be explained in part by changes in the stability of the complex formed between the Ag ions and the π -electrons of the double bond (see Refs. [11] and [12] for reviews of this topic). The increased electron release to the double bond by the stronger C- 2 H bonds (compared with C-H bonds) would result in increased Ag-complex stability. Thus substrates with deuterium atoms on the double bonds should be retained longer by Ag-HPLC.

The elution order of deuterium-labelled and non-labelled FAMES obtained by Ag-HPLC differs from the elution patterns obtained by capillary GC [13]. On both polar and non-polar capillary GC columns, the deuterium-labelled FAME elute first. Similar fractionations and elution orders have been documented in the separation of deuterated and non-deuterated carotenoids by reversed-phase HPLC [14]. The fractionation described in these examples occurs even when the deuterium atoms are not located on double bonds. With Ag-HPLC, however, the elution order is reversed, with non-deuterated FAMES eluting before their deuterated analogues.

This technology may have future applications in the analysis and isolation of deuterium-labelled fats and other metabolic products produced during the metabolism of deuterium-labelled precursors. Work is currently underway to develop semi-preparative applications.

References

- [1] W.W. Christie, *J. High Resolut. Chromatogr. Chromatogr. Commun.*, 10 (1987) 148.
- [2] W.W. Christie and G.H. McG. Breckenridge, *J. Chromatogr.*, 469 (1989) 261.
- [3] B. Nikolova-Damyanova, B.G. Herslof and W.W. Christie, *J. Chromatogr.*, 609 (1992) 133.

- [4] W.W. Christie, E.Y. Brechany and K. Stefanov, *Chem. Phys. Lipids*, 46 (1988) 127.
- [5] R.O. Adlof, *J. Chromatogr.*, 659 (1994) 95.
- [6] R.J. Cvetanovic, F.J. Duncan, W.E. Falconer and R.S. Irvin, *J. Am. Chem. Soc.*, 87 (1965) 1827.
- [7] R.O. Adlof and E.A. Emken, *J. Label. Comp. Radiopharm.*, 21 (1984) 75.
- [8] R.O. Adlof and E.A. Emken, *J. Am. Oil Chem. Soc.*, 70 (1993) 817.
- [9] W.H. Kunau, H. Lehmann and R. Gross, *Z. Physiol. Chem.*, 352 (1971) 542.
- [10] W.K. Rohwedder, E.A. Emken and D.J. Wolf, *Lipids*, 20 (1985) 303.
- [11] A.F. Thomas, *Deuterium Labeling in Organic Chemistry*, Appleton-Century-Crofts, New York, 1971, pp. 402ff.
- [12] C.L. de Ligny, *Adv. Chromatogr.*, 14 (1976) 284–294.
- [13] W.K. Rohwedder, S.M. Duval, D.J. Wolf and E.A. Emken, *Lipids*, 25 (1990) 401.
- [14] R. Baweja, *J. Liq. Chromatogr.*, 9 (1986) 2609.



ELSEVIER

Journal of Chromatography A, 685 (1994) 182–188

JOURNAL OF
CHROMATOGRAPHY A

Short communication

Single-run analysis of isomers of retinoyl- β -D-glucuronide and retinoic acid by reversed-phase high-performance liquid chromatography

Jörn Oliver Sass*, Heinz Nau

Institut für Toxikologie und Embryopharmakologie, Freie Universität Berlin, Garystrasse 5, D-14195 Berlin, Germany

First received 16 June 1994; revised manuscript received 23 August 1994

Abstract

Reversed-phase HPLC methods capable of separating several retinoic acid isomers are generally not designed for simultaneous analysis of isomers of other classes of retinoids. A reversed-phase HPLC method is presented which allows the separation of at least four retinoic acid (RA) isomers (13-*cis*-RA, 9,13-*dicis*-RA, 9-*cis*-RA, all-*trans*-RA) and of all isomers of retinoyl- β -D-glucuronide (RAG), which have been observed in vivo (13-*cis*-RAG, 9-*cis*-RAG, all-*trans*-RAG). The recovery of retinoids was generally between 80 and 90%. Intra-day reproducibility (expressed as relative standard deviation) was $\leq 7.0\%$. As little as 0.25 ng of RA isomers and of all-*trans*-RAG could be detected. This method allowed the study of the metabolism of 9-*cis*-retinoids, where isomerization reactions play a predominant role.

1. Introduction

Retinoids, derivatives of vitamin A alcohol (retinol), are involved in several physiological processes such as embryonic development, growth promotion, differentiation and vision [1,2]. Some retinoids have also attracted attention as important agents in dermatology [3] and oncology [4]. Three geometric isomers of vitamin A acid (retinoic acid, RA) have been found to be endogenously present in blood or tissues of animals and humans: all-*trans*-RA [5–7], 13-*cis*-RA [6,7] and 9-*cis*-RA [8,9] (Fig. 1).

It has been suggested that the retinoid action is mediated by the interaction of retinoids with

retinoid receptors and cellular retinoic acid binding proteins [1,8]. The various geometric isomers of the retinoic acid structure exhibit great differences towards the retinoic acid binding sites [10–12]. After administration of pharmacologic doses of all-*trans*-, 13-*cis*- and 9-*cis*-RA or 9-*cis*-retinaldehyde, the corresponding retinoyl- β -D-glucuronides (RAG) (Fig. 1) have been characterized as major plasma metabolites in monkeys, rats, mice and rabbits [13–20]. Recently, we have observed the in vivo formation of a further RA isomer: 9,13-*dicis*-RA (Fig. 1) was identified as a major metabolite after administration of 9-*cis*-RA and 9-*cis*-retinaldehyde to mice and rats [19,20]. Isomerization plays a major role in the metabolism of 9-*cis*-retinoids. Although some researchers have achieved separation of up

* Corresponding author.

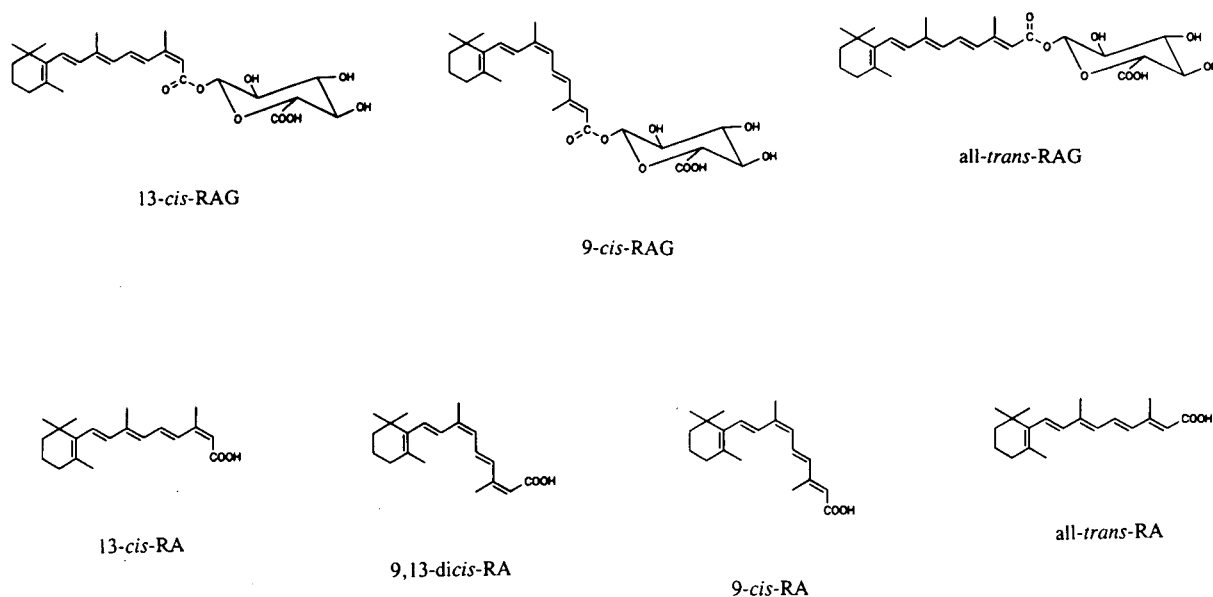


Fig. 1. Structures of isomers of retinoyl- β -D-glucuronide (RAG) and retinoic acid (RA).

to nine photoisomerization products of retinoic acid [21–23], the reversed-phase HPLC methods which are generally applied for analysis of biological samples, do not separate 9,13-dicis-RA from 13-cis-RA. Furthermore, the methods developed for separation of RA photoisomers are not designed for separation of isomers of retinoyl- β -D-glucuronides.

We have recently reported the separation of 9-cis-RAG from 13-cis- and all-trans-RAG using the HPLC method described by Collins et al. [24]. However, this method did not allow the separation of 13-cis-RA and 9,13-dicis-RA, and provided only limited separation of 13-cis-RA and 9-cis-RA as well as of 9-cis-RAG and all-trans-RAG.

We describe here a reversed-phase HPLC method, which allows the simultaneous analysis of all isomers of RAG and RA, which have been reported to be formed in mammalian species. This method has been used for analysis of photoisomers of RAG and RA and for examinations of the metabolism of retinoids, in particular of 9-cis-retinoids.

2. Experimental

2.1. Chemicals

Retinoic acid isomers as well as 4-oxoretinoic acids and all-trans-3,4-didehydroretinoic acid were provided by Hoffmann-La Roche (Basle, Switzerland; and Nutley, NJ, USA). All-trans-RAG was synthesized by Rühl [25] based on the method of Barua and Olson [26]. Isomers of RAG were prepared in a quartz cuvette by irradiation (30 min at room temperature) of a solution of all-trans-RAG in dimethyl sulfoxide or methanol–dimethyl sulfoxide, using a DESAGA duo-UV source (Desaga, Heidelberg, Germany) set to 366 nm. The RAG isomers were isolated using the newly developed HPLC method described herein and identified by enzymatic hydrolysis with β -glucuronidase (Boehringer Mannheim, Germany) [18], which yielded the corresponding retinoic acids. Bovine serum albumin (BSA; retinoid free) was obtained from Sigma (Deisenhofen, Germany).

Acetonitrile (HPLC grade) and all other chemicals (analytical grade) were purchased from Merck (Darmstadt, Germany). Water was purified with a Milli-Q system (Millipore, Eschborn, Germany).

Laboratory precautions. Due to the light sensitivity of retinoids, all work with these compounds was performed under dim amber light.

2.2. Animal experiment

Pregnant Wistar rats (gestational day 13) received a single intragastric dose of 100 mg 9-*cis*-RA per kg body mass. 9-*cis*-RA was suspended in peanut oil and a dosing volume of 5 ml/kg was administered. Two hours after treatment blood was collected and plasma was prepared from the heparinized blood by centrifugation at 4°C (1500 g for 10 min) [20].

2.3. Instrumentation and chromatographic conditions

The HPLC equipment used consisted of two type 64 pumps controlled by a gradient programmer 50B, a dynamic mixing chamber (all from Knauer, Berlin, Germany), a DEGASYS DG-1200 degasser (vds-optilab, Berlin, Germany), two Shimadzu UV detectors (SPD-6A and SPD 6-AV) for detection at 340 and 356 nm and a C-R4A integrator (Shimadzu, Duisburg, Germany). After the mixing chamber, the eluent mixture passed through a C-130B precolumn filled with Perisorb RP-18 material (Upchurch Scientific, Oak Harbour, WA, USA) and an on-line eluent filter (Knauer) before reaching an advanced automated sample processor (AASP; Varian, Darmstadt, Germany), which was followed by a second filter and a self-packed analytical column (120 × 4 mm), filled with Spherisorb ODS2 3 μm (silica modified with octadecyl groups, endcapped; Phase Separations, Deeside, UK). During chromatography, the analytical column was heated to 60°C. Analysis was performed with a multilinear gradient (Table 1) of solvent A [water with 0.2% (v/v) trifluoro-

Table 1
Composition of mobile phase (multilinear binary gradient)

Time (min)	A (%)	B (%)
0	70	30
30	25	75
35.5	25	75
36	1	99
39	1	99
39.5	70	30
42.5	70	30

Solvent A: water with 0.2% (v/v) trifluoroacetic acid; solvent B: acetonitrile with 0.2% (v/v) trifluoroacetic acid.

acetic acid] and solvent B [acetonitrile with 0.2% (v/v) trifluoroacetic acid] at a flow-rate of 0.7 ml/min. Between the analyses (run time 36 min) the column was washed with 99% of solvent B and subsequently re-equilibrated (cycle time 42.5 min). Injection was performed by introducing an AASP C2 cartridge (silica modified with ethyl groups; ICT, Bad Homburg, Germany), which was loaded with analytes, into the stream of mobile phase. The cartridge remained the whole run time in the AASP system. Before and after analysis the cartridge was purged with 500 μl of water.

2.4. Sample preparation

Sample enrichment was performed as recently described [24]. In brief, 125 μl of sample were mixed with 375 μl of isopropanol and shortly centrifuged; 400 μl of the supernatant were diluted with a threefold volume of 2% (w/v) aqueous ammonium acetate solution and poured with a nitrogen stream through a preconditioned AASP C2 cartridge. After washing with 1.5 ml of a mixture of 85% aqueous ammonium acetate solution (0.5%) and 15% acetonitrile the cartridge was loaded onto the AASP.

2.5. System validation

Standards for system validation as well as for calibration were prepared by spiking a filtered

5% (w/v) BSA solution with known amounts of reference retinoids (13-*cis*-RA, 9-*cis*-RA, all-*trans*-RA, all-*trans*-RAG). To determine recovery, peak areas of the standards were compared to those obtained after direct injection of respective amounts of retinoids. Reproducibility was tested on three subsequent days using standards with 15, 150 and 1500 ng/ml of 13-*cis*-RA, 9-*cis*-RA, all-*trans*-RA and all-*trans*-RAG. To examine linearity, further standards were analyzed which contained 2.5, 5, 50 and 500 ng/ml of each retinoid. Linear regression was performed by least squares analysis of the peak absorbance units and retinoid concentrations of the BSA standards. Quantification of retinoids in routine analysis was based on three standard concentrations, which covered the expected retinoid concentrations of the corresponding application. Concentrations of 9,13-*dicis*-RA were calculated using the standard values for 13-*cis*-RA at the 340 nm detection wavelength.

3. Results and discussion

The chromatogram in Fig. 2 demonstrates the separation of isomers of RAG and RA by the newly developed HPLC method. The corresponding k' values are given in Table 2. Fig. 3 shows a chromatogram of a plasma sample

Table 2
Retention factors (k') and resolution (R_s) of adjacent peaks (derived from Fig. 2)

Retinoid	k'	R_s
13- <i>cis</i> -RAG	11.78	1.22
9- <i>cis</i> -RAG	12.00	2.01
All- <i>trans</i> -RAG	12.33	
13- <i>cis</i> -RA	16.82	1.18
9,13- <i>dicis</i> -RA	17.05	1.51
9- <i>cis</i> -RA	17.35	2.43
All- <i>trans</i> -RA	17.89	

The resolution of two adjacent peaks (R_s) was calculated from the equation $R_s = 1.18(t_{R2} - t_{R1}) / (w_{1/2}^1 + w_{1/2}^2)$ with $w_{1/2}$ being the peak width at half maximum peak height.

obtained from a pregnant rat on gestational day 13 2 h after oral treatment with 100 mg/kg 9-*cis*-RA. Here the different isomers of RA and RAG are also well separated. Details on the metabolism of 9-*cis*-RA will be presented elsewhere [20]. The HPLC method allows also the detection of 4-oxo-retinoic acids. 13-*cis*-4-Oxo-RA, which is endogenously present in human blood [7], elutes 3 to 3.5 min before all-*trans*-RAG, but no reliable separation of the different

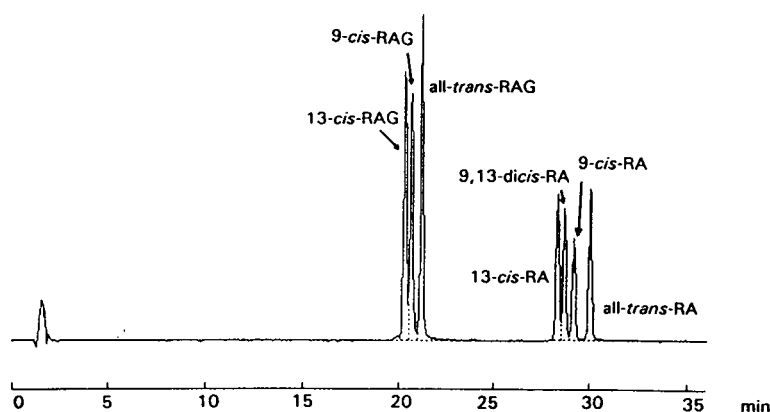


Fig. 2. Chromatogram of reference retinoids. Detection at 356 nm. A mixture of 13-*cis*-RAG, 9-*cis*-RAG, all-*trans*-RAG, 13-*cis*-RA, 9,13-*dicis*-RA, 9-*cis*-RA and all-*trans*-RA (total amount of each RAG isomer 40–50 ng, and of each RA isomer 14–18 ng) was submitted to solid-phase extraction and subsequently analyzed by reversed-phase HPLC, using the system described in the Experimental section.

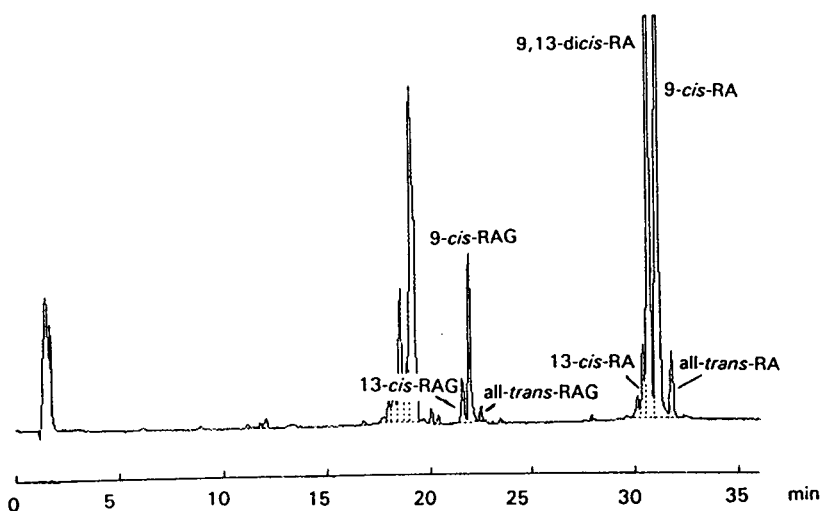


Fig. 3. Chromatogram of 100 μ l rat plasma, obtained from a pregnant rat (gestational day 13) 2 h after oral treatment with 100 mg 9-*cis*-RA per kg body mass. Detection at 356 nm. Retinoid concentrations: 13-*cis*-RAG: 60.2 ng/ml; 9-*cis*-RAG: 210 ng/ml; all-*trans*-RAG: 15.3 ng/ml; 13-*cis*-RA: 53.2 ng/ml; 9,13-*dicis*-RA: 591 ng/ml; 9-*cis*-RA: 768 ng/ml; all-*trans*-RA: 43.5 ng/ml.

isomers was achieved for 4-oxo-retinoic acids. In addition to the three RAG isomers which were also found *in vivo*, photoisomerization of all-*trans*-RAG also resulted in a fourth β -glucuronide ($k' = 11.54$), as indicated by enzymatic hydrolysis with β -glucuronidase, which yielded a compound eluting slightly in front of 13-*cis*-RA. Our method can also resolve 13-*cis*-RA from the preceding peak of all-*trans*-3,4-didehydroretinoic acid ($R_s = 2.07$) (data not shown).

Examination of linearity based on standards with 15, 150 and 1500 ng/ml retinoids yielded a coefficient of regression ≥ 0.9999 for all four retinoids all-*trans*-RAG, 13-*cis*-, 9-*cis*- and all-*trans*-RA on three consecutive days. If the four further standard concentrations were included into the regression analysis (2.5 to 1500 ng/ml) the coefficient of regression was ≥ 0.999 for all-*trans*-RAG, 13-*cis*-, all-*trans*-RA and 0.9517 for 9-*cis*-RA. As little as 0.25 ng/100 μ l of each retinoid could well be detected (signal-to-noise ratio > 10).

Table 3 demonstrates the recovery values obtained for the retinoid concentrations 15, 150 and 1500 ng/ml. Recovery was generally between 80 and 90%. The corresponding values for intra-day variation (relative standard deviation,

R.S.D.) are presented in Table 4. In comparison, the R.S.D. for direct injection of respective amounts of retinoids is about 4%. Table 4 contains also values for inter-day variation. These values are below 3% for all RA isomers at the highest concentration level examined and reach 10% for the lowest RA concentrations.

The described HPLC system allows rapid and simple resolution of all four RA isomers, which have been detected *in vivo*, and furthermore provides single-run separation of several RAG isomers. This method is suitable for analysis of a

Table 3

Recovery (compared with direct injections of the respective amount of retinoids)

Retinoid	Recovery (%)		
	15 ng/ml	150 ng/ml	1500 ng/ml
13- <i>cis</i> -RA	81.7	87.5	83.0
9- <i>cis</i> -RA	82.4	85.6	84.3
All- <i>trans</i> -RA	79.0	86.3	84.0
All- <i>trans</i> -RAG	77.9	83.2	80.7

Analysis of BSA standard samples with 15, 150 and 1500 ng/ml of 13-*cis*-RA, 9-*cis*-RA, all-*trans*-RA and all-*trans*-RAG. (Values given are based on the mean peak area values of 6 standard samples and 6 direct injections.)

Table 4
Intra-day and inter-day reproducibility expressed as R.S.D.

Retinoid	Intra-day R.S.D. (%) (n = 6)			Inter-day R.S.D. (%) (n = 3)		
	15 ng/ml	150 ng/ml	1500 ng/ml	15 ng/ml	150 ng/ml	1500 ng/ml
13- <i>cis</i> -RA	6.4	1.6	3.4	7.9	5.3	2.3
9- <i>cis</i> -RA	3.9	1.7	2.6	9.7	3.8	2.4
All- <i>trans</i> -RA	7.0	1.6	2.4	10.4	2.3	1.7
All- <i>trans</i> -RAG	2.2	2.1	1.7	12.1	2.7	13.1

Data are given for three concentrations of retinoids: 15, 150 and 1500 ng/ml.

variety of samples and is applied in our laboratory to determine retinoid concentrations in plasma and tissues as well as in microsomal preparations used for examining in vitro glucuronidation of RA isomers.

Acknowledgements

We are grateful to Ms. C. Plum for committed technical assistance. Mr. G. Tzimas provided helpful suggestions on the manuscript. We thank Dr. M. Klaus and Dr. A.A. Levin of Hoffmann-La Roche for providing retinoids as well as Mr. R. Rühl for the synthesis of all-*trans*-RAG. Ms. U. Schwikowski did the photographic work. Financial support was granted by the Deutsche Forschungsgemeinschaft (Sfb 174, C6), C.I.R.D Galderma and the European Commission (BIOTECH program BIO2TC-CT930471).

References

- [1] L.M. De Luca, *FASEB J.*, 5 (1991) 2924.
- [2] J.C. Saari, in M.B. Sporn, A.B. Roberts and D.S. Goodman (Editors), *The Retinoids: Biology, Chemistry, and Medicine*, Raven Press, New York, 1994, pp. 351–385.
- [3] A. Vahlquist, in R. Blomhoff (Editor), *Vitamin A in Health and Disease*, Marcel Dekker, New York, 1994, pp. 365–424.
- [4] M.A. Smith, D.R. Parkinson, B.D. Cheson and M.A. Friedman, *J. Clin. Oncol.*, 10 (1992) 839.
- [5] A.M. McCormick and J.L. Napoli, *J. Biol. Chem.*, 257 (1982) 1730.
- [6] G. Tang and R.M. Russell, *J. Lipid Res.*, 31 (1990) 175.
- [7] C. Eckhoff and H. Nau, *J. Lipid Res.*, 31 (1990) 1445.
- [8] A.A. Levin, L.J. Sturzenbecker, S. Kazmer, T. Bosakowski, C. Huselton, G. Allenby, J. Speck, C. Kratzeisen, M. Rosenberger, A. Lovey and J.F. Grippo, *Nature*, 355 (1992) 359.
- [9] R.A. Heyman, D.J. Mangelsdorf, J.A. Dyck, R.B. Stein, G. Eichele, R.M. Evans and C. Thaller, *Cell*, 68 (1992) 397.
- [10] A.A. Levin, T. Bosakowski, S. Kazmer and J.F. Grippo, *Toxicologist*, 12 (1992) 181.
- [11] G. Allenby, M.-T. Bocquel, M. Saunders, S. Kazmer, J. Speck, A. Rosenberger, A. Lovey, P. Kastner, J.F. Grippo, P. Chambon and A.A. Levin, *Proc. Natl. Acad. Sci. U.S.A.*, 90 (1993) 30.
- [12] G. Siegenthaler and J.-H. Saurat, in R. Marks and G. Plewig (Editors), *Acne and Related Disorders*, Martin Dunitz, London, 1989, pp. 169–174.
- [13] J. Creech Kraft, W. Slikker, Jr., J.R. Bailey, L.G. Roberts, B. Fischer, W. Wittfoht and H. Nau, *Drug Metab. Dispos.*, 19 (1991) 317.
- [14] A.B. Barua, D.B. Gunning and J.A. Olson, *Biochem. J.*, 277 (1991) 527.
- [15] M.D. Collins, G. Tzimas, H. Hummler, H. Bürgin and H. Nau, *Toxicol. Appl. Pharmacol.*, 127 (1994) 132.
- [16] J. Creech Kraft, Chr. Eckhoff, D.M. Kochhar, G. Bochert, I. Chahoud and H. Nau, *Teratogen. Carcinogen. Mutagen.*, 11 (1991) 21.
- [17] G. Tzimas, H. Bürgin, M.D. Collins, H. Hummler and H. Nau, *Arch. Toxicol.*, 68 (1994) 119.
- [18] J.O. Sass, G. Tzimas and H. Nau, *Life Sci.*, 54 (1994) PL69.
- [19] G. Tzimas, J.O. Sass, W. Wittfoht, M.M.A. Elmazar, K. Ehlers and H. Nau, *Drug Metab. Dispos.*, 22 (1994), in press.
- [20] J.O. Sass, G. Tzimas, M.M.A. Elmazar and H. Nau, in preparation.
- [21] M.G. Motto, K.L. Facchine, P.F. Hamburg, D.J. Burinsky, R. Dunphy, A.R. Oyler and M.L. Cotter, *J. Chromatogr.*, 481 (1989) 255.
- [22] A. Baillet, L. Corbeau, P. Rafidison and D. Ferrier, *J. Chromatogr.*, 634 (1993) 251.

- [23] A.R. Sundquist, W. Stahl, A. Steigel and H. Sies, *J. Chromatogr.*, 637 (1993) 201.
- [24] M.D. Collins, C. Eckhoff, I. Chahoud, G. Bochert and H. Nau, *Arch. Toxicol.*, 66 (1992) 652–659.
- [25] R. Rühl, *Diplomarbeit (Thesis)*, Fachbereich Chemie, Freie Universität Berlin, Berlin, 1993.
- [26] A.B. Barua and J.A. Olson, *Biochem. J.*, 263 (1989) 403.



ELSEVIER

Journal of Chromatography A, 685 (1994) 189–194

JOURNAL OF
CHROMATOGRAPHY A

Short communication

Formation of Schiff bases with acetone as a solvent in the determination of anilines

M. Kolb, M. Bahadir*

*Institute of Ecological Chemistry and Waste Analysis, Technical University of Braunschweig, Hagenring 30,
D-38106 Braunschweig, Germany*

First received 5 May 1994; revised manuscript received 28 July 1994

Abstract

The formation of Schiff bases, when using acetone as solvent in the determination of aniline and substituted basic anilines, was verified by GC–MS and GC–Fourier transform measurements. These reaction products are detected as additional peaks in GC, impairing calibration and quantification.

1. Introduction

Several papers have been published dealing with direct GC procedures for the determination of polar organic compounds such as chlorinated anilines and phenols [1–4]. Such polar compounds are determined utilizing certain capillary columns without being derivatized.

In residue analyses, acetone is a widely used solvent for extraction and clean-up procedures in analytical chemistry, because of its volatility and wide ability to dissolve different compounds, and for mixing with other solvents. Sometimes it is also used to dissolve polar reference substances. However, its volatility and effect as a sensitizer for photochemical reactions [5] can impair analytical results. We have detected two peaks in gas chromatograms of 4-chloroaniline standards that were dissolved in hexane–acetone mixtures. The peak ratio changed over several days, preventing

reliable calibration and quantification. This suggested a reaction of 4-chloroaniline. Böer et al. [2] also reported additional peaks in gas chromatograms of acetone eluates of substituted anilines after solid-phase extraction on RP-18 material. They concluded that the formation of Schiff bases (ketimines) was responsible for these peaks. However, other workers have utilized acetone as a solvent for substituted anilines, which are used as internal standards [6], or as an eluting solvent combined with methylene chloride in adsorption chromatography on silica gel as part of an analytical method for priority pollutants including anilines, without reporting additional peaks [7]. The preparative synthesis of ketimines with various anilines (aniline, 4-chloroaniline, 4-bromoaniline, etc.) and acetone at room temperature using a dehydrating agent has been reported [8]. In this work, various substituted anilines were investigated to establish whether they react in standard solutions with acetone to Schiff bases, as postulated.

* Corresponding author.

2. Experimental

2.1. Chemicals

Acetone and hexane were obtained from Baker (Deventer, Netherlands), diethyl ether from Promochem (Wesel, Germany) and aniline, 4-isopropylaniline (4-IPA), 2-chloroaniline (2-CA), 3-chloroaniline (3-CA), 4-chloroaniline (4-CA), 2,4-dichloroaniline (2,4-DCA), 3,4-dichloroaniline (3,4-DCA), 2,4,5-trichloroaniline (2,4,5-TCA), 4-bromoaniline (4-BA) and ben-zidine from Amchro (New Haven, CT, USA).

2.2. Preparation of standard solutions

Standard solutions of the investigated anilines were prepared at a concentration of $1 \mu\text{g}/\mu\text{l}$ by dissolving 10 mg of the aniline in 1 ml of diethyl-ether and diluting to 10 ml with hexane.

2.3. Gas chromatography with flame ionization (GC-FID) and nitrogen-phosphorus detection (GC-NPD)

An HP 5890 Series II gas chromatograph equipped with an HP 7673 autosampler (Hewlett-Packard, Avondale, PA, USA), a flame ionization detector and a DB-5 fused-silica capillary column ($30 \text{ m} \times 0.25 \text{ mm}$ I.D.; $0.25 \mu\text{m}$ film thickness) (J&W Scientific, Folsom, CA, USA) was employed. The carrier gas was helium at a flow of 1 ml/min. The column temperature was programmed from 60°C (1 min isothermal) to 190°C at $8^\circ\text{C}/\text{min}$ and then to 260°C at $10^\circ\text{C}/\text{min}$. Injection was performed in the splitless mode at an injector temperature of 260°C . The detector was operated at 280°C with hydrogen at 30 ml/min and synthetic air at 350 ml/min as burning gases and nitrogen at 30 ml/min as make-up gas. A second HP 5890 Series II gas chromatograph was equipped with a nitrogen-phosphorus detector and a Stabilwax-DB fused-silica capillary column ($15 \text{ m} \times 0.25 \text{ mm}$ I.D.; $0.1 \mu\text{m}$ film thickness) (Restek, Bellefonte, PA, USA). Helium was used as the carrier gas at a flow-rate of 1.2 ml/min. The column tempera-

ture was programmed from 100°C (1 min isothermal) at $5^\circ\text{C}/\text{min}$ to 200°C , held for 5 min, and then at $25^\circ\text{C}/\text{min}$ to 230°C , held for 5 min. Injection was performed manually in the splitless mode. The injector temperature was 250°C . The detector was operated at 250°C with hydrogen at 3 ml/min and synthetic air at 100 ml/min as burning gases and nitrogen at 30 ml/min as make-up gas.

2.4. Gas chromatography-mass spectrometry (GC-MS)

An HP 5890 A Series II gas chromatograph was interfaced to an HP 5971 A mass-selective detector. The gas chromatograph was equipped with an HP 7673 autosampler and an Ultra-1 fused-silica capillary column ($25 \text{ m} \times 0.2 \text{ mm}$ I.D.; $0.33 \mu\text{m}$ film thickness) (Hewlett-Packard). Helium was used as the carrier gas at a flow-rate of 0.8 ml/min. The temperature programme was the same as in GC-FID. Injection was performed in the splitless mode at an injector temperature of 260°C . The temperature of the transfer line was 280°C and the temperature of the mass spectrometer was 185°C . The mass spectrometer was operated in the electron impact mode at 70 eV and in the scan range 50–500 u. The multiplier voltage was 1.75 kV.

2.5. Gas chromatography-Fourier transform infrared spectrometry (GC-FT-IR)

GC-FT-IR was performed on an HRGC 5160 gas chromatograph (Carlo Erba, Milan, Italy), which was interfaced to a model 740 FT-IR spectrometer (Nicolet, Madison, WI, USA). The gas chromatograph was equipped with a DB-1 fused-silica capillary column ($30 \text{ m} \times 0.25 \text{ mm}$ I.D., $0.32 \mu\text{m}$ film thickness) (J & W Scientific). The carrier gas was helium at a head pressure of 150 kPa and the temperature programme was the same as in GC-FID. Injection was performed manually in the splitless mode at an injector temperature of 260°C . The transfer line was at 200°C and the light pipe at 200°C .

2.6. Procedures

A

About 15 ml of hexane were placed in 20-ml graduated flasks, then 200 μl of aniline standard solution were added to each flask, followed by 200 μl of acetone after mixing. The flask was filled up to 20 ml with hexane and shaken immediately. The mixtures were kept at 22°C. After 1, 2, 4 or 6 h, depending on the reaction rate, 0.5 ml of each mixture was transferred into GC vials and analysed by GC-FID. Further, part of each mixture was transferred into vials and analysed periodically, first at intervals of about 4 h and later at longer intervals of 8–24 h. This procedure was repeated for a period of 7 days. Acetone–aniline mixtures that provided GC-FID traces with additional peaks were analysed by GC-EI-MS for identification of these peaks. To confirm the GC-MS results, the solutions were also analysed by GC-FT-IR.

B

A 70-ml volume of water was spiked with 200 μl of either 4-CA or aniline standard solution. After adding 100 ml of acetone and 50 ml of hexane, the solutions were extracted on a horizontal shaker for 12 h (frequency 250 min^{-1}). The mixture was transferred into a separating funnel, mixed with 20 g of sodium-chloride and extracted with 30 ml of dichloromethane. The organic phase was separated, dried and evaporated and the residue was dissolved in 2 ml cyclohexane–ethyl acetate. These samples were analysed by GC-EI-MS.

3. Results and discussion

A 4-CA solution was analysed by GC-MS for the identification of the two peaks that were observed in GC-FID and GC-NPD (see Fig. 1). The mass spectra are presented in Fig. 2. The first peak gave a mass spectrum with a base peak of m/z 127 and an isotope peak of m/z 129. It could be assigned to chloroaniline. The molecular ion of the second peak was 40 u heavier than the molecular ion of 4-CA and showed the same

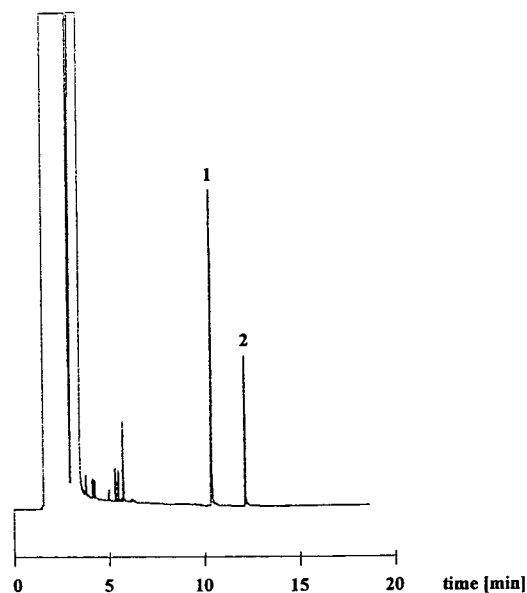


Fig. 1. GC-FID of a 4-CA solution (10 $\text{ng}/\mu\text{l}$) in hexane–acetone. Peaks: 1 = 4-CA; 2 = additional peak (Schiff base). Column, fused-silica coated with DB-5 bonded stationary phase (30 m \times 0.25 mm I.D., 0.25 μm film thickness); carrier gas, helium at 1.0 ml/min; temperature programme, from 60°C (1 min) at 8°C/min to 190°C and at 10°C/min to 260°C; injection, splitless (0.75 min) at 260°C.

chlorine cluster (m/z 167, 169). Additional information could be obtained from the fragmentations. The mass difference between the molecular and the fragment ion of 56 u pointed to the elimination of a $\text{C}_3\text{H}_6\text{N}$ fragment. The second fragment ion (m/z 152, 154) could be traced to the elimination of a CH_3 group. The detection of an additional peak using NPD confirmed that the compound contained nitrogen. From this information, the compound could be identified as Schiff base of 4-CA. The formation of the Schiff base could be verified by GC-FT-IR measurement. The IR spectrum of 4-CA exhibited two weak absorption bands with stretching vibrations at 3503 and 3411 cm^{-1} , which are characteristic of primary amines, and one band of medium intensity at 1623 cm^{-1} arising from the N–H deformation mode. These bands were absent in the spectrum of the second peak. Instead, a strong absorption band at 1667 cm^{-1} within the characteristic absorption region of the $-\text{N}=\text{C}$ -ketimine group appeared. GC-MS and GC-FT-

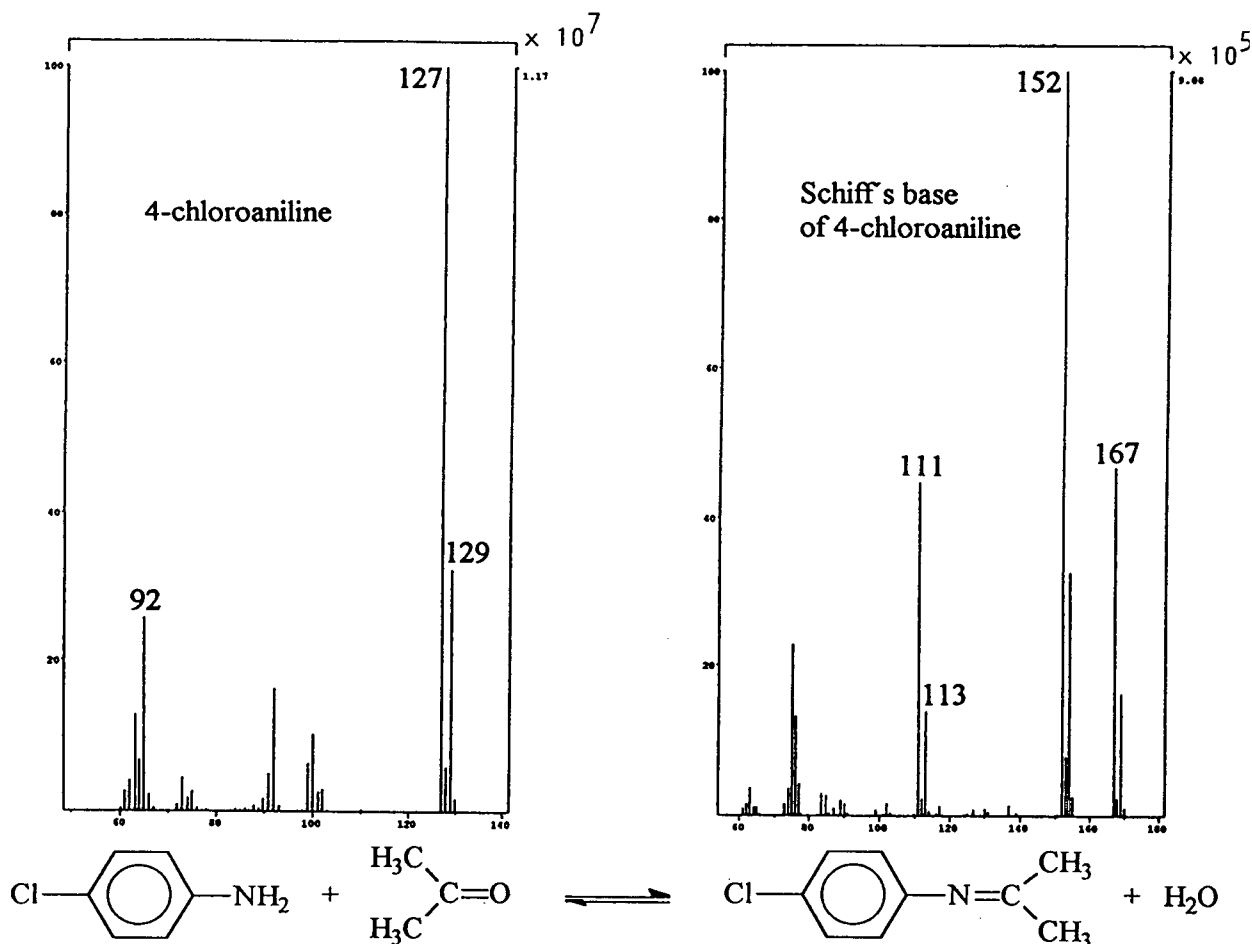


Fig. 2. EI mass spectra (scan range 50–500 u) of 4-CA (10 ng/ μ l) and the Schiff base of 4-CA formed in a solution containing acetone (1%, v/v). The reaction equation is also shown.

IR provided, in our opinion, the necessary evidence for the time-controlled formation of the Schiff base. It was also proved by Fig. 3, as will be discussed later.

The reaction extents and rates of formation of Schiff bases with further anilines were determined. After various reaction times, GC–FID of aniline, 4-IPA, 2-CA, 3-CA, 4-CA, 2,4-DCA and 4-BA mixtures with acetone showed an additional peak. The benzidine chromatogram even showed two additional peaks. No additional peak could be observed for the 2,4,5-TCA solution. By GC–MS measurement, all additional peaks could be identified as Schiff bases (N-

isopropylideneanilines), as the mass spectra of these peaks contained the characteristic mass difference of 40 u for the simultaneous formation of the ketimine group and elimination of water. The molecular and fragment ions of the anilines and their Schiff bases are listed in Table 1. The mass spectra of the reaction products of chloroanilines, bromoanilines and benzidine contained fragment ions with a mass difference of 56 u from the molecular ion masses, which is characteristic of the elimination of a C_3H_6N fragment. A further fragment ion of all ketimine mass spectra and the only in case of aniline and IPA ketimines resulted in elimination of a CH_3 frag-

Table 1
Molecular and fragment ions (GC–EI-MS) of anilines and their Schiff bases as reaction products with acetone (base peaks in italics)

Substance	Anilines (<i>m/z</i>)		Schiff bases with acetone (<i>m/z</i>)	
	Molecular ion	Fragment ion	Molecular ion	Fragment ion
Aniline	93	–	133	<i>118</i>
4-IPA	135	<i>120</i>	175	<i>160</i>
2-CA	127/129	–	167/169	<i>152/154, 111/113</i>
3-CA	127/129	–	167/169	<i>152/154, 111/113</i>
4-CA	127/129	–	167/169	<i>152/154, 111/113</i>
4-BA	171/173	92	211/213	<i>196/198, 155/157</i>
3,4-DCA	161/163	–	201/203	<i>186/188, 145/147</i>
2,4-DCA	161/163	–	201/203	<i>186/188, 145/147</i>
2,4,5-TCA	195/197	–	–	–
Benzidine	184	–	(a) 224 (b) 264	209, 168, 167 249, 152, 117

ment. The second product of the benzidine reaction was formed with two molecules of acetone (mass difference of another 40 u).

Fig. 3 shows the reaction rates and ratios of the different anilines. The ratios of the peak areas ($\text{area}_{\text{Schiff base}}/\text{area}_{\text{aniline}}$) depending on the reaction time are described here for selected anilines. As reference substances were unavailable, a quantification of the Schiff bases could not be performed. The order of the reaction ratios was $4\text{-IPA} > \text{aniline} > 4\text{-CA} > 3\text{-CA} > 4\text{-BA} > 3,4\text{-DCA} \gg 2\text{-CA} > 2,4\text{-DCA}$.

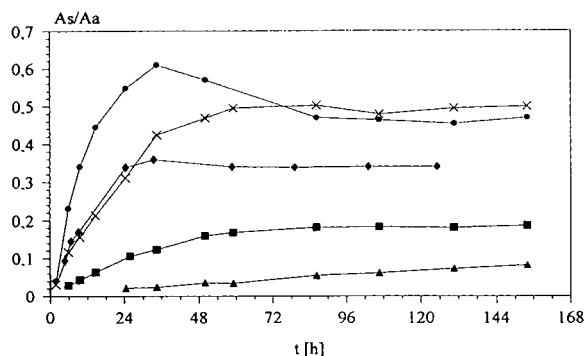


Fig. 3. Course of reaction for the formation of Schiff bases for selected anilines (10 ng/μl) and acetone (1%, v/v) in hexane at 22°C. Chromatographic conditions as in Fig. 1. As = peak area of Schiff base; Aa = peak area of aniline; t = time. \bullet = 4-IPA; \times = aniline; \blacklozenge = 4-CA; \blacksquare = 3-CA; \blacktriangle = 3,4-DCA.

After 5 and 15 days 2-CA and 2,4-DCA, respectively, showed a very small peak for the Schiff base. The order stated above is approximately related to the order of the basicity of the anilines and to the availability of the free electron pair at the nitrogen [9]. The first reaction product of benzidine was the ketimine with one molecule of acetone. The second ketimine with two molecules acetone was detected 6 h later.

Further, investigations were carried out to establish whether Schiff bases were formed from aniline and 4-CA during the common extraction of water with acetone–hexane, and whether they were stable during evaporation and dissolution procedures. By GC–MS the corresponding Schiff bases of both anilines were detected in the dissolved extracts despite the water content, which shifts the reaction balance to the disadvantage of Schiff base formation [10]. However, the peak areas of the Schiff bases were much smaller than with standard solutions, amounting to only 5% of the aniline peak areas.

The assumed formation of Schiff bases as reaction products of basic anilines and acetone could be verified at trace concentration levels. Therefore, aniline standards should not be dissolved using acetone. Acetone could be replaced by ethyl acetate, diethyl ether or other polar solvents. The formation of ketimines can cause problems during column chromatography when

using acetone as the eluent [2]. Further, small losses of anilines by formation of Schiff bases were observed during the extraction of spiked water with acetone.

References

- [1] R.M. Riggin, T.F. Cole and S. Billets, *Anal. Chem.*, 55 (1983) 1862.
- [2] G. Böer, C. Schlett and H.-P. Thier, *Z. Wasser Abwasser Forsch.*, 23 (1990) 220.
- [3] D.T. Williams, Q. Tran, P. Fellin and K. A. Brice, *J. Chromatogr.*, 549 (1991) 297.
- [4] M. Abdel-Rehin, M. Hassan and H. Ehrson, *J. High Resolut. Chromatogr.*, 14 (1991) 284.
- [5] H. Parlar and F. Korte, *Chemosphere*, 3 (1979) 792.
- [6] R. Scholz and N. Palauschek, *Fresenius' Z. Anal. Chem.*, 331 (1988) 282.
- [7] V. Lopez-Avilla, R. Northcutt, J. Onstot and M. Wickham, *Anal. Chem.*, 55 (1983) 881.
- [8] M. Tushimoto, S. Nishimura and H. Iwamura, *Bull. Chem. Soc. Jpn.*, 46 (1973) 675.
- [9] A. Streithwieser and C.H. Heathcock, *Organische Chemie*, Verlag Chemie, Weinheim, 1980, p. 1142.
- [10] E.P. Kyba, *Org. Prep. Proced.*, 2 (1970) 149.



ELSEVIER

Journal of Chromatography A, 685 (1994) 195–199

JOURNAL OF
CHROMATOGRAPHY A

Short communication

High-performance thin-layer chromatographic method for monitoring degradation products of rifampicin in drug excipient interaction studies

K.C. Jindal*, R.S. Chaudhary, S.S. Gangwal, A.K. Singla, S. Khanna

Lupin Laboratories Limited, MIDC, Chikalthana, Aurangabad-431210, India

First received 11 April 1994; revised manuscript received 3 August 1994

Abstract

A thin-layer chromatographic assay for the determination of rifampicin and its degradation components in drug–excipient interaction studies is described. The chromatography was performed on thin-layer plates (silica gel) with a mobile phase consisting of chloroform–methanol–water (80:20:2.5, v/v/v). The peaks were quantified by densitometric evaluation of the chromatograms. The method shows a limit of detection of 10 ng per band and good precision and linearity in the range 50–3000 ng per band for rifampicin, 3-formylrifamycin SV, rifampicin N-oxide and 25-desacetyl rifampicin and 100–350 ng per band for rifampicin quinone

1. Introduction

Rifampicin, (12*Z*,14*E*,24*E*)-(2*S*,16*S*,17*S*,18*R*,19*R*,20*R*,21*S*,22*R*,23*S*)-1,2-dihydro-5,6,9,17,19-pentahydroxy-23-methoxy-2,4,12,16,18,20,22-heptamethyl-8-(4-methylpiperazin-1-yliminomethyl)-1,11-dioxo-2,7-(epoxypentadeca-1,11,13-trienimino)naphtho[2,1-*b*]furan-21-yl acetate, is a semi-synthetic antibiotic, active against *Mycobacterium* species [1]. The structures of rifampicin, 3-formylrifamycin SV and 25-desacetyl rifampicin are shown in Fig. 1. Some physico-chemical properties such as stability of rifampicin in different media have been reported [2].

A liquid chromatographic method using an ODS Permaphase column employing gradient elution with water–methanol as the mobile phase

to determine simultaneously rifampicin and its degradation products has been described [3]. In another method, a microPak-NH₂ column was

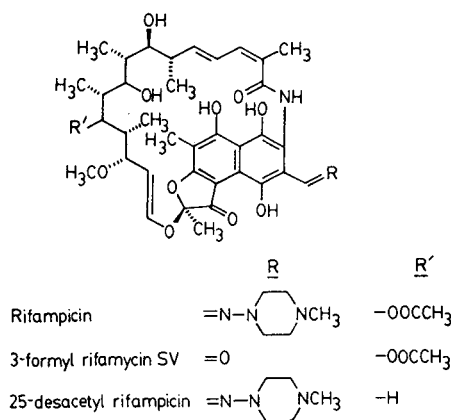


Fig. 1. Structures of rifampicin, 3-formylrifamycin SV and 25-desacetyl rifampicin.

* Corresponding author.

employed to determine rifampicin quinone alone [4], and several liquid chromatographic methods have been reported for the determination of rifampicin metabolites in blood, urine and saliva [5,6]. A qualitative thin-layer and paper chromatographic procedure has been reported for the detection of degradation products but detection was done visually [7–9].

The British Pharmacopoeia specifies a semi-quantitative TLC limit test for rifampicin and related compounds based on visual detection of bands by short-wavelength UV light [1]. The chromatographic purity test for rifampicin described in the US Pharmacopoeia is based on liquid chromatography [10]. The method is not sensitive enough to detect some of the degradation products of rifampicin.

In view of the various shortcomings of the tests mentioned above, this study was undertaken to develop a simple and sensitive TLC method making use of the UV absorbance characteristics of rifampicin and its degradation products. The suitability of this method was evaluated on preformulation study samples containing mixtures of rifampicin with various pharmaceutical excipients.

2. Experimental

2.1. Chemicals and materials

Rifampicin was supplied by Lupin Laboratories (Ankleshwar, India). Distilled water was obtained from a Milli-Q system (Millipore, Milford, MA, USA). Solvents, chemicals (analytical-reagent grade) and HPTLC plates were obtained from Merck (Bombay, India). The HPTLC plates (20 cm × 10 cm) were precoated with silica gel 60 (layer thickness 0.25 mm) and a fluorescent indicator. The plates were prewashed in methanol, air-dried and stored under normal conditions.

2.2. Instruments

Solutions of the test samples were applied to the HPTLC plates with a Linomat IV autospotter (Camag, Muttenz, Switzerland). The plates were

scanned with a Scanner II (Camag) and data were processed on PC/AT (Zenith, Pune, India) using Cats 3 software (Camag). A Model AE 163 analytical balance (Mettler Instruments, Highstown, NJ, USA) was used for weighing reagents.

2.3. Preparation of rifampicin, 3-formylrifamycin SV, rifampicin N-oxide and 25-desacetyl rifampicin standard solutions

Standard solutions containing 10 µg/ml of rifampicin, 3-formylrifamycin SV, rifampicin N-oxide and 25-desacetyl rifampicin were prepared separately by dissolution in chloroform. Aliquots of 5, 10, 15, 20, 25 and 30 µl of each standard solution were applied (6 mm band) on TLC plates (4 mm between bands) with a Linomat IV sample applicator to give 50, 100, 150, 200, 250 and 300 ng per band for the determination of linearity. The bands were dried with nitrogen.

2.4. Preparation of rifampicin quinone standard solution

A standard solution containing 25 µg/ml of rifampicin quinone was prepared by dissolution in chloroform. For the determination of linearity 4, 6, 8, 10, 12 and 14 µl of the standard solution were applied (6 mm band) on a TLC plate (4 mm between bands) with a Linomat IV sample applicator to give 100, 150, 200, 250, 300 and 350 ng per band. The bands were dried with nitrogen.

2.5. Preparation of rifampicin test solution

A standard solution containing rifampicin test sample was prepared in chloroform at 1000 µg/ml. A 20-µl volume of this solution was applied (6 mm band) on a TLC plate (4 mm between bands) with a Linomat IV sample applicator. The bands were dried with nitrogen.

2.6. Thin-layer chromatography

The TLC plates were developed in unlined glass twin-trough tanks (Camag) with chloroform–methanol–water (80:20:2.5, v/v/v) as mo-

bile phase [7]. The equilibration time to saturate the tank atmosphere was 1 h. The TLC plates were developed over a distance of 5 cm and finally air dried.

2.7. Densitometric measurement of the chromatograms

The developed plates were quantified by linear scanning at 4 mm/s with a Scanner II equipped with a PC/AT and Cats 3 software. The absorbance mode with a deuterium lamp and a monochromator setting of 330 nm and slit dimensions of 0.2×3 mm was used for determination of rifampicin, 3-formylrifamycin SV, rifampicin N-oxide, 25-desacetylriofampicin and other unknown impurities. Rifampicin quinone was determined at 490 nm. The determination of 3-formylrifamycin SV, rifampicin N-oxide, 25-desacetylriofampicin and rifampicin quinone was carried out by comparing the peak areas of the test samples with the peak areas of the respective standards. A 1% equivalent band of rifampicin was used to determine the unknown impurities for which reference standards were not available. The procedure adopted is based on the US Pharmacopeia recommendation.

2.8. Application of the method

The applicability of the method was demonstrated with rifampicin samples drawn from preformulation accelerated stability samples blended with various excipients. Samples were drawn after 1, 2, 3 and 6 months from the accelerated storage conditions at room temperature and 45, 60, 5 and 40°C at 75% relative humidity. All samples were treated in a similar manner to give solutions in chloroform.

3. Results

3.1. Chromatography

Under the conditions described, rifampicin showed no interference from 3-formylrifamycin SV, rifampicin N-oxide, 25-desacetylriofampicin, rifampicin quinone and other degradation com-

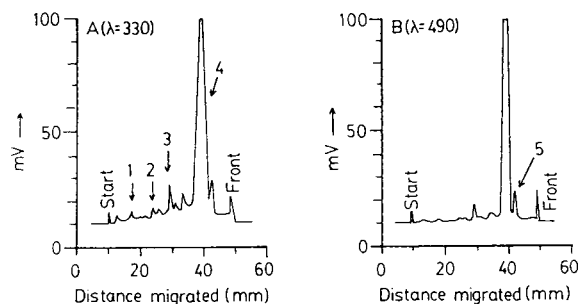


Fig. 2. Representative chromatograms of rifampicin. (A) Detection of degradation components at 330 nm: 1 = rifampicin N-oxide; 2 = 25-desacetylriofampicin; 3 = 3-formylrifamycin SV; 4 = rifampicin (4). (B) Detection of rifampicin quinone (5) at 490 nm.

ponents. Representative chromatograms of the pure drug and accelerated stability samples are given in Figs. 2 and 3.

3.2. Recovery

Recovery studies were performed by spiking a test solution with known concentrations of rifampicin, rifampicin quinone, 25-desacetylriofampicin, rifampicin N-oxide and 3-formylrifamycin SV. For calculation of recoveries, the resulting peak areas were compared with those of rifampicin, rifampicin N-oxide, 25-desacetylriofampicin, 3-formylrifamycin SV and rifampicin reference standards in chloroform. Reference standards and recovery samples had to be

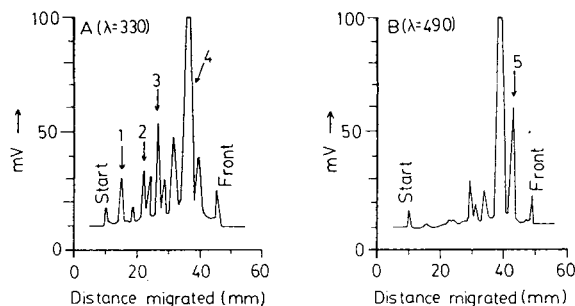


Fig. 3. Representative chromatograms of a rifampicin-sucrose mixture (1:1) kept at 45°C and analysed after 3 months. (A) Detection of degradation components at 330 nm: 1 = rifampicin N-oxide; 2 = 25-desacetylriofampicin; 3 = 3-formylrifamycin SV; 4 = rifampicin. (B) Detection of rifampicin quinone (5) at 490 nm.

prepared in the same solvent in order to run the sample applicator properly. Samples containing three different concentrations of rifampicin, rifampicin N-oxide, 25-desacetylriofampicin, 3-formylrifamycin SV and rifampicin quinone were determined ($n = 6$). The average recoveries were 99.4% for rifampicin, 99.6% for rifampicin quinone, 98.4% for 3-formylrifamycin SV, 99.8% for rifampicin N-oxide and 100.3% for 25-desacetylriofampicin. The results are summarized in Table 1.

3.3. Linearity

The calibration graphs were linear in the range 50–300 ng per band for rifampicin, 3-formylrifamycin SV, rifampicin N-oxide and 25-desacetylriofampicin and 100–350 ng per band for rifampicin quinone. Linearity for rifampicin, 3-formylrifamycin SV, rifampicin N-oxide and 25-desacetylriofampicin were tested with sample bands of 50, 100, 150, 200, 250 and 300 ng per band and rifampicin quinone with sample bands of 100, 150, 200, 250, 300 and 350 ng per band. The correlation coefficients were 0.9995 for rifampicin, 0.9996 for 3-formylrifamycin SV, 0.9989 for rifampicin N-oxide, 0.9976 for 25-

desacetylriofampicin and 0.9998 for rifampicin quinone.

3.4. Reproducibility

Reproducibility experiments were carried out for five components at three concentrations ($n = 6$). The results obtained are summarized in Table 1. The relative standard deviations ranged from 0.86 to 1.59% for rifampicin, 1.93 to 2.58% for rifampicin quinone, 1.32 to 1.96% for 3-formylrifamycin SV, 1.72 to 1.88% for rifampicin N-oxide and 1.23 to 1.86% for 25-desacetylriofampicin.

4. Discussion

The method described allows the simple and rapid determination of rifampicin, rifampicin quinone, 3-formylrifamycin SV, rifampicin N-oxide and 25-desacetylriofampicin levels without interference from each other or from other degradation components present in the sample. One of the main advantages of this assay is the very low limit of detection. The detection limit for each component was ca. 10 ng per band,

Table 1
Recovery and precision data

Compound	Concentration (ng per band)	n	Precision recovery		Average recovery (%)
			(R.S.D.)	(%)	
Rifampicin	50	6	1.59	99.6	99.4
	150	6	0.86	99.3	
	300	6	1.01	99.4	
Rifampicin quinone	100	6	2.01	98.3	99.6
	250	6	1.93	99.8	
	350	6	2.58	100.7	
3-Formylrifamycin SV	50	6	1.96	98.9	98.4
	150	6	1.32	99.7	
	300	6	1.68	96.8	
Rifampicin N-oxide	50	6	1.88	99.3	99.8
	150	6	1.72	98.9	
	300	6	1.77	101.3	
25-Desacetylriofampicin	50	6	1.54	102.1	100.3
	150	6	1.23	99.3	
	300	6	1.86	99.7	

which was possible because there was no dilution effect by the mobile phase at the time of detection. The HPLC methods described in literature are not suitable for separating all the degradation components simultaneously without any interference [3,10]. The method described here is sensitive, precise and involves a single-step sample preparation. Because almost 50 samples can be analysed within 4 h, the technique may be used for routine raw material purity analysis, stability monitoring studies and dosage form analysis.

References

- [1] *The British Pharmacopoeia, 1993*, Vol. 1, HMSO, London, 1993, p. 580.
- [2] N. Maggi, A. Vigevani, G.G. Gallo and C.R. Pasqualucci, *J. Med. Chem.*, 11 (1968) 936.
- [3] J.A. Schmit, R.A. Henry, R.C. Williams and J.F. Dieckman, *J. Chromatogr. Sci.*, 9 (1971) 645.
- [4] V. Vlasakova, J. Benes and K. Zivny, *J. Chromatogr.*, 151 (1978) 199.
- [5] J.B. Lecaillon, N. Febvre, J.P. Metayer and C. Souppart, *J. Chromatogr.*, 145 (1978) 319.
- [6] O.T. Kolos and L.L. Eidus, *J. Chromatogr.*, 68 (1972) 294.
- [7] W.L. Wilson, K.C. Graham and M.J. Lebel, *J. Chromatogr.*, 144 (1977) 270.
- [8] P. Sensi, C. Coronelli and B.J.R. Nicolaus, *J. Chromatogr.*, 5 (1961) 519.
- [9] K. Shimizu and O. Kunii, *Shinryo*, 23 (1972) 969.
- [10] *The United States Pharmacopoeia*, United States Pharmacopoeial Convention, Rockville, MD, 22nd ed., 1990, p. 1226.



ELSEVIER

Journal of Chromatography A, 685 (1994) 200–201

JOURNAL OF
CHROMATOGRAPHY A

Book Review

Modern Methods and Applications in Analysis of Explosives, by J. Yinon and S. Zitrin, Wiley, Chichester, New York, 1993, X + 305 pp., price £60.00, ISBN 0-471-93894-7.

The authors are both recognized experts in the explosives field and have published extensively, including a similar book on the analysis of explosives in 1981. New analytical advances have increased the sensitivity and specificity of methods for the analysis of explosives and this book concentrates on scientific contributions published during the 1980s and early 1990s. The book is organized into six chapters that take the reader through an introduction to explosive compounds and mixtures, followed by chromatographic and mass spectrometric analytical methods, residue and environmental analyses and finally methods for the detection of hidden explosives. Each chapter constitutes a complete entity, and while this style necessitates some repetition, it does not detract from the authors' ability to indicate the relevance of new explosive analysis methods for forensic, military and environmental applications. Referencing is consistent with the authors' objectives, with the majority of the over three hundred citations being published after 1980. The reader interested in specific information on explosives will find a complete index following the references.

The first chapter describes common explosives and mixtures, classifications of explosives and provides a comprehensive summary of the properties of common explosives and mixtures. Structures are provided for all the explosive compounds discussed as well as abbreviations for each compound. For the novice analyst the

continued use of abbreviations throughout the book will result in repeated referral to this chapter for abbreviation definition. A listing of the abbreviations used in the book would have been beneficial.

Chapters 2 and 3 discuss recent chromatographic and mass spectrometric advances and the use of these techniques for the analysis of explosives. Most of the chromatographic chapter deals with the use of fused-silica capillary column GC and HPLC, with an emphasis on the specificity and sensitivity of available detectors. The importance of the thermal energy analyzer (chemiluminescence detector) for explosive detection is highlighted and comparisons are made to other means of detection. Supercritical fluid and ion chromatographic methods are discussed, but only a brief mention of the utility of capillary electrophoresis for anion analysis is made at the end of Chapter 4.

The mass spectrometry chapter emphasizes novel developments and indicates the value of alternative ionization techniques such as chemical ionization and atmospheric pressure ionization for compound characterization. Tandem mass spectrometry has been commercially available for about a decade and the use of this technique for fragmentation studies and analysis problems is well illustrated. Capillary column GC-MS examples are presented to support the use of this method for the analysis of complex samples containing thermally stable, volatile

explosives. Less volatile or thermally labile compounds are more amenable to HPLC–MS, but discussion is limited to thermospray and direct liquid introduction. Newer interfaces for HPLC–MS, such as atmospheric pressure ionization, are not discussed. Applications in this area are likely too recent for inclusion in this book.

Chapters 4 and 5 discuss applications of the developed analytical methods for the analysis of explosive residues and environmental samples (e.g., aqueous and soil/sludge) for explosives. The importance of isolation schemes for sample clean-up is emphasized and examples illustrating the use of the described chromatographic and mass spectrometric techniques are provided. These chapters give the reader a good feel for the current status of methods for the analysis of explosives, but the book lacks a critical comparative summary of the analysis methods presented.

The final chapter deals with the detection of

hidden explosives in luggage, mail vehicles and aircraft, all situations where possible terrorist or criminal activity necessitates monitoring. The devices discussed include instruments that make use of electron capture, ion mobility spectrometric and mass spectrometric detection of explosive vapors. Bulk detection methods, including X-ray imaging and thermal-neutron activation, and explosive tagging are also presented.

Modern Methods and Applications in Analysis of Explosives is a good general reference book, providing the reader with a review of advances in the analysis of explosives over the past decade. The book emphasizes the use of chromatographic and mass spectrometric methods and applications and provides the reader with experimental details for each approach in a summary format.

Medicine Hat, Canada P.A. D'Agostino

PUBLICATION SCHEDULE FOR THE 1995 SUBSCRIPTION

Journal of Chromatography A and Journal of Chromatography B: Biomedical Applications

MONTH	O 1994	N 1994	D 1994	
Journal of Chromatography A	683/1 683/2 684/1	684/2 685/1 685/2 686/1	686/2 687/1 687/2 688/1 + 2	The publication schedule for further issues will be published later.
Bibliography Section				
Journal of Chromatography B: Biomedical Applications				

INFORMATION FOR AUTHORS

(Detailed *Instructions to Authors* were published in *J. Chromatogr. A*, Vol. 657, pp. 463–469. A free reprint can be obtained by application to the publisher, Elsevier Science B.V., P.O. Box 330, 1000 AH Amsterdam, Netherlands.)

Types of Contributions. The following types of papers are published: Regular research papers (full-length papers), Review articles, Short Communications and Discussions. Short Communications are usually descriptions of short investigations, or they can report minor technical improvements of previously published procedures; they reflect the same quality of research as full-length papers, but should preferably not exceed five printed pages. Discussions (one or two pages) should explain, amplify, correct or otherwise comment substantively upon an article recently published in the journal. For Review articles, see inside front cover under Submission of Papers.

Submission. Every paper must be accompanied by a letter from the senior author, stating that he/she is submitting the paper for publication in the *Journal of Chromatography A* or *B*.

Manuscripts. Manuscripts should be typed in **double spacing** on consecutively numbered pages of uniform size. The manuscript should be preceded by a sheet of manuscript paper carrying the title of the paper and the name and full postal address of the person to whom the proofs are to be sent. As a rule, papers should be divided into sections, headed by a caption (*e.g.*, Abstract, Introduction, Experimental, Results, Discussion, etc.). All illustrations, photographs, tables, etc., should be on separate sheets.

Abstract. All articles should have an abstract of 50–100 words which clearly and briefly indicates what is new, different and significant. No references should be given.

Introduction. Every paper must have a concise introduction mentioning what has been done before on the topic described, and stating clearly what is new in the paper now submitted.

Experimental conditions should preferably be given on a *separate* sheet, headed "Conditions". These conditions will, if appropriate, be printed in a block, directly following the heading "Experimental".

Illustrations. The figures should be submitted in a form suitable for reproduction, drawn in Indian ink on drawing or tracing paper. Each illustration should have a caption, all the *captions* being typed (with double spacing) together on a *separate sheet*. If structures are given in the text, the original drawings should be provided. Coloured illustrations are reproduced at the author's expense, the cost being determined by the number of pages and by the number of colours needed. The written permission of the author and publisher must be obtained for the use of any figure already published. Its source must be indicated in the legend.

References. References should be numbered in the order in which they are cited in the text, and listed in numerical sequence on a separate sheet at the end of the article. Please check a recent issue for the layout of the reference list. Abbreviations for the titles of journals should follow the system used by *Chemical Abstracts*. Articles not yet published should be given as "in press" (journal should be specified), "submitted for publication" (journal should be specified), "in preparation" or "personal communication".

Vols. 1–651 of the *Journal of Chromatography*; *Journal of Chromatography, Biomedical Applications* and *Journal of Chromatography, Symposium Volumes* should be cited as *J. Chromatogr.* From Vol. 652 on, *Journal of Chromatography A* (incl. Symposium Volumes) should be cited as *J. Chromatogr. A* and *Journal of Chromatography B: Biomedical Applications* as *J. Chromatogr. B*.

Dispatch. Before sending the manuscript to the Editor please check that the envelope contains four copies of the paper complete with references, captions and figures. One of the sets of figures must be the originals suitable for direct reproduction. Please also ensure that permission to publish has been obtained from your institute.

Proofs. One set of proofs will be sent to the author to be carefully checked for printer's errors. Corrections must be restricted to instances in which the proof is at variance with the manuscript.

Reprints. Fifty reprints will be supplied free of charge. Additional reprints can be ordered by the authors. An order form containing price quotations will be sent to the authors together with the proofs of their article.

Advertisements. The Editors of the journal accept no responsibility for the contents of the advertisements. Advertisement rates are available on request. Advertising orders and enquiries can be sent to the Advertising Manager, Elsevier Science B.V., Advertising Department, P.O. Box 211, 1000 AE Amsterdam, Netherlands; courier shipments to: Van de Sande Bakhuyzenstraat 4, 1061 AG Amsterdam, Netherlands; Tel. (+31-20) 515 3220/515 3222, Telefax (+31-20) 6833 041, Telex 16479 els vi nl. UK: T.G. Scott & Son Ltd., Tim Blake, Portland House, 21 Narborough Road, Cosby, Leics. LE9 5TA, UK; Tel. (+44-533) 753 333, Telefax (+44-533) 750 522. USA and Canada: Weston Media Associates, Daniel S. Lipner, P.O. Box 1110, Greens Farms, CT 06436-1110, USA; Tel. (+1-203) 261 2500, Telefax (+1-203) 261 0101.

Ovomucoid Bonded Column for Direct Chiral Separation

ULTRON ES-OVM

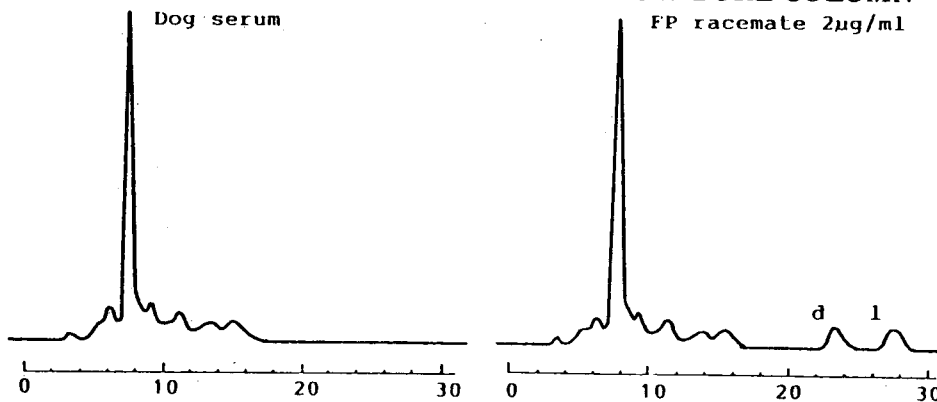
Narrow-Bore Column (2.0 I.D. x 150 mm) for Trace Analyses

Analytical Column (4.6 I.D. , 6.0 I.D. x 150 mm) for Regular Analyses

Semi-Preparative Column (20.0 I.D. x 250 mm) for Preparative Separation

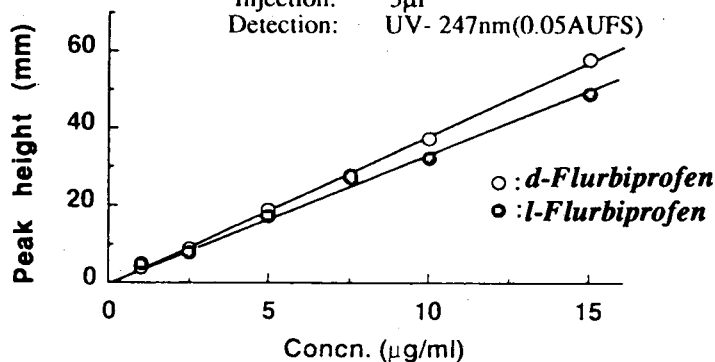
Analysis of Trace FLURBIPROFEN in Metabolite

with NARROW-BORE COLUMN



Conditions

Column: ULTRON ES-OVM(2.0I.D. x 150mm)
Mobile Phase: 20mM Phosphate Buffer(pH=3.0)/CH₃CN =100/15
Flow Rate: 0.1ml/min
Temperature: 25°C
Injection: 5µl
Detection: UV- 247nm(0.05AUFS)



Calibration Curve for Each Enantiomer of Flurbiprofen

SHINWA CHEMICAL INDUSTRIES, LTD.

50 Kagekatsu-cho, Fushimi-ku, Kyoto 612, JAPAN

Phone: +81-75-621-2360 Fax: +81-75-602-2660

In the United States and Europe, please contact:

Rockland Technologies, Inc.

538 First State Boulevard, Newport, DE 19804, U.S.A.

Phone: 302-633-5880 Fax: 302-633-5893

This product is licenced by Eisai Co., Ltd.

1 2 8 2538

11/20/28